Methods in Molecular Biology™

VOLUME 203

In Situ Detection of DNA Damage

Methods and Protocols

Edited by

Vladimir V. Didenko

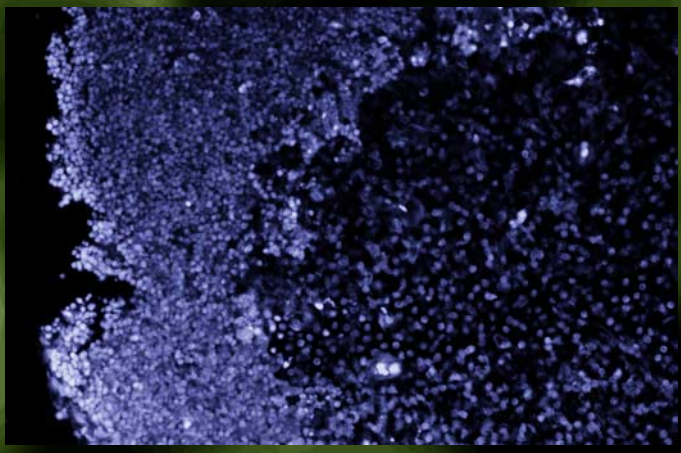

HUMANA PRESS

I

Labeling DNA Breaks Using Terminal Transferase (TUNEL Assay)

1

Labeling DNA Damage with Terminal Transferase

Applicability, Specificity, and Limitations

P. Roy Walker, Christine Carson, Julie Leblanc, and Marianna Sikorska

1. Introduction

Apoptotic and programmed cell death are characterized by, and indeed were first discovered from observations of, remarkable morphological changes that occur in the nucleus (see ***1*** for a comprehensive review of apoptosis and programmed cell death). Thus, light and electron microscopy were the first tools for the detection of apoptosis. This characteristic collapse of chromatin and ultimately the structural organization of the nucleus is triggered by the degradation of DNA, which is an active process and occurs prior to death of the cell. The degradation of DNA was subsequently found to be mediated by endonucleolytic activity that generated a specific pattern of fragments ***(2)***. The fragment sizes were multiples of approx 200 bp, the amount of DNA wound around a single nucleosome, and the pattern became known as the DNA ladder (**Fig. 1A**). Later it became apparent that DNA fragmentation is quite variable within cells and some cell types produce only high molecular weight (HMW) fragments (**Fig. 1B**, ***3***). The latter observations formed the basis of a convenient in vitro biochemical technique for the routine detection of apoptosis by resolving the fragmented DNA by conventional or pulsed field agarose gel electrophoresis. However, this technique requires relatively large amounts of material and DNA extraction. Subsequently, a variety of techniques have emerged to detect apoptotic DNA fragmentation *in situ* by exploiting the fact that the hydroxyl group at the 5' or 3' ends of the small DNA fragments becomes exposed. Nucleotide analogues can be attached to the ends by several enzymes, with **T**erminal **d**eoxynucleotide **T**ransferase (TdT) being the most popular ***(4,5)***. The assays

From: *Methods in Molecular Biology, vol. 203:* In Situ *Detection of DNA Damage: Methods and Protocols*
Edited by: V. V. Didenko

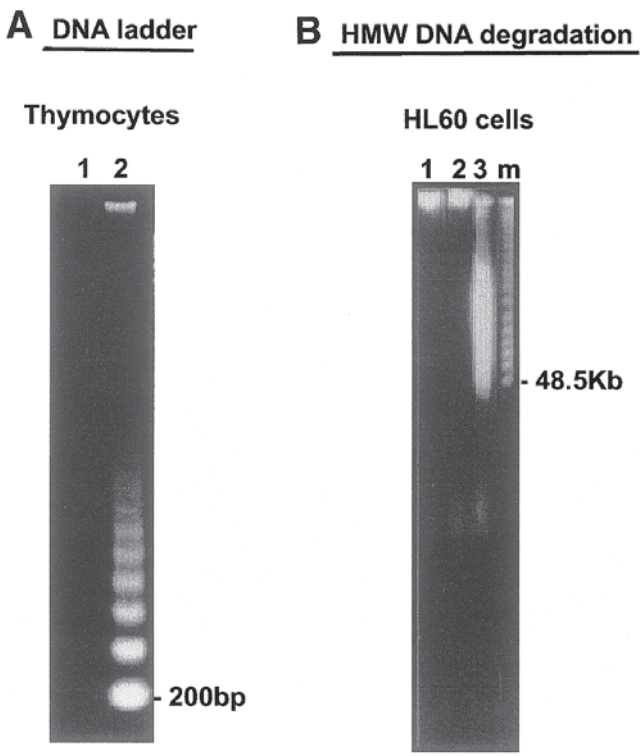

Fig. 1. Patterns of DNA fragmentation in apoptosis. (**A**) DNA extracted from control (lane 1) and glucocorticoid-treated (lane 2) thymocytes showing the DNA ladder of mono- and oligo-nucleosomes. (**B**) DNA extracted from untreated (lane 1), vehicle-treated (lane 2) and VM26-treated (lane 3) HL60 cells and resolved by pulsed field gel electrophoresis (*see* ***9***). Lane m is the lambda DNA ladder marker (multiples of 48.5Kb). In these cells, only high molecular weight (HMW) degradation occurs.

are typically fluorescence-based, either by the direct incorporation of a nucleotide to which a fluorochrome has been conjugated, or indirectly using fluorescent dye conjugated antibodies that recognize biotin- or digoxigenin-tagged nucleotides. Radioactively labeled nucleotides can also be used. Since several million fragments are generated during complete DNA fragmentation and low levels of fluorescence can be readily detected by photo-multipliers and CCD arrays, the assays are extremely sensitive. The assays have been formatted for light and confocal microscopy as well as flow cytometry, thereby greatly facilitating the detection and quantitation of apoptosis *in situ*. In addition, end-labeling techniques are employed in studies of the actual mechanism of DNA fragmentation, as well as the detection and characterization of endonucleases.

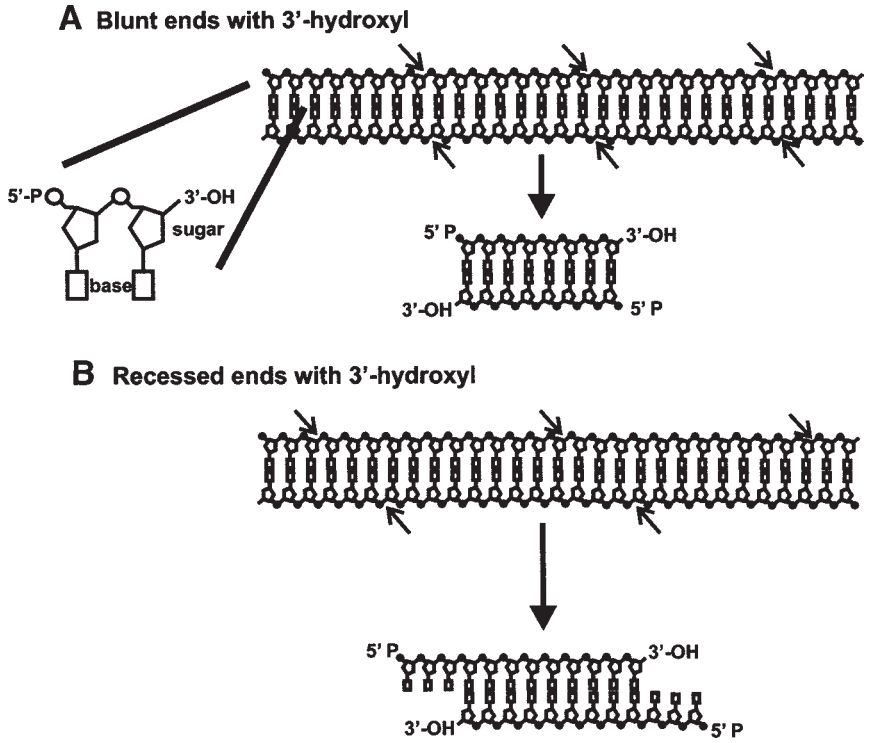

Fig. 2. Mechanisms of endonucleolytic attack on DNA. In **A** the arrows indicate the site of attack by an endonuclease cleaving the phosphodiester bond at the same point on each strand of the DNA duplex to generate multiple smaller fragments each with 3'-OH and 5'-P ends. In **B** the endonuclease cleavage of each strand of the DNA duplex is offset generating fragments with a 3' recess.

1.1. The Nature of the DNA Fragments

Endonucleases cleave DNA by attacking the phosphodiester bonds of the sugar-phosphate backbone of each strand (**Fig. 2A**). The phosphodiester bond can be cleaved in two ways such that the phosphate is left on either the 3' end of the DNA strand or the 5' end, the opposite end being a hydroxyl group in each case. In addition, the distance between the point at which the bond is broken on opposite strands of the DNA duplex also varies. If the breaks are exactly opposite, the fragment is considered blunt-ended. If they are offset, they generate either 3' or 5' overhangs (**Fig. 2B**). Thus, DNA can be cleaved by a variety of nucleases, operating by different mechanisms, and each type of nuclease generates a characteristic "signature" in terms of nature of the ends it creates.

The DNA fragments that are produced during apoptosis are usually, but not always, created by an endonuclease that cleaves the DNA strand at the

phosphodiester bond such that the 5' end of the DNA retains the phosphate group and the 3' end is an hydroxyl group (**Fig. 2A**). Generally there is little or no overhang *(6,7)*. The terminal transferase assays take advantage of this observation, and add nucleotide analogs to the 3'-hydroxyl of the DNA fragment. However, numerous exceptions to this observation have been documented. In some cells, the DNA is believed to be cleaved by DNAse II, an enzyme that produces 5'-OH *(8)*. Such ends would not be labeled with terminal transferase. In addition, the cleavage of each strand is sometimes offset, leaving a variety of sizes of overhang *(9)*. The reasons for this are not clear, but probably relate to the fact that different endonucleases cleave the DNA in different cell types or under different physiological conditions. Terminal transferase can still add nucleotides to the 3'-OH of many of these fragments and a variety of other enzymes can also be used to add fluorescent or radioactive nucelotides to those DNA strands, as discussed below.

In some cells undergoing apoptosis, the DNA is not cleaved into small fragments at all. Instead, larger fragments of about 50 Kb are produced (**Fig. 1B**) *(3)*. These fragments appear to have 3'-OH groups, but since the number of fragments per cell is orders of magnitude lower, their detection becomes more difficult.

1.2. Terminal Deoxynucleotidyl Transferase

DNA nucleotidylexotransferase. (E.C. 2.7.7.31, common name: **T**erminal **d**eoxynucleotidyl **T**ransferase, TdT) is a DNA polymerase that catalyzes the addition of deoxyribonucleotides to the 3'-OH end of DNA strands without the need for a template or a primer. This is in contrast to most enzymes that incorporate nucleotides into duplex DNA, since they require a string of nucleotides on the opposite strand to create a template so that the enzyme recognizes which nucleotides to select. A reaction mixture containing all four nucleotides is required by these enzymes. DNA polymerases and the smaller Klenow fragment are typical examples and these enzymes are ideally suited to incorporate nucleotides into DNA fragments that possess overhangs. On the other hand, TdT requires only 1 nucleotide type (typically, deoxyuridine triphosphate, dUTP) in end-labeling assays and will continue to add it to generate a homopolymer. TdT also has other advantages such as the ability to add nucleotides to very small fragments of DNA making it ideal for labeling fragments in apoptotic cells. The enzyme will also label single stranded DNA molecules containing a 3'-OH and will attach nucleotides to a single-strand nick in DNA. This is particularly useful since many single-strand breaks are also introduced into DNA during fragmentation in apoptotic cells *(10)*.

1.3. Nucleotides Used in Labeling Assays

Initially, radioactively-labeled nucleotides were used in DNA-labeling experiments, but more recently, fluorescent nucleotide analogs have been

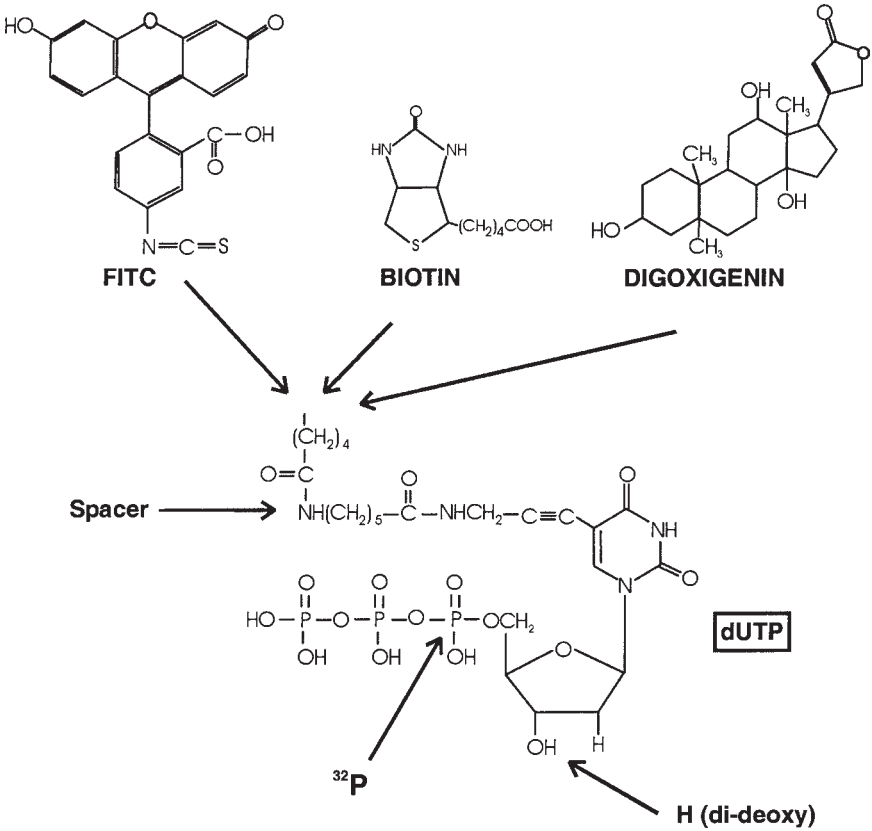

Fig. 3. Nucleotide analogs used in end-labeling assays. The three compounds commonly conjugated to dUTP are Fluoroscein, biotin and digoxigenin. The compounds are linked via a spacer to the C-5 of the nucleotide. Radioactively labeled dUTP is commonly on the alpha-Phosphate which becomes incorporated into the sugar phosphate backbone of DNA. Also shown is the substitution that terminates polymerization by removing the hydroxyl that interacts with the phosphate of the next nucleotide.

developed. The fluorochrome, usually fluorescein isothiocyanate (FITC), can be directly conjugated to the nucleotide and its green fluorescence readily detected using standard filter sets (**Fig. 3**). The nucleotide of choice is deoxyuridine triphosphate (dUTP) and conjugation is usually to the C-5 position of uridine which does not participate in hydrogen bonding. A spacer is used to decrease steric hindrance, with the length of the spacer dependent upon manufacturer and the nature of the molecule being conjugated. In other formats, the nucleotide is conjugated with biotin or digoxigenin derivatives and these molecules are detected with fluorescently-tagged proteins. This is fluo-

rochrome-conjugated streptavidin for biotin detection and anti-digoxigenin antibodies for digoxigenin detection. Because more than one molecule of FITC can be conjugated to the protein, the fluorescence signal is amplified. Thus, the indirect assays are more sensitive than direct FITC conjugation to the nucleotide *(11)*. Moreover, since digoxigenin is found only in plants, its antibody does not recognize any mammalian proteins, thereby reducing the background that is usually caused by non-specific binding. Other non-fluorescent detection systems have been used, particularly for tissue sections and blots, including alkaline phosphate-colorimetry, peroxidase, chemi-luminescence and colloidal gold.

Under optimal conditions, the sensitivity of fluorescence detection approaches that of radioactivity and the small number of fragments that occur during high molecular weight DNA fragmentation are readily detectable *(12)*. In addition, fluorescence affords the opportunity for multicolor counterstaining and labeling protocols, which are particularly useful for flow cytometry and confocal microscopy.

1.4. Assays Based on Terminal Transferase

The first end-labeling protocol developed for the detection of DNA fragmentation in apoptosis was the **T**erminal **U**ridine **N**ucleotide **E**nd **L**abeling (TUNEL) technique of Gavrielli et al *(4)*. This method exploited the ability of the enzyme, terminal transferase, to add biotin-conjugated nucleotides onto the 3' OH of a DNA strand. By using either a fluorescently tagged or radioactively labeled nucleotide analog, the DNA fragments become detectable. Formulation of the reaction buffer with cobalt ensures that the enzyme can add multiple bases to the 3'-end of each strand. As mentioned above, all types of 3'-end can be labeled, including those of single and double stranded DNA as well as recessed, protruding and blunt ends. The enzyme appears to have a preference for single stranded and 3'-protruding ends. The method can be used on cell suspensions and monolayers as well as frozen or paraffin tissue sections.

If only one nucleotide is to be incorporated onto each end of the double-stranded DNA fragment in order, for example, to accurately quantitate the number of fragments, then dideoxynucleotides can be used to create strand termination (**Fig. 3**). Usually, however, the objective is to increase sensitivity by incorporating multiple nucleotides and under optimal conditions as many as 50–100 monomers may be incorporated *(13)*. Unmodified nucleotides are included in the reaction mixture to "space out" the modified nucelotides in order to increase the ability of the binding protein to recognize its target. Typically, the methods use either digoxigenin-conjugated dUTP detected by staining with a FITC-conjugated anti-digoxigenin antibody or biotin-conjugated dUTP detected by staining with FITC-conjugated streptavidin.

If radioactivity is needed, the alpha-phosphate of dUTP is substituted with ^{32}P, since this is the phosphate that becomes incorporated into the sugar phosphate backbone of the DNA (**Fig. 3**).

1.5. Other Enzymes That Can Label DNA

Since some endonucleases also leave an overhang (i.e. a run of nucleotides on one strand only, **Fig. 2B**) the other strand can be extended or "filled in" by the Klenow fragment of DNA polymerase. The Klenow fragment of DNA polymerase I is used since it retains the ability to create a polymer, but does not possess the 5'–3' exonuclease activity which would degrade the fragment. In other situations, it is necessary to examine the 5' end of the DNA fragments. To confirm that the 5' end is indeed phosphorylated, the fragments can be incubated in the presence of the enzyme T4 kinase and ^{32}P-labeled inorganic phosphate. T4 kinase phosphorylates any 5'-OH. Thus, if the phosphate group is already present no radioactivity can be incorporated. However, if the phosphate is absent, or has been removed by incubation with alkaline phosphatase, the radioactively-labeled phosphate becomes attached to the fragment and this can be detected by autoradiography. Since T4 kinase can add only one phosphate, whereas terminal transferase or the Klenow fragment can add multiple nucleotides, the 5' labeling technique is much less sensitive than the 3' labeling techniques and is not generally used in routine assays. However, it is very useful for determining the nature of the ends of DNA from apoptotic cells.

1.6. Limitations

DNA fragments with 3'-OH ends can be produced in a number of situations where apoptosis is not occurring. For example, some forms of DNA damage produce DNA breaks or nicks with 3'-OHs. Moreover, the DNA degradation that occurs during necrosis also produces fragments with 3'-OH that would be labeled by TUNEL or ISEL (***I**n **s**itu* **E**nd **L**abeling, ***14***). Over-reliance on these techniques has led to considerable controversy in studies in brain where, following some insults, both apoptosis and necrosis occur simultaneously making it very difficult to establish and quantitate true apoptotic cell death ***(15–17)***.

It is evident, therefore, that TdT-based labeling techniques should not be used as the sole criterion for establishing the nature of the cell death mechanism. In order to establish that apoptosis is occurring, other criteria must also be used. Since it is possible to use multiple fluorochromes in the same experiments, another marker such as the appearance of annexin on the cell surface, can be used simultaneously. Once it has been established that the cell death is indeed apoptotic, then the TdT-based assays can be used for routine quantitation by microscopy or flow cytometry ***(3,18)***.

1.7. Terminal Transferase Labeling Examples

In the following sections are general protocols used in our laboratory for the detection of DNA fragmentation *in situ* using TdT. More detailed and application-specific protocols are given in the subsequent chapters of this section. **Fig. 4** shows apoptotic thymocytes prepared for electron, light and confocal microscopy as well as flow cytometry using the protocols described below. The electron micrograph shows a cell exhibiting classical apoptotic morphology alongside a normal thymocyte. The condensed apoptotic cells can easily be seen by light and fluorescence microscopy, particularly when the condensed chromatin is stained with Hoechst dye. The TUNEL assay labels all of the nuclei that are condensed and also shows two cells with TUNEL-positive fragmented DNA that have not yet undergone nuclear condensation (arrows). The extent of DNA fragmentation is demonstrated dramatically in the confocal image. In this example, the streptavidin is conjugated with Cy3 which fluoresces red and the anti-lamin B antibody is conjugated with FITC. The TUNEL positive (+) cells can be easily quantitated and sorted from the still normal (–) G_1 and G_2 populations by flow cytometry.

2. Materials

2.1. TUNEL Labeling of Cells for Light or Confocal Microscopy

1. 10× PBS: 1.31 *M* NaCl, 50 m*M* Na_2HPO_4, 16 m*M* KH_2PO_4. Composition per liter: 76.5 g NaCl, 7.25 g Na_2HPO_4, 2.12 g KH_2PO_4. Adjust pH to 7.0 after dilution, as pH changes over storage time. Store at room temperature.
2. Poly-L-lysine: 0.1% (w/v) in distilled H_2O.
3. Paraformaldehyde: 3% (w/v) in PBS. For 100 mL, heat 90 mL of distilled H_2O until boiling, add 3 g EM grade paraformaldehyde, 100 µL 1 *M* NaOH and stir to dissolve. Cool to room temperature, and add 10 mL of 10× PBS. Adjust pH to 7.0. Make fresh just before use, do not store.
4. 0.2% Triton-X-100 (v/v) in PBS. Composition per 100 mL: 2 mL 10% Triton-X-100 solution (Pierce, Rockford, IL), 10 mL 10× PBS, 88 mL distilled H_2O. Adjust pH to 7.0. Make fresh just before use.
5. TDT buffer: 30 m*M* Trizma base, 140 m*M* sodium cacodylate, 1 m*M* cobalt chloride. Available commercially from Gibco Life Technologies (Rockville, MD) with purchase of TDT enzyme.
6. Reaction buffer: 10 µ*M* biotin-16-dUTP (Roche Molecular Biochemicals, Indianapolis, IN), 0.3 U/µL TDT enzyme (Gibco Life Technologies, Rockville, MD) in TDT buffer. Make fresh just before use.
7. TB buffer: 300 m*M* NaCl, 30 m*M* sodium citrate. Composition per 100 mL of 2× stock: 3.5 g NaCl, 1.76 g sodium citrate. Store at room temperature.

2.2. TUNEL Labeling of Tissue Sections for Microscopy

1. Paraformaldehyde: 4% (w/v) in PBS. For 100 mL, heat 90 mL of distilled H_2O until boiling, add 4 g EM grade paraformaldehyde, 100 µL 1 *M* NaOH and stir to

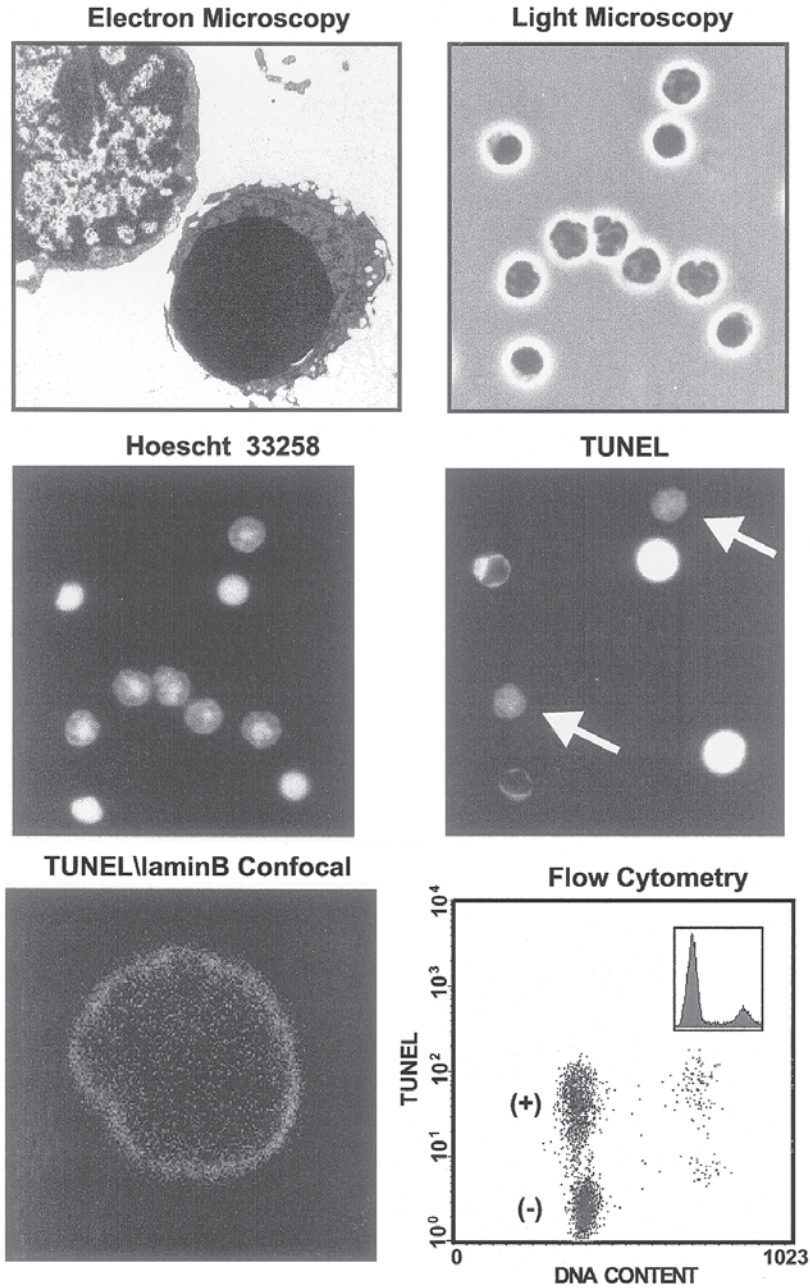

Fig. 4. Examples of the versatility of terminal transferase-based assays. Thymocytes were treated with dexamethasone for 2 h and then prepared for electron, light or fluorescence microscopy or TUNEL-labeled and examined by fluorescence or confocal microscopy and flow cytometry.

dissolve. Cool to room temperature, and add 10 mL of 10× PBS. Adjust pH to 7.0. Make fresh just before use, do not store.
2. Proteinase K buffer: 20 µg/mL Proteinase K (Invitrogen, Bethesda, MD) in 100 m*M* Tris-HCl, pH 8.0 plus 50 m*M* EDTA.

2.3. TUNEL Labeling of Cells for Flow Cytometry

1. 10× PBS: 1.31 *M* NaCl, 50 m*M* Na_2HPO_4, 16 m*M* KH_2PO_4. Composition per liter: 76.5 g NaCl, 7.25 g Na_2HPO_4, 2.12 g KH_2PO_4. Adjust pH to 7.0 after dilution, as pH changes over storage time. Store at room temperature.
2. Paraformaldehyde: 1% (w/v) in PBS. For 100 mL, heat 90 mL of distilled H_2O until boiling, add 1 g EM grade paraformaldehyde, 100 µL 1 *M* NaOH and stir to dissolve. Cool to room temperature, and add 10 mL of 10× PBS. Adjust pH to 7.0. Make fresh just before use, do not store.
3. Reaction buffer: 10 µ*M* biotin-16-dUTP (Roche Molecular Biochemicals, Indianapolis, IN.), 0.3 U/µL TDT enzyme (Gibco life Technologies, Rockville, MD), 0.2 *M* sodium cacodylate pH=6.6 (from 10× stock), 25 m*M* Tris-HCl pH=6.6 (from 10× stock), 2.5 m*M* $CoCl_2$ (from 10× stock), 0.25 mg/mL BSA. Make fresh just before use. All stocks stored at 4°C.
4. 2× TB buffer: 600 m*M* NaCl, 60 m*M* sodium citrate. Composition per 100 mL: 3.5 g NaCl, 1.76 g sodium citrate. Store at room temperature.
5. Staining buffer: 5% (w/v) dry milk powder, 0.1% (v/v) Triton-X-100 in 2× TB buffer. Composition per 5 mL: 50 µL 10% Triton-X-100 solution (Pierce, Rockford, IL), 0.25 g milk, 5 mL 2× TB buffer.

2.4. Determining the Nature of the Ends of the Fragments

1. Nuclear buffer (NB): 15 m*M* Tris-HCl, pH 7.4, 60 m*M* KCl, 15 m*M* NaCl, 1 m*M* EGTA, 2 m*M* EDTA, 0.5 m*M* Spermidine and 0.15 m*M* spermine. Composition per liter: 1.82 g Tris-HCl, 0.38 g EGTA, 0.74 g EDTA, 0.13 g spermidine (trihydrochloride, Sigma, St. Louis, MO), 0.05 g spermine (tetrahydrochloride, Sigma), 4.5 g KCl, 0.9 g NaCl. Adjust pH to 7.4 and store at 4°C.
2. TdT reaction buffer: 25 m*M* Tris-HCl buffer, pH 6.6, 200 m*M* potassium cacodylate, 5 m*M* $CoCl_2$, 0.5 m*M* DTT, 0.25 mg/mL BSA. Composition of a 2× stock per 10 mL: 0.06 g Tris-HCl, 0.67 g potassium cacodylate, 0.024 g $CoCl_2$, 1.54 mg DTT, 5 mg BSA. Adjust pH to 6.6 and store at 4°C.
3. T4 kinase reaction buffer: 50 m*M* glycine-NaOH buffer, pH 9.2, 5 m*M* DTT, 10 m*M* $MgCl_2$. Composition of a 10× stock per 100 mL: 3.75 g Glycine-NaOH, 0.77 g DTT, 2.03 g $MgCl_2$. Adjust pH to 9.2.
4. Lysis buffer: 5 m*M* Tris-HCl, pH 7.5, 5 m*M* EDTA and 0.5% (w/v) Triton X100. Composition per 100 mL: 0.061 g Tris-HCl, 0.19 g EDTA, 0.5 g Triton X 100. Adjust pH to 7.5 and store at 4°C.
5. TE buffer: 10 m*M* Tris-HCl + 1 m*M* EDTA, pH 7.5. Composition per liter: 1.26 g Tris + 0.37 g EDTA. Adjust pH to 7.5 with HCl and store at room temperature.
6. RNase solution: 2 mg/mL RNase A (Sigma, St. Louis, Missouri) Dissolved in 10 m*M* Tris-HCl + 15 m*M* NaCl at pH 7.5. Composition per 5 mL: 6.1 mg Tris,

4.5 mg NaCl, 10 mg RNase A . Adjust pH to 7.5, boil for 15 min and aliqout 0.5 mL into microfuge tubes and store at –20°C.

7. Proteinase K buffer: 10 m*M* Tris-HCl, pH 7.8, 5 m*M* EDTA and 0.5% (w/v) N-Lauroylsarcosine. Composition of a 10× stock per 100 mL: 1.21 g Tris-HCl, 1.86 g EDTA, 5 g N-lauroylsarcosine. Adjust pH to 7.8 and store at room temperature.

3. Methods

3.1. TUNEL Labeling of Cells for Light or Confocal Microscopy

3.1.1. Coating of Coverslips or Slides for Attachment of Suspension Cells or Tissue Sections

In order to stain suspension cells or tissue sections, they must be attached to coverslips or slides, respectively with a suitable bonding agent that maintains them in place and can withstand the multiple wash steps of the staining procedure, but does not interfere chemically with the staining or contribute to background fluorescence. We use poly-L-lysine although commercial bonding agents are also available.

1. Place coverslips or slides in a humid chamber, but do not add water to the chamber at this point (see **Note 1**). Coat with 0.1% poly-L-lysine solution and allow to sit 10 min at room temperature.
2. Drain coverslips and rinse by dipping briefly in a beaker of distilled water. Drain and return to humid chamber. Drain slides, but do not rinse. Air dry with the lid ajar (to promote air circulation, while preventing dust contamination)—typically 10–20 min.
3. Add water to the humid chamber. Allow suspension cells (typically at concentrations of 0.2–1 $\times 10^6$ cells/mL) or tissue sections 10 min to adhere.

3.1.2. TUNEL Labeling of Cells for Light Microscopy

All steps carried out at room temperature unless noted otherwise.

1. Grow cells on glass coverslips, or attach suspension cells to coverslips with poly-L-lysine or a suitable bonding agent. Rinse coverslips by immersing for 30 sec in PBS (*see* **Note 2**).
2. Fix for 5 min in 3% paraformaldehyde in PBS. Rinse twice for 30 sec each time in PBS.
3. Permeabilize for 20 min in 0.2% Triton X-100 in PBS. Rinse 3× for 4 min each time in PBS.
4. Incubate with reaction buffer or control buffer (no enzyme) for 1 h at 37°C in a humid chamber (*see* **Notes 3** and **4**).
5. Stop reaction by transferring to TB buffer for 15 min. Rinse 3× for 4 min each time in PBS.
6. Block for 10 min in PBS + 2% BSA. Rinse 3× for 4 min each time in PBS.
7. Incubate with fluorochrome-linked streptavidin (Jackson Laboratories, 1:200 in PBS) for 30 min in a humid chamber (*see* **Note 5**). Rinse 3× for 4 min each time in PBS.

8. Counterstain for 1 min with 1 µg/mL of Hoechst 33258 in PBS (*see* **Notes 6** and **7**). Mount onto slides, using 16–20 µL of mounting medium per 22 mm x 22 mm coverslip.
9. Examine the cells on a microscope equipped with epifluorescence optics, visualizing the nuclear morphology seen with the Hoechst signal using a UV filter set and the TUNEL label with the appropriate filter set for your fluorochrome (i.e., green for FITC, or red for CY3).

3.1.3. TUNEL Labeling of Tissue Sections for Microscopy

1. Adhere sections to poly-L-lysine coated slides.
2. Fixed samples embedded in paraffin must be deparaffinized and hydrated prior to staining. Samples can be gently heated to remove paraffin; either 10 min at 70°C or 30 min at 60°C should be appropriate. Sections are then hydrated by passing though a series of washes in fresh reagents: twice for 5 min each time in xylene, then twice for 3 min each time in 100% ethanol, then once for 3 min each in 90% ethanol, 80% ethanol 70% ethanol and 50% ethanol (*see* **Note 8**). Slides are then rinsed 3× for 5 min each time in PBS.
3. Fresh frozen tissue sections only should be fixed for 15 min in 4% paraformaldehye then rinsed 3× for 4 min each time in PBS.
4. Drain slides carefully. Permeabilize sections for 15 min in proteinase K buffer in a humid chamber (*see* **Notes 9** and **10**). Rinse three times for 4 min each time in PBS.
5. Incubate sections for 5 min in 3% H_2O_2 to inactivate endogenous peroxidase. Rinse three times for 4 min each time in PBS.
6. Equilibrate sections for 10 min in TdT buffer in a humid chamber. Drain slides carefully.
7. Proceed with staining as for cultured cells, as described in **3.1.2** steps 4–6, using 75 µL of reaction buffer per section.
8. Drain slides carefully. Incubate with ExtrAvidin-Peroxidase (Sigma, 1:20 in PBS) for 30 min in a humid chamber. Rinse 3× for 4 min each time in PBS.
9. Drain slides carefully. Stain with AEC (3-amino-9-ethyl-carbazole, Sigma) or alternate colorimetric substrate for 30 min in a humid chamber. Rinse 3× for 4 min each time in PBS. Drain slides carefully.
10. Mount coverslips onto slides if desired and examine using brightfield optics.

3.2. TUNEL Labeling of Cells for Flow Cytometry

3.2.1 Fixation of Cells

1. Spin down approximately 2×10^6 cells for 4 min at 220 *g* and carefully aspirate medium.
2. Resuspend while vortexing in 1 mL of ice-cold 1% paraformaldehyde in PBS. All vortexing is done at approximately 2/3 maximum on a variable speed vortex. Fix for 15 min on ice. Transfer to Eppendorf tubes during this step.

3. Spin down cells for 1 min at 1500 *g* at 4°C. Carefully aspirate formaldehyde (*see* **Note 11**).
4. Resuspend while vortexing in 200 µL of ice-cold PBS. Add, while vortexing, 1 mL of –20°C 70% ethanol. Samples may be stored in the freezer at this point for several days.

3.2.2. TUNEL Labeling of Cells for Flow Cytometry

All steps carried out at room temperature unless noted otherwise.

1. Spin down fixed cells and aspirate fixative. All spins are done at 1500 *g* for 1 min. Rehydrate for 15 min at room temperature in PBS + 1% BSA (*see* **Notes 12** and **13**). Spin down cells and aspirate wash.
2. Incubate while rocking for 30 min at 37°C in 100 µL reaction buffer or control buffer (no enzyme). Stop the reaction by diluting the sample with 1 mL of 2× TB buffer (*see* **Note 14**). Spin down cells and aspirate buffer.
3. Incubate while rocking for 1 h at room temperature in the dark in 100 µL of staining buffer containing 10 µg/mL of FITC-conjugated streptavidin. Wash by diluting the sample with 1 mL of 2× TB buffer + 0.1% TX-100. Spin down cells and aspirate buffer.
4. Incubate while rocking for 20 min at room temperature in the dark in 1 mL of PBS + 1% BSA, plus 100 µL of 0.1 mg/mL DNase-free RNase in PBS, plus 20 µL of 0.1 mg/mL propidium iodide in PBS. Spin down cells and aspirate buffer.
5. Resuspend in 0.5–1 mL of PBS.
6. Examine the cells on a flow cytometer using an excitation wavelength of 488 nm, and detecting the green TUNEL signal, indicative of the extent of DNA breaks, using a 525 bp filter and the red propidium iodide signal, indicative of total DNA content (cell cycle), using a 610 bp filter. The data is best analyzed on a two-parameter histogram displaying propidium iodide signal (DNA content) on the X axis and TUNEL labeling (DNA breaks) on the Y axis.

3.3. Determining the Nature of the Ends of the Fragments

3.3.1. Processing of Cells and Extraction of DNA

1. Each flask should contain a minimum of 10^7 cells. Remove the medium from each flask and set aside. Add 2 mL of trypsin/ T75 flask (0.15% trypsin in PBS containing 1 m*M* EDTA, pre-warmed to 37°C). After 1–2 min, add the medium back to each flask, remove the total suspension into a conical centrifuge tube and centrifuge at 200 *g* for 5' in a tabletop centrifuge.
2. Resuspend the pellet in 1 mL of nuclear buffer at room temperature (*see* **Note 15**). Centrifuge the suspension at 200 *g* for 5' as above.
3. Resuspend the pellet in 400 µL of lysis buffer in a microfuge tube and place on ice for 15 min.
4. Centrifuge the lysate at maximum speed in a refrigerated microfuge for 15' (*see* **Note 16**).

5. Discard the pellet and and add 40 µL of 2.5 *M* sodium acetate and 800 µL of absolute ethanol. Precipitate at –20°C for at least 12–16 h (*see* **Note 17**).
6. Centrifuge the lysate at maximum speed in a refrigerated microfuge for 15' and resuspend in 400 µL of 70% (v/v) ethanol. Centrifuge again and dissolve the pellet in 400 µL of TE buffer on ice. Add 50 µL of RNase solution and incubate at 65°C for 1 h.
7. Add 25 µL of Proteinase K (Gibco Life Technologies, Rockville, Maryland, 20 mg/mL stock in dH_2O) and 40 µL of 10× Proteinase K buffer to the same reaction tube. Incubate at 37°C for a further 2 h (*see* **Note 18**).
8. To the same tube, add 400 µL of phenol:chloroform-isoamyl alcohol 1:1 (v/v). The chloroform:isoamyl alcohol is a 40:1 (v/v) mixture. Vortex vigorously, centrifuge immediately at maximum speed in microfuge, and remove the upper layer into a new microfuge tube.
9. Precipitate the DNA from this supernatant as in step 5. Resuspend the precipitated DNA in 50 µL of TE buffer in a microfuge tube (*see* **Note 19**).

3.3.2. Labeling of 3'-OH Ends of DNA

1. Prepare a reaction tube by adding 25 µL of 2× TdT reaction buffer, 5 µL of sample from step 9 of **Subheading 3.3.1.**, 4 µL (60 Units) of TdT (Gibco Life Technologies, Rockville, Maryland), 1 µL (5 µci) of alpha [^{32}P]-ATP (NEN Life Science Products, Boston, MA) and water to a final volume of 50 µL.
2. Incubate for 1 h at 37°C.
3. Unincorporated radionucleotides are removed by transferring the reaction mixture to a G-50 Micro column (Amersham Pharmacia Biotech, Piscataway, NJ). The column is centrifuged at 750 g for 2' and the material that passes through the column is collected at the bottom of the tube.
4. Labeled DNA fragments are separated by agarose gel electrophoresis followed by autoradiography.

3.3.3. Labeling of 5'-OH Ends of DNA

1. Prepare a reaction tube by adding 5 µL of 10× T4 kinase reaction buffer, 5 µL of sample from step 9 of **Subheading 3.3.1.**, 5 µL (50 Units) of T4 Kinase (New England BioLabs, Beverly, MA), 1 µL (5µci) of gamma [^{32}P]-ATP (NEN Life Science Products, Boston, MA), 5 µL of phosphate (stock solution is 10 m*M* Na_2HPO_4\10 m*M* NaH_2PO_4 mixed at a ratio of 5:7.5 to give a pH of 9.2) and water to final volume of 50 µL (*see* **Note 20**).
2. Incubate for 1 h at 37°C.
3. Unincorporated radionucleodides are removed using G-50 Micro columns as described in step 3 of **Subheading 3.3.2.**
4. Labeled DNA fragments are separated by agarose gel electrophoresis followed by autoradiography.

4. Notes

1. A humid chamber consists of a small box or large glass Petri dish with a lid into which is placed a filter paper (which can be dampened to provide the source of

humidity) covered by a piece of Parafilm, onto which coverslips can be placed. With the lid on, cells on the coverslips can be left to incubate in small volumes of reagent without drying out.

2. Coverslips are typically placed cell side up in multiwell plates of appropriate size (6-well plates for 22 mm x 22 mm coverslips, 12 well plates for 15 mm round coverslips and 24 well plates for 12 mm round coverslips), and solutions are added from squeeze bottles and removed using a gentle water vacuum, taking care not to disturb the cells. Some suspension cells do not adhere well enough to withstand these manipulations. As a gentler alternative, solutions can be dispensed and coverslips moved from well to well in the plates or from weigh boat to weigh boat. 2–5 mL of solution per sample will be required for staining.
3. For incubations with enzymes, antibodies or steptavidin, which typically use very small volumes, coverslips are turned cell side down over a 25–50 µL drop of solution in a humid chamber. To remove, PBS is added to the drop so that the coverslip floats up and can be picked up without exerting undue shearing force on the cells. Gentle addition of PBS to the parafilm at the edge of the coverslip will result in the liquid being drawn under the glass by capillary action.
4. Gibco supplies a 5× TDT buffer with purchase of the enzyme which is convenient to use and of good quality. Alternatively, TUNEL labeling kits are available. The quality of these kits is reported to be good, but their cost is several times more than the purchase price of the separate components.
5. Prolonging the streptavidin incubation increases the background fluorescence markedly. Typically, attached cells display a noticeable level of background while suspension cells stain very cleanly.
6. DAPI may be used as an alternate counterstain. Incubate cells 3 min in 0.2 µg/mL DAPI, and rinse once in PBS.
7. To label fixed samples using both TUNEL and immunofluorescence staining for an antigen of interest, do the antibody incubations first, then block 20 min in 0.15% gelatin in PBS, rinse and proceed with the TUNEL labeling from step 4.
8. Slides are typically placed in Coplin jars into which solutions have already been dispensed and moved from jar to jar.
9. Slides with tissue sections are incubated cell side up in a humid chamber, with approximately 100 µL of solution covering each section.
10. The length of the incubation in proteinase K may need to be optimized to ensure adequate permeabilization and permit positive signals to be readily detected, while guarding against over-digestion, which loosens sections, leading to their loss in subsequent wash steps.
11. There is a marked loss of cells during the staining procedure. Take extreme care when aspirating solutions above the cell pellet, removing the bulk of the liquid with a GENTLE water vacuum and then the last 100 µL or so with a pipetman.
12. There is a tendency for some cell types to clump, especially when apoptotic. If this is the case, vortexing at each resuspension step usually solves the problem.

13. Cells in suspension are fragile, hence 1% BSA is added to the PBS throughout the protocol to enhance cell recovery.
14. In order to maximize recovery of cells from suspension, salt concentrations in the reaction and stop buffers used for flow cytometry are higher than those required for microscopy. This means that commercial buffer cannot be used.
15. This buffer has a relatively low ionic strength to assist in disruption of the cell and contains EDTA and EGTA to chelate divalent cations, as well as polyamines to bind to chromatin and protect the DNA.
16. We keep a regular microfuge in a cold cabinet for routine spins at 4°C.
17. Sodium acetate\ethanol ensures precipitation of DNA. Dry ice can also be used to lower the temperature and the tube can be left overnight at this stage for convenience.
18. RNase removes contaminating RNA and proteinase K removes residual protein and the RNase.
19. DNA fragments can be radioactively labeled at either the 3'-OH or 5'-OH end using terminal deoxynucleotidyl transferase (TdT) or T4 polynucleotide kinase, respectively. Since the presence of a phosphate group blocks both of these reactions, this approach can be used to determine the nature of the ends of the DNA fragments in apoptotic DNA, e.g. 5'P/3'-OH or 5'-OH/3'-P. This has important implications for the mechanism of action of nucleases involved in DNA fragmentation in apoptosis. To assess this, divide the reaction mixture in two tubes, one for TDT and other for the T4 kinase labeling reaction.
20. Phosphate, at 1 m*M* final concentration, is included in the reaction mixture to fully activate the forward reaction (i.e. phosphorylation of the 5'-OH) and inhibit the reverse reaction (i.e. an exchange reaction that would permit the incorporation of radioactive phosphate molecules onto 5-phosphorylated DNA).

References

1. Lockshin, R. A., Zakeri, Z. and Tilly, J. A. (1998) When Cells die: a comprehensive evaluation of apoptosis and programmed cell death. Wiley-Liss, New York.
2. Wyllie, A. H. (1980) Glucocorticoid induced thymocyte apoptosis is associated with endogenous endonuclease activation. *Nature* **284,** 555–556.
3. Walker, P. R., Pandey, S. and Sikorska, M. (1995) Degradation of chromatin in apoptotic cells *Cell Death and Differentiation* **2,** 93–100.
4. Gavrieli, Y., Sherman, Y. and Ben-Sasson, S. A. (1992) Identification of Programmed Cell Death In Situ via Specific Labeling of Nuclear DNA Fragmentation. *J. Cell Biol.* **119,** 493–501.
5. Mundle, S., Iftikhar, A., Shetty, V., Dameron, S., Wright-Quinones, V., Marcus, B., Loew, J., Gregory, S., Raza, A. (1994) Novel *in situ* double labeling for simultaneous detection of proliferation and apoptosis. *J. Histochem. Cytochem.* **42,** 1533–1537.
6. Alnemri, E. S. and Litwack, G. (1990) Activation of internucleosomal DNA cleavage in human CEM lymphocytes by glucocorticoids and novobiocin. *J. Biol. Chem.* **265,** 17323–17333.

7. MacManus, J. P., Fliss, H., Preston, E., Rashquinha, I. And Tour, U. (1999) Cerebral Ischemia produces laddered DNA fragments distinct from cardiac ischemia and archetypal apoptosis. *J. Cereb. Blood Flow Metab*. **19,** 502–510.
8. Barry, M. A. and Eastman, A. (1993) Identification of deoxyribonuclease II as an endonuclease involved in apoptosis. *Arch. Biochem. Biophys*. **300,** 440–450.
9. MacManus, J. P. and Rashqinha, I. (2001) Ischemic neuronal death is not by classic apoptosis: Are all DNA ladders the same? In "Apoptosis in Health and Disease". Ruffolo, R. R. and Walsh, F., eds. Harwood Academic Publishers, Amsterdam. pp. 33–46.
10. Walker, P. R. Leblance, J. and Sikorska, M (1997) Evidence that DNA fragmentation in apoptosis is initiated and propagated by single-strand breaks. *Cell Death & Differentiation* **4,** 506–515.
11. Li, X., James, W. M., Traganos, F. and Darzynkiewicz, Z. (1995) Application of biotin, digoxigenin or cluoroscein conjugated deoxyribonucleotides to label DNA strand breaks for analysis of cell proliferation and apoptosis using flow cytometry. *Biotech & Histochem.* **70,** 234–242.
12. Chapman, R. S., Chresta, C. M., Herberg, A. A., Beere, H., Heer, S., Whetton, A. D., Hickman, J. A. and Dive, C. (1995) Further characterisation of the *in situ* terminal deoxynucleotidyl transferase (TdT) assay for the flow cytometric analysis of apoptosis in drug resistant and drug sensitive leukemic cells. *Cytometry* **20,** 245–256.
13. Paladichuk, A. (1999) Fishing In A Molecular Sea. *The Scientist* **13,** 1–2 (http://www.the-scientist.com/yr1999/jan/profile1_990118.html).
14. FujiKawa, D. G. (2000) Confusion between neuronal apoptosis and activation of cell death mechanism in acute necrotic insults. *Trends NeuroSci.* **23,** 410–411.
15. Roy, M. and Sapolsky, R. (1999) Neuronal apoptosis in acute necrotic insults: why is this subject such a mess? *Trends NeuroSci.* **22,** 419–422.
16. Gilmore, E. C., Nowakowski, R. S., Caviness, V. S. and Herrup, K. (2000) Cell birth, cell death, cell diversity and DNA breaks: how do they all fit together? *Trends NeuroSci.* **23,** 100–105.
17. Chun, J. (2000) Cell death, DNA breaks and possible rearrangements: an alternative view. *Trends NeuroSci.* **23,** 407–409.
18. Darzynkiewicz, Z. (1993) Detection of DNA strand breaks associated with apoptosis in: Handbook of Flow Cytometry Methods ed: J. Paul Robinson, pub: Wiley-Liss, Inc., New York, N. Y. 206–207.

2

TUNEL Assay

An Overview of Techniques

Deryk T. Loo

1. Introduction

The study of DNA damage holds a wide interest within both basic and applied fields of research. Elucidating the mechanisms involved in the generation of DNA damage, and the consequences of this damage, will have an enormous impact on multiple fields of scientific research and will ultimately lead to a better understanding of human disease. One of the most widely used methods for detecting DNA damage *in situ* is TdT-mediated dUTP-biotin nick end labeling (TUNEL) staining ***(1)***. TUNEL staining was initially described as a method for staining cells that have undergone programmed cell death, or apoptosis, and exhibit the biochemical hallmark of apoptosis—internucleosomal DNA fragmentation ***(2–6)***. TUNEL staining relies on the ability of the enzyme terminal deoxynucleotidyl transferase to incorporate labeled dUTP into free 3'-hydroxyl termini generated by the fragmentation of genomic DNA into low molecular weight double-stranded DNA and high molecular weight single stranded DNA ***(1)***. While TUNEL staining has nearly universally been adopted as the method of choice for detecting apoptosis *in situ*, it should be recognized that TUNEL staining is not limited to the detection of apoptotic cells. TUNEL staining may also be used to detect DNA damage associated with non-apoptotic events such as necrotic cell death induced by exposure to toxic compounds and other insults ***(7)***, and TUNEL staining has also been reported to stain cells undergoing active DNA repair ***(8)***. Therefore TUNEL staining may be considered generally as a method for the detection of DNA damage (DNA fragmentation), and under the appropriate circumstances, more specifically as a method for identifying apoptotic cells.

From: *Methods in Molecular Biology, vol. 203:* In Situ *Detection of DNA Damage: Methods and Protocols*
Edited by: V. V. Didenko

The goal of this chapter is to provide the reader with step-by-step protocols for *in situ* TUNEL staining of nuclear DNA fragmentation in both cultured cells and tissue sections. These basic TUNEL protocols have been used on a wide variety of cell types and tissues with success. Methods for both colorimetric and fluorescent staining of cultured cells and tissues is presented thereby allowing investigators to utilize the TUNEL staining procedure with a minimal investment in laboratory reagents and equipment. In addition, methods to modify and optimize the basic protocols, as well as troubleshooting and control conditions, are provided in the **Notes** and **Troubleshooting** sections.

2. Materials

2.1. Cultured Cells

1. Phosphate-buffered saline (PBS), pH 7.4.
2. 2% buffered formaldehyde: dilute high quality formaldehyde (v/v) in PBS prior to use.
3. 70% ethanol
4. TdT equilibration buffer: 2.5 m*M* Tris-HCl (pH 6.6), 0.2 *M* potassium cacodylate, 2.5 m*M* $CoCl_2$, 0.25 mg/mL bovine serum albumin (BSA). Aliquots may be stored at –20°C for several months.
5. TdT reaction buffer: TdT equilibration buffer containing 0.5 U/µL of TdT enzyme and 40 pmol/µL biotinylated-dUTP (Roche Diagnostics Corp.; Indianapolis, IN). Prepare fresh from stock solutions prior to use.
6. TdT staining buffer: 4× saline-sodium citrate (0.6 *M* NaCl, 60 m*M* sodium citrate), 2.5 µg/mL fluorescein isothiocyanate-conjugated avidin (Amersham Pharmacia Biotech, Inc.; Piscataway, NJ), 0.1% Triton X-100, and 1% BSA. Prepare fresh from stock solutions prior to use.
7. Hoechst 33342 counterstain: 2 µg/mL in PBS (Molecular Probes; Eugene, OR). Stock solution may be stored at 4°C in the dark for several weeks.
8. Vectashield antifade mounting medium (Vector Laboratories, Burlingame, CA).

2.2. Tissue Sections

1. Phosphate-buffered saline (PBS), pH 7.4.
2. 4% buffered formaldehyde: dilute high quality formaldehyde (v/v) in PBS prior to use.
3. 20 µg/mL proteinase K (Roche Diagnostics Corp.). Stock solution may be stored at –20°C for several months.
4. 95, 90, 80, and 70% ethanol in Coplin jars
5. 2% hydrogen peroxide . Prepare fresh from hydrogen peroxide reagent stock prior to use.
6. 2% BSA solution: 2% BSA (w/v) dissolved in PBS and passed through a 0.45 µm filter. Sterile stock solution may be stored at 4°C for several weeks.
7. 2× SSC buffer: 300 m*M* NaCl, 30 m*M* sodium citrate. Stock solution may be stored at room temperature for several months.

8. TdT Equilibration Buffer: 2.5 m*M* Tris-HCl (pH 6.6), 0.2 *M* potassium cacodylate, 2.5 m*M* $CoCl_2$, 0.25 mg/mL BSA. Prepare from stock solutions. Aliquots may be stored at –20°C for several months.
9. TdT Reaction Buffer: TdT Equilibration Buffer containing 0.5 U/µL of TdT enzyme and 40 pmol/µL biotinylated-dUTP (Roche Diagnostics Corp.). Prepare fresh from stock solutions prior to use.
10. Vectastain ABC-peroxidase stock solution (Vector Laboratories, Burlingame, CA).
11. 3,3'-Diaminobenzidine (DAB) staining solution (Vector Laboratories).
12. TdT staining buffer: 4× saline-sodium citrate (0.6 *M* NaCl, 60 m*M* sodium citrate), 2.5 µg/mL fluorescein isothiocyanate-conjugated avidin (Amersham Pharmacia Biotech, Inc.), 0.1% Triton X-100, and 1% BSA. Prepare fresh from stock solutions prior to use.
13. Hematoxylin counterstain (Sigma-Aldrich; St. Louis, MO).
14. Hoechst 33342 counterstain: 2 µg/mL in PBS (Molecular Probes). Stock solution may be stored at 4°C in the dark for several weeks.
15. Vectashield antifade mounting medium (Vector Laboratories).

3. Methods (*see* Notes 1 and 2).

A flowchart of the general protocol for TUNEL staining of cells and tissues is shown in **Fig. 1**. Cells or tissues are fixed with formaldehyde then permeabilized with ethanol to allow penetration of the TUNEL reaction reagents into the cell nucleus. Following fixation and washing, incorporation of biotinylated-dUTP onto the 3' ends of fragmented DNA is carried out in a reaction containing terminal deoxynucleotidyl transferase. Depending on the specific needs of the investigator and/or available equipment, the incorporated biotinylated-dUTP may be visualized by ***(1)*** fluorescence microscopy or FACS analysis following staining with fluorescent-tagged avidin or ***(2)*** light microscopy following staining with horseradish peroxidase-conjugated avidin-biotin complex in conjunction with a colorimetric substrate (*see* **Notes 3** and **4**).

3.1. Cultured Cells

3.1.1. Suspension Cells

1. Collect cells by centrifugation, wash with PBS, and resuspend cells at a concentration of $1–2 \times 10^7$/mL in PBS. Transfer 100 µL of cell suspension to a V-bottomed 96-well plate.
2. Fix cells by addition of 100 µL of 2% formaldehyde in PBS, pH 7.4 *(*see **Note 5**). Incubate on ice for 15 min.
3. Collect cells by centrifugation, wash once with 200 µL of PBS, the postfix with 200 µL of 70% ice-cold ethanol. Cells may be stored in 70% ethanol at –20°C for several days.
4. Collect cells by centrifugation and wash twice with 200 µL PBS.
5. Resuspend cells ($1 \times 10^5 – 5 \times 10^5$) in 50 µL of TdT equilibration buffer. Incubate the cell suspension at 37°C for 10 min with occasional gentle mixing.

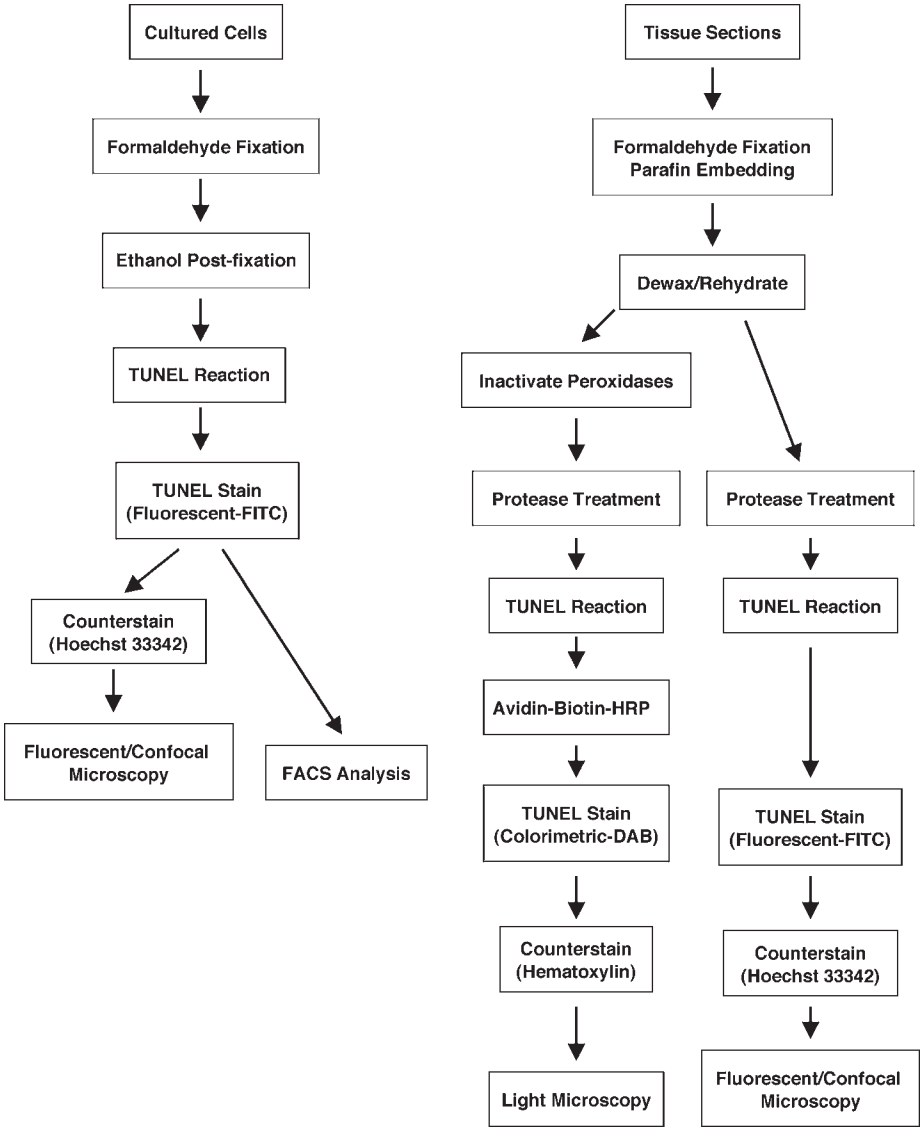

Fig. 1. General flow chart outlining the TUNEL assay protocols described in this chapter for staining cultured cells and tissue sections.

6. Resuspend cells in 50 µL of TdT reaction buffer. Incubate the cell suspension at 37°C for 30 min with occasional gentle mixing.
7. Collect cells by centrifugation and wash with 200 µL PBS.
8. Resuspend the cells in 100 µL of TdT staining buffer. Incubate the cell suspension at room temperature for 30 min in the dark.

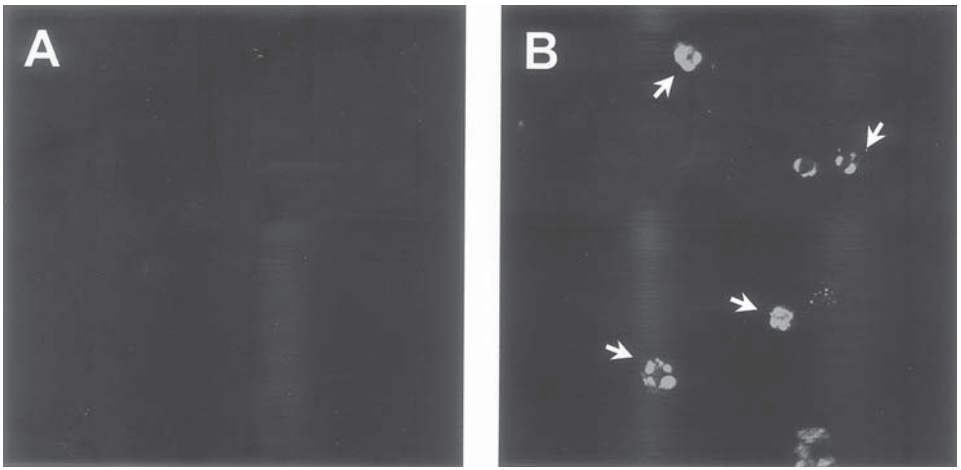

Fig. 2. Confocal micrograph of TUNEL-stained Jurkat T lymphocytes. **(A)** Untreated culture. **(B)** Fas ligand-treated culture undergoing apoptosis. Note the condensed TUNEL-positive chromatin within the nuclei of cells undergoing apoptosis (*see* arrows).

9. Collect cells by centrifugation, wash twice with 200 µL PBS, then resuspend in PBS at 2–8 × 10^6/mL. For fluorescence microscopy attach coverslips using Vectashield antifade mounting medium.
10. Examine cells by fluorescence microscopy, confocal microscopy or flow cytometry. See examples shown in **Fig. 2** and **3**.

3.1.2. Cytospin Preparation of Suspension Cells

TUNEL staining and subsequent fluorescent microscopic or confocal examination of suspension cells may be conveniently carried out on cells attached to glass slides. The cell suspension protocol may be easily modified to accommodate cytospin samples, as described below.

1. Collect cells by centrifugation, wash with PBS, then collect on glass slides pretreated with aqueous 0.01% poly-L-lysine using a cytospin device. Routinely 1 × 10^5 – 5 × 10^5 cells are collected on a single slide.
2. Fix cells by covering with a puddle of 1% formaldehyde in PBS for 15 min.
3. Rinse slides with PBS then transfer to a Coplin jar containing ice-cold 70% ethanol for 1 h. Slides may be stored overnight in 70% ethanol at 4°C.
4. Rinse slides with PBS and pipet 25–50 µL of TdT buffer onto the slides, enough to cover the cells. Incubate the slides in a humidified chamber for 30 min at 37°C. In order to conserve reagents a reduced volume of TdT buffer may be used and carefully covered with a glass coverslip during the incubation. Take care to avoid trapping air bubbles which may lead to staining artifacts.

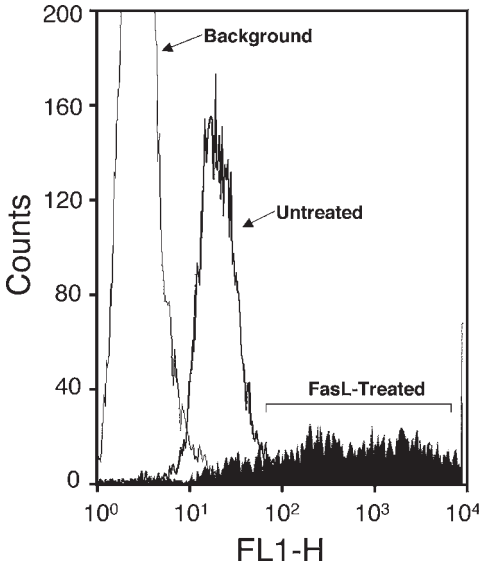

Fig. 3. FACS analysis of TUNEL-stained Jurkat T lymphocytes shown in **Fig. 2**. Note the broad peak of TUNEL-positive fluorescent cells in the FasL-treated sample, indicative of FasL-induced apoptosis.

5. Rinse the slides with PBS then pipet 25–50 µL of TdT staining buffer onto the slides. Incubate for 30 min at room temperature in the dark.
6. Rinse the slides with PBS, air dry, and attach coverslips using Vectashield antifade mounting medium.
7. Examine cells by fluorescence or confocal microscopy.

3.1.3. Adherent Cells

Adherent cells may be cultured on glass chamber slides and processed for TUNEL staining as described above for cytospin-processed cells.

3.2. Tissue Sections

3.2.1. Colorimetric Staining for Light Microscopic Examination

1. Fix tissue samples in 4% formaldehyde in PBS for 24 h and embed in paraffin. Adhere 4–6 µm paraffin sections to glass slides pretreated with 0.01% aqueous solution of poly-L-lysine.
2. Deparaffinize sections by heating the slides for 30 min at 60°C (or 10 min at 70°C) followed by two 5 min incubations in a xylene bath at room temperature in Coplin jars. Rehydrate the tissue samples by transferring the slides through a graded ethanol series: 2 × 3 min 96% ethanol, 1 × 3 min 90% ethanol, 1 × 3 min 80% ethanol, 1 × 3 min 70% ethanol, 1 × 3 min double-distilled water (DDW).

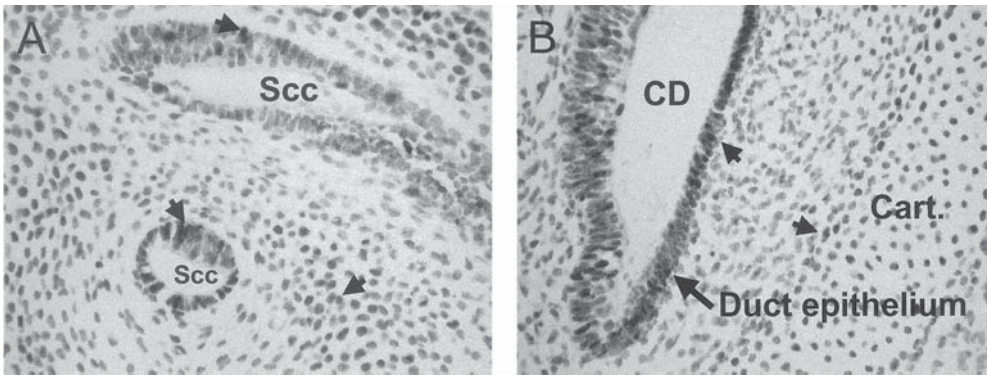

Fig. 4. Micrographs of TUNEL-stained mouse embryo tissue undergoing developmental restructuring (E11–12). **(A)** Semicircular canal area. **(B)** Cochlear duct and primordial cartilage. Apoptotic cells within the duct epithelium and adjacent primordial cartilage exhibiting DNA damage are stained brown (*see* arrowheads). Sections are counter-stained with hematoxylin (blue staining) to identify background TUNEL-negative cells and associated morphology.

3. Carefully blot away excess water and pipet 20 µg/mL proteinase K solution to cover sections. Incubate 15 min at room temperature.
4. Following proteinase K treatment, wash slides 3 × 5 min with DDW.
5. Inactivate endogenous peroxidases by covering sections with 2% hydrogen peroxide for 5 min at room temperature. Wash slides 3 × 5 min with DDW.
6. Carefully blot away excess water then cover sections with TdT equilibration buffer for 10 min at room temperature.
7. Remove TdT equilibration buffer and cover sections with TdT reaction buffer. Incubate slides in a humidified chamber for 30 min at 37°C. In order to conserve reagents a reduced volume of TdT buffer may be carefully covered with a glass coverslip during the incubation. Take care to avoid trapping air bubbles which may lead to staining artifacts.
8. Stop reaction by incubating slides 2 × 10 min in 2×SSC.
9. Rinse slides in PBS then block nonspecific binding by covering tissue sections with 2% BSA solution for 30–60 min at room temperature.
10. Wash slides 2 × 5 min in PBS then incubate in Vectastain ABC-peroxidase solution for 1 h at 37°C.
11. Wash slides 2 × 5 min in PBS then stain with DAB staining solution at room temperature. Monitor color development until desired level of staining is achieved (typically 10–60 min). Stop the reaction by incubating slides in DDW.
12. Lightly counter-stain tissue sections with hematoxylin stain.
13. Cover tissue sections with coverslips using Aqua-Poly/Mount mounting medium.
14. Observe sections under light microscopy. See examples shown in **Fig. 4**.

3.2.2. Fluorescent Staining

1. Follow steps 1–9 outlined above for the colorimetric staining of tissue sections (**Subheading 3.2.1**), omitting the hydrogen peroxide inactivation step.
2. Wash slides 2 × 5 min in PBS then cover tissue sections with TdT staining buffer. Incubate slides at room temperature for 30 min in the dark.
3. Wash slides 2 × 5 min in PBS.
4. Lightly counter-stain sections with hematoxylin, Hoechst 33342 or other appropriate counterstain (*see* **Note 6**).
5. Wash slides with PBS, air dry, and attach coverslips using Vectashield antifade mounting medium.
6. Examine tissue sections by fluorescence or confocal microscopy.

4. Notes

1. The protocols outlined here represent one method, together with several variations, that have been used successfully for TUNEL staining of a broad variety of cultured cells and tissues. However, specific cell types and tissues may require modification or optimization of the staining conditions to obtain successful results. Two of the steps that often require optimization are formaldehyde fixation and PK treatment. A lack of observed TUNEL staining in the positive control sample may result from over-fixation ***(9)***. This result may be remedied by using shorter fixation times and/or reducing the formaldehyde concentration. Additionally, over-treatment with PK may cause a loss of TUNEL staining in the positive control samples. Positive staining in the negative control sample may also result from inadequate inactivation of endogenous peroxidase activity (colorimetric detection), or non-specific binding of the FITC-conjugated avidin reagent (fluorescent detection). In the case of colorimetric detection ensure that the H_2O_2 reagent is fresh. Increasing the H_2O_2 concentration to 5% may also help to reduce the endogenous peroxidase activity. In the case of fluorescent detection, increasing the BSA concentration to 2–5% in the TdT staining buffer and/or reducing the FITC-conjugated avidin concentration may reduce the background fluorescence. It is important to optimize the staining conditions empirically with the control samples prior to examining and interpreting data from valuable experimental samples.
2. While this chapter provide the investigator with a step-by-step method for TUNEL staining that requires a modest amount of reagents, it should be noted that several TUNEL staining kits are now commercially available (R&D Systems, Inc., Minneapolis, MN; Roche Diagnostics Corp., Indianapolis, IN). Commercial kits may be appropriate under certain circumstances, such as for use by the casual or infrequent user or for use in a controlled clinical setting.
3. It is advisable to include control samples with each staining experiment to facilitate interpretation of the staining results. As a positive control, treat cells and tissues with DNAse I (1 µg/mL in 30 m*M* Tris-HCl (pH 7.2), 140 m*M* potassium cacodylate, 4 m*M* $MgCl_2$, 0.1 m*M* DTT) for 10 min at room temperature. Follow-

ing DNase I treatment, wash samples 3 × 2 min in DDW then proceed with TUNEL staining. As a negative control, omit the TdT enzyme from the TdT reaction buffer.

4. Immunohistochemical staining for cell surface or intracellular antigens may be performed simultaneously with TUNEL staining using colorimetric, fluorescent, or a combination of colorimetric and fluorescent detection systems. Careful selection of the detecting reagents will enable simultaneous two color staining of cells and tissue sections that can be observed microscopically, and in the case of suspension cell cultures also by FACS analysis. The reader is encouraged to consult the primary literature to obtain further information on specific systems of interest.
5. Formaldehyde-fixed cell culture samples have been successfully stored in 70% ethanol at –20°C for several weeks prior to TUNEL staining. The suitability of prolonged storage should be determined empirically for the individual culture system employed.
6. Hoechst 33342 binds to DNA and serves as a nuclear stain. Combining Hoechst 33342 staining with TUNEL staining allows one to compare TUNEL-positive nuclei with surrounding normal nuclei and observe changes in nuclear size and morphology. Hoechst 33342 also serves as a counterstain, allowing for the visualization of anatomical structures in both TUNEL-positive and TUNEL-negative cells in cultured cells and tissues ***(9)***.

Acknowledgments

The author wishes to thank Dr. Donna Dambach for providing the image of the TUNEL-stained tissue sections, Derek Hewgill for expert assistance with confocal microscopy and FACS analysis, Jill Rillema for critical discussion, and Fiona Apple.

References

1. Gavrieli, Y., Sherman, Y., and Ben-Sasson, S. A. (1992) Identification of programmed cell death *in situ* via specific labeling of nuclear DNA fragmentation. *J. Cell Biol.* **119,** 493–501.
2. Arends, M. J., Morris, R. G., and Wyllie, A. H. (1990) Apoptosis: the role of the endonuclease. *Am. J. Pathol.* **136,** 593–608.
3. Bortner, C. D., Oldenburg, N. B. E., and Cidlowski, J. A. (1995) The role of DNA fragmentation in apoptosis. *Trends Cell Biol.* **5,** 21–26.
4. Kerr, J. F. R., Wyllie, A. H., and Currie, A. R. (1972) Apoptosis: A basic biological phenomenon with wide-ranging implications in tissue kinetics. *Br. J. Cancer* **26,** 239–257.
5. Loo, D. T. and Rillema, J. R. (1998) Measurement of cell death, in *Methods in Cell Biol.* (Mather, J. P. and Barnes, D., ed.), Academic Press, San Diego, CA, vol. 57, pp. 251–264.
6. Wyllie, A. H. (1980) Cell death: The significance of apoptosis, in *Int. Rev. Cytol.*, (Bourne, G. H., Danielli, F. J., and Jeon, K. W., eds.) Academic Press, New York, NY, vol. **68,** pp. 251–306.

7. Ansari, B., Coates, P. J. Greenstein, B. D., and Hall, P. A. (1993) *In situ* end-labeling detects DNA strand breaks in apoptosis and other physiological and pathological states. *J. Pathol.* **170,** 1–8.
8. Kanoh, M., Takemura, G., Misao, J., Hayakawa, Y., Aoyama, T., Nishigaki, K., Noda, T., Fujiwara, T., Fukuda, K., Minatoguchi, S., and Fujiwara, H. (1999) Significance of myocytes with positive DNA *in situ* nick end-labeling (TUNEL) in hearts with dilated cardiomyopathy. Not apoptosis but DNA repair. *Circulation* **99,** 2757–2764.
9. Whiteside, G., Gougnon, N., Hunt, S. P., and Munglani, R. (1998) An improved method for detection of apoptosis in tissue sections and cell culture, using the TUNEL technique combined with Hoechst stain. *Brain Res. Prot.* **2,** 160–164.
10. Kishimoto, H., Surh, C. D., and Sprent, J. (1995) Upregulation of surface markers on dying thymocytes. *J. Exp. Med.* **181,** 649–655.

3

Electron Microscopic Detection of DNA Damage Labeled by TUNEL

Antonio Migheli

1. Introduction

1.1. DNA Damage, Apoptosis, and Necrosis

A number of exogenous and endogenous toxic agents may damage DNA, leading to genomic instability and transcriptional infidelity. Genetic or acquired defects in DNA repair mechanisms also contribute to exacerbate DNA damage. Progressive accumulation of DNA injury may alter the genetic control of cell proliferation and cause cancer. Alternatively, increased cell death may be a more likely consequence if DNA damage affects postmitotic cells, e.g., neurons ***(1)***. As a matter of fact, DNA damage is suspected to play a major role in the neuronal death that characterizes brain ischemia ***(2)*** and various neurodegenerative diseases ***(1,3)***.

At least two types of cell death are the consequence of extensive and irreversible DNA damage, i.e., apoptosis and necrosis. Apoptosis is recognized as a major mechanism of programmed cell death (PCD) ***(4)***. Morphologic criteria for apoptosis include cell shrinkage, blebbing of the cell surface, chromatin condensation and margination, nuclear pyknosis and late fragmentation into apoptotic bodies, with remarkable preservation of the integrity of cell membranes and organelles. All of these changes are due to cleavage of various cytoplasmic and nuclear substrates by caspases, a family of cysteine proteases that exist as latent zymogens and activate themselves in a cascade fashion, following apoptotic stimuli ***(5)***. A major biochemical change of apoptosis is the fragmentation of DNA into oligonucleosomal fragments multiples of 180–200 base pairs, that are visualized by agarose gel electrophoresis as a "ladder." Several DNases appear to induce apoptotic DNA fragmentation, including a caspase-activated DNase (CAD) ***(6)***.

From: *Methods in Molecular Biology, vol. 203:* In Situ *Detection of DNA Damage: Methods and Protocols*
Edited by: V. V. Didenko

DNA damage also occurs in necrosis. At variance with apoptosis, necrosis is not a programmed event, is characterized morphologically by early swelling, disintegration of membranes and organelles and absence of chromatin condensation ***(7)***, and is due to activation of calpains rather than caspases ***(8)***. Although early reports indicated that necrotic DNA fragmentation occurs in a "random" fashion, further studies showed that oligonucleosomal fragmentation may be also a feature of necrosis. Indeed, the DNA damage that occurs in necrosis is not easily distinguishable from that of apoptosis, as 3'-OH and 5'-OH ends of DNA strand breaks are generated in both cases, although with a different ratio ***(9)***. Furthermore, double strand breaks with single-base 3' overhangs appear to be specific for apoptosis but not for necrosis ***(10)***.

1.2. DNA Damage Detection In Situ: *Potentials and Pitfalls*

The development of techniques for *in situ* end-labeling (ISEL) of fragmented DNA has allowed the recognition of DNA damage in single cells both in vitro and in vivo. ISEL techniques reveal the presence of DNA breaks through the exogenous application of labeled nucleotides and incorporating enzymes such as DNA polymerase and terminal deoxynucleotidyl transferase (TdT). In the TUNEL assay ***(11)***, that employs TdT, only 3'-OH ends are labeled; on the contrary, both 3'-OH and 5'-OH ends are labeled with the DNA polymerase *in situ* nick translation (ISNT) assay ***(12,13)***. Comparative in vitro ***(14)*** and in vivo ***(15)*** studies have shown that TUNEL has a greater labeling capacity than ISNT, possibly because of differences in enzyme kinetics, TdT being faster than DNA polymerase.

While the various ISEL assays had been originally developed to detect apoptotic DNA breaks and help recognizing apoptotic cells in tissues, subsequent studies showed that both ISNT and TUNEL may detect necrosis-related DNA fragmentation as well ***(16,17)***. The ISNT assay might be more specific for necrosis and the TUNEL assay for apoptosis ***(18,19)***; however, the fact that the two death processes often occur simultaneously contributes to the difficulty in assessing the nature of labeled cells ***(9)***.

In addition to apoptotic and necrotic DNA fragmentation, ISEL techniques may reveal DNA breaks that are not necessarily related to actual death of the labeled cell. Examples of such labeling include DNA damage due to reactive oxygen species, radiation, metals and toxins ***(20–24)***. This finding has allowed to demonstrate the occurrence of DNA damage even in disease conditions that had not been previously linked to genotoxicity, such as Alzheimer's disease ***(3)***. In such events, labeled cells do not typically display a clear-cut apoptotic or necrotic morphology. On the other hand, it is often difficult to establish whether the labeling refers or not to a death phenotype by examining the labeled cell at the light microscopic level only.

Finally, there are a number of artifactual situations in which DNA breaks may occur and be revealed by ISEL, in the absence of a specific pathologic event. These include postmortem autolysis ***(15)***, delay in fixation ***(15,25)***, improper fixation ***(25–27)***, and excessive section pretreatment with proteinase K or microwave heating, both of which are often necessary steps to allow the access of the incorporating enzymes to the DNA breaks. In all of these cases, ISEL will produce a significant degree of nuclear (and sometimes cytoplasmic) non-specific labeling.

1.3. Why an Ultrastructural Assay for DNA Damage Detection?

It should be clear from the preceding paragraph that establishing the significance of DNA damage as revealed by ISEL may not be a trivial task, especially if the analysis is done at the light microscopic level, where the morphologic detail of labeled cells has often a poor resolution. These difficulties may be overcome if the ISEL assay is performed at the electron microscopic (EM) level. An EM-ISEL assay offers several advantages:

1. As a genotoxicity assay, it allows the visualization of DNA damage induced e.g., by free radicals or by radiation, metals, toxins etc.
2. As a cell death assay, by showing at the same time the nuclear labeling of DNA breaks and the overall ultrastructural morphology of the cell, it allows to definitely establish whether the labeling affects an apoptotic or a necrotic cell. Furthermore, it helps identifying other types of non-apoptotic PCD, such as cytoplasmic and autophagic PCD ***(28)***, in which DNA fragmentation is absent ***(29)***.

Several papers on the use of EM-ISEL assays have now appeared. Examples of application of this technique include: apoptotic and nonapoptotic cell death in neurodegenerative diseases ***(29,30)***; activation of DNA repair mechanisms in dilated cardiomyopathy ***(31)***; metal-induced genotoxicity ***(22)***. The EM-ISEL assay described in the present chapter ***(30)*** is both simple and advantageous, in that it has been developed on tissues routinely processed for electron microscopy. For this reason, retrospective studies on archival material can be easily performed.

2. Materials

2.1. Tissues

Tissue blocks are prepared according to routine electron microscopy procedures, i.e. fixation in 2.5% glutaraldehyde for 1–3 h, postfixation in 1–2% osmium for 1–2 h and embedding in an epoxy resin (*see* **Notes 1–3**). After selecting the area of interest on toluidine blue-stained semithin sections, thin sections are cut with an ultramicrotome, collected on Formvar-coated nickel grids and stored until use.

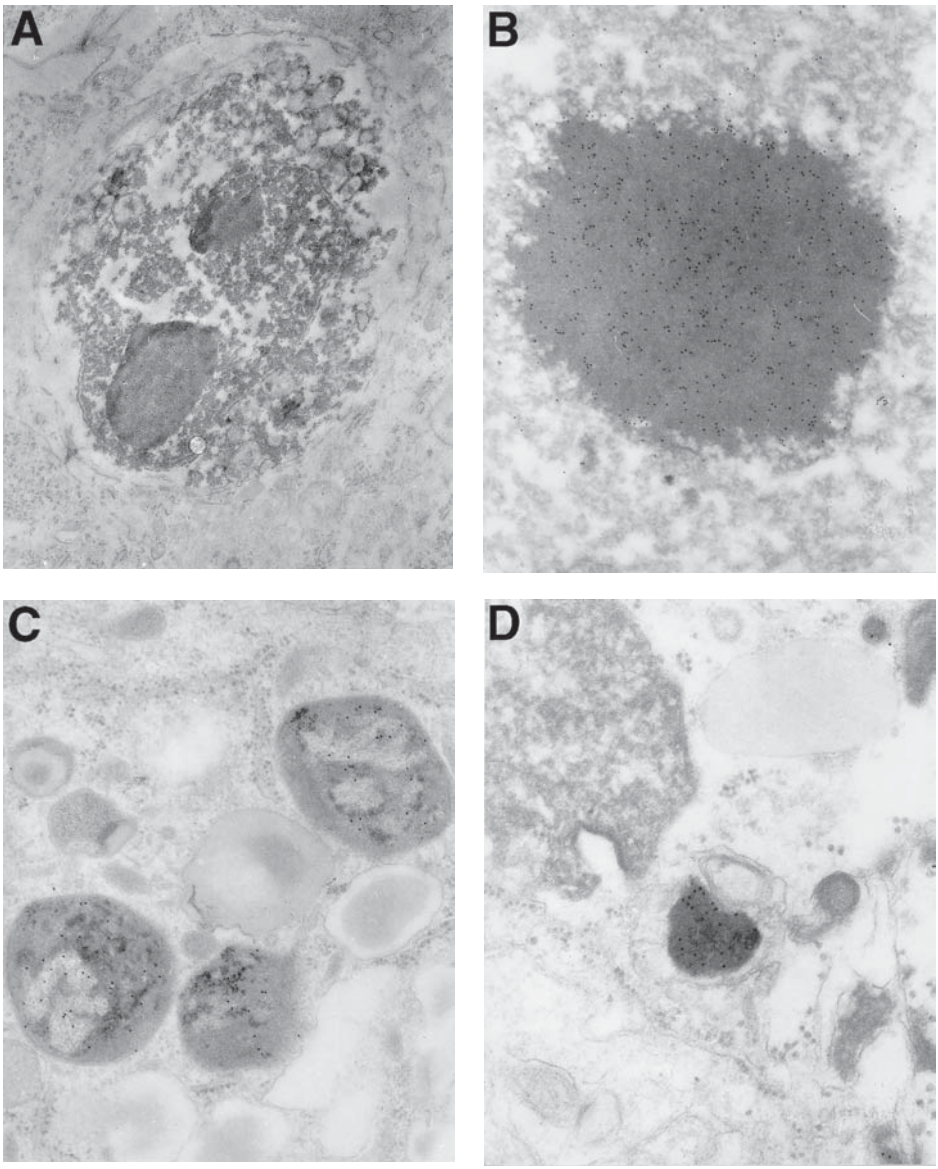

Fig. 1. Weaver mouse cerebellum. **(A)** A granule cell undergoing an advanced stage of apoptotic cell death shows detachment from the surrounding neuropil, integrity of the plasma membrane and condensation of both nucleus and cytoplasm. Diffuse gold labeling can be seen over the two large nuclear fragments. Original magnification 7,000×. **(B)** Intense gold labeling in an apoptotic nucleus. Original magnification 20,000×. **(C)** Three apoptotic bodies within a phagocyte show discrete labeling of their nuclear component. Note complete lack of labeling of the other organelles.

2.2. Reagents

All solutions are prepared using double distilled water (DDW).

1. Terminal deoxynucleotidyl transferase (TdT) is available from Boehringer (Mannheim, Germany) as 50 U/µL solution and is stored at –20°C.
2. Digoxigenin-11-dUTP is available from Boehringer as 1 n*M*/µL solution and is stored at –20°C (*see* **Note 4**).
3. Anti-digoxigenin goat immunoglobulins coupled with 10 nm colloidal gold are available from BioCell (Cardiff, UK) and are stored at 4°C (*see* **Note 4**).
4. TdT buffer: 25 m*M* Tris-HCl, 200 m*M* potassium cacodylate, 2.5 m*M* cobalt chloride, pH 6.6. This buffer is prepared using two 2× stock solutions: (A) 50 m*M* Tris-HCl, 0.4 *M* potassium cacodylate, pH 6.6; (B) 5 m*M* cobalt chloride in DDW. After autoclaving, the two stock solutions can be stored at room temperature. Prepare the TdT buffer by mixing equal volumes of A and B just before use.
5. 2× saline sodium citrate (SSC) solution: 300 m*M* sodium chloride, 30 m*M* sodium citrate, pH 7.0. Prepare a 20× stock solution: 3 *M* sodium chloride, 0.3 *M* sodium citrate, pH 7.0. After autoclaving, the stock solution can be kept at room temperature. Make a 2× solution with DDW just before use.
6. Tris buffered saline (TBS). Prepare a 10× stock solution: 6.055 g Tris base, 40.91 g NaCl in 500 mL DDW, pH 7.4. After autoclaving, the stock solution can be kept at room temperature. Make a 1× solution with DDW just before use.
7. TBS-BSA buffer. Dissolve 100 mg bovine serum albumin, fraction V, in 10 mL TBS, pH 8.2. Store at 4°C.
8. 2% uranyl acetate in DDW. Prepare fresh before use and keep in the dark.

2.3. Other Requirements

1. Anti-static tweezers are needed to handle nickel grids.
2. Incubation chamber: to create a humid chamber, a convenient way is to use a glass Petri dish. On the bottom, place a wet round filter paper and apply a square sheet of Parafilm™ over the filter. Prepare two such chambers.
3. Oven: set at 37°C and used for the TdT reaction.

3. Methods

1. Collect silver-gold thin sections on Formvar coated nickel grids and store until use.
2. Place each grid over a 30 µL drop of TdT buffer inside the first humid chamber.
3. While grids are floating, prepare the labeling solution in an Eppendorf tube (keep all tubes on ice, as TdT can be easily degraded) as follows: 1 U of TdT, 1 n*M* digoxigenin-dUTP in 100 µL of TdT buffer.
4. Divide the labeling solution into 20 µL drops in the first humid chamber and place the chamber in the oven set at 37°C for 10 min.

Fig. 1. *(continued)* Original magnification 20,000×. **(D)** A small apoptotic body shows strong gold labeling. A normal nucleus (upper left) is completely unlabeled. Original magnification 24,000×.

5. Quickly transfer grids from the drops of TdT buffer to the drops of labeling solution and keep the chamber inside the oven at 37°C for 10 min (*see* **Notes 5–6**).
6. While grids are being incubated in the oven, prepare two series of 50 µL drops of 2× SSC and one series of 50 µL drops of TBS in a second humid chamber, and keep it at room temperature.
7. At the end of the incubation in the labeling solution, remove the grids from the first chamber and rinse them on the 50 µL drops of 2× SSC in the second chamber (two changes, 5 min each).
8. Place each grid on the 50 µL drop of TBS for 5 min.
9. While grids are being rinsed in TBS, prepare a 1/30 solution of colloidal gold-coupled anti-digoxigenin goat immunoglobulins in TBS-BSA, pH 8.2, and divide it into 50 µL drops in the second humid chamber.
10. Incubate grids in the anti-digoxigenin antiserum overnight at 4°C.
11. The following day, rinse extensively the grids in several drops of TBS and DDW.
12. Stain grids with 2% uranyl acetate for 20 min.

4. Notes

1. Best results are obtained with tissues that have been routinely processed for electron microscopy. We have found that fixation in glutaraldehyde-osmium gives more reproducible results compared to glutaraldehyde alone, or when paraformaldehyde is used instead of glutaraldehyde. Tissues can be fixed both by immersion and by perfusion (e.g., laboratory animals). Sections of biopsy material retrieved from paraffin blocks and re-embedded in epoxy resin have been also found to be suitable (unpublished observations).
2. Two types of epoxy resins have been studied, i.e., Epon 812 and Araldite, without any appreciable difference.
3. As an alternative to epoxy resins, acrylic resins such as LR White and LR Gold can be used ***(30)***. However, the morphologic detail is greatly decreased.
4. Recently, fluorescein-12-dUTP labeled nucleotides (Boehringer) and 10 nm gold-conjugated anti-fluorescein immunoglobulins (BioCell) have been used instead of digoxigenin-11-dUTP and anti-digoxigenin antibodies, with an equivalent intensity of reaction (unpublished observations).
5. No etching of the resin is needed prior to staining. In fact, etching with oxidizing agents (10% H_2O_2 or 10% $NaIO_4$) resulted in weak to absent staining, suggesting that the 3'-OH ends of DNA breaks are altered by the oxidizing agents and are no longer recognized by TdT ***(30)***.
6. The concentration of TdT and the length of the incubation step in the labeling solution indicated in the protocol are those that have given the best results in most cases. Higher TdT concentrations, or longer incubation times, generally result in a progressive increase in the background staining of nuclei of normal cells. The reason for the latter finding is unclear. DNA nicks might be produced by the cutting procedure itself and be revealed under favorable staining conditions. Alternatively, the labeling might refer to sites of active gene transcription, that are located in the condensed chromatin and have been demonstrated using a

TdT-based approach ***(32)***. The latter finding, however, usually require DNase I pretreatment of sections. However, since differences in the labeling intensity may occur with different tissues, it is strongly suggested that a series of grids be initially prepared, varying both TdT concentration and the incubation time in the labeling mix.

Acknowledgments

The financial support of Fondazione Cavalieri Ottolenghi is gratefully acknowledged.

References

1. Rolig, R. L. and McKinnon, P. J. (2000) Linking DNA damage and neurodegeneration. *Trends Neurosci*. **23,** 417–424.
2. Love, S. (1999) Oxidative stress in brain ischemia. *Brain Pathol*. **9,** 119–131.
3. De la Monte, S. M., Luong, T., Neely, T. R., Robinson, D. and Wands, J. R. (2000) Mitochondrial DNA damage as a mechanism of cell loss in Alzheimer's disease. *Lab. Invest*. **80,** 1323–1335.
4. Kerr, J. F. R., Wyllie, A. H. and Currie, A. R. (1972) Apoptosis: A basic biological phenomenon with wide-ranging implications in tissue kinetics. *Br. J. Cancer* **26,** 239–257.
5. Budihardjo, I., Oliver, H., Lutter, M., Luo, X. and Wang, X. (1999) Biochemical pathways of caspase activation during apoptosis. *Annu. Rev. Cell Dev. Biol.* **15,** 269–290.
6. Enari, M., Sakahira, H., Yokoyama, H., Okawa, K. and Nagata, S. (1998) A caspase-activated DNase that degrades DNA during apoptosis, and its inhibitor ICAD. *Nature* **391,** 43–50.
7. Majno, G. and Joris, I. (1995) Apoptosis, oncosis, and necrosis: an overview of cell death. *Am. J. Pathol.* **146,** 3–15.
8. Wang, K. K. (2000) Calpain and caspase: can you tell the difference? *Trends Neurosci*. **23,** 20–26.
9. Hayashi, R., Ito, Y., Matsumoto, K., Fujino, Y. and Otsuki, Y. (1998) Quantitative differentiation of both free 3'-OH and 5'-OH DNA ends between heat-induced apoptosis and necrosis. *J. Histochem. Cytochem.* **46,** 1051–1059.
10. Didenko, V. V. and Hornsby, P. J. (1996) Presence of double-strand breaks with single-base 3' overhangs in cells undergoing apoptosis but not necrosis. *J. Cell Biol*. **135,** 1369–1376.
11. Gavrieli, Y., Sherman, Y. and Ben-Sasson, S. A. (1992) Identification of programmed cell death in situ via specific labeling of nuclear DNA fragmentation. *J. Cell Biol.* **119,** 493–501.
12. Gold, R., Schmied, M., Rothe, G., Zischler, H., Breitschopf, H., Wekerle, H. and Lassmann, H. (1993) Detection of DNA fragmentation in apoptosis: application of an in situ nick translation to cell culture systems and tissue sections. *J. Histochem. Cytochem.* **41,** 1023–1030.

13. Wijsman, J. H., Jonker, R. R., Keijzer, R., Van de Velde, C. J. H., Cornelisse, C. J. and Van Dierendonck, J. H. (1993) A new method to detect apoptosis in paraffin sections: in situ end-labeling of fragmented DNA. *J. Histochem. Cytochem.* **41,** 7–12.
14. Gorczyca, W., Gong, J. and Darzynkiewicz, Z. (1993) Detection of DNA strand breaks in individual apoptotic cells by the in situ terminal deoxynucleotidyl transferase and nick translation assays. *Cancer Res.* **53,** 1945–1951
15. Migheli, A., Cavalla, P., Marino, S. and Schiffer, D. (1994) A study of apoptosis in normal and pathologic nervous tissue after in situ end-labeling of fragmented DNA. *J. Neuropathol. Exp. Neurol.* **53,** 606–616.
16. Grasl-Kraupp, B., Ruttkay-Nedecky, B., Koudelka, H., Bukowska, K., Bursch, W. and Schulte-Hermann, R. (1995) In situ detection of fragmented DNA (TUNEL assay) fails to discriminate among apoptosis, necrosis and autolytic cell death: a cautionary note. *Hepatology* **21,** 1465–1468.
17. van Lookeren Campagne, M., Lucassen, P. J., Vermeulen, J. P. and Balasz, R. (1995) NMDA and kainate induce internucleosomal DNA cleavage associated with both apoptotic and necrotic cell death in the neonatal rat brain. *Eur. J. Neurosci.* **7,** 1627–1640.
18. Mundle, S., Gao, X. Z., Khan, S., Gregory, S. A., Preisler, H. D. and Raza, A. (1995) Two *in situ* labeling techniques reveal different patterns of DNA fragmentation during spontaneous apoptosis *in vivo* and induced apoptosis *in vitro*. *Anticancer Res.* **15,** 1895–1904.
19. Gold, R., Schmied, M., Giegerich, G., Breitschopf, H., Hartung, H. P., Toyka, K. V. and Lassmann, H. (1994) Differentiation between cellular apoptosis and necrosis by the combined use of in situ tailing and nick translation techniques. *Lab. Invest.* **71,** 219–225.
20. Lopes, S., Jurisicova, A., Sun, J. G. and Casper, R. F. (1998) Reactive oxygen species: potential cause for DNA fragmentation in human spermatozoa. *Hum. Reprod*. **13,** 896–900.
21. Coates, P. J., Save, V., Ansari, B. and Hall, P. A. (1995) Demonstration of DNA damage/repair in individual cells using in situ end labeling: association of p53 with sites of DNA damage. *J. Pathol*. **176,** 19–26.
22. Assad, M., Lemieux, N. and Rivard, C. H. (1997) Immunogold electron microscopy in situ end-labeling (EM-ISEL): assay for biomaterial DNA damage detection. *Biomed. Mater. Eng*. **7,** 391–400.
23. Brooks, P. J. (2000) Brain atrophy and neuronal loss in alcoholism: a role for DNA damage? *Neurochem. Int*. **37,** 403–412.
24. Kisby, G. E., Kabel, H., Hugon, J. and Spencer, P. (1999) Damage and repair of nerve cell DNA in toxic stress. *Drug Metab. Rev*. **31,** 589–618.
25. Tateyama, H., Tada, T., Hattori, H., Murase, T., Li, W. X. and Eimoto, T. (1998) Effects of prefixation and fixation times on apoptosis detection by in situ end-labeling of fragmented DNA. *Arch. Pathol. Lab. Med.* **122,** 252–255.
26. Schallock, K., Schulz-Schaeffer, W. J., Giese, A. and Kretzschmar, H. A. (1997) Postmortem delay and temperature conditions affect the in situ end-labeling (ISEL) assay in brain tissue of mice. *Clin. Neuropathol.* **16,** 133–136.

27. Labat-Moleur, F., Guillermet, C., Lorimier, P., Robert, C., Lantuejoul, S., Brambilla, E. and Negoescu, A. (1998) TUNEL apoptotic cell detection in tissue sections: critical evaluation and improvement. *J. Histochem. Cytochem.* **46,** 327–334.
28. Clarke, P. G. H. (1990) Developmental cell death: morphological diversity and multiple mechanisms. *Anat. Embryol.* **181,** 195–213.
29. Migheli, A., Piva, R., Wei, J., Attanasio, A., Casolino, S., Dlouhy, S. R., Bayer, S. A. and Ghetti, B. (1997) Diverse cell death pathways result from a single missense mutation in weaver mouse. *Am. J. Pathol.* **151,** 1629–1638.
30. Migheli, A., Attanasio, A. and Schiffer, D. (1995) Ultrastructural detection of DNA strand breaks in apoptotic neural cells by in situ end-labeling techniques. *J. Pathol.* **176,** 27–35.
31. Kanoh, M., Takemura, G., Misao, J., Hayakawa, Y., Aoyama, T., Nishigaki, K., Noda, T., Fujiwara, T., Fukuda, K., Minatoguchi, S. and Fujiwara, H. (1999) Significance of myocytes with positive DNA in situ nick end-labeling (TUNEL) in hearts with dilated cardiomyopathy-Not apoptosis but DNA repair. *Circulation* **99,** 2757–2764.
32. Thiry, M. (1991) In situ nick translation at the electron microscopic level: a tool for studying the location of DNAse I-sensitive regions within the cell. *J. Histochem. Cytochem*. **39,** 871–874.

4

Quantitative Differentiation of Both Free 3' OH and 5' OH DNA Ends Using Terminal Transferase-Based Labeling Combined with Transmission Electron Microscopy

Yoshinori Otsuki and Yuko Ito

1. Introduction

The initial concept of apoptosis was proposed by Kerr et al. (1972) ***(1)*** and was based on characteristic morphological criteria. Transmission electron microscopy (TEM) allows visualization of fine details of cellular morphology and is one of the most reliable methods for detecting of apoptotic cells. However, TEM has a number of limitations as an apoptosis detection method. First, apoptotic cells detected by TEM are those at the terminal stage of apoptosis. Therefore, TEM cannot identify apoptotic cells entering early stages of apoptotic process. For this purpose, investigators prefer to use fluorescent probes such as a combination of Hoechst 33342 and propidium iodide ***(2)***. Second, chromatin condensation detected by TEM does not necessarily indicate extensive DNA fragmentation. In the thymus, thymocytes with chromatin condensation do not always exhibit extensive nuclear DNA fragmentation ***(3,4)***. Recently, Sahara et al. reported the discovery of a caspase-3-activated protein that is required for apoptotic chromatin condensation without DNA fragmentation ***(5)***. Therefore, chromatin condensation and DNA fragmentation are independent events of apoptosis. Both agarose gel electrophoresis using extracted DNA and *in situ* end labeling of DNA strand breaks (ISEL) technique using light microscopy (ISEL/LM) have been widely used for the detecting of DNA fragmentation. To overcome the above-mentioned limitations of TEM, we applied the ISEL technique to TEM (ISEL/TEM technique) (**Fig. 1**). The procedure of the ISEL/TEM technique is fundamentally the same as that of the

From: *Methods in Molecular Biology, vol. 203:* In Situ *Detection of DNA Damage: Methods and Protocols*
Edited by: V. V. Didenko

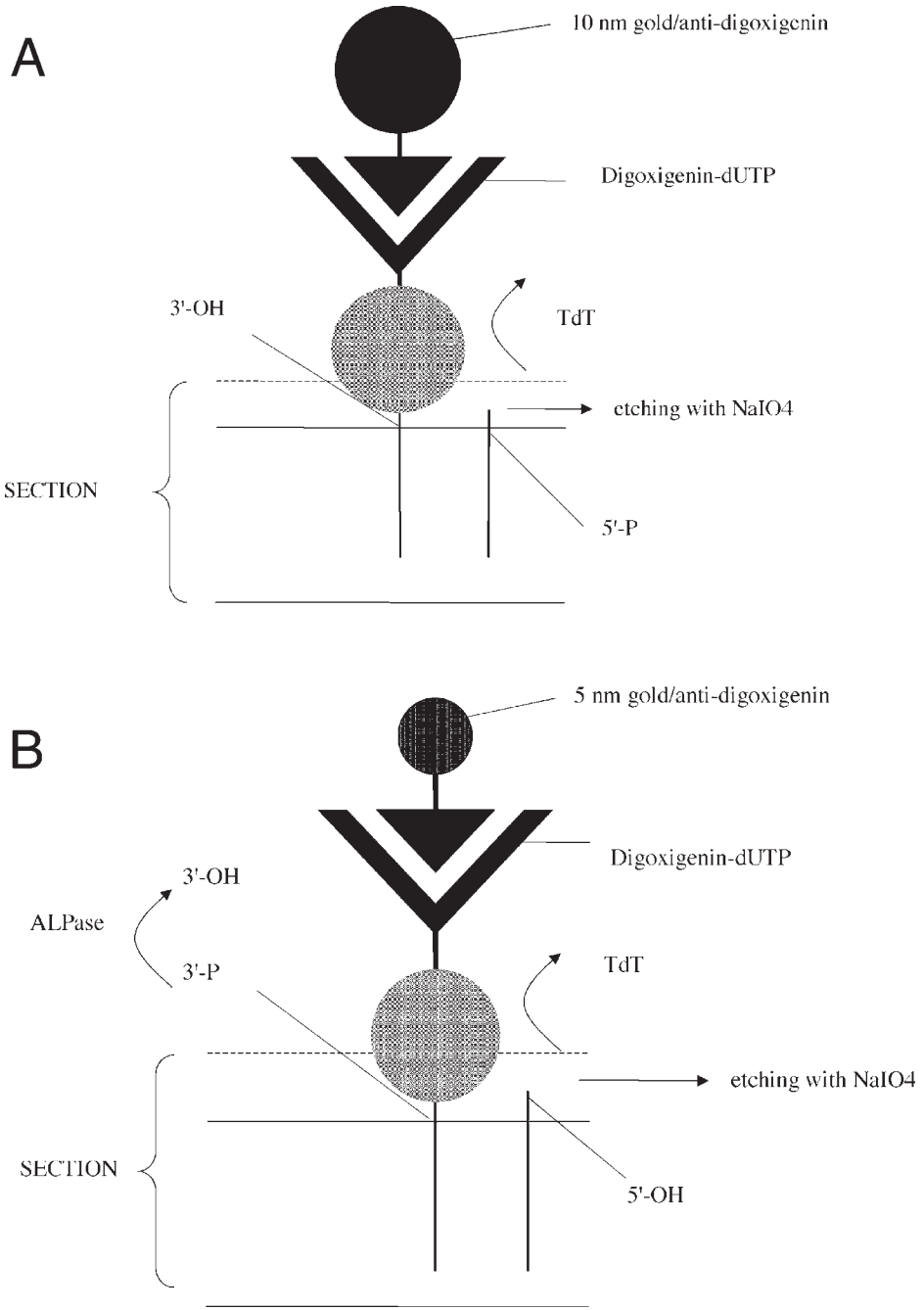

Fig. 1. Principle of ISEL/TEM **(A)** and ALP/ ISEL/TEM **(B)** (Explanation in the text).

ISEL/LM technique, except for the incorporation of immunogold particles, as a substitution for the immunoperoxidase in the ISEL/LM technique ***(6,7,8)***. Briefly, dideoxynucleotides labeled with digoxigenin are bound to the 3' OH DNA ends by reacting with the TdT enzyme in ultrathin sections on a nickel grid. After incubation with an anti-digoxigenin antibody conjugated with 10-nm colloidal gold, the sections are then stained with uranyl acetate and lead citrate and are examined by TEM. The ISEL/TEM technique using immunogold staining has some advantages in terms of detection of apoptotic cells and semiquantification of free 3' OH DNA ends. First, the ISEL/TEM technique enables determination of apoptotic cells entering early stages of apoptosis. It is well known that the increase in the number of sites of newly formed free 3' OH DNA ends precedes morphological changes associated with apoptosis ***(6,9)***. The ISEL/TEM study clearly shows apoptotic cells in the early stage of apoptosis: the moderately increased number of immunogold particles on the initial chromatin condensation but otherwise normal ultrastructural appearance, and in the late stage, the typical chromatin condensation with a numerous immunogold particles in the nuclei ***(6,8)***. Second, the ISEL/TEM technique provides information on the mode of DNA cleavage for both apoptosis and necrosis. More than 10 endonucleases have been identified and classified into the following two DNA cleavage types: the 3' OH/5' P type and the 3' P/5' OH type ***(8,10)***. There are only few studies on the mode of DNA cleavage, particularly the 3' P/5' OH type, for both apoptosis and necrosis ***(8,11,12)***, although several studies have reported that apoptotic cells possess abundant DNA termini of the 3' OH/5' P type ***(13,14,15)***. In order to detect the free 5' OH DNA ends using a nonradioactive method, the 3' P ends located on the opposite side which hold the 5' OH ends that were generated by cleavage, were dephosphorylated into 3' OH ends using alkaline phosphatase (ALP). In this chapter, we describe two techniques for detecting both 3' OH and 5' OH ends in a nucleus (*see* **Subheadings 3.3.1**, **3.3.2**). As described in **Subheading 3.3.1**, the exact number of 5' OH ends in a nucleus was determined by calculating the difference between the number of immunogold particles labeled by ISEL/TEM using ALP (ALP/ISEL/TEM) and that by ISEL/TEM, because the ALP/ISEL/TEM technique recognizes both inherent 3' OH ends and 3' OH ends newly formed by dephosphorylation. As shown in 3.3.2. (**Fig. 1**), we can simultaneously detect 3' OH ends labeled with 5-nm immunogold particles and 3' P ends labeled with 10-nm immunogold particles in a nucleus, although the number of labeled immunogold particles may decrease due to double staining using different sizes of immunogold particles. Third, the ISEL/TEM technique provides objective data due to the image analysis of quantitative changes for both the 3' OH and 5' OH DNA ends in each apoptotic or necrotic cell, when images are processed by employing NIH Image and Adobe Photoshop programs ***(6,8)*** (**Figs. 2**, **3**).

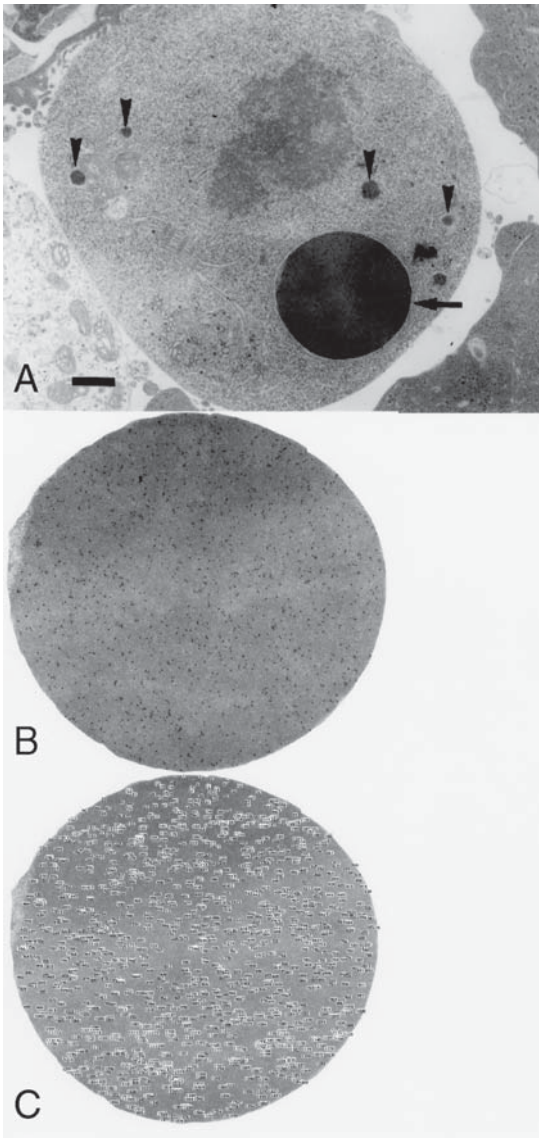

Fig. 2. Electron micrographs of an apoptotic NP3 cell stained by the ISEL/TEM technique and the image of the nucleus on a computer. **(A)** The nuclei (arrow and arrowheads) are characterized by the presence of condensed chromatin with many immunogold particles. Bar = 1 μm. **(B)** The images of the nucleus (arrow in **A**) is reserved using a software (Adobe Photoshop™) on a computer. **(C)** Both the number of immunogold particles and area of the nucleus are automatically measured by the NIH Image program. The labeling density of free 3' OH ends (the number of immunogold particles/nuclear area) was 196.8/μm^2.

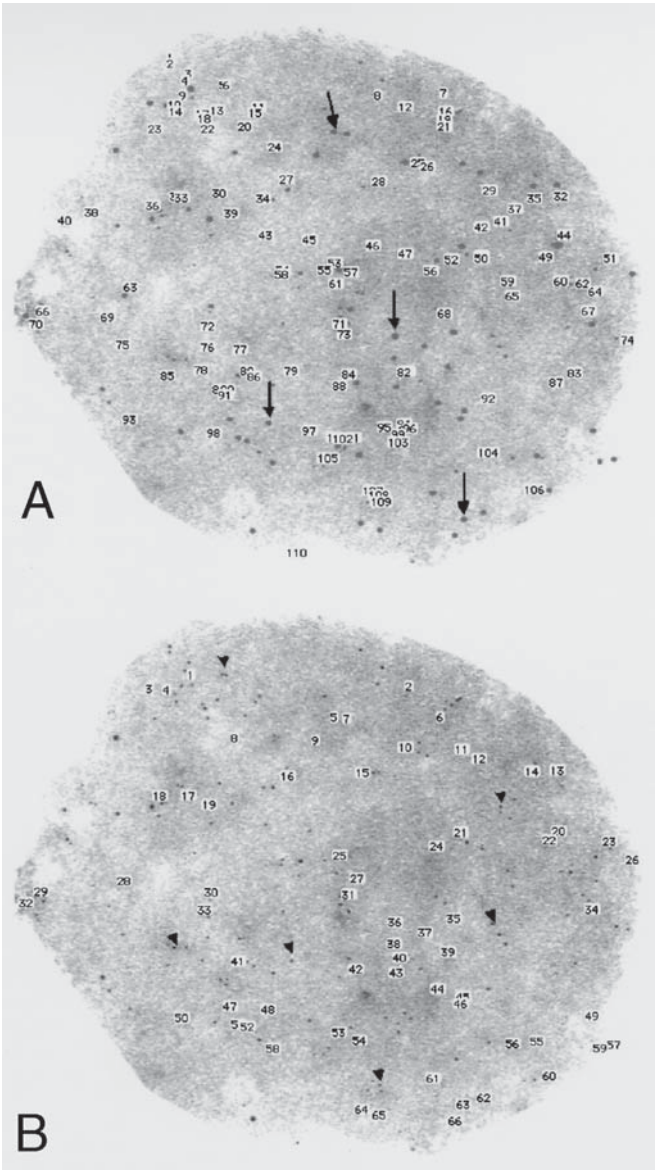

Fig. 3. Nuclear images of an apoptotic NP3 cell stained by both the ISEL/TEM and ALP/ISEL/TEM techniques. The labeling density of 3' OH ends labeled with 5 nm immunogold particles is 70.6/μm^2 **(A)** and that of 5' OH ends labeled with 10 nm immunogold particles is 28.0/μm^2 **(B)**. When you properly use "min particle" and "max particle size" of the NIH image program, 10 nm immunogold particles indicating 5' OH ends (arrows) are not numbered in **A**, in contrast to no number for 5 nm immunogold particles indicating 3' OH ends (arrowheads) in **B**.

2. Materials

2.1. Fixation, Embedding, and Staining

1. Fixative:
   a. Pre-fixative: 2% (w/v) paraformaldehyde and 2.5% (v/v) glutaraldehyde in 0.1 *M* phosphate buffer (PB) (pH 7.4). Prepare the following reagents: [Solution A] Dissolve the 8 g paraformaldehyde in 90 mL distilled water (dH_2O) at 60°C, add 40 µL of 1 *N* NaOH and make up to 100 mL with dH_2O (*see* **Note 1**). [Solution B] 0.2 *M* PB, pH 7.4 (*see* **Subheading 2.1 item 2**). Mix 25 mL of Solution A with 10 mL of 25% glutaraldehyde and 50 mL of Solution B, and adjust volume to 100 mL with dH_2O.
   b. Post-fixative: 1% (w/v) osmium tetroxide in 0.1 *M* PB (pH 7.4).
   Dissolve the 1 g osmium tetroxide in a glass capsule in 50 mL of dH_2O (*see* **Note 2**).
2. Buffer: 0.2 *M* phosphate buffer (PB), pH 7.4. Dissolve 5.93 g $NaH_2PO_4 \cdot 2H_2O$ and 58 g $Na_2HPO_4 \cdot 12H_2O$ in dH_2O, store at room temperature (RT), and make up to 1 L with dH_2O. Prepare 0.1 *M* PB then simply dilute 0.2 *M* PB with dH_2O.
3. A series of graded ethanol solution: 30%, 50%, 70%, 80%, 90%, 99.5% (v/v in dH_2O), absolute 100% ethanol.
4. C_3H_6O: Propylene oxide
5. Embedding resin: Epoxy resin (total volume: 20.4 mL). Mix 9.4 mL of Epon 812 with 5.65 mL of methyl nadic anhydride (MNA), 4.95 mL of dodecenyl succinic anhydride (DDSA) and 0.4 mL of 2,4,6-dimethylaminomethyl phenol (DMP-30) (*see* **Note 3**).
6. Staining solution for electron microscopy: 2% (w/v) uranyl acetate in 70% (v/v in dH_2O) ethanol. Lead citrate staining solution: Mix 1 g Pb $(NO_3)_2$ with 1 g Pb $(CH_3COO)_2 \cdot 3H_2O$, 1 g $Pb_3(C_6H_5O_7)_2 \cdot 3H_2O$ and 2 g $Na_3C_6H_5O_7 \cdot 2H_2O$ in 82 mL dH_2O, and dissolve with adding 18 mL 1 *N* NaOH.

2.2. 3' OH Labeling using Terminal Deoxynucleotidyl Transferase (TdT) for ISEL/TEM

1. Saturated $NaIO_4$: Dissolve 1 g $NaIO_4$ in 8 mL dH_2O and store at RT.
2. Apop Tag® *In Situ* Apoptosis Detection Kit: Available from Serologicals Corp. (formerly Intergen) Gaithersburg, MD (*see* **Note 4**).
3. Tris-bovine serum albumin (BSA) buffer: 0.02 *M* Tris-HCl, pH 7.4 containing 0.1% BSA and store at 4°C.
4. 10% normal sheep serum in Tris-BSA buffer.
5. 5 and 10 nm colloidal gold conjugated sheep IgG anti-digoxigenin antibody: Available from British BioCell Int. (Golden Gate, UK). Dilute to 1:50 with Tris-BSA buffer.

2.3. Dephosphorylation of 3' P Ends for ALP/ISEL/TEM

1. Calf Intestinal Alkaline phosphatase (CIAP) and 10 x CIAP buffer: Available from Gibco-BRL (Gaithersberg, MD) and stored at –20°C. Dilute 5 µL of CIAP with 195 µL of 1 × CIAP buffer.

2. CIAP/Stop solution: 5 m*M* ethylenediaminetetraacetic acid (EDTA) (pH 8.0), 0.5% sodium dodecyl sulfate (SDS) and 100 µg/mL proteinase K in dH_2O.

3. Methods

3.1. Preparation of TEM Samples

1. Fix specimens with the pre-fixative at 4°C for 2 h (*see* **Note 5**).
2. Rinse and immerse in 0.1 *M* PB at 4°C overnight.
3. Fix with post-fixative at RT for 2 h (*see* **Note 5**).
4. Rinse with 0.1 *M* PB for 5 min, 3×.
5. Dehydrate in a series of graded ethanol solutions for each 15 min.
6. Clear with propylene oxide for 15 min, 2×.
7. Immerse in 50% epoxy resin (v/v in propylene oxide) for 2 h.
8. Immerse in epoxy resin for 2 h.
9. Embed in epoxy resin at 60°C for 72 h.
10. Make ultra-thin sections by ultramicrotome (*see* **Note 6**) and mount on nickel grids.

3.2. ISEL/TEM Technique for 3' OH Ends

Several buffers for the ISEL/TEM technique described in the **Note 4** are taken from studies dealing with TdT-mediated dUTP-biotin nick end labeling ***(15,16)***. We recommend a commercially available non-radioactive apoptosis detection kit (*see* **Subheading 2.2 item 2**). In the reaction the droplets of the medium are placed on Parafilm M® so that ultra-thin sections float on the surface of the droplets and then are moved to the new droplets for incubation and rinse. Do not allow sections to dry during the staining process.

1. Etch the ultra-thin sections with saturated $NaIO_4$ for 2–3 min at RT (*see* **Note 7**).
2. Rinse with dH_2O for 5 min, 3×.
3. Incubate with the equilibration buffer (Apop Tag®) for 10–15 sec.
4. Incubate with the mixture of the reaction buffer and TdT enzyme (Apop Tag®) for 60 min at 37°C (*see* **Note 8**).
5. Incubate with the stop/wash buffer (Apop Tag®) for 30 min at 37°C (*see* **Note 8**).
6. Rinse with Tris-BSA buffer 5 min, 3× (*see* **Note 9**).
7. Incubate with normal sheep serum for 15 min.
8. Incubate with the anti-digoxigenin antibody conjugated to 10 nm colloidal gold for 60 min.
9. Rinse with Tris-BSA buffer for 5 min.
10. Rinse with dH_2O for 5 min, 3× (*see* **Note 10**).
11. Stain with uranyl acetate for 5 min and then stain with lead citrate for 2 min.

Fig. 4 (A, B) shows the localization of free 3' OH ends in the nucleus of an apoptotic cell visualized by the ISEL/TEM technique with immunogold particles.

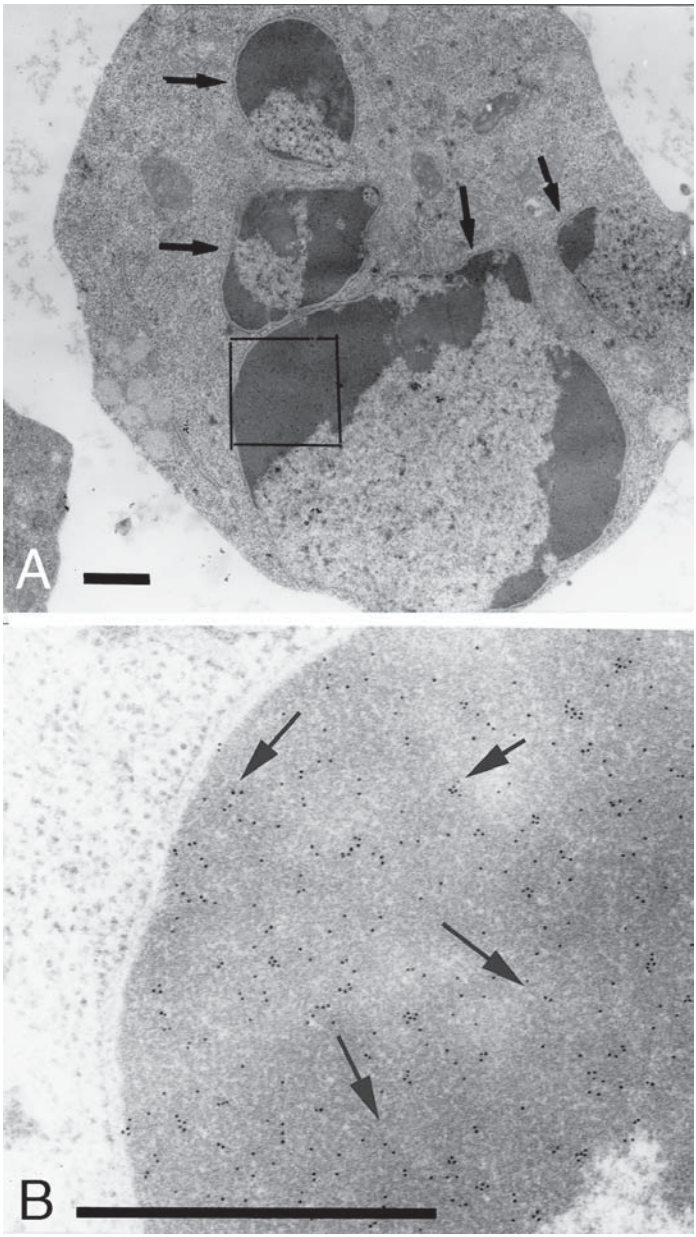

Fig. 4. Photographs of the ISEL/TEM technique. **(A)** An apoptotic mouse B lymphoma cell (NP3 cell) after treatment of heating at 43°C is characterized by fragmented nuclei with condensed chromatin (arrows) . **(B)** Higher magnification of the boxed area of A. 3' OH ends are labeled with 10 nm immunogold particles (arrows). Bar = 1 μm.

3.3. ALP/ISEL/TEM for Both 3' OH and 3' P (5' OH) Ends

3.3.1. Staining for 3' OH and 3' P (5' OH) Ends Using 10 nm Immunogold Particles

In this method, free 3' OH ends are at first stained on the right side of the grid with ultra-thin sections as described in **3.2**, and then 3' P (5' OH) ends are detected on the opposite side of the grid (*see* **Note 11**). In an individual nucleus, the true number of 3' P (5' OH) ends is shown as the number that is subtracted from the number of immunogold particles labeled by the ISEL/TEM from that labeled by the ALP/ISEL/TEM.

1. Etch the ultra-thin sections with saturated $NaIO_4$ for 2 to 3 min at RT (*see* **Note 7**).
2. Rinse with dH_2O for 5 min, 3×.
3. Incubate with the equilibration buffer (Apop Tag®) for 10–15 sec.
4. Incubate with the mixture of the reaction buffer and TdT enzyme (Apop Tag®) for 60 min at 37°C (*see* **Note 8**).
5. Incubate with the stop/wash buffer (Apop Tag®) for 30 min at 37°C (*see* **Note 8**).
6. Rinse with Tris-BSA buffer 5 min, 3× (*see* **Note 9**).
7. Incubate with normal sheep serum for 15 min.
8. Incubate with the anti-digoxigenin antibody conjugated to 10 nm colloidal gold for 60 min.
9. Rinse with Tris-BSA buffer for 5 min.
10. Rinse with dH_2O for 5 min, 3× (*see* **Note 10**).
11. Stain with uranyl acetate for 5 min and then stain with lead citrate for 2 min.
12. Take TEM photos.
13. Count the number of the immunogold particles (*see* **Note 3**,**4**).
14. Etch the ultra-thin sections on the opposite surface with saturated $NaIO_4$ for 2–3 min at RT.
15. Rinse with dH_2O for 5 min, 3×.
16. Incubate with CIAP solution for 60 min at 37°C.
17. Incubate with CIAP/stop solution for 30 min at 56°C.
18. Rinse with dH_2O for 5 min, 3×.
19. Incubate with the equilibration buffer (ApopTag® kit) for 10–15 sec.
20. Incubate with the mixture of the reaction buffer and TdT enzyme (ApopTag® kit) for 60 min at 37°C.
21. Incubate with the Stop/wash buffer (ApopTag® kit) for 30 min at 37°C.
22. Rinse with Tris-BSA buffer for 5 min, 3×.
23. Incubate with normal sheep serum for 15 min.
24. Incubate with the anti-digoxigenin antibody conjugated to 10 nm immunogold particles for 60 min.
25. Rinse with Tris-BSA buffer for 5 min.
26. Rinse with dH_2O for 5 min, 3×.
27. Stain with uranyl acetate for 5 min, then with lead citrate for 2 min.
28. Take TEM photos.

29. Count the number of the immunogold particles (*see* **Note 3**,**4**).
30. The labeling density is determined by subtracting the number (obtained in 13) from the number (obtained in 29).

3.3.2. Double Immunogold Staining for 3' OH and 3' P (5' OH) Ends

This method enables us to observe both 3' OH and 5' OH ends on the same surface of grids with ultra-thin sections: 3' OH ends labeled with 5 nm immunogold particles and 3' P (5' OH) ends labeled with 10 nm immunogold particles.

1. Etch the ultra-thin sections with saturated $NaIO_4$ for 2–3 min at RT (*see* **Note 7**).
2. Rinse with dH_2O for 5 min, 3×.
3. Incubate with the equilibration buffer (Apop Tag®) for 10 to 15 sec.
4. Incubate with the mixture of the reaction buffer and TdT enzyme (Apop Tag®) for 60 min at 37°C (*see* **Note 8**).
5. Incubate with the stop/wash buffer (Apop Tag®) for 30 min at 37°C (*see* **Note 8**).
6. Rinse with Tris-BSA buffer 5 min, 3× (*see* **Note 9**).
7. Incubate with normal sheep serum for 15 min.
8. Incubate with the anti-digoxigenin antibody conjugated to 5 nm colloidal gold for 60 min (*see* **Note 12**).
9. Rinse with Tris-BSA buffer for 5 min.
10. Rinse with dH_2O for 5 min, 3× (*see* **Note 10**).
11. Incubate with CIAP solution for 60 min at 37°C.
12. Incubate with CIAP/stop solution for 30 min at 56°C.
13. Rinse with dH_2O for 5 min, 3×.
14. Incubate with the equilibration buffer (ApopTag® kit) for 10–15 sec.
15. Incubate with the mixture of the reaction buffer and TdT enzyme (ApopTag® kit) for 60 min at 37°C.
16. Incubate with the Stop/wash buffer (ApopTag® kit) for 30 min at 37°C.
17. Rinse with Tris-BSA buffer for 5 min, 3×.
18. Incubate with normal sheep serum for 15 min.
19. Incubate with the anti-digoxigenin antibody conjugated to 10 nm immunogold particles for 60 min.
20. Rinse with Tris-BSA buffer for 5 min.
21. Rinse with dH_2O for 5 min, 3×.
22. Stain with uranyl acetate for 5 min and then stain with lead citrate for 2 min.
23. Take TEM photos.
24. Count the number of the immunogold particles (*see* **Note 3**,**4**).

Fig. 5 shows double immunogold staining for 3' OH and 3' P (5' OH) ends.

3.4. Image Analysis Using NIH Image Program

1. Observe the ultra-thin sections by TEM and take photographs of the labeled cell at high magnification (**Figs. 2B**, **4B**, **5B**) (*see* **Note 12**).

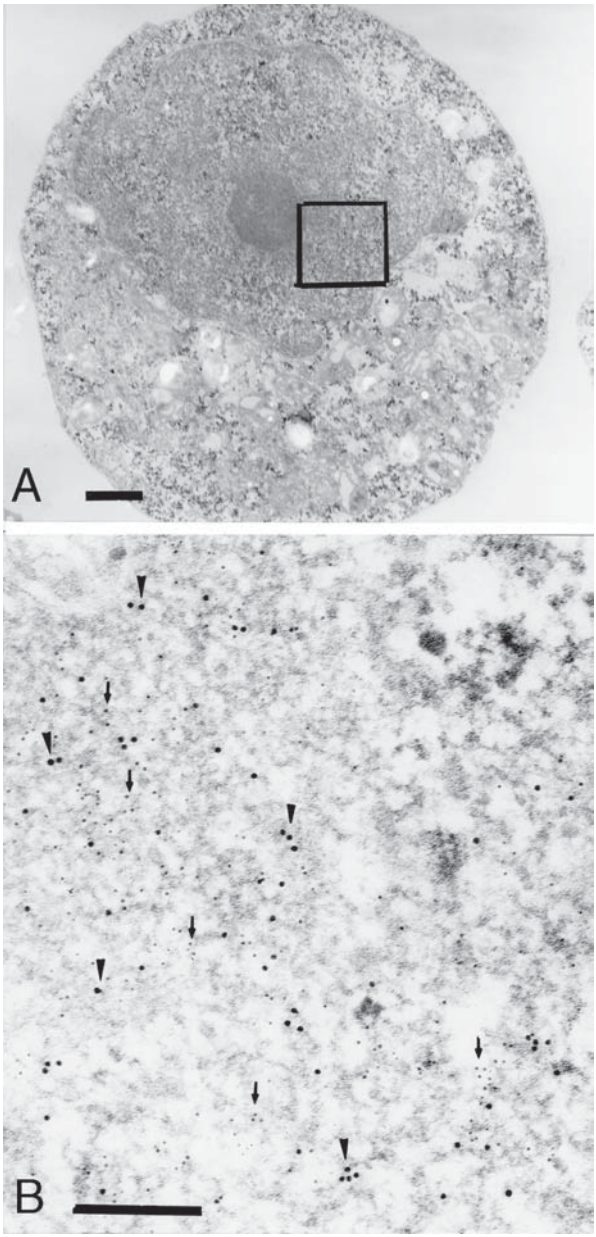

Fig. 5. Electron micrographs of the double immunogold staining for the detection of both 3' OH and 5' OH ends. **(A)** A necrotic NP3 cell after treatment of heating at 47°C. Bar = 1 µm. **(B)** Higher magnification of the boxed area of A. 3' OH ends and 3' P (5' OH) ends are labeled by 5-nm immunogold particles (arrows) and 10-nm immunogold particles (arrowheads), respectively. Bar = 0.25 µm.

2. Import the images of the cell captured by a scanner from electron micrographs, on a computer.
3. Reserve only the images of the nucleus using a drawing software (**Fig. 2B**).
4. Automatically, measure the nuclear area (μm^2) and count the number of the immunogold particles using the NIH Image program (*see* **Note 13**) (**Fig. 2C** and **Fig. 3**).
5. Calculate the labeling density (the number of immunogold particles/μm^2).

4. Notes

1. Cover the flask with aluminum film to avoid the vapor from paraformaldehyde in a fume hood.
2. Dissolve OsO_4 at 1~2 days before the use, because it is hard to dissolve OsO_4 in H_2O within a short time.
3. Cover a beaker with Parafilm M® to prevent absorption of water and store in a refrigerator until the nearly future use. Since epoxy resin is a potent carcinogen, it should be handled with gloves.
4. This kit supplies equilibration buffer, reaction buffer, TdT enzyme, stop/wash buffer and anti-digoxigenin antibody conjugated to peroxidase. Instead of anti-digoxigenin antibody conjugated to peroxidase, we use anti-digoxigenin antibody conjugated to immunogold particles in this chapter. This kit is convenient, but you can use 30 m*M* Tris-HCl buffer (pH 7.2) containing 140 m*M* $(CH_3)_2AsO_2Na{\cdot}3H_2O$ and 1 m*M* $CoCl_2$ (TDT buffer) instead of the equilibration buffer, TdT (0.3 e.u./μL) and digoxigenin—dUTP in TDT buffer instead of the reaction buffer and TdT enzyme, and 300 m*M* NaCl, 30 m*M* $Na_3C_6H_5O_7{\cdot}2H_2O$ instead of the stop/wash buffer ***(15,16)***.
5. Cut the specimen into small pieces ($5 \times 5 \times 5$ mm in maximal size). This fixation time (2 h) is for tissue samples. The fixation time should be shortened when culture cells are used in your study.
6. Make thicker ultra-thin sections (80 nm in thickness) than those (60–70 nm in thickness) used in the conventional TEM, because DNA amounts contained in 60–70 nm-thick sections may be scanty.
7. If you detect only a few immunogold particles on the labeled sections, change the time for etching (usually, only 2 min is optimal for etching time).
8. Put a small-sized petri dish into a moisture chamber, and place the chamber in the incubator. When only a few immunogold particles are observed on the labeled sections, try to increase the amounts of TdT enzyme or the incubation time.
9. We use locking forceps to surely grip the grids, when washing in the beaker. Anti-capillary forceps should be used when the grid is transported to the droplet of the different medium. A wire loop is used for the transport between the droplets of the same medium. After the incubation with the medium, carefully blot the excessive medium from both the tip of the forceps and the face of the grid, using small pieces of filter paper.
10. Rinsing is an important step because incomplete rinse cause the contamination.
11. Check the grid under a light microscope and confirm the glossy right side of grids, because ultra-thin sections were constantly placed on the right side of grids.

12. We usually take photographs with the high magnification, ×20,000 which is adequate to observe 5 and 10 nm immunogold particles.
13. Erase contaminants with high electron-density from the images and decrease the density of the whole nucleus by the drawing software (Adobe Photoshop™, Adobe Systems Inc., CA.). The NIH Image program (written by Wayne Rasband at the U.S. National Institutes of Health and available from the Internet by anonymous ftp from http://rsb.info.nih.gov/nih-image/download.html) recognizes and counts the immunogold particles based on the difference of the contrast between immunogolds and other substances. Choose "min particle size" and "max particle size" of the NIH Image program for the detection of 5 and 10 nm immunogold particles, respectively (*see* **Fig. 3**).

References

1. Kerr, J. F. R., Wyllie, A. H. and Currie, A. R. (1972) A basic biological phenomenon with wide-ranging implications in tissue kinetics. *Br. J. Cancer* **26,** 239–257.
2. Shimizu, S., Eguchi, Y., Ito, Y., HasegawaJ., Yamabe K., Otsuki, Y., Matsuda H. and Tsujimoto Y. (1996) Induction of apoptosis as well as necrosis by hypoxia and predominant prevention of apoptosis by Bcl-2 and Bcl-X_L. *Cancer Res.* **56,** 2161–2166.
3. Nakamura, M., Yagi, H., Ishii, T., Kayabe, S., Soga, H., Gotoh, S., Ogata, M. and Itoh, T (1997) DNA fragmentation is not the primary event in glucocorticoid-induced thymocyte death in vivo. *Eur. J. Immunol.* **27,** 999–1004.
4. Nakamura, M., Yagi, H., Kayaba, S., Ishii, T., Gotoh, T., Ohtsu, S. and Itoh, T. (1996) Death of germinal center B cells without DNA fragmentation. *Eur. J. Immunol.* **26,** 1211–1216.
5. Sahara, S., Aota, M., Eguchi, Y., Imamoto, N., Yoneda, Y. and Tsujimoto, Y. (1999) Acinus is a caspase-3-activated protein required for apoptotic chromatin condensation. *Nature* **401,** 168–172.
6. Inoki, C., Ito, Y., Yamashita, H., Ueki, K., Fukuda, Y., Ninomiya, E., Nakamura, K., Hayashi, R., Ueki, M. and Otsuki, Y. (1997) Image analysis and ultrastructural detection of DNA strand breaks in human endometrium by *in situ* end-labeling techniques. *J. Histotechnol.* **20,** 321–328.
7. Nakamura, K., Ito, Y., Matsumoto, K., Daikoku, E., Kiyokane, K. Otsuki, Y. (1999) The relationship between apoptosis and keratinization in human epidermis. *Acta Histochem. Cytochem.* **32,** 77–83.
8. Hayashi, R., Ito, Y., Matsumoto, K., Fujino, Y. and Otsuki, Y. (1998) Quantitative differentiation of both free 3' OH and 5' OH DNA ends between heat-induced apoptosis and necrosis. *J. Histochem. Cytochem.* **46,** 1051–1059.
9. Walker, P. R., Kokileva, L., Leblanc, J. and Sikorska, M. (1993) Detection of the initial stages of DNA fragmentation in apoptosis. *Biotechniques* **15,** 1032–1047.
10. Shiokawa, D., Ohyama, H., Yamada, T., Takahashi, K. and Tanuma, S. (1994) Identification of an endonuclease responsible for apoptosis in rat thymocytes. *Eur. J. Biochem.* **226,** 23–30.
11. Mundle, S., Gao, X. Z., Khan, S., Gregory, S. A., Preisler, H. D. and Raza, A. (1995) Two in situ labeling techniques reveal different patterns of DNA fragmentation during

spontaneous apoptosis in vivo and induced apoptosis in vitro. *Anticancer Res.* **15,** 1895–1904.
12. Gold, R., Schmied, M., Giegerich, G., Breitschopf, H., Hartung, H. P., Toyka, K. V. and Lassmann, H. (1994) Differentiation between cellular apoptosis and necrosis by combined use of in situ tailing and nick translation techniques. *Lab. Invest.* **71,** 219–225.
13. Tanuma, S. and Shiokawa, D. (1994) Multiple forms of nuclear deoxyribonuclease in rat thymocytes. *Biochem. Biophys. Res. Commun.* **203,** 789–797.
14. Park, H. J. (1995) Effects of intracellular pH on apoptosis in HL-60 human leukemia cells. *Yonsei Med. J.* **36,** 473–479.
15. Verhaegen, S., McGowan, A. J., Brophy, A. R., Fernande, R. S. and Cotter, T. G. (1996) Inhibition of apoptosis by antioxidants in the human HL-60 leukemia cell line. *Biochem. Pharmacol.* **50,** 1021–1029.

5

Determination of Three-Dimensional Distribution of Apoptotic DNA Damage by Combination of TUNEL and Quick-Freezing and Deep-Etching Techniques

Shinichi Ohno, Takeshi Baba, Nobuo Terada, and Yasuhisa Fujii

1. Introduction

1.1. Apoptosis and Prostatic Epithelial Cells

Apoptosis is a widespread phenomenon, which plays an important role in many physiological events as well as pathological processes ***(1)***. It was originally defined by its unique ultrastructural features, which were detected by electron microscopy ***(2,3)***. They are cytoplasmic shrinkage, nuclear chromatin condensation along nuclear margin, cell fragmentation into apoptotic bodies, and phagocytosis by adjacent epithelial cells or macrophages. It is also known that normal epithelial cell proliferation and death in mammalian prostatic glands depend upon an appropriate level of circulating androgen in blood ***(4,5)***. Therefore, the prostatic epithelial cells routinely undergo apoptosis by androgen withdrawal following castration in experimental male animals ***(6,7,8)***.

1.2. Endonuclease Activation with Apoptosis

In apoptosis, nuclear changes such as chromatin condensation and pyknosis, followed by budding into apoptotic bodies ***(2,3)***, are linked to activation of a calcium-dependent endonuclease which cleaves DNA into oligonucleosomal fragments ***(7,9,10)***. In some cells, a rise in cytoplasmic ionized calcium occurs in an early phase ***(9)***. Even in the absence of the DNA ladder hallmark, some degrees of high molecular weight DNA fragmentation first occur during the apoptosis, leading to further oligonucleosomal degradation. The leaked DNA molecules appear to be not small molecular fragments but condensed heterochromatin clumps, which have been seen leaking out apparently without rupture of the nuclear envelope ***(2)***.

From: *Methods in Molecular Biology, vol. 203:* In Situ *Detection of DNA Damage: Methods and Protocols*
Edited by: V. V. Didenko

Although the nuclear breakdown is widely considered to be a hallmark of apoptosis *(2,3,10)*, its mechanism remains poorly understood. A little is known about the correlation between the DNA cleavage and appearance of the described ultrastructural chromatin modifications. Biochemically, the large-scale DNA is digested into low molecular weight DNA fragments. Such a cleavage of DNA by endonucleases is known to represent a biochemical hallmark of apoptosis and can be demonstrated in agarose gel DNA electrophoresis as a "ladder" *(10)*.

1.3. Normal DNA Structure

A normal eukaryotic cell forms a complex higher order nuclear structure, in which there is coiling of double-stranded nucleic acid polymers *(11,12,13)*. In addition, the organization of such a higher order DNA structure around histone proteins arranges a basic architecture of intranuclear chromatin *(12,13)*. In the interphase nucleus, each chromosome is anchored to protein scaffolds composed of a peripheral nuclear lamina and an intranuclear network. During the cell cycle, both S and G_2 stages are assumed to be the most sensitive to apoptosis. Some deoxyribonucleases (DNases) in eukaryotic cells play important roles in nucleic acid metabolism, such as DNA repair, recombination and degradation. By the use of DNases, actively transcribing genes are identified, but inactive chromatin is relatively protected from the digestion by its tight structure and presence of associated proteins. Therefore, euchromatin domains in nuclei are generally DNase-sensitive sites, while other heterochromatin domains are DNase-insensitive.

1.4. Apoptosis Detection Techniques

Some methods have been described to identify apoptotic cells in animal tissues, which are light or electron microscopy, flow cytometry, TUNEL (terminal deoxynucleotidyl transferase-mediated dUTP-biotin nick end-labeling) technique and agarose gel DNA electrophoresis *(14,15,16,17)*. Morphological features especially at the electron microscopic level were accepted as a most reliable criterion to identify apoptosis *(2,3,14)*. In addition to the electron microscopy, the TUNEL technique, which labels free 3'-OH ends *(14,15,17)*, was developed and widely used for detection of apoptotic cells. The TUNEL technique is positive not only for apoptotic cells, but also for necrotic cells *(18)*. In the agarose gel DNA electrophoresis, when a sample contains small amounts of apoptotic cells, there is no demonstration of a DNA ladder *(16)*. Therefore, the electron microscopy still remains an essential and helpful technique in the study of apoptosis to characterize the form of cell death *(2,3,14)*.

1.5. TUNEL Technique

The TUNEL technique has been used to identify apoptosis of cells *(5,14,15, 17,18)*, but some apparently non-apoptotic cells are found to be TUNEL-positive *(18)*. Such DNA fragmentation has been formed in some cells undergoing necrosis. There had been very little data correlating TUNEL findings with electron microscopic evaluation of nuclear chromatins. For the past several years, the TUNEL technique has been adapted for electron microscopy, called the EM-TUNEL method *(16,18,19,20,21)*. The principle of the TUNEL technique is that the DNA of apoptotic cells becomes fragmented into regular nucleosome-sized units *(15)*. It is based on the specific binding of terminal deoxynucleotidyl transferase (TdT) to 3'-OH ends of DNA, ensuring a synthesis of a polydeoxynucleotide polymer. Therefore, the overhanging 3'-OH ends of the nucleosome-sized units in apoptosis can be identified by the immunohistochemical detection of enzymatically incorporated digoxigenin-labeled triphosphates as dUTP.

The TUNEL technique relies on the presence of DNA strand fragments in apoptotic cells caused by activation of endonucleases during the process of cell death *(7)*. However, it is not specific for apoptosis and its findings must be interpreted with caution and correlated with morphological criteria of apoptosis. Some changes in DNA-histone interactions also represented a major modulating factor of chromatin condensation *(22)*. Such chromatin changes in apoptosis may be characterized by a three-dimensional array of nucleosomes different from that prevailing in the interphase nucleus *(23)*. Therefore, our attention has been turned to application of the QF-DE method (*see* next three sections), which can define three-dimensional ultrastructures of natural chromatin organization *(12)*. We have used the TUNEL technique in combination with the QF-DE method at the electron microscopic level *(8)*, in order to clarify if apoptotic nuclei are indeed associated with evidence of small DNA strand fragments in vivo.

1.6. Methodological Problems of Conventional Preparations for Electron Microscopy

The conventional procedure to prepare biological samples for electron microscopic study includes the following steps; chemical fixation of cells and tissues, their dehydration and embedding in epoxy resin, ultrathin sectioning and electron staining with heavy metals, including uranium and lead. The first step is commonly carried out by serial double fixations with glutaraldehyde and osmium tetroxide. These chemical fixatives are believed to preserve cellular ultrastructures in situ. It is generally accepted that the fixation mechanism of glutaraldehyde is a cross-linking of the extracellular and intracellular proteins

via its bifunctional aldehyde residues and that osmium tetroxide binds with intracellular components, such as proteins and membrane lipids.

However, there are some disadvantages to using these chemical fixatives to preserve the in vivo ultrastructures in cells and tissues. First, components such as ions and metals cannot be immobilized by the chemical cross-linking mechanism and are easily extracted during the subsequent buffer washing and dehydration steps. Second, fast cellular events cannot be captured by the chemical fixations, because the methods require at least several seconds to fix the cells and tissues. Finally, their ultrastructures are unavoidably altered, and soluble proteins that are not associated with cytoskeletons and membranous organelles are translocated.

Moreover the fixed biological specimens are subjected to the subsequent dehydration and embedding steps. In the dehydration step, ethanol is generally used to substitute for any water in the specimens. However, considerable amounts of lipids and other ethanol-soluble components are easily extracted at this step. The dehydrated specimens are then embedded in viscous epoxy resin, which is polymerized by heating up to 60°C. The highly aqueous biological cells and tissues are thus embedded in the matrix of the resin network via these harsh manipulations.

Next, the specimens are cut into sections 0.05–0.1 μm thick with an ultramicrotome and mounted on copper grids. Thus, only a two-dimensional single plane is usually obtained from the three-dimensional cells and tissues and observed under an electron microscope. The ultrathin section staining with lead and uranium is necessary to enhance the contrast of ultrastructural images. In these steps we cannot avoid the artifacts produced by coating the ultrathin sections with heavy metals or the heat damage that occurs during the final electron microscopic observation under a high vacuum condition.

Although conventional electron microscopy with ultrathin sections has the disadvantages described in the preceding paragraphs, such ultrastructural studies have provided much important morphological information about nuclei that has greatly contributed to the progress in a biological field. Meanwhile, some researchers have been trying to improve the sample preparation methods and have been looking for other techniques to preserve the three-dimensional ultrastructures of cells and tissues in vivo.

1.7. Quick-Freezing (QF) Method

A promising approach to studying less artificial biological morphology is the QF method, in which cells and tissues are usually brought into contact with copper or silver metal cooled in liquid helium or nitrogen to be quickly frozen. The QF method has a high time resolution for dynamic ultrastructures, which is sufficient to capture ultrastructural changes of water-rich cells and tissues. It

has been also accepted that the QF method is the best way to preserve antigenecity and chemical compositions of biological specimens. Therefore, ultrastructural artifacts produced by the conventional chemical fixation and dehydration steps can be avoided by the QF method, whose goal is to preserve cellular ultrastructures and components in their natural states. Since the mid 1980s, the QF method has become a popular tool for the ultrastructural study of biological specimens, followed by deep-etching or freeze-substitution method.

1.8. Deep-Etching (DE) Method

To obtain three-dimensional images of cells and tissues, the previously frozen biological specimens are generally freeze-fractured, deeply etched under vacuum conditions to evaporate tiny ice crystal and shadowed with platinum and carbon. The replica membranes are prepared and observed in electron microscopes (*see* **Subheading 3.1.**). Although the three-dimensional structure of cells and tissues is not well defined in conventional ultrathin sections (*see* **Subheading 1.6.**), the DE method is highly versatile for visualizing three-dimensional intracellular ultrastructures and extracellular matrices. Therefore, the three-dimensional ultrastructure of nuclei can be clarified by the QF-DE method.

1.9. Quick-Freezing and Deep-Etching (QF-DE) Method

The QF-DE method, which is one of the useful techniques in electron microscopy as described above, has an advantage of directly examining three-dimensional ultrastructures of cells and tissues at high resolution ***(24,25)***. We have already analyzed three-dimensional ultrastructures of apoptotic nuclear chromatin in rat prostatic epithelial cells after the castation ***(8)***. By the QF-DE method, the destruction of chromatin fibers, nucleosomal filaments and DNA strands was morphologically detected in the apoptotic nuclei (**Fig. 1A**). Such destruction of intranuclear chromatin networks randomly appeared and was spotty throughout the apoptotic nucleus at an early stage (**Fig. 1B**). At a late stage, the definite chromatin destruction occurred in a center of the apoptotic nucleus, and broken chromatin networks were condensed along the nuclear margin (**Fig. 1C**). These findings obtained by the QF-DE method probably corresponded to alteration of the intranuclear chromatin ***(8)***, as observed on conventional ultrathin sections (**Fig. 1D**) ***(19,21)***.

2. Materials

2.1. Animal Treatment

According to a general survey on the occurrence of TUNEL-positive cells in prostatic tissues, the following animal samples are used for the apoptosis study ***(8)***.

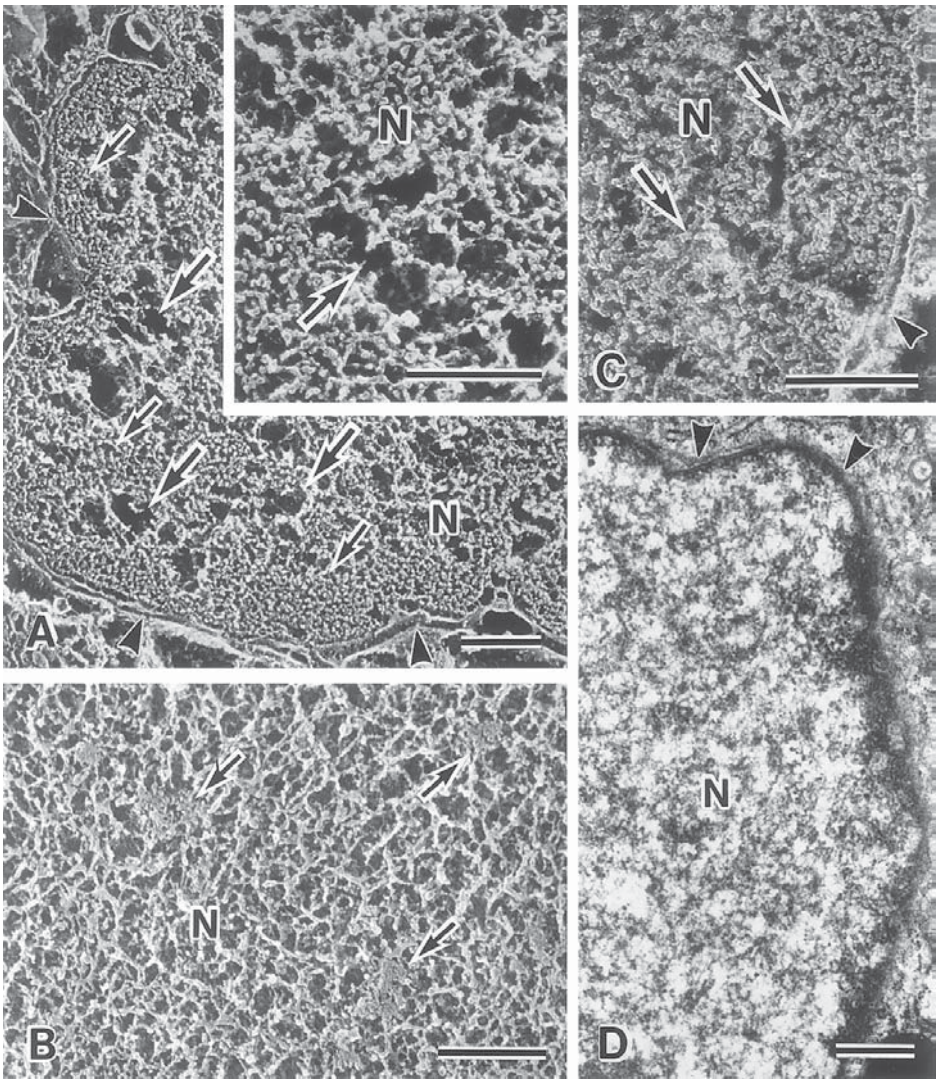

Fig. 1. **(A–C)** Replica electron micrographs of apoptotic nuclei. N; nuclei. Scale bars = 0.5 μm. **(A)** Filamentous networks in a nucleus (N) are broken (large arrows) and aggregated (small arrows) along its nuclear membrane (arrowheads) at late apoptotic stages. Inset; higher magnification. **(B)** and **(C)** Replica electron micrographs of apoptotic nuclei treated by the TUNEL technique. **(B)** The DAB reaction products are scattered in an early apoptotic nucleus (arrows). **(C)** They are aggregated (arrows) along the nuclear membrane (arrowhead) at late apoptotic stages. **(D)** Conventional electron micrograph of an early apoptotic nucleus. The chromatin destruction is hardly detected at this stage. N; Nucleus. Arrowheads; nuclear membrane. Scale bar = 0.5 μm.

1. Male Wistar rats at ages of 11–15 weeks are housed in an air-conditioned room.
2. The castration of some rats is performed under intraperitoneal anesthesia with sodium pentobarbital (50 µg/kg body weight).
3. They are sacrificed 1, 2, 3, 4, and 5 d after the castration, as described in the following paragraphs. In the control group, non-castrated normal rats are sacrificed in the same way.
4. Under anesthesia with the sodium pentobarbital, the castrated or normal rats are perfused with 2% paraformaldehyde (PF) in 0.1 *M* phosphate buffer (PB), pH 7.4, via the left cardiac ventricle.
5. Their ventral prostatic lobes are excised and weighed to check the atrophy of prostates. In this series of experiment, the number of TUNEL-positive nuclei rapidly increases on d 2 and gradually decreases on d 5, as reported before ***(8)***. The percentage of TUNEL-positive nuclei was about 11% at a peak time, as obtained from morphometric data ***(8)***.

2.2. Chemicals and Enzymes

1. DAB (3, 3'-diaminobenzidine tetrahydrochloride) solution: carcinogen and must be freshly prepared.
   a. Dissolve 25 mg DAB in ~75 mL of 0.05 *M* Tris-HCl buffer, pH 7.6.
   b. Readjust pH to 7.6 with 0.05 *M* Tris-aminomethane.
   c. Make up to 100 mL with 0.05 *M* Tris-HCl buffer, pH 7.6.
2. DAB-H_2O_2: make 5% H_2O_2 solution from concentrated ***(30%)*** H_2O_2 solution and add 0.1 mL of the 5% H_2O_2 solution to 100 mL of DAB solution.
3. 0.05 *M* Tris-HCl buffer:
   a. Prepare 100 mL of 0.1 *N* HCl and 500 mL of 0.2 *M* Tris-aminomethane.
   b. Mix 25 mL of 0.2 *M* Tris-aminomethane and 40 mL of 0.1 *N* HCl.
   c. Make up to 100 mL with distilled water.
4. Proteinase K (EM Science, Gibbstown, NJ): 1~5 µg/mL in PBS. Store at –20°C.
5. DNase (Deoxyribonuclease) I (Worthington Biochemical Corporation, Lakewood, NJ): 1 µg/mL in digestion buffer (*see* **Subheading 3.3.2.**).
6. Digestion buffer: 0.02 *M* Tris-HCl, pH 7.5, 5 m*M* $MgCl_2$, 1 m*M* $CaCl_2$ (*see* **Subheading 3.3.2.**).
7. Paraformaldehyde and glutaraldehyde fixatives: both are toxic, which may be absorbed by contact through skin or by respiration.
8. 10% methanol: pure methanol is flammable and poisonous. Poisoning may occur from ingestion, inhalation or percutaneous absoption.
9. 0.5% Formvar (Ladd Research, Williston, VT) in chloroform: must be used in a fume hood, its vapor is toxic.
10. 2% collodion in amylacetate (n-pentyl acetate) (Diatome US, Fort Washington, PA): must be used in a fume hood, its vapor is toxic.
11. 0.1 *M* phosphate buffer (PB) solution, pH 7.4: dissolve 11.86 g of $NaH_2PO_4 \cdot 2H_2O$ and 115.99 g of $Na_2HPO_4 \cdot 12H_2O$ in 4 L of distilled water.
12. PBS: PB containing 0.15 *M* sodium chloride (NaCl).

13. 1% saponin in PB: foams strongly when shaken with PB and acts as a powerful hemolytic after oral ingestion.
14. In Situ Apoptosis Detection Kit [ApopTag® Peroxidase; Serologicals Corp. (formerly Intergen) Gaithersburg, MD] (*see* **Subheading 3.2.**)

3. Methods

3.1. Quick-Freezing and Deep-Etching (QF-DE) Method

In our previous report ***(8)***, the QF-DE method clarified three types of fibrous structures in normal nuclei of rat prostatic epithelial cells (**Fig. 2A**). They were 20–30 nm thick fibers, 5–10 nm filaments and also 2–5 nm fine filaments, forming network structures. At higher magnification, the chromatin fibers showed substructures, consisting of nucleosomal filaments (**Fig. 2A**, left upper inset). In the replica membrane preparations, total thickness of platinum metal coating is controlled as a thin layer (1~2 nm), therefore the above-mentioned fibrous structures in the nuclear matrix are probably not much different from their native states in vivo. By the QF-DE method ***(8)***, it is easier to recognize such substructures of the in situ chromatin fibers than the conventional ultrathin section technique (**Fig. 2A**, right lower inset).

1. Cut the PF-perfused prostatic tissues into small pieces with razor blades and wash in PB for 10 min (**Fig. 3A–B**).
2. Treat them with 1% saponin in PB for 60 min to remove cytoplasmic soluble proteins from prostatic epithelial cells and wash in PB for 30 min (**Fig. 3B**).
3. Treat additionally them with 5 μg/mL proteinase K in PBS for 30 min and wash in PB for 30 min.
4. Postfix the treated specimens with 0.25% GL in PB for 30 min and wash in PB for 10 min.
5. Immerse them in distilled water for removal of salts and further rinse with 10% methanol to prevent ice crystal formation during the following quick-freezing step.
6. Mount them on a specimen copper holder (**Fig. 3C**) and quickly freeze in a JFD-RFA quick-freezing apparatus (JEOL, Tokyo, Japan) after removal of excess fluid with filter paper, using a pure copper metal block cooled in liquid nitrogen (–196°C) (**Fig. 3D**).
7. Freeze-fracture tissue surface areas of the frozen specimens with a scalpel in liquid nitrogen to expose cracked nuclear matrices (**Fig. 3E**).
8. Transfer them onto a stage precooled at –160°C in an Eiko FD-3AS freeze-fracture apparatus equipped with a turbo molecular pump (Eiko Engineering Co., Mito, Japan) and deeply etch at a temperature of –95°C under vacuum conditions of $2–6 \times 10^{-7}$ Torr for 15–20 min (**Fig. 3F**).
9. Shadow the specimens on a rotary stage with platinum metal at an angle of 28° without rotation for several seconds and then rotary-shadow up to a total thickness of 2 nm (**Fig. 3F**). Shadow them additionally with carbon at an angle of 90°.

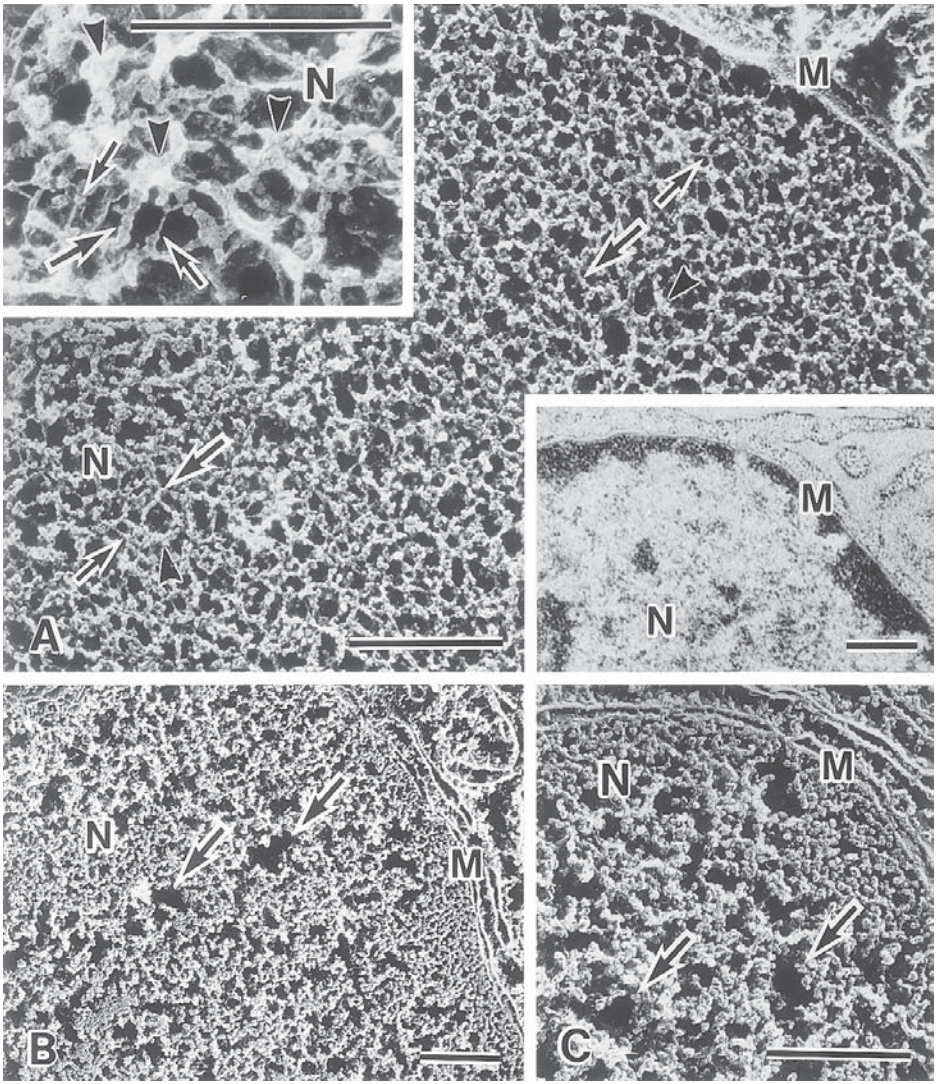

Fig. 2. Replica electron micrographs of normal nuclei **(A)** and DNase-treated nuclei (**B** and **C**). N; nucleus. M; nuclear membrane. Scale bars=0.5 μm. **(A)** Three types of fibrous structures are seen in the normal nucleus, including 20–30 nm fibers (arrowheads), 5–10 nm filaments (large arrows), and 2–5 nm fine filaments (small arrow). Left upper inset; higher magnification. Right lower inset; ultrathin section image. **(B)** and **(C)** The 2–5 nm fine filaments are rarely seen in nuclei after the DNase I treatment (arrows). **(C)** Higher magnification.

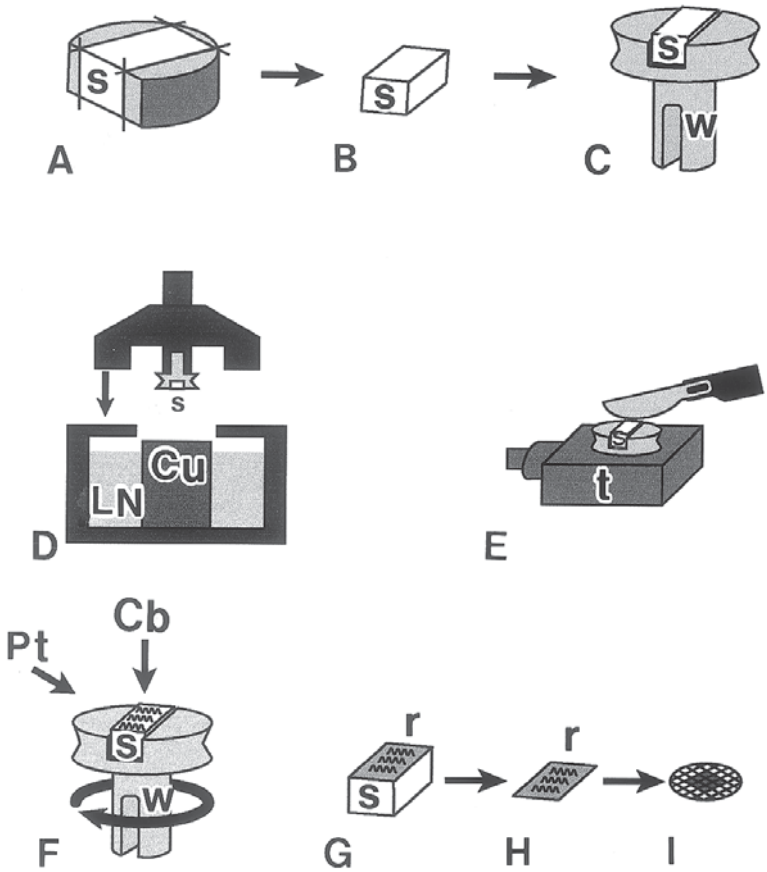

Fig. 3. **(A)** and **(B)** Prostatic specimen preparation. s; specimen. **(C)** Put on a copper holder (w). **(D)** Quick-freezing step. LN; liquid nitrogen. Cu; cooled copper block. **(E)** Freeze-fracturing step in liquid nitrogen. t; transfer carrier **(F)** Deep-etching and rotary-shadowing with platinum (Pt) and carbon (Cb). **(G)** and **(H)** Replica membrane (r) preparation. s; specimen. **(I)** Put on Formvar-filmed grid.

10. Coat the replica membranes with the specimens, upon being taken out of the apparatus, with drops of 2% collodion diluted in amylacetate to prevent their breaking into pieces during the following digestion procedure (**Fig. 3G**) (*see* **Note 1**).
11. Check the collodion dryness by a stereomicroscope, while the frozen tissue is thawing. Put the whole sample into the household bleach, when the collodion is judged to be almost dried up (*see* **Note 2**).
12. Dissolve the wet prostatic tissues with the replica membranes and dried collodion film in solution of commercialized household bleach, for 15–30 min to dissolve away the tissue components (**Fig. 3H**).

13. Pick up the replica membrane with the collodion kept in the household bleach and transferred into distilled water using a tiny piece of filter paper held with a pair of titanium tweezers, because the household bleach is corrosive.
14. Wash thoroughly the replica membrane in distilled water to remove the household bleach from it, at least 3×, 5 min each.
15. Wash the large replica membranes (2 mm × 3 mm) with the collodion film in distilled water and cut into small pieces with scissors. Pick them up on Formvar-filmed copper grids (*see* **Note 3**).
16. Dip the replica membranes with the dried collodion on the copper grid in amylacetate solution for a few seconds and immediately dried up again at room temperature. In such a treatment, the replica membranes are firmly attached to the Formvar membrane.
17. Immerse them in amylacetate solution to dissolve out the dried collodion for 30 min (**Fig. 3I**).
18. Observe them in an electron microscope at an accelerating voltage of 75 kV. Print electron micrographs from the inverted negative films, so that areas of platinum deposition look bright, in contrast with dark backgrounds. Take some electron micrographs in stereo at ±5° tilting angles.

3.2. TUNEL Technique for QF-DE Method

In Situ Apoptosis Detection Kit, ApopTag® Peroxidase [Serologicals Corp. (formerly Intergen) Gaithersburg, MD] is commercially available ***(8,18)***, it is based on the method developed by Gavrieli et al. ***(15)*** with minor modifications.

1. Cut the PF-perfused prostatic tissues into small pieces with razor blades, and additionally fix with 2% PF in PB for 1 h.
2. Treat them with 1% saponin in PB for 60 min and 1 μg/mL proteinase K in PBS at room temperature for 10 min, followed by washing in PB for 30 min.
3. Quench such treated tissues with 0.1% sodium azide in PBS for 15 min to block endogenous peroxidase.
4. Immerse them in equilibration buffer solution after washing in PBS for 15 min, and react with terminal deoxynucleotidyl transferase (TdT) enzyme containing TdT and digoxigenin-labeled deoxyuridine triphosphate at 37°C for 60 min. As a negative control, omit the TdT treatment from the labeling mixture.
5. React them with anti-digoxigenin-peroxidase conjugate for 30 min at room temperature after their immersion in working strength stop/wash buffer at 37°C for 30 min and wash in PBS for 20 min.
6. Visualize them with DAB-H_2O_2 solution for 2 min.
7. Process them for the QF-DE method (*see* **Subheading 3.1.5.**).

3.3. DNase I Treatment for QF-DE Method

We use DNase I treatment to detect DNA strand structures. When normal nuclei are treated with DNase I, their intranuclear networks are changed into

some fragments resembling apoptotic ones (**Fig. 2B**). The number of 2–5 nm fine filaments decreased after the DNase I treatment (**Fig. 2C**). The DNase I might be different from their active DNase during apoptosis ***(26)***, but it was assumed to act like an original DNase.

1. Process some normal PF-fixed prostatic tissues through the routine 1% saponin and 5 µg/mL proteinase K treatments, as described before (*see* **Subheading 3.1.2.**).
2. Treat them with 1 µg/mL deoxyribonuclease I (DNase I) in the digestion buffer for 20 min at room temperature, and then wash in PBS.
3. Process them for the QF-DE method as described before after the postfixation with 0.25% GL in PB for 15 min (*see* **Subheading 3.1.5.**).

4. Notes

1. The liquid collodion must be quickly applied onto a replica membrane with the frozen prostatic tissue to avoid frost attachment at low temperature (probably the sample temperature is very low, –100 to –150°C, when it is taken out from the freeze-fracture apparatus).
2. Please don't dry up the tissue specimen. Because, if you dry up not only the collodion but also the specimen, the replica membrane can be easily collapsed and fragmented later during the collodion dissolution in amylacetate. So, it is important to put the wet tissue specimen with the dried collodion into the household bleach.
3. When the replica membrane with the collodion is picked up from distilled water onto a Formvar-filmed copper grid and dried again at room temperature, it is not yet firmly attached to the Formvar membrane. In this step, the replica membrane side, not the collodion side, must be facing the Formvar membrane.

References

1. Ansari, B., Coates, P. J., Greenstein, B. D. and Hall, P. A. (1993) In situ end-labeling detects DNA strand breaks in apoptosis and other physiological and pathological states. *J. Pathol.* **170,** 1–8.
2. Dini, L., Coppola, S., Ruzittu, M. T. and Ghibelli, L. (1996) Multiple pathways for apoptotic nuclear fragmentation. *Exp. Cell Res.* **223,** 340–347.
3. Falcieri, E., Zamai, L., Santi, S., Cinti, C., Gobbi, P., Bosco, D., Cataldi, A., Betts, C. and Vitale M. (1994) The behaviour of nuclear domains in the course of apoptosis. *Histochemistry* **102,** 221–231.
4. Evans, G. S. and Chandler, J. A. (1987) Cell proliferation studies in the rat prostate: II. the effects of castration and androgen-induced regeneration upon basal and secretory cell proliferation. *The Prostate* **11,** 339–351.
5. Furuya, T., Kubo, M., Ueno, A., Fujii, Y., Baba, T. and Ohno, S. (2000) Histochemical study of apoptotic epithelial cells depending on testosterone in primary cultured rat prostatic tissues. *Histol. Histopathol.* **15,** 385–394.
6. Banerjee, P. P., Banerjee, S., Tilly, K. I., Tilly, J. L., Brown, T. R. and Zirkin, B. R. (1995) Lobe-specific apoptotic cell death in rat prostate after androgen ablation by castration. *Endocrinology* **136,** 4368–4376.

7. English, H. F., Kyprianou, N. and Isaacs, J. T. (1989) Relationship between DNA fragmentation and apoptosis in the programmed cell death in the rat prostate following castration. *The Prostate* **15,** 233–250.
8. Kubo, M., Uchiyama, H., Ueno, A., Terada, N., Fujii, Y., Baba, T. and Ohno, S. (1998) Three-dimensional ultrastructure of apoptotic nuclei in rat prostatic epithelial cells revealed by a quick-freezing and deep-etching method. *The Prostate* **35,** 193–202.
9. Kyprianou, N., English, H. F. and Isaacs, J. T. (1988) Activation of a Ca^{2+}-Mg^{2+}-dependent endonuclease as an early event in castration-induced prostatic cell death. *The Prostate* **13,** 103–117.
10. Montague, J. W. and Cidlowski, J. A. (1996) Cellular catabolism in apoptosis: DNA degradation and endonuclease activation. *Experientia* **52,** 957–962.
11. Allen, T. D. (1989) The organization and substructure of chromatin fibres in the interphase nucleus as studied by scanning electron microscopy. *Scanning Microsc. [Suppl.]* **3,** 77–86.
12. Haggis, G. H. and Bond, E. F. (1978) Three-dimensional view of the chromatin in freeze-fractured chicken erythrocyte nuclei. *J. Microsc.* **115,** 225–234.
13. Tanaka, K. and Iino, A. (1973) Demonstration of fibrous components in hepatic interphase nuclei by high resolution scanning electron microscopy. *Exp. Cell Res.* **81,** 40–46.
14. Gaffney, E. F., O'Neill, A. J. and Staunton, M. J. (1995) In situ end-labeling, light microscopic assessment and ultrastructure of apoptosis in lung carcinoma. *J. Clin. Pathol.* **48,** 1017–1021.
15. Gavrieli, Y., Sherman, Y. and Ben-Sasson, S. A. (1992) Identification of programmed cell death in situ via specific lebeling of nuclear DNA fragmentation. *J. Cell Biol.* **119,** 493–501.
16. Kasagi, N., Adachi, H., Ueno, E., Hayashi, H. and Ito, H. (1996) Initial phase of apoptosis detected by terminal deoxynucleotidyl transferase-mediated dUTP-biotin nick end-labeling in UV-irradiated HL-60 cells: morphological and biochemical findings of DNA fragmentation. *Biomed. Res.* **17,** 385–393.
17. Wijsman, J. H., Jonker, R. R., Keijzer, R., van de Velde, C. J. H., Cornelisse, C. J. and van Dierendonk, J. H. (1993) A new method to detect apoptosis in paraffin sections: in situ end-labeling of fragmented DNA. *J. Histochem. Cytochem.* **41,** 7–12.
18. Hayashi, R., Ito, Y., Matsumoto, K., Fujino, Y. and Otsuki Y. (1998) Quantitative differentiation of both free 3'-OH and 5'-OH DNA ends between heat-induced apoptosis and necrosis. *J. Histochem. Cytochem.* **46,** 1051–1059.
19. Migheli, A., Attanasio, A. and Schiffer, D. (1995) Ultrastructural detection of DNA strand breaks in apoptotic neural cells by in situ end-labeling techniques. *J. Pathol.* **176,** 27–35.
20. Saitoh, T. (2000) Detection of VP-16-treated HL-60 cell apoptosis by TUNEL electron microscopy. *Ultrastruc. Pathol.* **24,** 99–103.
21. Sanders, E. J. and Wride, M. A. (1996) Ultrastructural identification of apoptotic nuclei using the TUNEL technique. *Histochem. J.* **28,** 275–281.

22. Allera, C., Lazzarini, G., Patrone, E., Alberti, I., Barboro, P., Sanna, P., Melchiori, A., Parodi, S. and Balbi, C. (1997) The condensation of chromatin in apoptotic thymocytes shows a specific structural change. *J. Biol. Chem.* **272,** 10,817–10,822.
23. Weaver, V. M., Carson, C. E., Walker, P. R., Chaly, N., Lach, B., Raymond, Y., Brown, D. L. and Sikorska, M. (1996) Degradation of nuclear matrix and DNA cleavage in apoptotic thymocytes. *J. Cell Sci.* **109,** 45–56.
24. Ohno, S. and Fujii, Y. (1990) Three-dimensional and histochemical studies of peroxisomes in cultured hepatocytes by quick-freezing and deep-etching method. *Histochem. J.* **22,** 143–154.
25. Ohno, S. and Fujii, Y. (1991) Three-dimensional studies of the cytoskeleton of cultured hepatocytes: a quick-freezing and deep-etching study. *Virchows Arch. [A] Pathol. Anat.* **418,** 61–70.
26. Anzai, N., Kawabata, H., Hirama, T., Masutani, H., Ueda Y., Yoshida, Y. and Okuma, M. (1995) Types of nuclear endonuclease activity capable of inducing internucleosomal DNA fragmentation are completely different beween human $CD34^+$ cells and their granulocytic descendants. *Blood* **86,** 917–923.

6

In Situ Detection of DNA Strand Breaks in Analysis of Apoptosis by Flow- and Laser-Scanning Cytometry

Zbigniew Darzynkiewicz, Elzbieta Bedner, and Piotr Smolewski

1. Introduction

The presence of a multitude of DNA strand breaks resulting from fragmentation of nuclear DNA by the caspase-activated DNase is one of the most characteristic features of apoptotic cells ***(1,2)***. A widely used methodology to detect apoptotic cells, thus, relies on labeling DNA strand breaks in situ, within the nuclear chromatin, either with fluorochromes ***(3–5)*** or absorption dyes ***(6–8)***. The overview of the techniques (TUNEL techniques), which were developed independently by Gavrieli et al., ***(6)*** and by us ***(3–5)*** is presented in Chapter 3. One advantage of strand break labeling with fluorochromes is that such cells can rapidly be analyzed by flow cytometry. When cellular DNA content also is measured in these cells, the bivariate analysis of such data provides information about DNA ploidy or the cell cycle phase specificity of apoptosis ***(3,9)***.

The method presented in this Chapter can be applied to cells measured by flow cytometry, and its modification, also included here, to cells attached on microscope slides The latter can be analyzed by a new type of the instrument, the Laser Scanning Cytometer (LSC). LSC is the microscope-based cytofluorimeter which allows one to measure rapidly, with high sensitivity and accuracy, fluorescence of individual cells ***(10,11)***. The instrument combines advantages of both flow and image cytometry. Cells staining on slides eliminates their loss that otherwise occurs during repeated centrifugations in sample preparation for flow cytometry. Another advantage of LSC stems from the possibility of localization of cells on slide for their visual inspection or morphometry after the initial measurement of large cell population and electronic selection (gating)

From: *Methods in Molecular Biology, vol. 203:* In Situ *Detection of DNA Damage: Methods and Protocols*
Edited by: V. V. Didenko

of cells of interest. Visual examination is of particular importance because the characteristic changes in cell morphology ***(12)*** are still considered the gold standard for positive identification of apoptotic cells. Furthermore, the measured cells can be bleached and re-stained with another set of dyes ***(13)***. The cell attributes measured after re-staining can be correlated with the attributes measured before, on a cell by cell basis ***(13,14)***.

Fixation and permeabilization of the cells are the initial essential steps to successfully label DNA strand breaks. Cells are briefly fixed with a crosslinking fixative such as formaldehyde, and then permeabilized by suspending them in ethanol or using detergents in the subsequent rinses. By crosslinking low MW DNA fragments to other cell constituents, formaldehyde prevents extraction of the fragmented DNA, which otherwise occurs during repeated centrifugations and rinses required by this procedure ***(3–5)***. The 3'OH-termini of the DNA breaks serve as primers and become labeled in this procedure with BrdU when incubated with BrdUTP in a reaction catalyzed by exogenous terminal deoxynucleotidyl transferase (TdT) ***(15,16)***. The incorporated BrdU is immunocytochemically detected by BrdU antibody conjugated to FITC ***(15)***. The latter is a reagent widely used in studies of cell proliferation to detect BrdU incorporated during DNA replication ***(17)***. The overall cost of reagents is significantly lower and sensitivity of DNA strand breaks detection is higher when BrdUTP is used as a marker, compared to the alternative labeling with biotin- (or digoxygenin-) or directly fluorochrome-tagged deoxynucleotides ***(15)***. However, the alternate procedures, utilizing digoxygenin, biotin or directly labeled deoxynucleotides, also are described in the Chapter.

2. Materials

2.1. Reagents and Glassware

1. Phosphate-buffered saline (PBS), pH 7.4.
2. 1% Formaldehyde (methanol-free, "ultrapure," Polysciences, Warrington, PA), in PBS, pH 7.4.
3. 70% Ethanol.
4. TdT (Boehringer Mannheim, Indianapolis, IN). TdT 5× reaction buffer: 1 *M* potassium (or sodium) cacodylate, 125 m*M* HCl, pH 6.6 (this 5× reaction buffer may be purchased from Boehringer Mannheim), 1.25 mg/mL bovine serum albumin (BSA, Sigma, St. Louis, MO).
5. 5-Bromo-2'-deoxyuridine-5'-triphosphate (BrdUTP) stock solution (50 µL): 2 m*M* BrdUTP (Sigma) in 50 m*M* Tris-HCl, pH 7.5.
6. 10 m*M* $CoCl_2$ (Boehringer Mannheim).
7. Rinsing buffer: 0.1% Triton X-100 (Sigma) and 5 mg/mL BSA dissolved in PBS.
8. FITC-conjugated anti-BrdU monoclonal antibody (mAb): Dissolve 0.3 µg of FITC-conjugated anti-BrdU mAb (Becton Dickinson, Immunocytometry Systems, San Jose CA) in 100 µL of PBS containing 0.3% Triton X-100 and 1% (w/v) BSA.

9. Propidium iodide (PI) staining buffer: 5 µg/mL PI (Molecular Probes, Eugene, OR) , 100 µg/mL of RNase A (DNase-free) (Sigma) in PBS.
10. Microscope slides (to be used in conjunction with LSC).
11. Coplin jars (to be used in conjunction with LSC).
12. Parafilm "M" (American National Can, Greenwich, CT) (to be used in conjunction with LSC).
13. Glycerol (to be used in conjunction with LSC).

2.2. Commercial Kits

Several kits for labeling DNA strand breaks are commercially available. Three kits have been tested by us. The APO-BRDU kit (Phoenix Flow Systems, San Diego, CA) uses a BrdUTP methodology similar to that described in this chapter. As mentioned, this methodology offers the most sensitive means of DNA strand break detection ***(15)***. The APO-DIRECT kit (also from Phoenix) offers a single-step labeling of DNA strand breaks with the fluorochrome-tagged deoxynucleotide. Its virtue is simplicity, but it is less sensitive than the APO-BRDU. The positive and negative control cells are supplied with each of these Phoenix kits. Widely used is the two-step kit utilizing digoxygenin-dUTP (ApopTag) provided by Serologicals Corp. (formerly Intergen) Gaithersburg, MD. A plethora of other kits for DNA strand break labeling is available from different vendors

2.3. Instrumentation

Flow cytometers of different types, offered by several manufacturers, can be used to measure cell fluorescence following staining according to the procedures described below. The manufacturers of the most common flow cytometers are Coulter Corporation (Miami, FL), Becton Dickinson Immunocytometry Systems (San Jose, CA), Cytomation (Fort Collins, CO) and PARTEC (Zurich, Switzerland). The multiparameter Laser Scanning Cytometer (LSC) is available from CompuCyte, Inc., (Cambridge, MA). Cytospin centrifuge, which is used in conjunction with LSC, is provided by Shandon (Pittsburgh, PA).

The software to deconvolute the DNA content frequency histograms, to analyze the cell cycle distributions, is available from Phoenix Flow Systems (San Diego, CA) and Verity Software House (Topham, MA).

3. Methods

3.1. DNA Strand Break Labeling with BrdUTP for Analysis by Flow Cytometry

1. Suspend 1–2 × 10^6 cells in 0.5 mL PBS. With a Pasteur pipette transfer this suspension into a 5 mL polypropylene tube (*see* **Note 2**) containing 4.5 mL of ice cold 1% formaldehyde (*see* **Note 3**). Keep the tube for 15 min on ice.

2. Centrifuge at 300*g* for 5 min and resuspend cell pellet in 5 mL of PBS. Centrifuge again and resuspend cell pellet in 0.5 mL of PBS. With a Pasteur pipette transfer the suspension to a tube containing 4.5 mL of ice-cold 70% ethanol. The cells can be stored in ethanol, at –20°C for several weeks.
3. Centrifuge at 200*g* for 3 min, remove ethanol, resuspend cells in 5 mL of PBS and centrifuge at 300*g* for 5 min.
4. Resuspend the pellet in 50 µL of a solution containing:
   - 10 µL TdT 5× reaction buffer.
   - 2.0 µL of BrdUTP stock solution.
   - 0.5 µL (12.5 units) TdT.
   - 5 µL $CoCl_2$ solution.
   - 33.5 µL distilled H_2O.
5. Incubate the cells in this solution for 40 min at 37°C (*see* **Notes 4** and **5**).
6. Add 1.5 mL of the rinsing buffer, and centrifuge at 300*g* for 5 min).
7. Resuspend cell pellet in 100 µL of FITC-conjugated anti-BrdUrd mAb solution.
8. Incubate at room temperature for 1h.
9. Add 1 mL of PI staining solution.
10. Incubate for 30 min at room temperature, or 20 min at 37°C, in the dark.
11. Analyze cells by flow cytometry.
    - illuminate with blue light (488 nm laser line or BG12 excitation filter)
    - measure green fluorescence of FITC-anti BrdUrd mAb at 530 ±20 nm.
    - measure red fluorescence of PI at >600 nm.

Fig. 1 shows apoptotic cells detected by the method described in the protocol. Although the cell fluorescence in this Figure was measured by LSC, nearly identical scatterplots are obtained after measurements by flow cytometry.

3.2. DNA Strand Break Labeling with Other Markers for Analysis by Flow Cytometry

As mentioned in **Subheading 1** DNA strand breaks can be labeled with deoxynucleotides tagged with variety of other fluorochromes. For example, the Molecular Probes, Inc., catalog lists several types of dUTP conjugates, including BODIPY dyes (e.g., BODIPY-FL-dUTP), fluorescein, Cascade Blue, Texas Red or dinitrophenyl. Several cyanine dyes conjugates (e.g., CY-3-dCTP) are available from Biological Detection Systems (Pittsburgh, PA). Indirect labeling, *via* biotinylated or digoxygenin conjugated deoxynucleotides offers a multiplicity of commercially available fluorochromes (fluorochrome-conjugated avidin or streptavidin, as well as digoxygenin antibodies) with different excitation and emission characteristics. DNA strand breaks, thus, can be labeled with a dye of any desired fluorescence color and excitation wavelength.

The procedure described in **Subheading 3.1** can be adopted to utilize any of these fluorochromes. In the case of the direct labeling ***(18)***, the fluorochrome-

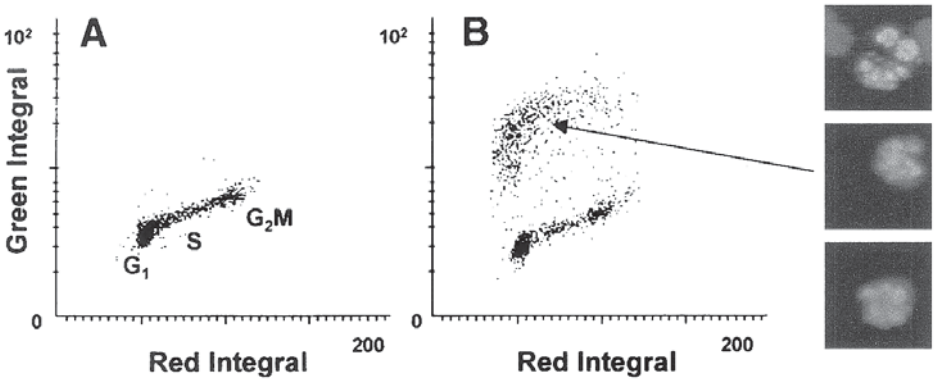

Fig. 1. Detection of apoptotic cells after labeling DNA strand breaks with BrdUTP. U-937 cells were untreated **(A)** or treated with tumor necrosis factor-α in the presence of cycloheximide (**B**, refs. ***22,23)***. The cells were then subjected to DNA strand break labeling and DNA staining as described in the protocol. Cell fluorescence was measured by LSC. The bivariate distributions (scatterplots) allow one to identify apoptotic cells as the cells with labeled DNA strand breaks (strong green fluorescence intensity), and also reveal the cell cycle position of cells in either apoptotic or nonapoptotic population. The cells that showed DNA strand break labeling were relocated, their morphology examined by microscopy and photomicrographs of three such cells are presented. The cells show nuclear fragmentation and chromatin condensation, the typical features of apoptosis ***(12)***.

conjugated deoxynucleotide is included in the reaction solution (0.25–0.5 nmoles per 50 µL) instead of BrdUTP, as described in **step 4** of **Subheading 3.1**. Following the incubation step (**step 5**), omit steps 6–8, and stain cells directly with PI (**step 9**). In the case of the indirect labeling, instead of BrdUTP, digoxygenin- or biotin-conjugated deoxynucleotides are included into the reaction buffer (0.25–0.5 nmoles per 50 µL) at **step 4**. The cells are then incubated either with the fluorochrome conjugated anti-digoxigenin MAb (0.2–0.5 µg per 100 µL of PBS containing 0.1% Triton X-100 and 1% BSA), or with fluorochrome conjugated avidin or streptavidin (0.2–0.5 µg per 100 µL, as above) at **step 7** and then processed through **steps 8–10** as described in the protocol. Analysis by flow cytometry is carried out with excitation and emission wavelengths appropriate to the used fluorochrome.

3.3. DNA Strand Break Labeling for Analysis by LSC

1. Transfer 300 µL of cell suspension (in tissue culture medium, with serum) containing approximately 20,000 cells into a cytospin chamber. Cytocentrifuge at 1,000 rpm for 6 min to deposit the cells on a microscope slide.

2. Without allowing the cytospins to completely dry, prefix the cells by transferring the slides for 15 min to a Coplin jar containing 1% formaldehyde in PBS, cooled to ice temperature.
3. Rinse the slides in PBS and transfer to 70% ethanol; fix in ethanol for at least 1 h; the cells can be stored in ethanol for weeks at –20°C.
4. Follow **steps 4–8** of **Subheading 3.1** as described for flow cytometry. Carefully layer small volumes (approximately 100 µL) of the respective buffers, rinses or staining solutions on the cytospin area of the horizontally placed slides. At appropriate times remove these solutions with Pasteur pipet (or vacuum suction pipet). To prevent drying, place a 2 × 4 cm strip of Parafilm on the slide over the cytospin, atop the drop of the solutions used for cell incubations (*see* **Note 8**).
5. Replace the PI staining solution with a drop of a mixture of glycerol and PI staining solution (9:1) and mount under the coverslips. To preserve the specimen for longer period of time or transport, seal the coverslip with nail polish or melted paraffin.
6. Measure cell fluorescence on LSC.
   - excite fluorescence with 488 nm laser line.
   - measure green fluorescence of FITC-anti BrdUrd MAb at 530 ±20 nm.
   - measure red fluorescence of PI at >600 nm.

The typical results are shown in **Fig. 1**.

3.3. Controls

The procedure of DNA strand break labeling is rather complex and involves many reagents. Negative results, therefore, may not necessarily mean the absence of DNA strand breaks but may be due to methodological problems, such as loss of TdT activity, degradation of BrdUTP, etc. It is necessary, therefore, to include a positive and negative controls. An excellent control is to use HL-60 cells treated (during their exponential growth) for 3–4 h with 0.2 µ*M* of the DNA topoisomerase I inhibitor camptothecin (CPT). Because CPT under these conditions induces apoptosis selectively during S phase, cells in G_1 and G_2/M may serve as negative control populations, while the S phase cells in the same sample, represent the positive control.

Another negative control consist cells processed identically as described in **Subheading 3.1** except that TdT is excluded from **step 4**.

4. Notes

1. This method is useful for clinical material, such as obtained from in leukemias, lymphomas and solid tumors ***(19,20)***, and can be combined with surface immunophenotyping. The cells are first immunophenotyped, then fixed with 1% formaldehyde (which stabilizes the antibody bound on the cell surface) and subsequently subjected to the DNA strand break detection assay using different color fluorochromes (*see* **Subheading 3.1**) than those used for immunophenotyping.

2. If the sample initially contains small number of cells, cell loss during repeated centrifugations is a problem. To minimize cell loss, polypropylene, or siliconized glass tubes are recommended. Since transferring cells from one tube to another results in irreversible electrostatic attachment of a large fraction of cells to the surface of each new tube all steps of the procedure (including fixation) should be done in the same tube. Addition of 1% BSA into rinsing solutions also decreases cell loss. When the sample contains very few cells, the carrier cells, which later can be recognized based on differences in DNA content (e.g., chick erythrocytes) may be included. Cell analysis by LSC, of course, has no such problem.
3. Cell cell pre-fixation with a crosslinking agent such as formaldehyde is required to prevent extraction of the fragmented DNA from apoptotic cells ***(3,4)***. This ensures that despite the repeated cell washings during the procedure, the DNA content of apoptotic cells (and with it the number of DNA strand breaks) is not markedly diminished.
4. Alternatively, incubate at room temperature overnight.
5. Control cells may be incubated in the same solution, but without TdT.
6. It is generally easy to identify apoptotic cells, due to their intense labeling with FITC conjugated anti-BrdU mAb. The high fluorescence intensity often requires use of the exponential scale (logarithmic amplifiers of the flow cytometer or LSC) for data acquisition and display (**Fig. 1**). As it is evident in this Figure, because cellular DNA content of both apoptotic and nonapoptotic cell populations is measured, the cell cycle distribution and/or DNA ploidy of these both populations can be estimated.
7. While the presence of extensive DNA breakage, detected following strand break labeling, by the strong fluorescence, is a very characteristic feature of apoptosis, a weak fluorescence may not necessarily mean the lack of apoptosis. In some cell systems DNA fragmentation stops at 300–50 kb size DNA fragments and does not progress into internucleosomal sections ***(21)***.
8. It is essential that the incubations are carried out in moist atmosphere to prevent drying at any step of the procedure. Even minor drying produces severe artifacts.

Acknowledgment

Supported by NCI grant RO1 28704, “This Close” Foundation for Cancer Research and Chemotherapy Foundation.

References

1. Nagata, S. (2000) Apoptotic DNA fragmentation. *Exp. Cell Res.* **256,** 12–18.
2. Enari, M., Sakahira, H., Yokoyama, H., Okawa, K., Iwamatsu, A and Nagata, S. (1998) A caspase-activated DNase that degrades DNA during apoptosis and its inhibitor ICAD. *Nature* **391,** 43–50.
3. Gorczyca, W., Bruno, S., Darzynkiewicz, R. J., Gong, J., and Darzynkiewicz, Z. (1992) DNA strand breaks occurring during apoptosis: Their early *in situ* detection by the terminal deoxynucleotidyl transferase and nick translation assays and prevention by serine protease inhibitors. *Int. J. Oncol.* **1,** 639–648.

4. Darzynkiewicz, Z., Bruno, S., Del Bino, G., Gorczyca, W., Hotz, M. A., Lassota, P., and Traganos, F. (1992) Features of apoptotic cells measured by flow cytometry. *Cytometry* **13,** 795–808.
5. Darzynkiewicz, Z., Juan, G., Li, X., Gorczyca, W., Murakami, T., and Traganos, F. (1997) Cytometry in cell necrobiology: analysis of apoptosis and accidental cell death (necrosis). *Cytometry* **27,** 1–20.
6. Gavrieli, Y., Sherman Y., and Ben-Sasson S. A. (1992) Identification of programmed cell death in situ via specific labeling of nuclear DNA fragmentation. *J. Cell Biol.* **119,** 493–501.
7. Gold, R., Schmied, M., Rothe, G., Ziechler, H., Breitschopf, H., Wekerle, H., and Lassman, H. (1993) Detection of DNA fragmentation in apoptosis: Application of *in situ* nick translation to cell culture systems and tissue sections. *J. Histochem. Cytochem.* **41,** 1023–1030.
8. Wijsman, J. H., Jonker, R. R., Keijzer, R., Van De Velde, C. J. H., Cornelisse, C. J., and Van Dierendonck, J. H. (1993) A new method to detect apoptosis in paraffin sections: In situ end-labeling of fragmented DNA. *J. Histochem. Cytochem.* **41,** 7–12.
9. Gorczyca, W., Gong, J., Ardelt , B., Traganos, F. and Darzynkiewicz, Z. (1993) The cell cycle related differences in susceptibility of HL-60 cells to apoptosis induced by various antitumor drugs. *Cancer Res.* **53,** 3186–3192
10. Kamentsky, L. A. (2001) Laser scanning cytometry. *Meth Cell Biol.* **63,** 51–87.
11. Darzynkiewicz, Z., Bedner, E., Li, X., Gorczyca, W., and Melamed, M. R. (1999) Laser scanning cytometry. A new instrumentation with many applications. *Exp. Cell Res.* **249,** 1–12.
12. Kerr, J. F. R., Wyllie, A. H., and Curie, A.R, (1972) Apoptosis: a basic biological phenomenon with wide-ranging implications in tissue kinetics. *Br. J. Cancer* **26,** 239–257.
13. Bedner, E., Du, L., Traganos, F., and Darzynkiewicz, Z. (2001) Caffeine dissociates complexes between DNA and intercalating dyes: application for bleaching fluorochrome-stained cells for their subsequent restaining and analysis by laser scanning cytometry. *Cytometry* **43,** 38–45.
14. Li, X., and Darzynkiewicz, Z. (1999). The Schrödinger's cat quandary in cell biology: integration of live cell functional assays with measurements of fixed cells in analysis of apoptosis. *Exp. Cell Res.* **249,** 404–412.
15. Li, X., and Darzynkiewicz, Z. (1995) Labeling DNA strand breaks with BrdUTP. Detection of apoptosis and cell proliferation. *Cell Prolif.* **28,** 571–579.
16. Li, X., Melamed, M. R., and Darzynkiewicz, Z. (1996) Detection of apoptosis and DNA replication by differential labeling of DNA strand breaks with fluorochromes of different color. *Exp. Cell Res.* **222,** 28–37.
17. Dolbeare, F., and Selden, J. R. (1994) Immunochemical quantitation of bromodeoxyuridine: Application to cell cycle kinetics. *Meth. Cell Biol.* **41,** 297–316.
18. Li, X., Traganos, F., Melamed, M. R., and Darzynkiewicz, Z. (1995) Single-step procedure for labeling DNA strand breaks with fluorescein- or BODIPY-conjugated deoxynucleotides: Detection of apoptosis and bromodeoxyuridine incorporation. *Cytometry* **20,** 172–180.

19. Halicka, H. D., Seiter, K., Feldman, E. J., Traganos, F., Mittelman, A., Ahmed, T., and Darzynkiewicz, Z. (1997) Cell cycle specificity during treatment of leukemias. *Apoptosis* **2,** 25–39.
20. Li, X, Gong, J., Feldman, E., Seiter, K., Traganos, F., and Darzynkiewicz, Z. (1994) Apoptotic cell death during treatment of leukemias. *Leukemia and Lymphoma* **13,** 65–72.
21. Oberhammer, F., Wilson, J. W., Dive, C., Morris, I. D., Hickman, J. A., Wakeling, A. E., Walker, P. R., and Sikorska, M. (1993) Apoptotic death in epithelial cells: Cleavage of DNA to 300 and 50 kb fragments prior to or in the absence of internucleosomal degradation. of DNA. *EMBO J.* **12,** 3679–3684.
22. Li, X., and Darzynkiewicz, Z.(2000) Cleavage of poly(ADP-ribose) polymerase measured in situ in individual cells: relationship to DNA fragmentation and cell cycle position during apoptosis. *Exp. Cell Res.* **255,** 125–132.
23. Bedner, E., Smolewski, P., Amstad, P., and Darzynkiewicz, Z. (2000) Activation of caspases measured in situ by binding of fluorochrome-labeled inhibitors of caspases (FLICA): correlation with DNA fragmentation. *Exp. Cell Res.* **260,** 308–313.

7

DNA Damage Detection Using DNA Polymerase I or its Klenow Fragment

Applicability, Specificity, Limitations

Jan Hein van Dierendonck

1. Introduction

Mainly as a result of the booming interest in apoptosis and of the discovery of the occurrence of massive DNA breaks as a major feature of this type of cell death, during the past few years polymerase-based assays for detection of DNA breaks in cellular nuclei have found worldwide application in many fields of cellular biology and medicine. This interest has greatly stimulated research on technical improvements of the assays and has led to the availability of a variety of commercial kits for that purpose.

The basic concept is as follows:

1. Fixed cells or tissue sections are permeabilized, e.g. by using proteolytic enzymes.
2. A mixture is added of labeled nucleotides and either enzymes that, under proper conditions, are able to incorporate these nucleotides into gaps or nicks in one of the strands of the double DNA helix—or on recessing strands at double strand breaks—or enzymes that do not need a single-strand DNA template, but can produce a polymer of labeled nucleotides on blunt ended breaking points; this type of DNA labeling reactions is performed in special buffers containing divalent cations.
3. A method is applied to visualize the DNA-incorporated labeled nucleotides, appropriate either for detection of cells with DNA breaks by flow cytometry or for *in situ* detection of these cells, e.g. for evaluation by microscopy.

It should not be forgotten though that this type of DNA-labeling procedures were already in use many decades ago for quite different purposes and it is the primary aim of this chapter to present a general overview of key publications

From: *Methods in Molecular Biology, vol. 203:* In Situ *Detection of DNA Damage: Methods and Protocols*
Edited by: V. V. Didenko

on the applicability of DNA polymerases for detection of DNA breaks in various experimental conditions. But because of its importance for apoptosis research, a special subparagraph is devoted to the process of apoptosis in the context of what is known about endonuclease activities, followed in **Subheading 3.2** by a discussion of the relevance of these activities—and thus of the specificity and limitations of DNA break detection in cell death research.

Subsequently it is described how different research groups rediscovered DNA labeling assays to visualize apoptosis and studies are reviewed in which different approaches were compared with respect to their specificities towards different types of cell death. A special paragraph is devoted to different pretreatments of paraffin-embedded tissue sections.

This chapter is followed by technical reviews presenting several detailed protocols and troubleshooting, electron microscopic modification of the labeling procedure, and colabeling of DNA damage and specific cellular proteins.

2. Development of *In Situ* DNA Labeling

2.1. Characterization of DNA Polymerase Activities and the Invention of In Situ DNA Labeling

In the late fifties, Kornberg's research group purified from extracts of *E. coli,* an enzyme that catalyzed the incorporation of deoxyribonucleotides into DNA. All four deoxynucleotide triphosphates (dNTPs), a certain amount of polymerized DNA, and magnesium ions were required for its activity and the enzyme was named 'polymerase' ***(1)***. Independently, Bollum described the partial purification of an enzyme activity from mammalian tissue with similar characteristics ***(2)***; when ethanol-fixed cells on glass slides were incubated with calf thymus polymerase and dNTPs including ^{3}H-dATP, autoradiography revealed activity in interphase nuclei and mitotic chromosomes, provided that low-pH conditions had been applied prior to the polymerase reaction ***(3)***. Application to paraffin sections from ethanol-fixed chicken embryo lenses confirmed requirement of acid- or alkali-denaturation of DNA to detect nuclear label and revealed that highest labeling intensity was present in pycnotic nuclei. In line with earlier biochemical analyses that had demonstrated a net loss of DNA from the fiber area in bovine lenses, this *in situ* DNA end labeling (ISEL) method demonstrated extensive DNA strand scission in degenerating nuclei ***(4)***.

Subsequently, Modak & Bollum applied on similar sections calf thymus deoxynucleotidyl transferase (Terminal deoxynucleotide Transferase, TdT), an enzyme known to catalyze on single-stranded DNA with free 3'-OH an end-addition synthesis of a deoxynucleotide homopolymer. Now they also observed incorporation of ^{3}H-dATP in non-denatured DNA of degenerating fiber cell nuclei and occasionally in nuclei with no altered gross morphology. DNA dena-

turation turned all types of nuclei positive, but again, the advanced pycnotic nuclei showed the strongest labeling intensity ***(5)***. Was this a result of hypothetical endogenous DNases that use the 3'-OH site as target? Because during lens fiber differentiation not only the proportion of positive nuclei increased but also the relative number of breaks per nucleus: was there a gradual loss of DNA repair function ***(6)***? Interestingly, determination of the size of DNA present in central fiber cells from 15–21 d embryos revealed low molecular weight DNA appearing as multiples of a monomeric unit and being similar to the fragments produced by digestion of nuclei by micrococcal nuclease (MNase). Thus, double-strand breaks indeed seemed to occur as part of a normal process of nuclear autodigestion ***(7)***.

The further characterization of activities of *E. coli* DNA polymerase (Pol I) had led to the discovery that double stranded DNA serves as a template primer when the DNA contains a single strand break (a 'nick') with a 3'-OH terminus. Initiation of replication was found to entail covalent extension of the 3'OH-terminus and a concurrent 5'→3' nuclease action by the enzyme—the primer strand being hydrolyzed at the 5' side of the nick, while the synthetic activity catalyzed the addition of nucleotides to the 3' side. Thus, the ability to promote hydrolysis and synthesis simultaneously resulted in the translation of the nick along the DNA duplex in the 5'→3' direction ***(8)***. It was also discovered that cleavage of the polymerase by limited proteolytic action (preferably by the enzyme subtilisin) resulted into two fragments of 76 kDa and 34 kDa, the former still having the polymerizing but not the 5'→3' nuclease activity ***(9)***, whereas the latter retained only 5'→3' exonuclease activity ***(10)***. This phenomenon was independently described by Klenow & Henningsen and the large fragment is now generally referred to as 'Klenow fragment' ***(11)***.

In addition to its 5'→3' exonuclease activity, the Pol I holoenzyme can also function as a 3'→5' exonuclease (and even has a RNase activity); the 3'→5' exonuclease proofreading activity, which is more active on single-stranded than on double-stranded DNA and is retained in the Klenow fragment, results in removal of 3' protruding termini. In fact, this activity also removes nucleotides from the double strand, but in the presence of dNTPs the polymerase activity counteracts further degradation: the nucleotide at the 3'OH end will then be continuously replaced ***(12,13)***. Under certain conditions, the Klenow fragment can even add a single nucleotide to the 3'OH of a blunt end—thus not requiring coding information from the DNA template ***(14)***.

2.2. Early Improvements and Applications of Nick Translation with Pol I or Klenow Fragment

Levitt and coworkers pioneered the use of nick translation reactions with Pol I on intact nuclei (*in situ* nick translation, ISNT). It had been found that

when nuclei of many types of organisms were partially digested with DNase I, the active genes were in a special sensitive conformation; by treating DNase I-treated oviduct nuclei with Pol I and dNTPs (including ^{32}P-dTTP) they were able to show that over 85% of the label was incorporated into the sequences that were transcribed into RNA ***(15)***. Subsequently it was established that DNase I, DNase II, and MNase preferentially nicked active chromosomal segments. The finding that active genes were sensitive to DNase I to the same degree in mitotic chromosomes and interphase nuclei indicated that these enzymes could be used as structural probes for gene expression ***(16,17)***.

The sensitivity and accuracy of this approach was substantially increased with the introduction of biotinylated dUTP, that was found to be able to replace dTTP ***(18)***, and the use of avidin-biotin-peroxidase complex in combination with the peroxidase reaction with H_2O_2/diaminobenzidine, which results in precipitation of a brown complex ***(19)***. Excellent results visualizing biotin-dUTP in metaphase chromosomes were obtained by using streptavidin-peroxidase complex ***(20)***, or a goat anti-biotin IgG followed by a biotinylated rabbit anti-goat antibody and streptavidin-biotin-peroxidase complex (sABC) ***(21)***. By using this protocol, it became evident that the specific chromosomal banding pattern from this technique (dark D-bands) corresponded with bands obtained by Giemsa staining (light G-bands) known to represent early replicating DNA or potentially active gene regions ***(22)***. Because the exonuclease activity of Pol I was thought to be an important determinant of sensitivity, it came to a surprise that no difference in sensitivity could be detected between Pol I and the Klenow fragment in this respect; it was conjectured that this could be due at least in part to the lower molecular weight of the latter, a feature that would guarantee a more easy access to the chromatin breaks ***(23)***.

An entirely different application of nick translation was introduced by Nose & Okamoto: the detection of DNA breaks induced by DNA damaging agents. Fibroblasts were treated with these agents, harvested with trypsin and permeabilized with lysolecithin. Nick translation was performed in the presence of ^{3}H-dCTP and Pol I and radioactivity was measured on sonicated and filtrated cell samples. Performance of the procedure at different time intervals after removal of the genotoxic agent revealed that the radioactivity rapidly decreased to control levels, indicating loss (repair) of initial damage ***(24)***. Application of this assay to monitor DNA damage and repair of 28 carcinogens led to the conclusion that it had predictive capability at least equal to that of unscheduled DNA synthesis assays, but allowed a much broader spectrum of genotoxic effects to be analyzed ***(25)***.

A very similar approach was independently developed by Iseki and Mori: cells treated with the genotoxic compound bleomycin were fixed in aceton/methanol and nick translation was performed *in situ* on cover slips; acid-

insoluble materials were adsorbed on glass fiber filters and radioactivity was measured. In addition, they applied the dUTP-ABC strategy for histochemical detection *in situ* ***(26)***. Subsequently, the presence of DNA stand breaks was visualized in frozen sections from various rat tissues, comparing incorporation of ^{3}H-dTTP and ABC-detected biotin-dUTP, as well as the influence of various fixation procedures. To examine if incorporation was due to 'nick translation' or to 'gap filling' of single-stranded DNA regions, also the Klenow enzyme was tested: the latter resulted in about only 30% of the incorporation obtained with Pol I. Strong reactivity was observed when cells were fixed in ethanol, aceton, or their combination, and strongly reduced reactivity when cells were fixed in methanol/acetic acid or treated with this fixative after ethanol/acetone. But in combination with DNase I there was also a strong reactivity in the acid-treated material, whereas tissues fixed in 10% buffered formalin were negative. Evaluation of nuclear staining in various tissues revealed that especially certain cell populations in hematopoietic tissues were strongly positive ***(27)***.

Probably unfamiliar with the above-cited work, Dawson & Lough invented ISNT to monitor transient DNA strand breaks in differentiating chicken myotubes. Myogenic cells were isolated, plated, fixed in methanol/acetic acid, and nick translated in the presence of biotin-dUTP. The latter was visualized by rabbit anti-biotin and fluorescein isothiocyanate (FITC)-labeled goat anti-rabbit IgG; incubation with DNase I prior to nick translation was used as a positive control. They concluded that extensive DNA-nicking occurs in nuclei of young myotubes, followed by repair as terminal differentiation ensues ***(28)***.

Other investigators wondered if these staining patterns could be explained by artificially induced breaks due to the exonuclease activity of Pol I. They performed a rigorous investigation on the *in situ* localization of nuclear DNA breaks in a mouse model for Duchenne muscular dystrophy: in this model, muscle lesions contain necrotic fibres and regenerating myotubes and inflammatory cell infiltrate. Frozen sections of skeletal muscle were fixed in 1% paraformaldehyde and permeabilized with Triton X-100; DNA polymerization was performed with digoxigenin-dUTP (detectable with a FITC- or alkaline phosphatase-conjugated specific Fab fragment of polyclonal sheep anti-digoxigenin antibody) and either Pol I or the Klenow enzyme or a form of the Klenow fragment lacking the 3'→5' exonuclease activity. In each case a nuclear reaction was visible within a subpopulation of small cells in the inflammatory infiltrate (whereas nuclei of myotubes and mature muscle fibers remained unstained). It was concluded that labeling was due to naturally occurring DNA breaks, presumably resulting in single-stranded gaps ***(29)***.

A remarkable feature of Pol I is its ability to incorporate dideoxynucleotides (ddNTPs) onto the 3' end of a growing DNA strand; continued polymerization is blocked by this reaction as the ddNTP cannot act as a primer site for further

polymerization ***(30)***. When ddNTPs were added prior to polymerization with dNTPs, subsequent nuclear staining was completely eradicated and this was thought to be consistent with the presence of gaps ***(29)***. However, these investigators did not mention the possibility that nuclear staining could also result from a significant amount of (ddNTP-blockable) double strand breaks, such as induced by the action of endonucleases. Because endonuclease-induced DNA damage is believed to be a major feature of apoptotic cell death and because the majority of readers will be particularly interested in the application of *in situ* labeling for apoptosis detection, in the next paragraph I will briefly summarize investigations related to apoptotic nucleases as well as to studies that have questioned the general use of DNA labeling for that purpose.

3. Apoptotic DNA Fragmentation: Cautionary Notes

3.1. The Hunt for Apoptotic Nucleases

It had been observed in the early seventies that irradiation of cells can induce fragmentation of chromatin in a very regular pattern, implicating the occurrence of DNA breaks between nucleosomes, and it was Wyllie who linked these internucleosomal DNA breaks with a special form of cell death, associated with chromatin condensation and fragmentation of the nucleus. This type of cell death had already been described in some detail in the second half of the nineteenth century by Flemming ("chromatolysis") ***(31)*** and its significance in counterbalancing mitosis and the relevance of the swift clearance of these cells by phagocytes (either professional scavengers or neighboring cells) was recognized 30 years later by Gräper ***(32)***. After the World Wars, Glücksmann wrote a classic overview on many observations on cell death in the field of embryology ***(33)*** and Lockshin & Williams realized that death of metamorphosing larval cells should have a genetic background ("programmed cell death") ***(34)***.

The pathologist Kerr studied dying hepatocytes on a submicroscopical level and noticed that many cells showed a morphology he called "shrinkage necrosis" ***(35)***; building on this observation, he and his colleagues Wyllie and Currie established that most physiological forms of cell death, observed both in normal and pathological conditions, in fact follow a common morphological pattern. The powerful insight that this was a "basic biological phenomenon with wide-ranging implications for tissue kinetics" justified a special name: "apoptosis," to be discriminated from the type of degenerative accidental cell death referred to as "necrosis" ***(36)***. Independently, other investigators were aware of "active" or "suicidal" cell death in various organs after treatment with anticancer drugs ***(37)*** and it became clear that this drug-induced cell death was in fact indistinguishable from "physiological" apoptosis ***(38)***.

Wyllie was the first to take a biochemical approach to apoptosis, analyzing by agarose gel electrophoresis DNA isolated from thymocytes treated in vitro with methylprednisolone succinate: the characteristic morphological changes occurred in parallel with excision of nucleosome chains from nuclear chromatin, as evidenced by a characteristics 180–200 bp repeat-ladder pattern on the gels ***(39)***. This pattern appeared to be in sharp contrast with DNA isolated from cells with a typical necrotic morphology, as the latter produced a smear of DNA debris likely reflecting totally random DNA degradation ***(40)***. Further studies revealed that in thymocyte apoptosis, double-stranded cleavage of DNA generated two classes of chromatin fragments: 70% of DNA existing as long, histone H1-rich oligonucleosomes bound to the nucleus, and 30% comprising short oligonucleosomes and even mononucleosomes, which were depleted in H1 and not attached to the nucleus. The finding that the whole phenomenon was closely mimicked by MNase digestion of normal thymocyte nuclei hinted at the activation of an endogenous endonuclease ***(41)***, possibly dependent on Ca^{2+} and/or Mg^{2+} ions ***(41–44)***. As condensation of chromatin and its margination at the nuclear periphery was now generally considered to be a cardinal feature of apoptotic cell death, the implication that this condensation was due to internucleosomal cleavage made the 'DNA ladder' a biochemical hallmark ***(45)***.

These findings stimulated the search for the responsible nucleases. Freshly isolated nuclei from intact and castrated rats were assayed for Ca^{2+}/Mg^{2+}-dependent endonuclease activity and this was found to parallel the emergence of nucleosomal oligomers ***(46)***. Circumstantial evidence was provided for a role of DNase I, an enzyme requiring Mg^{2+} an Ca^{2+} for maximal activity and having a strong preference for internucleosomal sites ***(47)***.

DNase I first binds at the minor groove, cutting one DNA strand, and this mechanism is subsequently repeated for the other strand, resulting in sticky-end like fragments. It was assumed that if such fragmentation products even leave free 3'-OH ends, the nucleosomal ladder should be detected by simply end-labeling the purified DNA by Klenow enzyme in the presence of ^{32}P-dCTP or ^{32}P-dATP; it was shown that this method indeed substantially enhanced the detectability of the apoptotic ladder sports and thus that at least a portion of the DNA fragments should have 5'-protruding ends ***(48)***. Together with data from experiments with S_1-nuclease, known to cleave the second strand opposite of nicked DNA ***(49)***, this strongly suggested the DNA fragmentation to be the result of single-strand cleavage and that two single strand nicks on opposite strands within 14 bases (in nucleosomal linker regions) were sufficient for dissociation of the DNA molecule. Further studies revealed that the DNAse activity extracted from apoptotic nuclei could be immunoprecipitated with antibodies specific for DNase I and was inhibitable by actin ***(50)***.

A somewhat different Ca^{2+}/Mg^{2+}-dependent endonuclease, not inhibitable by actin, but capable of producing a ladder, was purified from human spleen ***(51)***, and from apoptotic rat thymocytes a calcium-dependent, Zn^{2+}-inhibitable nuclease was purified (NUC18) showing similarity to the cyclophilins, ubiquitous proteins first identified as the intracellular receptors of the immunosuppressant drug cyclosporin A ***(52,53)***. Subsequently it was described that cyclophilins in fact can degrade both single and double stranded DNA, producing 3'-OH termini in linear double-stranded substrates, and being stimulated by Ca^{2+} and/or Mg^{2+} ***(54)***.

Barry and Eastman advocated that intracellular acidification rather than Ca^{2+} concentrations correlated with apoptotic DNA digestion ***(55)*** and that cleavage probably resulted from a cation-independent endonuclease active below pH 7, possibly DNase II ***(56)***. However, this nuclease produces 5'-OH ends, being inconsistent with labeling by Klenow fragment. Bortner et al. proposed that the predominant subcellular localization of DNase II in acidic lysozymes would make it to work well under conditions of necrosis. But they also stressed that DNase I contains a signal peptide for extracellular transport; access to nuclei would probably require the type of rupture of the nuclear membrane seen in necrotic cell death ***(57)***.

Another interesting candidate was identified by Shiokowa and coworkers in rat thymocyte nuclei; apart from DNases α and β, which appeared to have properties similar to DNAase II, they described DNase γ, being Ca^{2+}/Mg^{2+}-dependent, Zn^{2+}-inhibitable, and producing 3'-OH and 5'-P ends ***(58)***.

Recently, two independent research groups have discovered still another candidate that seems to fit nicely in the concept of apoptosis. It is now well established that most of the apoptosis-related morphological changes are induced by a set of apoptosis-specific cystein proteases that belong to the family known as caspases, which has over a dozen members in humans. The enzymes selectively cleave a restricted set of target proteins and always after an aspartate residue. This may lead to inactivation of the target protein, but can also activate proteins, either directly, by cleaving off a negative regulatory domain, or indirectly, by inactivating a regulatory subunit. Liu and colleagues identified and purified a protein (DNA Fragmentation Factor, DFF) that after its activation by caspase-3 induces DNA fragmentation in coincubated nuclei ***(59)***. Others described the mouse homologue, caspase-activated DNase (CAD) and its inhibitor (ICAD). ICAD is complexed with CAD to inhibit its DNase activity and cleavage of ICAD allows CAD to cause internucleosomal DNA degradation ***(60,61)***.

Of course, it may well be possible that a variety of different nucleases is involved in apoptosis. E.g., recent analyses of ISEL performed on nuclear spreads provided data suggesting that also the initial larger chromatin loops are cut off

from their underlying matrix by the action of caspase-activated endonuclease activity ***(62)***. Despite all this progress, a variety of studies have questioned the dogma that the morphology of apoptosis depends on DNA fragmentation.

3.2. Is Apoptotic DNA Fragmentation a Dispensable Phenomenon?

In the presence of Zn^{2+}, thymocytes could be made apoptotic according to all morphological criteria but without evidence of internucleosomal fragmentation ***(63)***. A similar observation was made for murine fibroblasts: as targets for cytotoxic T lymphocytes, these cells show apoptotic morphology and genome digestion, but a mutant was cloned that lacked the Ca^{2+}-dependent DNase activity, showed no signs of excessive DNA fragmentation, but had still an apoptotic morphology ***(64)***.

Despite the observation of chromatin condensation in leukemia cells treated with staurosporin, no DNA ladders could be detected ***(65)***. Ladders were also absent in DNA from interdigital embryonic mouse limbs or from the labial gland and intersegmental muscle of metamorphosing insects; only by enhancing the sensitivity of ladder detection by using DNA end-labeling, DNA fragmentation was found at a very late stage in cell death in the labial glands ***(66)***. This end-labeling had been developed by Tilli and coworkers: isolated DNA was 3'-OH end-labeled by TdT with α^{32}P-ddATP, leading to a more than 100-fold increase in sensitivity compared to the widely used ethidium bromide staining method ***(67)***.

In fibrosarcoma cells, apoptosis could be induced while DNA fragmentation was blocked by the presence of the DNase inhibitor aurintricarboxylic acid and cells enucleated with cytochalasin B were demonstrated to undergo apoptosis by a variety of triggers ***(68)***. Also induction of apoptosis in cultured hepatocytes by treatment with TGF-β1 was not associated with excessive DNA fragmentation, while activation of endonuclease activity by Ca^{2+} in isolated nuclei led to almost complete degradation of the chromatin to mononucleosomes—but not to chromatin condensation, dissolution of the nucleolar structure, and/or nuclear fragmentation ***(69)***.

In thymocytes, zinc completely inhibited the generation of oligonucleosomal fragments, but not of high molecular weight fragments. Latter fragments, induced by an activity other than Ca^{2+}/Mg^{2+}-dependent endonuclease, seemed to correlate with the earliest morphological features of apoptosis ***(70)***. Application of field inversion gel electrophoresis with DNA of a number of epithelial and mesenchymal cells in which apoptosis was induced by a variety of treatments provided data indicating that internucleosomal fragmentation, if occurring at all, was a relatively late step and always preceded by cleavage to 300.000 and/or 50.000 kb fragments: could release of chromatin loop domains be more fundamental to apoptosis than cleavage at internucleosomal sites ***(71)***?

More recently, changes in cell surface and nuclear morphology of cultured ovarian and carcinoma cells treated with either taxol or ricin were studied by time-lapse video phase contrast: whereas the first signs of apoptosis, such as cell rounding (presumably through loss of substrate adhesion) and intense surface blebbing occurred almost simultaneously with nuclear morphological changes, DNA fragmentation was clearly a very late event in the apoptotic process *(72)*. The question was raised if major DNA fragmentation detected at the terminal lytic stage of apoptosis would really be fundamentally different from that of necrosis, except for the fact that in the former process the nuclear DNA had been previously condensed. Some systems would show clear early 'laddering' with late 'smearing,' but other systems more smearing than laddering. The presence of a ladder would imply apoptosis, but its absence would not rule it out.

However, even the ladder does not seem to stand up in all circumstances. Conditions were described in which DNA extracted from P815 cells forced to die by necrosis showed a clear 'apoptotic' ladder pattern *(73)*. This issue was investigated in depth by Dong and coworkers in cells treated with compounds that led to ATP depletion, necrotic morphology, and, surprisingly, progressive fragmentation of DNA in a ladder pattern. DNA breakdown was immediately preceded by increased permeability of the plasma membrane to macromolecules and this process was found to be prerequisite for activation of a Ca^{2+}/Mg^{2+}-dependent, Zn^{2+} and aurintricarboxylic acid inhibitable endonuclease. Additional data suggested that this DNase is not activated by a caspase, but by a serine protease, and that it may also play a role in apoptosis *(74)*.

The morphology of programmed cell death of cells in which caspases have been inactivated often shows great resemblance with classical necrotic cell death *(75,76)*. It seems therefore that the distinction between apoptosis and necrosis is not as absolute as originally thought and that, eventually, classification will be determined by molecular pathways rather than by morphology. If left undisturbed, the death program would predominantly yield an apoptotic-like morphology, whereas when elements of the program are disturbed or inhibited, or when the insult is so high that some of the subroutines cannot be terminated, the shape of death can change *(77)*.

Although DNA breakdown certainly represents an irreversible step in apoptotic cell death, it has not proven to be a mandatory feature of apoptosis in all cell systems and it may well be that it rather has a clean up function, relevant in some instances and at specific locations *(78)*. DNA fragmentation ensures irreversibility and prevents the spread of possibly infectious or mutated DNA. In immune cells or in cells killed by immune mediators, DNA fragmentation is generally extensive and rapid, but for instance not after the size regres-

sion that follows liver hypertrophy ***(79)***. Nevertheless, the use of ISEL to detect *in situ* DNA damage is still one of the most frequently used techniques with which to highlight apoptotic cells in tissues ***(80)***.

4. Detection of Cell Death by Labeling DNA Breaks

4.1. Independent Development of Several Protocols

One of the first reports on the application of Pol I and biotin-dUTP with the intention to detect apoptosis-related DNA damage was from Fehsel and colleagues; the reaction (referred to as *in situ* nick translation, ISNT) was performed on TNFα-treated mouse fibroblasts fixed in acetone and methanol. But although the presented images demonstrated excessive DNA breaks, starting about 3 hours after TNF-treatment, the lack of apoptotic morphology would be more in line with a necrosis-type of lysis ***(81)***. Subsequently these investigators applied ISNT on acetone-fixed frozen sections from thymus tissue and on cultured thymocytes and validated the method for apoptosis detection by making electron micrographs ***(82)***.

Jonker et al. used both biotin- and digoxigenin-labeled nucleotides subsequently labeled for flow cytometry to detect apoptosis in haemopoietic cells and cell lines after irradiation or treatment with various apoptosis-inducing compounds. The method allowed detection of a fraction of apoptotic cells down to 0.01% and double staining with a cell surface marker allowed for further analysis of subpopulations ***(83)***. Using a similar approach with TdT, biotinylated dUTP, and fluorescinated avidin, Gorczyca et al. were able to demonstrate in thymocytes and leukemia cells that apoptotic DNA degradation was preceded by a proteolytic step, probably catalyzed by a serine protease ***(84)***.

A great advantage of the flow cytometric approach is that both the incorporated dUTP and cellular DNA content can be measured in individual cells simultaneously, making it possible to estimate the kinetics of the labeling reaction and relate DNA breaks to cell position in the cell cycle. Comparing the TdT and Pol I assays on leukemia cells treated with cytostatics, a somewhat better distinction of cells with DNA breaks was obtained with TdT. It was also confirmed that these methods did not detect the protein-associated DNA breaks in the ‘cleavable’ DNA-topoisomerase complexes as resulting from treatment with topoisomerase inhibitors ***(85)***.

Several research groups independently worked on the application of end labeling for sections from paraffin embedded tissues fixed in 4% buffered formaldehyde. Gavrieli and colleagues applied TdT, biotin-dUTP, and avidin-peroxidase on sections mildly digested with proteinase K to allow penetration of the enzyme; this procedure became known as TdT-mediated dUTP-biotin nick end labeling (TUNEL) ***(86)***.

Wijsman and coworkers used Pol I or its Klenow fragment and named their method *in situ* end labeling (ISEL). They compared proteinase K pretreatment with the effect of pepsin (pH 2) and in addition evaluated if incubation in the chaotropic agent NaSCN or in 2 × SSC at 80°C before protease treatment enhanced the effect. Best results were obtained with 2 × SSC at 80°C followed by pepsin digestion as a pretreatment and no differences in staining intensities or frequency of positive events were observed between the use of Pol I and Klenow fragment. Large apoptotic bodies occasionally remained unstained in their center, even in case sections had been treated with DNase I; as stronger protease digestion increased the stainability of these bodies, this indicated poor accessibility. Most often the cytoplasm of apoptotic cells was stained too, suggesting leakage of DNA fragments out of the nucleus. Because apoptosis is relatively easily recognized in haematoxylin & eosin-stained sections of involuting prostates of castrated rats, this was used as a model system to validate ISEL for the quantification of apoptotic cells ***(87)***.

A very similar approach was followed by another research group, leading to similar conclusions; in addition they compared biotin-dATP, biotin-dUTP, and digoxigenin-dUTP (the latter detected with alkaline phosphatase-conjugated Fab fragments) and reported equivalent sensitivity ***(88)***.

A third validation of ISNT/ISEL for apoptosis, both for irradiated thymocytes in flow cytometry and for the application on (4% paraformaldehyde-fixed) tissue sections, was reported by Gold et al. They also evaluated a model for excitotoxic nerve cell necrosis and concluded that DNA fragmentation is a very late event in this type of cell death ***(89)***.

4.2. Comparison of Different Protocols

A number of investigators started to compare Pol I/Klenow-based end labeling (ISNT) with TUNEL, both in conditions of apoptosis and necrosis. Migheli and his team observed that in physiological and pathological conditions of the nervous system, TUNEL detected a higher fraction of cells, including cells without a clearcut apoptotic morphology ***(90)***. Gold and coworkers claimed that in the early phase of thymocyte apoptosis in vitro, DNA breaks were more efficiently labeled by TUNEL, whereas early stages of necrosis in vivo were more efficiently labeled by ISNT. They theorized that if necrosis was associated with a lot of single strand breaks, the signal at these breaks would be amplified by the exonuclease activity of Pol I ***(91)***.

However, these statements have been criticized ***(92)***, as Wijsman did not detect any difference between Pol I and its Klenow fragment in that respect ***(87)***, and others failed to discriminate between apoptosis and necrosis and/or autolytic cell death when using TUNEL ***(93–96)***. In case of focal brain ischemia,

somewhat larger areas were detected by ISNT and very similar results were obtained by Pol I and Klenow fragment ***(97)***.

Mundle and coworkers found that ISNT and TUNEL had similar levels of detectability in biopsies from lymphomas or squamous cell carcinomas, but that breast cancers were only labeled by TUNEL. Moreover, etoposide-treated HL60 cells showed a higher apoptotic index determined by TUNEL. They hypothesized that different endonucleases could result in fragments with either 3' recessed, 5' recessed or blunt ends and that whereas TUNEL could label all three types, ISNT would label only those with 3' recessed ends ***(98)***.

However, comparison of Pol I and TdT in anti-Fas antibody-induced apoptosis in leukemia cells lines revealed that only Pol I strongly reacted with nonfragmented nuclei of early apoptotic cells ***(99)*** and Mainwaring and coauthors concluded that ISNT (Klenow fragment) and TUNEL were not significantly different when applied on human breast cancer; the methods gave an excellent correlation, both in case of 'physiological' apoptosis and in material from patients who had received chemotherapy. They stated that disappointing results with ISNT could be due to the absence of full optimization of the ISNT technique ***(100)***.

4.3. Attempts to Differentiate Between Different Types of Cell Death

A number of researchers attempted to elucidate the nature of the DNA breaks in the context of apoptotis versus necrosis and autolysis. One approach was based on pretreatment with alkaline phosphatase (AP), which dephosphorylates both 3'-P ends and 5'-P ends. Using both TdT and T4 polynucleotide kinase (which labels 5'-OH ends) and agarose gel electrophoresis, Shiokawa and coworkers were able to demonstrate that apoptotic thymocytes contain 3'-OH/5'-P cleavage ends and no 3'-P/5'-OH ends ***(58)*** and Lucassen and colleagues applied AP pretreatment in ISEL to establish that post mortem autolysis was not associated with phosphorylation of 3'-OH ends ***(101)***.

In contrast, in a more recent study in which AP was applied in a study combining ISEL and transmission electron microscopy it was shown in a model of heat-induced apoptosis and necrosis in mouse lymphoma cells that in apoptotic cells the labeling intensity of both 5'-OH and 3'-OH ends increased, that cells in early stages of necrosis had higher levels of 3'-OH/5'-P than 5'-OH/3'-P, but that at late stages this ratio reversed ***(102)***. DNase I gives rise to double strand cuts with 1, 2, or 3 bases of 3' overhang, whereas DNase II cleavage of DNA yields 3' overhangs of an average of 4 bases ***(103)***; these staggered cleavage patterns result from the helical twist of the DNA in chromatin ***(104)***. TdT and Pol I and Klenow fragment can easily label protruding 3'-OH termini, the latter two by virtue of their 3'→5' exonuclease activity which removes the protruding 3' tails and creates a recessed 3' terminus. Double stranded DNA fragments

synthesized by *Taq* DNA polymerase in the polymerase chain reaction have a single 3' base extension beyond the templated sequence ***(105)*** and thus can be ligated to double strand breaks with single-base 3' overhangs. Similarly, the blunt-ended fragments prepared by *Pfu* polymerase can be ligated to blunt ended DNA breaks. Using labeled double-stranded DNA fragments, Didenko & Hornsby elegantly showed by *in situ* DNA ligation with T4 DNA ligase that both single-base 3' overhangs and blunt ends were detectable in apoptotic rat thymocytes. However, DNA from nuclei with non-apoptotic DNA damage (necrosis, in vitro autolysis, peroxide damage, and heating) hardly showed single-base 3' overhangs and much lower intensity of blunt end staining compared to DNA from apoptotic cells ***(106)***.

By contrast, others observed strong labeling with blunt-ended fragments in necrotic areas in human placental tissue ***(107)***. Because a major problem encountered with these DNA probes was ligase-independent binding to tissue sections, biotin-labeled hairpin oligonucleotides have been prepared that resulted in a substantial reduction of non-specific background ***(108,109)***.

Recently, Kanoh and colleagues used the *Taq* Pol-based ligation assay to verify if TUNEL positive myocyte nuclei in hearts with dilated cardiopathy should be considered apoptotic or not; based on the negative results with the ligase assays they conjectured that TUNEL in fact detected increased activity of DNA repair ***(110)***.

Finally, two other DNA-based apoptosis-detection techniques are worth mentioning. One is based on the fact that nuclear DNA of early apoptotic cells shows an increased susceptibility to denaturation ***(111)***, especially A-T rich regions, which have lower melting temperatures than regions with a higher G-C content. A-T-rich Alu repeats are present in many thousands of copies and are excellent targets for *in situ* hybridization with poly(A) oligonucleotide probes that hybridyze to poly(T) repeats. It has been claimed that application of 30 bp probes (labeled with dUTP by TdT) on formalin fixed tissue sections was more specific than ISEL in detecting apoptosis ***(112)***.

The other method is basically a modification of the random oligonucleotide primed synthesis (ROPS) assay: single stranded DNA fragments generated by endonuclease-mediated strand breaks are initially separated by a denaturation step. Subsequently the strand are (randomly) reassociated; the DNA fragments serve as a primer and the excess high molecular weight DNA serves as a template. The Klenow fragment is then used to polymerase from 3'-OH ends and incorporate radiolabeled dNTPs; provided that strictly defined conditions are being used (time, temperature, concentration of precursors) the measured radioactivity will be proportional to he initial number of 3'OH breaks ***(113)***.

5. ISEL Retrieval Methods for Paraffin-Embedded Tissue Sections

5.1. Use of Protein Digesting Enzymes

One of the enormous advantages of ISEL is that it can be applied on archival material, i.e., on tissues fixed in 4% formaldehyde solutions (formalin) and embedded in paraffin. Formaldehyde is required to preserve tissue morphology and to render it non-infectious. The aldehyde molecule reacts with tissue nucleophiles to produce a methylene bridge with other molecules and it also disrupts hydrogen bonds. The process of cross-linking is time dependent, so it matters if tissue is fixed for several hours or for many weeks.

It is believed that in the apoptotic nucleus, both the progressive DNA hypercondensation (pyknosis) and the protein environment of DNA (histones) seriously impair the accessibility of ISEL reagents and that these condition are markedly worsened by crosslinking (and precipitating) fixatives. Therefore, to make the formalin-fixed tissues amenable to ISEL, protein-digesting enzymes were introduced. However, excess digestion may disrupt the excellent morphology and result in considerable DNA extraction, leading to a diffuse nonspecific staining with a "washed-out" aspect of nuclei ***(90)***.

In fact, a variety of different proteolytic enzymes can be used, such as proteinase K (PK), pepsin, trypsin, protease XIV, and protease XXIV—provided of course that these preparations are absolutely free of nucleases. The effect of the latter three enzymes was reported to be enhanced by subsequent treatment with hydrochloric acid ***(114)***. Davidson and coworkers investigated the consequences of fixation duration for apoptosis detection with Klenow enzyme after pretreatment with PK. They found that the time of digestion with PK is crucial is case material is fixed for several hours, but not if fixed overnight, and that apoptotic cells become indetectable after several weeks of fixation. They attributed this to irreversible crosslinking between different DNA strands and between DNA and amino acids. In case of overnight fixation the DNA exposed by proteolysis would not be an ideal template for polymerases: free ends and single-strand regions would be rendered inaccessible by prolonged fixation ***(115)***.

Once properly fixed, storage duration of the material—even if lasting for decades—does not seem to affect staining results ***(116)***.

5.2. Application of Heat

Approaches used to enhance the detectability of DNA breaks in long-term fixed cells were essentially the same as used in antigen retrieval and based on breaking the formaldehyde linkages by high temperature. It is believed that the quality of heating is superior in case microwave (MW) radiation is used for that purpose, because microwaves would cleave peptide bonds in a more selective fashion than simple heating, probably by increasing molecular agitation ***(117–119)***.

Lucassen et al. reported that a marked increase in apoptosis-specific labeling could be obtained by MW heating of prolonged-fixed tissue sections in citrate buffer (up to 90–100°C) and best results were achieved when performing this under acid conditions (pH 3). The same method applied on shortly fixed material resulted in strong nonspecific labeling ***(101)***.

A potential drawback of MW heating is the possible occurrence of local superheating, resulting in non-uniform heating of the buffer. Assuming that these temperature variations could be large enough to affect the efficiency of antigen retrieval, the high-pressure cooker was introduced in immunohistochemistry: this not only assured uniform heat distribution, but also a higher temperature (up to 130°C) ***(120)***. Cooking under pressure (for 2 min) has been successfully applied both for ISNT and TUNEL, generating very similar and consistent results ***(121)***.

Negoescu and coworkers confirmed that for TUNEL, combined MW-PK pretreatment was never more efficient than MW alone. Testing cultured cells fixed by a variety of fixatives, they found a 4–30-fold increase in the percentage of labeled cells with apoptotic morphology as compared with no pretreatment. They proposed that the pretreatment modality for ISEL should become standardized, that labeling should only be accepted as specific when being strong as compared to general background, and that cells devoid of apoptotic morphology should be accepted as preapoptotic—provided that they are associated with strongly stained elements with classical apoptotic features on the same cell or tissue preparation ***(122)***.

Further studies revealed that sections from formalin-fixed material were maximally stained by TUNEL if MW heating was performed in extreme pH-value solutions (pH 3), but material fixed in Bouin's fixative was optimally stained after heating in pH 10.6. This indicates that optimalization not necessarily comes from retrieval reenforcement, but rather from qualitative adaptations of retrieval techniques ***(123)***.

The major problems with ISEL can be summarized as follows: (i) without pretreatment sensitivities are far too low; (ii) pretreatments with acknowledged efficiency (PK, MW) easily induce general labeling of morphological normal nuclei ***(90,101,106,124)***; (iii) ISEL is very sensitive to fixation, which makes sample size critical: in large samples—which are rule in archives—fixation is uneven from the periphery to the central area; (iv) altogether this may lead to the presence in the same tissue of blank areas, together with specifically labeled spots and areas in which all nuclei are stained ***(125)***.

6. Final Remarks

There are many known causes of DNA breaks apart from apoptosis-associated endonuclease activities ***(7)***, including DNA recombination, replication,

repair, compaction-relaxation during mitosis, RNA synthesis and splicing ***(127)***, tissue electrocoagulation, autolysis (postmortem interval) ***(128)***, fixation, paraffin embedding, cutting, and pretreatments with H_2O_2, detergent, PK, microwaves, etc. ISEL can be a convenient method for demonstrating genotoxic insults unrelated to apoptosis- or necrosis-associated DNA fragmentation. The idea to use TdT to label radiation-induced DNA strand breaks goes back to the early 70s ***(129)*** and in the mid-80s, Pol I and ^{3}H-dCTP were used to monitor DNA damage by genotic agents and the repair thereof ***(24,25,130)***.

Maehara and coworkers subsequently applied Pol I and ^{3}H-dTTP *in situ* on cultured cells to evaluate the effects of heat ***(131)***, γ-irradiation ***(132)***, and adriamycin ***(133)*** and the method was used to prove that asbestos is a genotoxic agent ***(134)*** and to demonstrate an increase in single strand breaks in small samples of human ultraviolet-irradiated skin ***(135)***. Kodym and Hörth introduced digoxigenin-dUTP to study *in situ* radiation-induced DNA strand breaks and their repair ***(137)*** and Coates and coworkers used Pol I and biotin-dATP to demonstrate UV light-induced DNA damage/repair, both in vitro and in vivo ***(137)***. More recent examples of the *in situ* application of Pol I or Klenow fragment and biotin-labeled nucleotides unrelated to apoptosis detection are studies on the mutagenic effects of biomaterials ***(138)***, on the protective effects of mineral sunscreen against ultraviolet radiation ***(139)*** and on the kinetics of bleomycin-induced DNA damage in the lung ***(140)***.

However, in the overwhelming majority of studies from the past decade in which ISEL was applied it was done with the aim to verify, localize and/or even quantitate apoptosis. In fact, ISEL owes its popularity mainly to the phenomenon that many cell types at some point in the execution phase of their apoptotic process are subjected to a degree of DNA fragmentation by far exceeding the amount of DNA breaks resulting from transcription, replication, and mitotic activities, or from factors related to tissue preparation. Moreover, many companies introduced 'apoptosis detection' kits relying on labeling DNA breaks, the majority of which being based on TdT, probably because earlier reports had suggested that TdT had a greater specificity towards apoptotic DNA breaks than Klenow fragment ***(91)***.

But whatever kind of enzyme is being applied, it is clear that the reliability and specificity of ISEL-kits as advocated by these companies are simply not justified. As has been repeatedly stressed in the literature, it is fair to say that ISEL methods assist with the identification and quantification of apoptosis, but must be employed in conjunction with (simple) morphological examination to exclude artifactual staining caused by technical aspects and staining as a result of DNA strand breaks resulting from other physiological or pathological processes ***(127,141)***. To some extent a similar argument holds for all other current methods to detect cell death, such as *in situ* detection with biotin-Annexin V

(142) and with antibodies against activated caspase-3 ***(143)*** or against epitopes that emerge from specific caspase-induced protein cleavage ***(144)***.

A major advantage of ISEL is that it can easily be combined with immunostaining on the same tissue section, even if it involves nuclear antigens ***(145)***. Although at present no single technique seems fully adequate to unequivocally determine under all conditions both the presence and nature of dying cells, the increasing choice of different methods available ***(146–149)*** may provide ample opportunity to combine a number of complementary techniques that are suited to any individual situation.

References

1. Lehman, I. R., Bessman, M. J., Simms, E. S., and Kornberg, A. (1958) Enzymatic synthesis of deoxyribonucleic acid. I. Preparation of substrates and partial purification of an enzyme from *Escherichia coli*. *J. Biol. Chem*. **233,** 163–170.
2. Bollum, F. J. (1960) Calf thymus polymerase. *J. Biol. Chem.* **234,** 2733–2734.
3. Borstel, R. C. von, Prescott, D. M., and Bollum, F. J. (1966) Incorporation of nucleotides into nuclei of fixed cells by DNA polymerase. *J. Cell Biol*. **29,** 21–28.
4. Modak, S. P., von Borstel, R. C., and Bollum, F. J. (1969) Terminal lens cell differentiation II. Template activity of DNA during nuclear degeneration. *Exp. Cell Res*. **56,** 105–113.
5. Modak, S. P., and Bollum, F. J. (1970) Terminal lens cell differentiation III. Initiator activity of DNA during nuclear degeneration. *Exp. Cell Res*. **62,** 421–432.
6. Modak, S. P., and Bollum, F. J. (1972) Detection and measurement of single-strand breaks in nuclear DNA in fixed lens sections. *Exp. Cell Res*. **75,** 307–313.
7. Appleby, D. W., and Modak, S. P. (1977) DNA degradation in terminally differentiating lens fiber cells from chick embryos. *Proc Natl. Acad. Sci. USA* **74,** 5579–5583.
8. Kelly, R. B., Cozzarelli, N. R., Deutscher, M. P., Lehman, I. R., and Kornberg, A. (1970) Enzymatic synthesis of deoxyribonucleic acid. XXII. Replication of duplex deoxyribonucleic acid by polymerase at a single strand break. *J. Biol. Chem*. **245,** 39–45.
9. Brutlag, D., Atkinson, M. R., Setlow, P., and Kornberg, A. (1969) An active fragment of DNA polymerase produced by proteolytic cleavage. *Biochem. Biophys. Res. Commun*. **37,** 982–989.
10. Setlow, P., Brutlag, D., and Kornberg, A. (1972) Deoxyribonucleic acid polymerase: two distinct enzymes in one polypeptide. *J. Biol. Chem*. **247,** 224–231.
11. Klenow, H., and Henningsen, I. (1970) Selective elimination of the exonuclease activity of the deoxyribonucleic acid polymerase from *Escherichia coli* B by limited proteolysis. *Proc. Natl. Acad. Sci*., **65,** 168–175.
12. Maunders, M. J. (1993) DNA polymerases (EC 2.7.7.7), in *Methods in Molecular Biology, vol 16: Enzymes of Molecular Biology*. (Burrell M. M. ed.) Humana, Totowa, NJ, pp. 17–30.

13. Joyce, C. M., and Steitz, T. A. (1994) Function and structure relationships in DNA polymerases. *Annu. Rev. Biochem.* **63,** 823–867.
14. Clarke, J. M., Joyce, C. M., and Beardsley, G. P. (1987) Novel blunt-end addition reactions catalyzed by DNA polymerase I of *Escherichia coli*. *J.Mol. Biol.* **198,** 123–127.
15. Levitt, A., Axel, H., and Cedar, H. (1979) Nick translation of active genes in intact nuclei. *Dev. Biol,* **69,** 469.
16. Gazit, B., Cedar, H., Lerer, I., and Voss, R. (1982) Active genes are sensitive to deoxyribonuclease I during metaphase. *Science* **217,** 648–650.
17. Kerem, B.-S., Goitein, R., Richler, C., Marcus, M., and Cedar, H. (1983) *In situ* nick-translation distinguishes between active and inactive X chromosomes. *Nature* **304,** 88–90.
18. Langer, P. R., Waldrop, A. A., and Ward, D. C. (1981) Enzymatic synthesis of biotin-labeled polynucleotides: noble nucleid acid affinity probes. *Proc. Natl. Acad. Sci. USA* **78,** 6633–6637.
19. Hsu, S.-M., Raine, L., and Fanger, H. (1981) The use of avidin-biotin-peroxidase complex (ABC) in immunoperoxidase techniques: a comparison between ABC and unlabeled antibody (PAP) procedures. *J. Histochem. Cytochem*, **29,** 577–580.
20. Adolph, S., Hameister, H. (1985) *In situ* nick translation of metaphase chromosomes with biotin-labeled d-UTP. *Human Genet*. **69,** 117–121.
21. Murer-Orlando M. L., Peterson, A. C. (1985) *In situ* nick translation of human and mouse chromosomes detected with a biotinylated nucleotide. *Exp. Cell Res*. **157,** 322–334.
22. Kerem, B.-S., Goitein, R., Diamond, G., Cedar, H., and Marcus, M. (1984) Mapping of DNAse I sensitive regions on mitotic chromosomes. *Cell* **38,** 493–499.
23. Patkin, E. L., Kustova, M. E., and Noniashvili, E. M. (1995) DNA-strand breaks in chromosomes of early mouse embryos as detected by *in situ* nick translation and gap filling. *Genome* **38,** 381–384.
24. Nose, K., and Okamoto, H. (1983) Detection of carcinogen-induced DNA breaks by nick translation. *Biochem. Biophys. Res. Commun*. **111,** 383–389.
25. Snyder, R. D., and Matheson, D. W. (1985) Nick translation-a new assay for monitoring DNA damage and repair in cultured human fibroblasts. *Environ. Mutagen*. **7,** 267–279.
26. Iseki, S., and Mori, T. (1985) Histochemical detection of DNA strand scissions in mammalian cells by *in situ* nick translation. *Cell Biol. Int. Rep*. **9,** 471–477.
27. Iseki, S. (1986) DNA strand breaks in rat tissues as detected by *in situ* nick translation. *Exp. Cell Re*s. **167,** 311–326.
28. Dawson, B., and Lough, J. (1988) Immunocytochemical localization of transient DNA strand breaks in differentiating myotubes using *in situ* nick-translation. *Dev. Biol*. **127,** 362–367.
29. Coulton, G. R., Rogers, B., Strutt, P., Skynner, M. J., and Watt, D. J. (1992) *In situ* localisation of single-stranded DNA breaks in nucleiof a subpopulation of cells within regenerating skeletal muscle of the dystrophic mdx mouse. *J. Cell Sci*. **102,** 653–662.

30. Sanger, F., Nicklen, S., and Coulson, A. R. (1977) DNA sequencing with chain terminating inhibitors. *Proc. Nat. Acad. Sci. USA* **74,** 54–63.
31. Flemming, W. (1885) Über die Bildung von Richtungsfiguren in Säugetiereiern beim Untergang Graaf'scher Follikel. *Arch. Anat. EntwGesch*. 221–244.
32. Gräper, L. (1914) Eine neue Anschauung über physiologische Zellausschaltung. *Arch. Zellforschung* **12,** 373–294.
33. Glücksmann, A. (1951) Cell deaths in normal vertebrate ontogeny. *Biol. Rev. Camb. Philo. Soc*. **26,** 59–86.
34. Lockshin, R. A. and Williams, C. M. (1964) Programmed cell death. II Endocrine potentiation of the breakdown of intersegmetal muscles of silk moths. *J. Insect Physiol*. **10,** 643–649.
35. Kerr, J. F. R. (1971) Shrinkage necrosis: a distinct mode of cellular death. *J. Pathol*. **105,** 13–20.
36. Kerr, J. F. R., Wylie, A. H., and Currie, A. R. (1972) Apoptosis: a basic biological phenomenon with wide-ranging implications in tissue kinetics. *Br. J. Cancer* **26,** 239–257.
37. Farber, E., Verbin, R. S., and Liberman, M. (1971) Cell suicide and cell death. In: A Symposium on Mechanisms of Toxicology. Aldridge, N. (ed.) Macmillan, N.Y. pp 163–173.
38. Searle, J., Lawson, T. A., Abbott, P. J., Harmon, B., and Kerr, J. F. R. (1974) An electron-microscope study of the mode of cell death induced by cancer-chemotherapeutic agents in populations of proliferating normal and neoplastic cells. *J. Pathol*. **166,** 129–137.
39. Wyllie, A. H. (1980) Glucocorticoid-induced thymocyte apoptosis is associated with endogenous endonuclease activation. *Nature* **284,** 555–556.
40. Harmon, B. V., Corder, A. M., Collins, R. J., Gobé, G. G., Allen, J., Allan, D. J., and Kerr, J. F. R. (1990) Cell death induced in a murine mastocytoma by 42–47°C heating in vitro: evidence that the form of death changes from apoptosis to necrosis above a critical heat load. *Int. J. Radiat. Biol*. **58,** 845–858.
41. Arends, M. J., Morris, R. G., and Wyllie, A. H. (1990) Apoptosis. The role of endonucleases. *Am. J. Pathol*. **136,** 593–608.
42. Hewish, D. R., and Burgoyne, L. A. (1973) Chromatin substructure. The digestion of chromatin at regularly spaced sites by a nuclear deoxyribonuclease. *Biochem. Biophys. Res. Commun*. **52,** 504–510.
43. Ishida, R., Akiyoshi, H., Takahoshi, T. (1974) Isolation and purification of calcium and magnesium dependent endonuclease from rat liver nuclei. *Biochem. Biophys. Res. Commun*. **56,** 703–710.
44. Cohen, J. J., and Duke, R. C. (1984) Glucocorticoid activation of a calcium-dependent endonuclease in thymocyte nuclei leads to cell death. *J. Immunol*. **132,** 38–42.
45. Compton, M. M. (1992) A biochemical hallmark of apoptosis: internucleosomal degradation of the genome. *Cancer Metastasis Rev*. **11,** 105–119.

46. English, H. F., Kyprianou, N., and Isaacs, J. T. (1989) Relationship between DNA fragmentation and apoptosis in the programmed cell death in the rat prostate following castration. *Prostate* **15,** 233–250.
47. Peitsch, M. C., Hesterkamp, T., Polzar, B., Mannherz, G. H., and Tschopp, J. (1992) Functional characterization of serum DNase I in MRL-^{lpr}/lpr mice. *Biochem. Biophys. Res. Commun*. **186,** 739–745.
48. Rösl, F. (1992) A simple and rapid method for detection of apoptosis in human cells. *Nucleic Acids Res*. **20,** 19.
49. Peitsch, M. C., Müller, C., and Tschopp, J. (1993) DNA fragmentation during apoptosis is caused by frequent single-strand cuts. *Nucleic Acids Res*. **21,** 4206–4209.
50. Peitsch, M. C., Polzar, B., Stephan, H., Crompton, B., MacDonald, H. R., Mannherz, H. G., and Tschopp, J. (1993) Characterization of the endogenous deoxyribonuclease involved in nuclear DNA degradation during apoptosis (programmed cell death). *EMBO J*. **12,** 371–377.
51. Ribeiro, J. M. and Carson, D. A. (1993) Ca^{2+}/Mg^{2+}-dependent endonuclease from human spleen: purification, properties, and role in apoptosis. *Biochemistry* **32,** 9129–9136.
52. Gaido, M. L., and Cidlowski, J. A. (1991) Identification, purification, and characterization of a calcium-dependent endonuclease (NUC18) from apoptotic rat thymocytes. *J. Biol. Chem*. **266,** 18,580–18,585.
53. Montague, J. W., Gaido, M. L., Frye, C., and Cidlowski, J. A. (1994) A calcium-dependent nuclease from apoptotic rat thymocytes is homologous with cyclophilin. *J. Biol. Chem*. **269,** 18,877–18,880.
54. Montague, J. W., Hughes, F. M., and Cidlowski, J. A. (1997) Native recombinant cyclophilins A, B, and C degrade DNA independently of peptidylprolyl cis-trans-isomerase activity. *J. Biol Chem*. **272,** 6677–6684.
55. Barry, M. A., and Eastman, A. (1992) Endonuclease activation during apoptosis: the role of cytosolic Ca^{2+} and pH. *Biochem. Biophys. Res. Commun*. **186,** 782–789.
56. Barry, M. A., and Eastman, A. (1993) Identification of deoxyribonuclease II as an endonuclease involved in apoptosis. *Arch. Biochem. Biophys*. **300,** 440–450.
57. Bortner, C. D., Oldenburg, N. B. E., and Cidlowski, J. A. (1995) The role of DNA fragmentation in apoptosis. *Trends Cell Biol*. **5,** 21–26.
58. Shiokawa, D., Oyama, H., Yamada, T., Takahashi, K., and Tanuma, S. (1994) Identification of an endonuclease responsible for apoptosis in rat thymocytes. *Eur. J. Biochem*. **226,** 23–30.
59. Liu, X., Zou, H., Slaughter, C., and Wang, X. (1997) DFF, a heterodimeric protein that functions downstream of caspase-3 to trigger DNA fragmentation during apoptosis. *Cell* **89,** 175–184.
60. Enari, M., Sakahira, H., Yokoyama, H., Okawa, K., Iwamatsu, A., and Nagata, S. (1998) A caspase-activated DNase that degrades DNA during apoptosis, and its inhibitor ICAD. *Nature* **391,** 43–50.
61. Sakahira, H., Enari, M., and Nagata, S. (1998) Cleavage of CAD inhibitor in CAD activation and DNA degradation during apoptosis. *Nature* **391,** 96–99.

62. Chan, D. W., and Yager, T. D. (1998) Preparation and imaging of nuclear spreads from cells of the zebrafish embryo. Evidence for large degradation intermediates in apoptosis. *Chromosoma* **107,** 39–60.
63. Cohen, C. M., Sun, X.-M., Snowden, R. T., Dinsdale, D., and Skilleter, D. N. (1992) Key morphological features of apoptosis may occur in the absence of internucleosomal DNA fragmentation. *Biochem. J.* **286,** 331–334.
64. Ucker, D. S., Obermiller, P. S., Eckhart, W., Apgar, J. R., Berger, N. A., and Meyers, J. (1992) Genome digestion is a dispensable consequence of physiological cell death mediated by cytotoxic T lymphocytes. *Mol. Cell. Biol.* **12,** 3060–3069.
65. Falcieri, E., Martelli, A. M., Bareggi, R., Cataldi, A., and Cocco, L. (1993) The protein kinase inhibitor staurosporin induces morphological changes typical of apoptosis in MOLT-4 cells without concomitant DNA fragmentation. *Biochem. Biophys. Res. Commun*. **193,** 19–25.
66. Zakeri, Z. F., Quaglino, D., Latham, T., and Lockshin, R. A. (1992) Delayed internucleosomal DNA framentation in programmed cell death. *FASEB J*. **7,** 470–478.
67. Tilly, J. L., Kowalski, K. I., Johnson, A. L., Hsueh, A. J. W. (1991) Involvement of apoptosis in ovarian follicular atresia and postovulatory regression. *Endocrinol*. **129,** 2799–2801.
68. Schulze-Osthoff, K., Walczak, H., Dröge, W., and Krammer, P. H. (1994) Cell nucleus and DNA fragmentation are not required for apoptosis. *J. Cell Biol.* **127,** 15–20.
69. Oberhammer, F., Fritsch, G., Schmied, M., Pavelka, M., Printz, D., Purchio, T., Lassmann, H., and Schulte-Hermann, R. (1993) Condensation of the chromatin at the membrane of an apoptotic nucleus is not associated with activation of an endonuclease. *J. Cell Sci*. **104,** 317–326.
70. Brown, D. G., Sun, X.-M., and Cohen, G. M. (1993) Dexamethasone-induced apoptosis involves cleavage of DNA to large fragments prior to internucleosomal fragmentation. *J. Biol. Chem*. **268,** 3037–3039.
71. Oberhammer, F., Wilson, J. W., Dive, C., Morris, I. D., Hickman, J. A., Wakeling, A. E., Walker, P. R., and Sikorska, M. (1993) Apoptotic death in epithelial cells: cleavage of DNA to 300 and/or 50 kb fragments prior to or in the absence of internucleosomal fragmentation. *EMBO J.* **12,** 3679–3684.
72. Collins, J. A., Schandle, C. A., Young, K. K., Vesely, J., and Willingham, M. C. (1997) Major DNA fragmentation is a late event in apoptosis. *J. Histochem. Cytochem.* **45,** 923–934.
73. Collins, R. J., Harmon, B. V., Gobé, G. C., and Kerr, J. F. R. (1992) Internucleosomal DNA cleavage should not be the sole criterion for identifying apoptosis. *Int. J. Radiat. Biol*. **61,** 451–453.
74. Dong, Z., Saikumar, P., Weinberg, J. M., and Venkatchalam, M. A. (1997) Internucleosomal DNA cleavage triggered by plasma membrane damage during necrotic cell death. Involvement of serine but not cysteine proteases. *Am. J. Pathol*. **151,** 1205–1213.
75. Kitanka, C, and Kuchino, Y. (1999) Caspase-dependent programmed cell death with necrotic morphology. *Cell Death Differ*. **6,** 508–515.

76. Chautan, M., Chazal, G., Cecconi, F., Gruss, P., nnd Goldstein, P. Interdigital cell death can occur through a necrotic and caspase-independent pathway. *Curr. Biol.* **9,** 967–970.
77. Leist, M., and Nicotera, P. (1997) Breakthroughs and views. The shape of cell death. *Biochem. Biophys. Res. Commun*. **236,** 1–9.
78. Peitsch, M. C., Mannherz, H. G., and Tschopp, J. (1994) The apoptosis endonucleases: cleaning up after cell death? *Trends Cell Biol*. **4,** 37–41.
79. Oberhammer, F., Bursch, W., Tiefenbacher, R., Fröschl, G., Pavelka, M., Purchio, T., and Schulte-Hermann, R. (1993) Condensation of the chromatin at the membrane of an apoptotic nucleus is not associated with activation of an endonuclease. *Hepatology* **18,** 1238–1246.
80. Stadelmann, C., and Lassmann, H. (2000) Detection of apoptosis in tissue sections. *Cell Tissue Res*. **301,** 19–31.
81. Fehsel, K., Kolb-Bachofen, V., and Kolb, H. (1991) Analysis of TNFα-induced DNA strand breaks at the single cell level. *Am. J. Pathol*. **139,** 251–254.
82. Fehsel, K., Kroncke, K. D., Kolb, H., and Kolb-Bachofen, V. (1994) *In situ* nick-translation detects focal apoptosis in thymuses of glucocorticoid- and lipopolysaccharide-treated mice. *J. Histochem. Cytochem*. **42,** 613–619.
83. Jonker R. R., Bauman, J. G. J., and Visser, J. W. M. (1991) Detection of apoptosis with *in situ* nick translation. *Cytometry* **S5,** 44.
84. Gorczyca, W., Bruno, S., Darzynkiewicz, R. J., Gong, J., and Darzynkiewicz, Z. (1992) DNA strand breaks occurring during apoptosis: their early *in situ* detection by the terminal deoxynucleotidyl transferase and nick translation assays and prevention by serine protease inhibitors. *Int. J. Oncol*. **1,** 639–648.
85. Gorczyca, W., Gong, J., and Darzynkiewicz, Z. (1993) Detection of DNA strand breaks in individual apoptotic cells by the *in situ* terminal deoxynucleotidyl transferase and nick translation assays. *Cancer Res*. **53,** 1945–1951.
86. Gavrieli, Y., Sherman, Y., and Ben-Sasson, A. A. (1992) Identification of programmed cell death *in situ* via specific labeling of nuclear DNA fragmentation. *J. Cell Biol*. **119,** 493–501.
87. Wijsman, J. H., Jonker, R. R., Keijzer, R., van de Velde, C. J. H., Cornelisse, C. J., van Dierendonck, J. H. (1993) A new method to detect apoptosis in paraffin sections: *in situ* end-labeling of fragmented DNA. *J. Histochem. Cytochem*. **41,** 7–12.
88. Ansari, B., Coates, P. J., Greenstein, B. D., and Hall, P. A. (1993) *In situ* end-labeling detects DNA strand breaks in apoptosis and other physiological and pathological states. *J. Pathol*. **170,** 1–8.
89. Gold, R., Schmied, M., Rothe, G., Zischler, H., Breitschopf, H., Wekerle, H., and Lassmann, H. (1993) Detection of DNA fragmentation in apoptosis: application of *in situ* nick translation to cell culture sections. *J. Histochem. Cytochem*. **41,** 1023–1030.
90. Migheli, A., Cavalla, P., Marino, S., and Schiffer, D. (1994) A study of apoptosis in normal and pathologic nervous tissue after *in situ* end-labeling of DNA breaks. *J. Neuropathol. Exp. Neurol*. **53,** 606–616.

91. Gold, R., Schmied, M., Giegerich, G., Breitschopf, H., Hartung, H. P., Toyka, K. V., and Lassmann, H. (1994) Differentiation between cellular apoptosis and necrosis by the combined use of *in situ* tailing and nick translation techniques. *Lab. Invest*. **71,** 219–225.
92. Mundle, S. D., Raza, A. (1995) The two *in situ* techniques do not differentiate between apoptosis and necrosis but rather distinct patterns of DNA fragmentation in apoptosis. Reply by Gold *et al*. *Lab. Invest*. **72,** 611–613.
93. Grasl-Kraupp, B., Ruttkay-Nedecky, B., Koudelka, H., Budowska, K., Bursch, W., and Schulte-Hermann, R. (1995) *In situ* detection of fragmented DNA (TUNEL assay) fails to discriminate among apoptosis, necrosis, and autolytic cell death: a cautionary note. *Hepatol.* **21,** 1465–1468.
94. Charriaut-Marlangue, C., and Ben-Ari, Y. (1995) A cautionary note on the use of the TUNEL stain to determine apoptosis. *NeuroRep*. **7,** 61–64.
95. Nishiyama, K., Kwak, S., Takekoshi, S., Watanabe, K., and Kanazawa, I. (1996) *In situ* end-labeling detects necrosis of hippocampal pyramidal cells induced by kainic acid. *Neurosci. Lett*. **212,** 139–142.
96. Fujita, K., Ohyama, H., and Yamada, T. (1997) Quantitative comparison of *in situ* methods for detecting apoptosis induced by X-ray irradiation in mouse thymus. *Histochem. J*. **29,** 823–830.
97. Tagaya, M, Liu, K.-F., Copeland, B., Seiffert, D., Engler, R., Garcia, J. H., and Zoppo, G. J. del (1997) DNA scission after focal brain ischemia. *Stroke*, **28,** 1245–1254.
98. Mundle, S. D., Gao, X. Z., Khan, S., Gregory, S. A., Preisler, H. D., and Raza, A. (1995) Two *in situ* labeling techniques reveal different patterns of DNA fragmentation during spontaneous apoptosis *in vivo* and induced apoptosis *in vitro*. *Anticancer Res*. **15,** 1895–1904.
99. Yamadori, I., Yoshino, T., Kondo, E., Cao, L., Akagi, T., Matsuo, Y., and Minowada, J. (1998) Comparison of two methods of staining apoptotic cells of leukemia cell lines: terminal deoxynucleotidyl transferase and DNA polymerase I reactions. *J. Histochem. Cytochem*. **46,** 85–90.
100. Mainwaring, P. N., Ellis, P. A., Detre, S., Smith, I. E., and Dowsett, M. (1998) Comparison *of in situ* methods to asses DNA cleavage in apoptotic cells in patients with breast cancer. *J. Clin. Pathol*. **51,** 34–37.
101. Lucassen, P. J., Chung, W. C. J., Vermeulen, J. P., van Lookeren Campagne, M., van Dierendonck, J. H., and Swaab, D. F. (1995) Microwave-enhanced *in situ* end-labeling of fragmented DNA: parametric studies in relation to postmortem delay and fixation of rat and human brain. *J. Histochem. Cytochem*. **43,** 1163–1171.
102. Hayashi, R., Ito, Y., Matsumoto, K., Fujino, Y., and Otsuki, Y. (1998) Quantitative differentiation of both free 3'-OH and 5'-OH DNA ends between heat-induced apoptosis and necrosis. *J. Histochem. Cyto*chem. **46,** 1051–1059.
103. Cusick, M. E., Wasserman, P. M., and DePamphilis, M. L. (1989). Application of nucleases to visualizing chromatin organization at replication forks. *Methods Enzymol.* **170,** 290–316.

104. Sollner-Webb, B., Melchior, W Jr, and Felsenfeld, G. (1978). DNase I, DNAse II, and staphylococcal nuclease cut at different, yet symmetrical located sites in the nucleosome core. *Cell* **14,** 611–627.
105. Hu, G. (1993) DNA polymerase-catalyzed addition of nontemplated extra nucleotides to the 3' end of a DNA fragment. *DNA Cell Biol*. **12,** 763–770.
106. Didenko, V., and Hornsby, P. J. (1996). Presence of double-strand breaks with single-base 3' overhangs in cells undergoing apoptosis but not necrosis. *J. Cell Biol.* **135,** 1369–1376.
107. Al-Lamki, R. A., Skepper, J. N., Loke, Y. W., King, A., and Burton, G. J. (1998) Apoptosis in the early human placental bed and its discrimination from necrosis using the *in situ* DNA ligation technique. *Hum. Reprod.* **13,** 3511–3519.
108. Didenko, V. V., Tunstead, J. R., and Hornsby, R. J. (1998 Biotin-labeled hairpin oligonucleotides. Probes to detect double-strand breaks in DNA in apoptotic cells. *Am. J. Pathol*. **152,** 897–902.
109. Didenko, V. V., Boudreaux, D. J., and Baskin, D. S. (1999) Substantial background reduction in ligase-based apoptosis detection using newly designed hairpin oligonucleotide probes. *Biotechiques* **27,** 1130–1132.
110. Kanoh, M, Takemura, G., Misao, J., Hayakawa, Y, Aoyama, T., Nishigaki, K., Noda, T., Fujiwara, T., Fukuda, K., Minatoguchi, S., and Fujiwara, H. (1999) Significance of myocytes with positive DNA *in situ* nick end-labeling (TUNEL) in hearts with dilated cardiomyopathy. *Circulation* **99,** 2757–2764.
111. Hotz, M. A., Gong, J., Traganos, F., and Darzynkiewicz, Z. (1994) Flow cytometric detection of apoptosis: comparison of assays *in situ* DNA degradation and chromatin changes. *Cytometry*, **15,** 237–244.
112. Hilton, D. A., Love S., and Barber, R. (1997) Demonstration of apoptotic cells in tissue sections by *in situ* hybridization using dioxigenin-labeled poly(A) oligonucleotide probes to detect thymidine-rich DNA sequences. *J. Histochem. Cytochem*. **45,** 13–20.
113. Basnakian, A., and James, S. J. (1994) A rapid and sensitive assay for the detection of DNA fragmentation during early phase of apoptosis. *Nucleic Acids Res*. **22,** 2714–2715.
114. Carr, N. J., and Talbot, I. C. (1997) *In situ* end labeling: effect of proteolytic enzyme pretreatment and hydrochloric acid. *J. Clin. Pathol.: Mol. Pathol*. **50,** 160–163.
115. Davidson, F. D., Groves, M., and Scaravilli, F. (1995) The effects of formalin fixation on the detection of apoptosis in human brain by *in situ* end-labeling of DNA. *Histochem. J*. **27,** 982–988.
116. Bardales, R. H., Xie, S.-S., Hsu, S.-M. (1996) *In situ* DNA fragmentation assay for detection of apoptosis in paraffin-embredded tissue sections. Technical considerations. *Am. J. Clin. Pathol.* **107,** 332–336.
117. Shi, S., Key, M. E., and Kalra, K. L. (1991) Antigen retrieval in formalin-fixed paraffin-embedded tissues: an enhancement method for immunohistochemical staining based on microwave oven heating of tissue sections. *J. Histochem. Cytochem*. **39,** 741–748.

118. Wu, C. Y., Chen, S. T., Chiou, S. H., and Wag, K. T. (1992) Specific peptide-bond cleavage by microwave irradiation in weak acid solution. *J. Prot. Chem*. **11,** 45–50.
119. Sträter, J., Günther, A. R., and Brüderlein, S. (1995) Microwave irradiation of paraffin-embedded tissue sensitizes the TUNEL method for *in situ* detection of apoptotic cells. *Histochem*. **103,** 157–160.
120. Norton, A. J., Jordan, S., and Yeomans, P. (1994) Brief, high temperature heat denaturation (pressure cooking): a simple and effective method of antigen retrieval for routinely processed tissues. *J. Pathol*. **173,** 371–379.
121. Panchalingam, S., Reynolds, G. M., Lammas, D. A., Rowlands, D. C., and Kumararatne, D. S. (1996) Simple method for pretreatment of tissue sections for the detection of apoptosis by *in situ* end-labeling and *in situ* nick translation. *J. Clin. Pathol: Mol. Pahol*. **49,** M273–M277.
122. Negoescu, A., Lorimier, P., Labat-Moleur, F., Drouet, C., Robert, C., Guillermet, C., Brambilla, C., and Brambilla, E. (1996) *In situ* apoptotic cell labeling by the TUNEL method: improvement and evaluation on cell preparations. *J. Histochem. Cytochem*. **44,** 959–968.
123. Labat-Moleur, F., Guillermet, C., Lorimier, P., Robert, C., Lantuejoul, S., Brambilla, E., and Negoescu, A. (1998) TUNEL apoptotic cell detection in tissue sections: critical evaluation and improvement. *J. Histochem. Cytochem*. **46,** 327–334.
124. Stähelin, B. J., Marti, U., Solioz, M., Zimmermann, H., and Reichen, J. (1998) False positive staining in the TUNEL assay to detect apoptosis in liver and intestine is caused by endogenous nucleases and inhibited by diethyl pyrocarbonate. *J. Clin. Pathol.: Mol. Pathol*. **51,** 204–208.
125. Negoescu, A., Guillermet, C., Lorimier, P., Brambilla, E., and Labat-Moleur, F. (1998) Importance of DNA fragmentation in apoptosis with regard to TUNEL specificity. *Biomed. Pharmacother*. **52,** 252–258.
126. Eastman, A., and Barry, M. B. (1992) The origins of DNA breaks: a consequence of DNA damage, DNA repair, or apoptosis? *Cancer Invest*. **10,** 229–240.
127. Kockx, M. M., Muhring, J., Knaapen, M. W. M., and Meyer, G. R. Y. de (1998) RNA synthesis and splicing interferes with DNA *in situ* end labeling techniques used to detect apoptosis *Am. J. Pathol*. **152,** 885–888.
128. Petito, C. K., and Roberts, B. (1995) Effect of postmortem interval on *in situ* end-labeling of DNA oligonucleotides. *J. Neuropathol. Exp. Neurol*. **54,** 761–765.
129. Modak, S. P., and Price, G. B. (1971) Exogenous DNA polymerase-catalysed incorporation of deoxyribonucleotide monophosphates in nuclei of fixed mouse-brain cells. *Exp. Cell Res*. **65,** 289–296.
130. Manoharan, K., Kinder, D., and Banerjee, M. R. (1987) DMBA induced DNA damage and repair in mammary epithelial cells *in vitro* measured by a nick translation assay. *Cancer Biochem. Biophys*. **9,** 127–132.
131. Anai, H., Maehara, Y., and Sugimachi, K. (1988) *In situ* nick translation method reveals DNA strand scission in HeLa cells following heat treatment. *Cancer Lett*. **40,** 33–38.

132. Maehara, Y., Anai, H., Kusumoto, T., Sakaguchi, Y., and Sugimachi, K. (1989) Nick translation detection *in situ* of cellular DNA strand breaks induced by radiation. *Am. J. Pathol*. **134,** 7–10.
133. Maehara, Y., Emi, Y., Anai, H., Sakaguchi, Y., Kohnoe, S., Tsuichi, S., and Sugimachi, K. (1989) Adriamycin-induced DNA strand breaks in HeLa and in P388 leukemia cells detected using *in situ* nick translation. *J. Pathol*. **159,** 323–327.
134. Libbus, B. L., Illenye, S. A., and Graighead, J. E. (1989) Induction of DNA strand breaks in cultured rat embryo cells by crocidolite asbestos as assessed by nick translation. *Cancer Res*. **49,** 5713–5718.
135. Berlingin, E., Sass, U., Roza, L., and Heenen, M. (1992) UV-induced DNA strand breaks detected by *in situ* nick translation in human epidermis. *Arch. Dermatol. Res*. **284,** 184–185.
136. Kodym, R., and Hörth, E. (1995) Determination of radiation-induced DNA strand breaks in individual cell by non-radioactive labeling of 3'OH ends. (1995) *Int. J. Radiat. Biol*. **68,** 133–139.
137. Coats, P. J., Save, V., Ansari, B., and Hall, P. A. (1995) Demonstration of DNA damage/repair in individual cells using *in situ* end labeling: association of p53 with sites of DNA damage. *J. Pathol*. **176,** 19–26.
138. Assad, M., Lemieux, N., and Rivard, C. H. (1997) Immunogold electron microscopy *in si*tu end-labeling (EM-ISEL): assay for biomaterial DNA damage detection. *Bio-Med. Mat. Engin*. **7,** 291–400.
139. Cayrol, C., Sarraute, J., Tarroux, R., Redoules, D., Charveron, M., and Gall, Y. (1999) A mineral sunscreen affords genomic protection against ultraviolet (UV) B and UV A radiation: *in vitro* and *in situ* assays. *Br. J. Dermatol.* **141,** 250–258.
140. Okudela, K., Ito, T., Mitsui, H., Hayahi, H., Udaka, N., Kanisawa, M., and Kitamura, H. (1999) The role of p53 in bleomycin-induced DNA damage in the lung. *Am. J. Pathol.* **155,** 1341–1351.
141. Coates, P. J. (1994) Molecular methods for the identification of apoptosis in tissues. *J. Histochem.* **17,** 261–267.
142. Eijnde, S. M. van den, Luijsterburg, A. J. M., Boshart, L., Zeeuw, C. I. de, Dierendonck, J. H. van, Reutelingsperger, C. P. M., and Vermeij-Keers, C. (1997) *In situ* detection of apoptosis during embryogenesis with Annexin V: from whole mount to ultrastructure. *Cytometry*, **29,** 313–320.
143. Srinivasan, A., Roth, K. A., Sayers, R. O., Schindler, K. S., Wong, A. M., Fritz, L. C., and Tomaselli, K. (1998). *In situ* immunodetection of activated caspase-3 in apoptotic neurons in the developing nervous system. *Cell Death Differ.* **5,** 1004–1016.
144. Leers, M. P. G., Kolgen, W., Björklund, V., Bergman, T., Tribbick, G., Persson, B., Björklund, P., Ramaekers, F. C. S., Bjorkland, B., Nap, M., Jornvall, H., and Schutte, B. (1999) Immunocytochemical detection and mapping of a cytokeratin 18 neoepitope exposed during early apoptosis. *J. Pathol*. **187,** 567–572.
145. Mundle, S. D., Iftikhar, A., Shetty, V., Dameron, S., Wright-Quinones, V., Marcus, B., Loew, J., Gregory, S. A., and Raza, A. (1994) Novel *in situ* double

labeling for simultaneous detection of proliferation and apoptosis. *J. Histochem. Cytochem*. **42,** 1533–1537.
146. Sanders, E. J. (1997) Methods for detecting apoptotic cells in tissues. *Histol. Histopathol*. **12,** 1169–1177.
147. Willingham, M. C. (1999) Cytochemical methods for the detection of apoptosis. *J. Histochem. Cytochem*. **47,** 1101–1109.
148. Saraste, A., and Pulkki, K. (2000) Morphologic and biochemical hallmarks of apoptosis. *Cardiovasc. Res*. **45,** 528–537.
149. Stadelmann, C., and Lassmann, H. (2000) Detection of apoptosis in tissue sections. *Cell Tissue Res.* **301,** 19–31.

8

Labeling DNA Breaks *In Situ* by Klenow Enzyme

Katherine A. Wood

1. Introduction

The Klenow fragment of DNA polymerase I, first described by Klenow and Henningson in 1970 ***(1)***, consisted of a 75 kDa proteolytic fragment of the Kornberg polymerase of *Escherichia coli*. Klenow is now usually obtained as a recombinant protein expressed from a truncated *polA* gene ***(2)***. To polymerize the addition of nucleotides to the 3'-OH end of DNA, Klenow requires a single stranded DNA template and a DNA or RNA primer with a 3'-hydroxyl terminus. Klenow lacks the 5'–3' exonuclease activity of DNA polymerase I, but retains both the 3'–5' exonuclease activity, which degrades single stranded or double stranded DNA from a 3'-OH terminus, and the displacement activity of the intact polymerase ***(3)***. Applications using Klenow include: end-filling and end-labeling DNA with a 5'-overhang, labeling single stranded DNA by random priming, chain termination sequencing, second strand cDNA synthesis, second strand synthesis in site directed mutagenesis, and production of single stranded probes by primer extension. Of these applications, end-labeling DNA with a 5'-overhang by Klenow has been developed into an *in situ* technique for the detection of DNA breaks using incorporation of modified nucleotides that may then be detected and visualized by a variety of direct and indirect methods.

The most common use of Klenow *in situ* has been for the detection of DNA fragmentation associated with apoptosis ***(4–6)***. DNA fragmentation during apoptosis is a common, although not universal, event in cells and tissues, ***(7,8)***. DNA fragmentation is induced by caspase mediated cleavage of the inhibitor of caspase-activated DNase (ICAD) which in turn allows DNA cleavage by the caspase activated DNase (CAD) ***(9)***. The cascade commonly leads to the characteristic double stranded breaks in the internucleosomal regions of DNA. The cleavage is not sequence specific and occurs randomly within the exposed

From: *Methods in Molecular Biology, vol. 203:* In Situ *Detection of DNA Damage: Methods and Protocols*
Edited by: V. V. Didenko

linker regions generating up to a million DNA breaks per cell or more. The majority of the internucleosomal breaks leave a free 3'-hydroxyl group. For detection of DNA fragmentation associated with apoptosis, no difference has been observed between labeling with Klenow and DNA polymerase I, suggesting that the 5'–3' exonuclease activity is not required for labeling apoptotic cells *in situ* ***(10,11)***.

In addition to apoptosis, there are other circumstances when DNA fragmentation occurs *in situ*, although DNA breaks during physiological processes other than apoptosis are usually limited and of insufficient number to be detected directly using Klenow. However, necrotic cells contain a high number of random single stranded breaks. Since the nick translation activity of polymerase I can improve labeling of single stranded breaks, necrotic cells may be preferentially labeled by DNA polymerase I and this would be the enzyme of choice for identifying necrosis ***(10)***. DNA breaks occur normally during mitosis, meiosis, DNA damage, and DNA repair but at levels too low to be detected routinely *in situ*. In an adaptation of the basic *in situ* technique, Klenow has also been used to detect abasic sites in DNA: after treatment of DNA with Exonuclease III to convert abasic sites to single stranded DNA breaks, Klenow is used to label the DNA ends ***(12)***.

Damage to DNA can also be introduced during sample fixation, processing, and handling ***(13)***. Accurate interpretation of the results of *in situ* labeling for DNA breaks using Klenow can only be made with data obtained from positive and negative controls included in each study. Similarly, the conclusions drawn from a positive result with *in situ* labeling using Klenow should be supported with data obtained using other techniques such as morphological methods, to determine the biological relevance of the DNA breaks detected, *e.g.* electron microscopy to determine apoptosis versus necrosis.

The typical labeling reaction to detect DNA breaks *in situ* using Klenow involves sample preparation, fixation and immobilization, followed by permeabilization and Klenow-based labeling at the sites of DNA breaks, and finally detection of the incorporated label, and visualization. The method presented here describes a detailed protocol for the detection of DNA breaks in tissue sections, using Klenow to incorporate a biotinylated nucleotide. The incorporated biotinylated nucleotides are bound by a streptavidin-horseradish peroxidase conjugate that is detected by the conversion of diaminobenzamide tetrahydrochloride (DAB) to an insoluble brown precipitate at the sites of peroxidase activity. The samples are viewed with a standard light microscope after counterstaining. There are a variety of options available for the specific label and detection method used that are discussed in the notes section at the appropriate point in the protocol.

2. Materials

See **Note 1**. The majority of solutions should be prepared on the day of use, therefore, a list of stock solutions is provided.

1. For sample preparation, access to standard facilities and equipment for tissue fixation and processing, and for preparation of frozen sections or paraffin embedded sections will be required.
2. For cryosectioning: sucrose, Optimum Cutting Temperature (OCT) Matrix, *e.g.,* from TissueTEK, isopentane, dry ice.
3. For paraffin embedding; absolute alcohol (100% ethanol), xylene, low or middle point melting temperature paraffin.
4. For fixation of tissues: 37% formaldehyde, 10× phosphate buffered saline (pH 7.4), magnesium and calcium free (75 m*M* disodium hydrogen phosphate, 25 m*M* sodium dihydrogen phosphate, 1.45 *M* sodium chloride). The 10× phosphate buffered saline (PBS) is diluted with water to prepare the 1× PBS that is used throughout the labeling procedure.
5. Autoclaved deionized water (18 mΩ) should be used for dilutions of all reagents unless otherwise indicated. Molecular biology grade reagents should be used for the labeling reaction.
6. For permeabilization: stock solutions of 100 m*M* Tris-HCl (pH 7.5), 200 m*M* EDTA, 10% SDS, 1 mg/mL proteinase K (20 units/mg) in water (store at –20°C).
7. For DNase I treatment: stock solutions of 1 mg/mL DNase I (2000 Kunitz units/mg) prepared in 10 m*M* $CaCl_2$, 50% glycerol and stored at –20°C, 100 m*M* $MnCl_2$, 200 m*M* $CaCl_2$, 100 mg/mL bovine serum albumin (BSA).
8. For peroxidase quenching: 30% hydrogen peroxide, methanol.
9. For labeling reaction: Klenow enzyme (2 unit/μL), stock solutions of 1 *M* Tris-HCl (pH 7.5), 100 m*M* $MgCl_2$, 10 m*M* 2-mercaptoethanesulfonic acid (MESNA), 100 mg/mL BSA, 1 m*M* dATP, 1 m*M* dTTP, 1 m*M* dGTP, 1 m*M* biotin-14-dCTP, 3 *M* NaCl, and 300 m*M* sodium citrate.
10. For detection and visualization: streptavidin-horseradish peroxidase (1 mg/mL), diaminobenzamide tetrahydrochloride (DAB), Harris modified hematoxylin solution, Tween-20, ammonium hydroxide, mounting medium, *e.g.* Permount, 30% hydrogen peroxide, 10× PBS, absolute alcohol or denatured alcohol, and xylene. Do not reuse the ethanol or xylene left after paraffin embedding or deparaffinization of sections.

3. Methods

3.1. Sample Preparation

It is essential to control the quality of the sample during harvesting and preparation for labeling. False positives can be generated by the introduction of DNA breaks through excessive heating, *e.g.* during paraffin embedding, by certain fixatives, *e.g.* picric acid, and by physical shearing, *e.g.* during sectioning. In analysis of post mortem tissue using DNA polymerase I for the detection of DNA damage, there was no change in the number of labeled cells when

rodent tissue was harvested up to 24 h post mortem ***(12)***, however, caution must be used when interpreting samples harvested at later times post mortem or from other species. Cell or tissue samples should be harvested quickly and efficiently but without undue physical handling, and be frozen or fixed as soon as possible to halt the actions of endogenous nucleases and to prevent autolysis.

3.1.1. Frozen Samples and Fixation of Small Tissue Pieces or Biopsies

1. Rapidly freeze sample by dropping into liquid nitrogen, followed by embedding in optimum cutting temperature (OCT) matrix and immersion into isopentane prechilled on dry ice. Alternatively, the sample can be quickly blotted dry on gauze, placed directly on OCT matrix and rapidly frozen by immersing into isopentane prechilled on dry ice.
2. Attach the frozen embedded sample to a cryostat chuck (pre-chilled to below –20°C) using OCT matrix. Position the chuck and sample in the cryostat and allow to equilibrate to the temperature of the cryostat (approximately –18°C) before sectioning.
3. Cut sections of approximately 10–15 microns and collect onto slides pretreated for electrostatic adherence. Allow slides to dry thoroughly for 1–2 h at 45°C on a slide drier or overnight at room temperature (*see* **Note 2**).
4. Fix the dried sections by immersion in 3.7% formaldehyde in 1× PBS for 10 min at room temperature, followed by washing in 1× PBS to remove traces of fixative. Proceed with labeling (*see* **Section 3.2**).

3.1.2. Fixed Tissues

Klenow may be used for *in situ* detection of DNA fragmentation on tissues fixed in formaldehyde, paraformaldehyde, glutaradehyde, with or without alcohols. Strong acids or bases should be avoided. Formaldehyde is the most commonly used fixative in the published literature using Klenow *in situ*. After fixation, samples may be processed for paraffin embedding or for frozen sectioning. The latter may be of benefit if immunohistochemistry is to be performed in addition to the detection of DNA fragmentation when paraffin embedding is known to interfere with the antigen of interest.

Fresh tissue or material from perfused specimens should be fixed in 4% formaldehyde in 1× PBS at room temperature for up to 24 h. Change the fixative every 2 h for a minimum of two changes. Proceed with either paraffin embedding or cryosectioning.

3.1.3. Cryosectioning of Fixed Tissues

Freezing of fixed tissues, unless they are small pieces, usually requires cryoprotection before freezing to reduce artifacts due to the formation of ice. This is achieved by equilibration into sucrose prior to freezing.

1. Immerse the fixed sample into a large excess of 30% sucrose in water at room temperature. Leave for a minimum of 12 h or until the sample floats to the top. Rinse briefly in water.
2. Freeze and cut sections according to the procedure in **Subheading 3.1.1** (**Steps 1–4**).

3.1.4. Paraffin Embedding and Sectioning

The process of embedding is commonly automated. It is important to note that the temperature of the paraffin should not exceed 65°C otherwise DNA breaks may be introduced. For manual processing:

1. Place the fixed tissue in a cassette and immerse in an excess volume of 95% ethanol for 30 min. Repeat.
2. Immerse the sample in an excess volume of absolute ethanol for 30 min.
3. Immerse the sample in an excess volume of absolute ethanol for 60 min.
4. Immerse the sample in an excess volume of a 1:1 mix of xylene:absolute ethanol for 60 min.
5. Immerse the sample in an excess volume of xylene for 30 min.
6. Immerse the sample in an excess volume of xylene for 60 min.
7. Immerse the sample in an excess volume of molten paraffin at 65°C for 30 min.
8. Immerse the sample in an excess volume of molten paraffin at 65°C for 60 min. Repeat.
9. Place tissue in the required orientation in a mold and fill with molten paraffin at 65°C.
10. Chill for a few seconds on a freezer plate.
11. Position cassette on top of mold and fill with molten paraffin at 65°C.
12. Chill at –5°C on freezer plate for 15 min.
13. Remove cassette and tissue block from mold and allow to warm to room temperature (for storage *see* **Note 3**).
14. Cut sections from block at 3–6 microns and collect onto slides pretreated for electrostatic adherence (for storage *see* **Note 4**).
15. Just prior to labeling with Klenow, remove paraffin from specimen by immersing for 5 min sequentially in 2 changes each of xylene, 100% ethanol, 95% ethanol, then 70% ethanol.
16. Wash twice in 1× PBS to remove traces of ethanol then proceed with labeling (*see* **Subheading 3.2**).

3.2. Labeling Reaction

The labeling reactions are performed on fixed samples, immobilized on glass slides. For washing, buffer equilibration, and counterstaining steps when reagents are not limiting it is convenient to immerse the slide vertically in Coplin jars designed for this purpose. Small volumes of reagents are pipetted directly on top of the specimens without touching the specimen with the pipet tip but ensuring the entire specimen in covered. Volumes of between 50 and 100 µL are usually sufficient. A cover slip may be used for coverage of large sections.

The protocol is broken down into separate steps to indicate convenient stopping points in the procedure: the samples may be left in the last buffer used in each section for several hours. Optimal labeling will be obtained if the procedure is carried out in its entirety in the same day.

3.2.1. Permeabilization

Based on results from a wide variety of laboratories, permeabilization of the tissue to allow access to the nucleus by the DNA labeling reagents is crucial. Although some samples do not require a permeabilization step, controlled treatment with a permeabilization reagent, combined with the use of appropriate positive and negative controls, will generate the optimal results. A wide variety of agents have been used including solvents, detergents, heat (antigen retrieval), and enzymatic digestion. Optimal labeling will require empirical determination of this step for the tissue under investigation, although a brief digestion using proteinase K will be appropriate for the majority of samples. Frozen sections (fixed after sectioning) typically require little permeabilization, if any, after fixation. For a summary of alternative permeablization methods, *see* ***(14)***.

1. Prepare on ice a 20 µg/mL solution of proteinase K in 10 m*M* Tris-HCl (pH 7.5), 0.05 m*M* EDTA, 0.5% SDS from stock solutions.
2. Remove slide from 1× PBS and blot away excess buffer from around sample.
3. Lay slide flat and immediately pipet the prepared proteinase K solution on top of sample and incubate for 5–30 min at 37°C in a humidified chamber to prevent evaporation and sample drying. Empirical determination of incubation time will be needed (*see* **Note 5**).
4. Wash slide in 1× PBS.
5. Generate a positive control with DNase I on at least one sample (*see* **Note 5**).

3.2.2. Quenching Endogenous Peroxidase Activity

Some specimens will naturally contain peroxidase activity, *e.g.* spleen. When using a peroxidase-based detection system, it is important to remove endogenous peroxide. This step is not required for non-peroxidase detection methods.

1. Immerse slide in a freshly prepared solution of 3% hydrogen peroxide in methanol for 5 min at room temperature. Do not leave samples in hydrogen peroxide solution for longer periods because hydrogen peroxide will cause DNA breaks via free radical production.
2. Rinse slide briefly in 1× PBS.

3.2.3. Labeling of DNA Breaks

Typical incubation times are 60 min at 37°C in a humidified chamber. Prepare the solutions just prior to use. Controls must be included to validate the

data obtained. These controls include: an experimental negative control, *e.g.,* normal tissue, prepared in the same way as the experimental sample (*see* **Subheading 3.1.**), to control for tissue handling and processing; a negative labeling control in which the Klenow enzyme is omitted from the labeling mix (*see* **Step 3**, **Subheading 3.2.3.**) to confirm specific labeling; a positive control generated on an experimental sample using DNase I (*see* **Step 5**, **Subheading 3.2.1.**, and **Note 5**) to confirm that permeabilization was optimal; and a standard positive control obtained from an alternate source *e.g.* commercially available sections of tissues containing apoptotic cells (*see* **Subheading 2**) to confirm that all the reagents were functioning and that the procedure was carried out correctly.

1. Equilibrate sample by immersing slide in 1× Klenow labeling buffer (50 m*M* Tris (pH 7.5), 5 m*M* $MgCl_2$, 60 µ*M* 2-mercaptoethanesulfonic acid (MESNA), 50 µg/mL BSA for 2 min.
2. Meanwhile, prepare the enzyme labeling mix on ice consisting of 0.15 m*M* dATP, 0.15 m*M* dGTP, 0.15 m*M* dTTP, 5 µm biotinylated dCTP, in 1× Klenow labeling buffer, and 0.04 units/µL Klenow. Generate a labeling negative control by omitting the Klenow from the mixture applied to at least one experimental sample. Alternative labeled nucleotides are also available (*see* **Note 6**).
3. Remove equilibrated slide and blot excess buffer from around sample with a tissue. Immediately, pipette the enzyme labeling mix onto the sample, ensuring the entire sample is covered, and incubate for 1 h at 37°C in a humidified chamber.
4. Immerse for 2 min in 300 m*M* NaCl, 30 m*M* sodium citrate to stop the reaction, then rinse briefly in PBS.

3.3. Detection and Visualization of Incorporated Label

Biotin is recognized and bound by streptavidin. A convenient and well characterized method for the detection of biotin is the use of streptavidin conjugated to horseradish peroxidase. Since endogenous peroxidase activity is readily quenched, peroxidase based systems are more commonly used over phosphatase based systems (*see* **Note 7**). The peroxidase is then visualized using DAB to generate a dark brown precipitate in cells that have incorporated the biotin. A variety of commercial proprietary peroxidase substrates are available that may be used instead of DAB: follow the manufacturers' guidelines for buffers, incubations, selection of counterstain etc.

1. Blot excess buffer from around sample, then cover specimen with 2 µg/mL streptavidin-horseradish peroxidase in 1× PBS, 0.05% Tween-20 for 20 min at room temperature.
2. Wash slide three times in an excess volume of 1× PBS, 0.05% Tween-20, then once in 1× PBS. The presence of Tween helps reduce non-specific interaction of the streptavidin-conjugate with the specimen.

3. Prepare a solution of 50 mg/mL diaminobenzamide tetrahydrochloride (DAB), 0.03% hydrogen peroxide, in 1× PBS (*see* **Note 8**). Immerse washed slide from step 2 and incubate for 3 to 10 min. View periodically during development under microscope (*see* **Note 9**).
4. Stop the color development by washing in 1× PBS.
5. Immerse slide in hematoxylin for up to one min. Rinse briefly in tap water then dip ten times in 0.01% ammonium hydroxide tap. Rinse briefly again in tap water. Care is needed not to counterstain the specimen too darkly or the DAB will be obscured (*see* **Note 10**).
6. Dehydrate by passing through two changes each of 95% ethanol then 100% ethanol.
7. Clarify by passing through two changes of mixed xylenes for 5 min each.
8. Lay slide horizontally and place two drops of Permount onto specimen. Lay glass cover slip onto Permount and press gently to expel any bubbles. Allow sample to harden overnight.
9. View at up to 400× magnification. *See* **Note 11** for data interpretation. Store slides in the dark.

4. Notes

1. Some of the reagents that are used for *in situ* Klenow labeling of DNA may be hazardous, therefore, wear gloves, lab coat and eye protection when handling any of the reagents. Use of a chemical fume hood is recommended for certain reagents, *e.g.* xylene. Refer to the appropriate materials safety data sheets prior to use.
2. Optimal labeling is obtained if the sections are labeled immediately after sectioning and drying. If necessary, store the sections at –80°C after sectioning for short periods of time, dry for 2 h at 45°C on a plate drier, then rinse with 1× PBS before proceeding with the labeling reaction.
3. Specimens are ideally stored in paraffin blocks. Store them at room temperature.
4. The quality of labeling of DNA breaks with Klenow is optimal when the sections are freshly cut and labeled within 48 h. If necessary, store paraffin embedded sections for up to one month at room temperature in a sealed box with desiccant.
5. A brief treatment with DNase I will generate DNA breaks that are substrates for Klenow end-labeling. If the tissue was permeabilized adequately, each nucleus in the DNase I treated sample will be labeled. The inclusion of Mn^{+2} in the DNase I buffer causes double stranded DNA breaks ***(3)***. If single stranded breaks are required Mg^{+2} may be substituted.
   a. After permeabilization, incubate the sample in 1 µg/mL of DNase I in 50 m*M* Tris-HCl (pH 7.5), 10 m*M* $MnCl_2$, 20 m*M* $CaCl_2$, 0.1 mg/mL BSA (prepared fresh from stock solutions) for 10 min at 37°C.
   b. Wash twice in 1× PBS. Proceed with quenching step.
6. Other labels include digoxigenin-labeled nucleotides, and FITC-labeled nucleotides. The detection method used will be dependent upon the label utilized. FITC-labeled nucleotides incorporated by Klenow can be viewed directly after labeling by epifluorescence microscopy. Incorporation of digoxigenin-labeled

nucleotides require use of an anti-digoxigenin antibody conjugate for detection. Follow the manufacturers' recommendation for use.

7. If preferred, phosphatase-based detection systems may be used, *e.g.* substitute the streptavidin-horseradish peroxidase conjugate for a streptavidin-phosphatase conjugate. Organic phosphate buffers should not be used with phosphatases, therefore, substitute the 1× PBS used throughout the procedure for 1× Tris buffered saline. A variety of phosphatase substrates can be used: follow the manufacturers recommendations for use. Note that the counterstain must be compatible with the detection system, *e.g.* do not use hematoxylin if the phosphatase reaction product is blue or black.
8. DAB should be disposed of according to local, state and federal regulations.
9. The color reaction product may be monitored by rinsing the slide briefly in water, and viewing the slide with a light microscope at 100–200× magnification. Positive cells will appear pale brown. If a longer time is needed, return the slide to the DAB solution and continue the incubation.
10. To ensure that the counterstaining is appropriate, it is worthwhile staining one or two specimens prior to labeling the sections to determine the immersion times needed for a pale blue staining of all cells.
11. The presence of DNA breaks in a cell is indicated by a dark brown coloration (DAB) usually confined to the nucleus, visible against the pale blue of the counterstain. The staining may be diffuse or punctate, indicating whether the chromatin (with DNA breaks) is also condensed.

    The DNase I treated positive control allows for the investigator to determine that the permeabilization was adequate: this sample should contain nuclei that are universally labeled with a brown diffuse DAB stain. If few or no nuclei are stained this suggests that the permeabilization is inadequate and the incubation time in proteinase K should be increased. No staining in this sample could also indicate that one of the reagents has failed, *e.g.* the Klenow enzyme was stored incorrectly, or the protocol was not carried out correctly *e.g.* a reagent was omitted by mistake.

    Confirmation that the procedure was carried out correctly is ruled out using a standard positive control, *e.g.* a sample known to contain cells with DNA breaks for which optimal conditions have been determined. There are commercial sources for these positive controls, *e.g.* murine thymus (positive for apoptotic cells) available from Trevigen Inc. It is important to note that commercially available controls allow novice users to become familiar with the technique but they can confirm only that all the reagents are working and that the procedure was carried out correctly. Each experimental specimen will require optimization.

    A negative control allows for the investigator to determine the background level of staining. The negative labeling control must be treated in an identical manner to the positive control sample and the experimental sample except the Klenow enzyme is omitted from the labeling reaction. After labeling, the negative labeling control should not contain any brown DAB staining. Labeling over the entire sample (nuclei and cytoplasm) indicates that the streptavidin-conjugate

has bound non-specifically. This background staining can be reduced by decreasing the concentration of the streptavidin-conjugate, or by increasing the numbers of washes. Bovine serum albumin (1%) may be added to the washes prior to the incubation with the streptavidin-conjugate to block non-specific binding sites. Cytoplasmic DAB staining in the negative control may also be observed with inadequate quenching of endogenous peroxidases. Patches of DAB staining in the negative control usually indicates that the sample may have dried out during the labeling procedure.

An experimental negative control can be very important for troubleshooting and data interpretation. In normal adult tissue very few cells will contain DNA breaks, although some neonatal and embryonic tissue may contain high numbers of apoptotic cells with DNA breaks, *e.g.* cerebellum in neonatal mice. The inclusion in the assay of normal tissue, *e.g.* from untreated animal, that is harvested, prepared and labeled in the same way as the experimental material helps validate the data. Labeling of the majority of nuclei in the experimental negative control usually indicates that the permeabilization with proteinase K was too aggressive and should be reduced. Less commonly, high numbers of stained nuclei in the experimental negative control may indicate hydrolysis of the DNA during storage, improper fixation, autolysis, or heat damage during paraffin embedding, which would render the samples useless for end-labeling under most circumstances.

References

1. Klenow, H. and Henningsen, I. (1970) Selective elimination of the exonuclease activity of the deoxyribonucleic acid polymerase from *Escherichia coli* B by limited proteolysis. *Proc. Natl. Acad. Sci.* USA **65,** 168–175.
2. Joyce, C. M. and Grindley, N. D. F. (1983) Construction of a plasmid that overproduces the large proteolytic fragment (Klenow fragment) of DNA polymerase I of *Escherichia coli*. *Proc. Natl. Acad. Sci. USA* **80,** 1830.
3. Brown, T. A., ed. (1991) *Molecular Biology LabFax.* BIOS Scientific Publishers, Oxford, UK.
4. Ansari, B., Coates, P. J., Greenstein, B. D. and Hall, P. A. (1993) *In situ* end-labeling detects DNA strand breaks in apoptosis and other physiological and pathological states. *J. Pathol.* **170,** 1–8.
5. Wijsman, J. H., Jonker, R. R., Keijzer, R., Velde, C. J. van de, Cornelisse, C. J. and Dierendonck, J. H. (1993) A new method to detect apoptosis in paraffin sections: *in situ* end-labeling of fragmented DNA. *J. Histochem. Cytochem.* **41,** 7–12.
6. Davison, F. D., Groves, M. and Scaravilli, F. (1995) The effects of formalin fixation on the detection of apoptosis in human brain by *in situ* end-labeling of DNA. *Histochem. J.* **27,** 983–988
7. Wyllie, A. H. (1980) Glucocorticoid-induced thymocyte apoptosis is associated with endogenous endonuclease activation. *Nature* **284,** 555–556.
8. Oberhammer, F., Wilson, J.W, Dive, C., Morris, I. D., Hickman, J. A., Wakeling, A. E., Walker, P. R., and Sikorska, M. (1993) Apoptotic death in epithelial cells: cleavage of DNA to 300 and/or 50 kb fragments prior to or in the absence of internucleosomal fragmentation. *EMBO J.* **12,** 3679–3684.

9. Sakahiri, H., Enari, M., and Nagata, S. (1998) Cleavage of CAD inhibitor in CAD activation and DNA degradation during apoptosis. *Nature* **391,** 96–99.
10. Gold, R. Schmied, M., Giegerich, G., Breitschopf, H., Hartung, H. P., Toyka, K., Lassmann H. (1994) Differentiation between cellular apoptosis and necrosis by combined use of *in situ* tailing and nick translation techniques. *Lab Invest.* **71,** 219–225.
11. Tagaya, M., Liu, K.-F., Copeland, B., Seiffert, D., Engler, R., Garcia, J. H., and Zoppo, G. J. del (1997) DNA scission after focal brain ischemia. *Stroke* **28,** 1245–1254.
12. Huang, D., Shenoy, A., Cui, J., Huang, W., and Liu, P. K. (2000) *In situ* detection of AP sites and DNA strand breaks bearing 3'-phosphate termini in ischemic mouse brain. *FASEB J.* **14,** 407–417.
13. Petito, C. K. and Roberts, B. (1995) Effect of postmortem interval on *in situ* end-labeling of DNA oligonucleosomes. *J. Neuropathol Exp Neurol*. **54,** 761–765.
14. Stadelmann, C. and Lasmann, H. (2000) Detection of apoptosis in tissue sections. *Cell Tissue Res.* **301,** 19–31.

9

In Situ Nick Translation at the Electron Microscopic Level

Marc Thiry

1. Introduction

The nick translation procedure has been introduced in 1977 by Righy et al. ***(1)***. It is commonly used to label purified DNA in vitro. This technique relies on combined 5'→3' polymerase and 5'→3' exonuclease activities of *Escherichia coli* DNA polymerase I. If a nick or single strand break with a 3' hydroxyl terminus is present in a duplex DNA molecule, the enzyme will translocate it, removing nucleotides ahead of it by 5'→3' exonuclease activity and synthesizing the new DNA strand behind it using 5'→3' polymerase activity ***(2)***. When labeled deoxyribonucleotides are used as substrates, the original unlabeled nucleotides in the DNA template are replaced by the labeled ones.

In addition to DNA damage detection ***(3)*** the method was adapted to study the location of DNase I-sensitive regions within cellular DNA. In this case, the breaks are introduced into an undamaged DNA duplex by adding trace amounts of DNase I to study active regions of chromatin. Initially, Levitt et al. ***(4)*** selectively labeled nuclease-sensitive sites in DNA in isolated nuclei by nick-translation using treatment with low concentrations of DNase I. Later this method was successfully used to study the location of DNase I-sensitive sequences within chromosomes and cells ***(5–14)***. It was recently adapted to the electron microscopic level in order to discriminate between active and inactive regions of interphase chromatin ***(15–16)***.

The technique is applied to the ultrathin sections of biological material and includes two successive steps, the enzymatic labeling reaction followed by an immunocytochemical detection step (**Fig. 1**). In the enzymatic reaction, pancreatic DNase I introduces single-strand breaks with 3' hydroxyls in susceptible

From: *Methods in Molecular Biology, vol. 203:* In Situ *Detection of DNA Damage: Methods and Protocols*
Edited by: V. V. Didenko

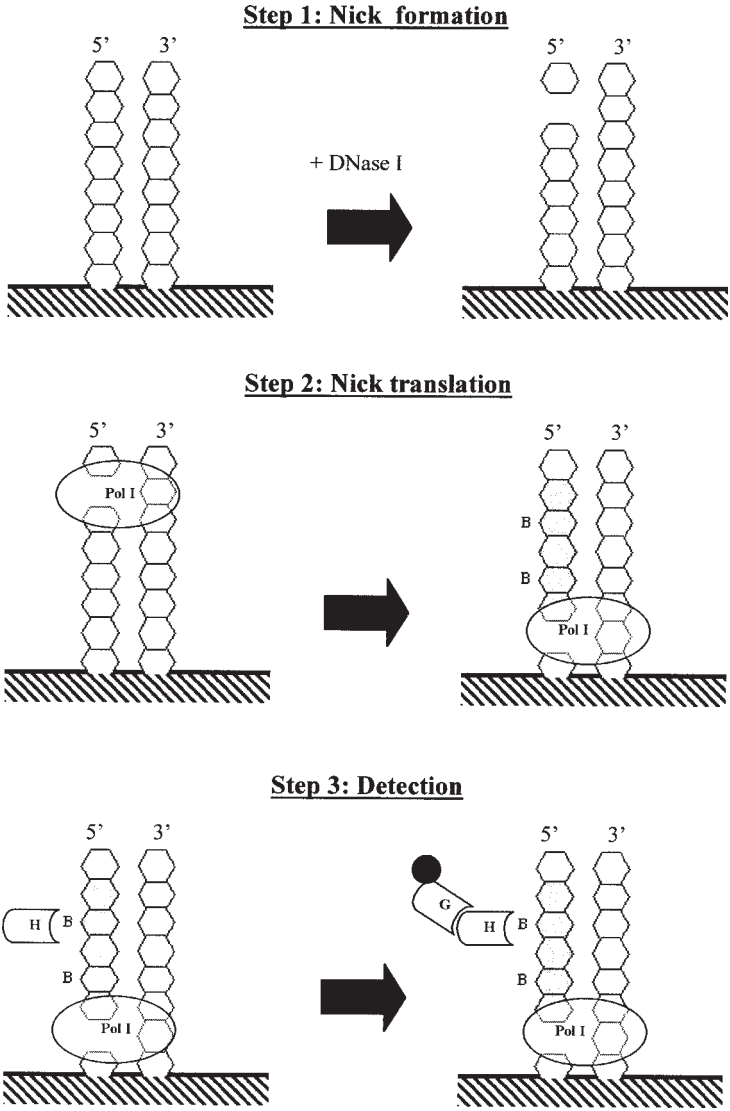

Fig. 1. Schematics of the *in situ* nick-translation-immunogold technique.

1. Step 1—nick formation: DNA exposed by sectioning at the surface of ultrathin sections (hatched lines) is nicked by DNase I.
2. Step 2—nick translation*: E. coli* DNA polymerase I (Pol I) recognizes the nicks and synthesizes a new DNA strand using the opposite strand as a template. The newly synthesized DNA strand is labeled using biotin-11-dUTP (B).
3. Step 3—detection: The incorporated nucleotide analogues are reacted with anti-biotin antibody (H) and visualized using secondary antibody coupled to colloidal gold (G).

sites in DNA. These breaks are subsequently labeled by the nick translation procedure with DNA polymerase I and modified nucleotides. In the detection step, the newly synthesized DNA strands are visualized by an indirect immunogold labeling technique.

Nick translation using mild digestion with DNase I allows preferential labeling of actively transcribing DNA regions. In case when DNase I treatment is omitted the technique detects the pre-existing single-stranded DNA breaks and can be used for visualization of DNA damage *in situ* at the electron microscopic level ***(17)***.

2. Materials

2.1. Equipment

1. Material for ultramicrotomy.
2. Material for embedding at low temperature in Lowicryl K4M (*see* **Note 1**).

2.2. Reagents

2.2.1. Fixatives

1. Sörensen's buffer : 0.1 *M* Na_2HPO_4, 0.1 *M* NaH_2PO_4, pH 7.4, store at 4°C, stable for up to 3 mo.
2. 0.2% glutaraldehyde in Sörensen's buffer , store at 4°C, stable for up to 3 months.
3. 4% formaldehyde or paraformaldehyde in Sörensen's buffer, store at 4°C, stable for 15–21 d.
4. Mixture: formaldehyde 4% and 0.1% glutaraldehyde in Sörensen's buffer, store at 4°C, stable for 15–21 d.

2.2.2. Resin

1. Lowicryl K4M (Chemische Werke Lowi, Waldkraiburg, Germany), store at room temperature (*see* **Note 1**).
2. We currently use the following mixture: 2.7 g crosslinker A, 17.3 g monomer B, 0.1 g initiator C.

2.2.3. Nick Translation

1. Nick translation buffer: 50 m*M* Tris-HCl, 5 m*M* $MgCl_2$, 10 m*M* β-mercaptoethanol, 50 µg/mL bovine serum albumin (BSA; Fraction V, Sigma-Aldrich Chemie, Steinheim, Germany), pH 7.9, stable at 4°C for up to one year.
2. Bovine pancreatic DNase I (Sigma-Aldrich): a stock solution of 1 mg DNase I/100 µL H_2O, store at –20°C in small aliquots, use once.
3. Nucleotides : a 0.4 m*M* stock solution of dGTP, dATP (BRL, Pomona, NY), store at –20°C in aliquots; a stock 0.4 m*M* solution of biotin–11-dCTP (Enzo Diagnostics, Farmingdale, NY), store at –20°C; a stock 0.4 m*M* solution of biotin–11-dUTP (Roche Molecular Biochemicals, Indianapolis, IN), store at –20°C.

2.2.4. Immunocytochemical Detection

1. PBS buffer stock : 0.17 *M* NaCl, 3.35 m*M* KCl, 10 m*M* Na_2HPO_4, 1.8 m*M* KH_2PO_4, stable at 4°C for up to one year.
2. PBSB buffer : 1 volume of PBS buffer stock, 4 volumes of H_2O, add extemporaneously 1% BSA and adjust the pH to 7.2 or 8.2.
3. Goat anti-biotin antibody (Sigma-Aldrich) 1 mg/mL, store at –20°C in aliquots.

2.2.5. Contrasting

1. 50% ethanolic uranyl acetate: 0.5 g uranyl acetate, 12.5 mL boiled H_2O, 12.5 mL ethanol, store at 4°C in a brown glass container or otherwise protected from direct light, stable at 4°C for up to one year, filter (0.22 µm in pore size) before use.
2. Aqueous lead citrate: 4.2% sodium citrate, 2.6% lead nitrate, add concentrated NaOH until clearing up of mixture, stable at 4°C for up to one year, filter (0.22 µm in pore size) before use.

3. Methods

3.1. Preparation of Cells for Electron Microscopy

1. Fix cell pellets (< 0.5 mm^3) at 4°C in either glutaraldehyde or formaldehyde (or paraformaldehyde) or mixture for 15 min or 60 min or 30 min respectively (*see* **Note 1**).
2. Wash samples three times in Sörensen's buffer.
3. Dehydrate samples in a graded series of ethanol solutions:
   - Ethanol 30° 4°C 30 min
   - Ethanol 50° –20°C 30 min
   - Ethanol 70° –20°C 2 × 30 min
   - Ethanol 95° –20°C 30 min
   - Ethanol 100° –20°C 3 × 30 min,
4. Infiltrate samples in Lowicryl K4M at –30°C (*see* **Note 2**) as follows:
   - Ethanol/Lowicryl K4M 2/1 60 min
   - Ethanol/Lowicryl K4M 1/1 60 min
   - Ethanol/Lowicryl K4M 1/2 60 min
   - Pure Lowicryl K4M 2 × 60 min
   - Pure Lowicryl K4M overnight.
5. Transfer samples to the BEEM capsules, fill capsules with fresh pre-cooled resin and close, fill capsules to the top, to minimize dead space over the resin.
6. Polymerize resin for 24 h at –30°C, then for another 2–4 d period at room temperature by indirect (diffuse) ultraviolet irradiation from a Philips TLAD 15W/05 fluorescent lamp (Wavelength peak at 360 nm).
7. Cut ultrathin sections (60–90 nm) of Lowicryl K4M-embedded cells with a diamond knife.
8. Mount sections on 200–400 mesh nickel grids having a collodion film.

3.2. Nick Translation Reaction

1. Incubate grids for 5 min at room temperature on a drop of nick translation buffer (*see* **Note 3**).
2. Transfer grids for 5–45 min at 37°C on a drop (5–10 µL) of nick translation buffer containing 0.1–1,000,000 ng/mL pancreatic DNase I (*see* **Notes 4** and **5**), 10 U/mL *Escherichia coli* DNA polymerase I, 4 µ*M* dGTP, dATP, biotinylated-11-dCTP and biotinylated-11-dUTP (*see* **Note 6**).
3. Rinse grids in five 15 mL-beakers filled with bidistilled water.

3.3. Immunolabeling Procedure

1. Incubate grids for 30 min at room temperature on a drop of PBSB buffer (pH 7.2) containing normal rabbit serum diluted 1/30.
2. Transfer grids for 60 min at room temperature on a drop of goat anti-biotin antibody diluted 1/500 in PBSB buffer containing normal rabbit serum diluted 1/50.
3. Rinse grids in four 15 mL-beakers filled with PBSB buffer (pH 7.2).
4. Rinse grids in a 15 mL-beaker filled with PBSB buffer (pH 8.2).
5. Incubate grids for 60 min at room temperature with medium containing rabbit anti-goat IgG coupled to gold particles either 5 or 10 nm diameter (*see* **Notes 4** and **7**), the gold-coupled IgG being diluted 1/50 in PBSB buffer (pH 8.2).
6. Rinse grids in four 15 mL-beakers filled with PBSB buffer (pH 8.2).
7. Rinse grids in four 15 mL-beakers filled with bidistilled water.
8. Blot and dry grids.

3.4. Staining of Sections

1. Transfer grids into a Petri dish with reduced CO_2 concentration (sodium hydroxide pellets in a Petri dish). Incubate for 30 sec at room temperature in darkness, on drops of 50% ethanolic uranyl acetate.
2. Rinse grids in three 25 mL-beakers filled with boiled bidistilled water.
3. Dry grids on filter paper.
4. Transfer grids into a Petri dish with reduced CO_2 concentration (sodium hydroxide pellets in a Petri dish) for 30 sec at room temperature, on drops of aqueous lead citrate.
5. Rinse grids in three 25 mL-beakers filled with boiled bidistilled water.
6. Dry grids on filter paper.
7. Examine sections in a transmission electron microscope at 60–80 KV (*see* **Notes 8** and **9**).

4. Notes

1. Sterilize glassware, tools and H_2O to be used in the procedure. When the cells are fixed in 1.6% glutaraldehyde, no labeling occurs.
2. Lowicryl K4M is prepared in a brown glass container the day before use. The resin is a skin and eye irritant. All manipulations are carried out in a well-ventilated fume hood. We use gloves for all steps involving use of this resin.

We use a low-temperature embedding in Lowicryl K4M, which is suitable for immunocytochemistry ***(18)*** because it provides optimal conditions for preserving fine cellular structure and for locating antigenic cellular material. In addition to Lowicryl sections ***(15–16,19–22)***, *in situ* nick translation-immunogold technique has been applied successfully to cryosections ***(23)***. It reveals with great precision specific DNA-containing structures in various biological materials, including animal and plant cells. Examples of sensitive, high-resolution detection include the DNA present in mitochondria and DNA viruses ***(16,22)***.

3. Each step is performed on drops of medium placed on parafilm in a moist Petri dish, the face of the grid with ultrathin sections is floated or incubated on the drops of the medium. The washing procedure is performed in beakers by agitating the grids for 10 sec using anticapillary forceps. Before each incubation of grids on drops, the edge of grids and the face of grids devoid of ultrathin sections have to be blotted on filter paper to avoid dipping of grids.
4. The labeling pattern depends on the DNase I concentration in the nick translation medium ***(15,16)***: whereas small nuclear sites at and/or near the border of condensed chromatin blocks are labeled at 1 ng/mL of DNase I concentrations for 5 min (*see* **Fig. 2**, upper), labeling of the condensed chromatin requires higher concentrations in the nick-translation medium (**Fig. 2**, middle). Very high DNase I concentrations cause the label to disappear (**Fig. 2**, below), most likely because the DNA sequences are digested rapidly and solubilized. The evolution of labeling in these experiments thus appears to reflect the selective nicking activity of DNase I. Since DNase I acts preferentially on active chromatin ***(4,24)***, the procedure can be used to distinguish active from inactive sequences of DNA in cells.

   In practice, for each new biological material used, it is recommended to use a graded series of DNase I concentration in nick-translation medium (between 0.1–1,000,000 ng/mL), to discriminate between active and inactive regions.
5. EM-level *in situ* nick-translation reveals DNase I-sensitive sites within in the cell similar to the direct DNase I-colloidal gold labeling technique described by Bendayan ***(25)***. However the direct approach has several disadvantages compared to our procedure. DNase activity in it may be reduced if the active site of the enzyme is involved in the binding with the gold particle, in addition steric hindrance problem can arise when the enzyme is coupled to gold particles. Another limitation of the DNase-gold technique is the affinity of the complex for actin and chitin ***(26,27)***. The indirect method avoids such undesirable labeling because only nucleotides incorporated into DNA at nicked sites are detectable.
6. The signal is more intense when two different biotinylated deoxyribonucleoside triphosphates are used.
7. Label is distributed identically regardless of the diameter of the gold particle, although the labeling intensity is lower for 10 nm particles than for 5 nm particles. However, considering that results are more visible with the larger gold particles, we have frequently illustrated our results with 10 nm gold particles.

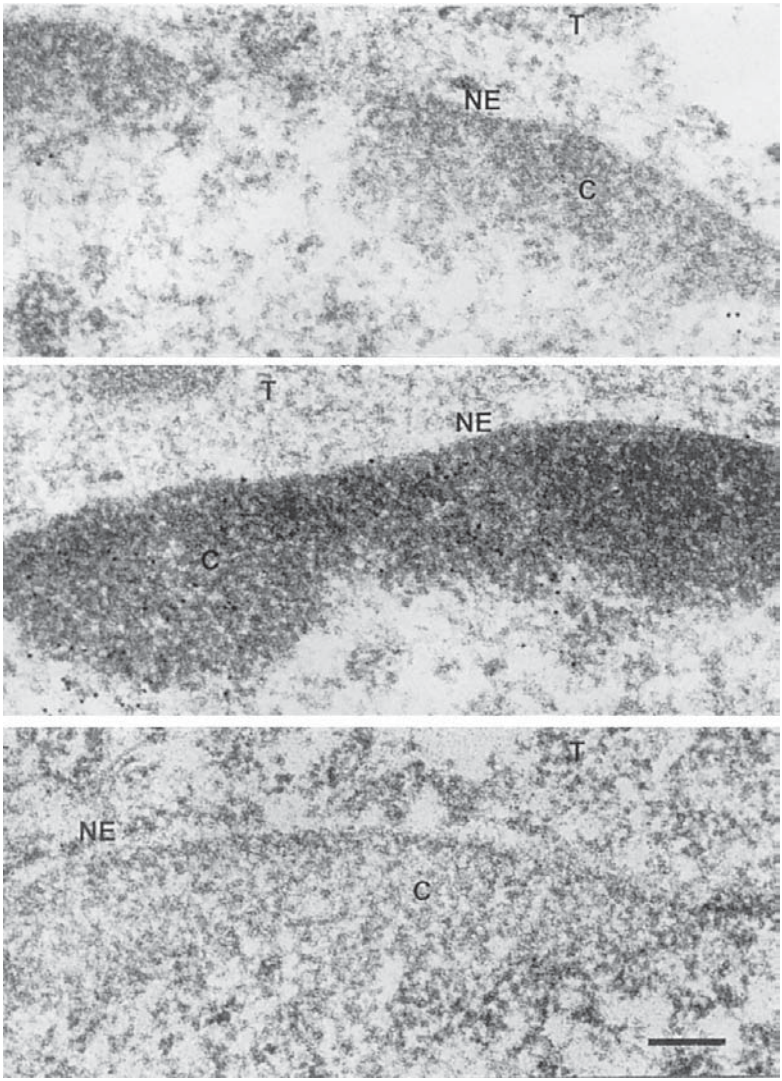

Fig. 2. The distribution of gold particles in the Ehrlich tumor cell nucleus depends on the concentration of DNase I in nick translation medium. At a low concentration of DNase I (1 ng/mL of DNase I for 5 min; upper) only a few labeled sites are present at or near to the blocks of condensed chromatin (C) associated with the nuclear envelope (NE). The labeling of condensed chromatin required higher DNase I concentrations (500 ng/mL for 45 min; middle). At a very high DNase I concentration (1,000,000 ng/mL for 30 min; below) no label occurs, most likely because the DNA sequences present at the surface of ultrathin sections are digested rapidly and solubilized.
(T—cytoplasm; Bar represents 0.2 μm)

8. To verify the specificity of the labeling obtained by *in situ* nick-translation-immunogold procedure, various controls are necessary. The following controls are recommended:
   - Pretreatment of sections with RNase, RNase should not affect labeling.
   - Omission of DNase I from the nick-translation medium. It is worth mentioning that some very scant labeling of DNA-containing structures occurs when ultrathin sections are incubated in a DNase I-free nick-translation medium ***(28)***. This signal probably results from the 3'→5' exonuclease activity of DNA polymerase I., in this reaction the enzyme degrades double-stranded DNA from the 3'-hydroxyl terminus and creates a recessed 3 ‘terminus which can then serve as a primer for DNA synthesis catalyzed by DNA polymerase I. By this exchange reaction, labeled nucleotides can be incorporated into blunt-ended DNA present at the surface of sections. On the other hand, all the naturally occurring DNA breaks such as those generated during apoptosis or by DNA repair systems can also be detected.
   - Omission of DNA polymerase I from the nick-translation medium.
   - Omission of modified nucleotides from the nick-translation medium.
   - Omission of the primary antibody.
   - Substitution of the secondary antibody coupled colloidal gold with a solution of gold lacking the antibody tag.
   - Biological control. No positive label should be found in structures devoid of DNA.
9. Troubleshooting.

   No labeling:
   - Inadequate fixation; fixative concentration is high.
   - Insufficient DNase digestion; increase the incubation time or the amount of enzyme.
   - Check the quality of reagents.

   High background:
   - Insufficient washing.
   - Care must be taken not to dry up samples, when you blot excess buffer around specimens.
   - Immunolabeling conditions are inappropriate; decrease the immunolabeling time and/or temperature; increase the dilution of antibodies.

Acknowledgments

The author acknowledges the skillful technical and secretarial assistance provided by F. Skivée, D. Bourguignon and S. Bodson. This work received financial support from the “Fonds de la Recherche Scientifique Médicale” (grant no. 3.4578.98). M. T. is a research associate of the National Fund for Scientific Research (Belgium).

References

1. Rigby, P., Dieckmann, M., Rhodes, C., and Berg, P. (1977) Labeling deoxyribonucleic acid to high specific activity *in vitro* by nick translation with DNA polymerase I. *J. Mol. Biol*. **113,** 237–251.

2. Kelly, R., Cozzarelli, N. R., Deutscher; M. P., Lehman, I. R., and Kornberg, A. (1970) Enzymatic synthesis of deoxyribonucleic acid. XXXII. Replication of duplex deoxyribonucleic acid by polymerase at a single strand break. *J. Biol. Chem.* **245,** 39–45.
3. Hashimoto, S., Koji, T., Niu, J., Kanematsu, T., and Nakane, P. K. (1995) Differential staining of DNA strand breaks in dying cells by non-radioactive *in situ* nick translation. *Arch. Histol. Cytol.* **58,** 161–170
4. Levitt, A., Axel, R., and Cedar, H. (1979) Nick translation of active genes in intact nuclei. *Dev. Biol.* **69,** 496–505.
5. Gazit, B., Cedar, H., Lerer, I., and Voss, R. (1982) Active genes are sensitive to deoxyribonuclease I during metaphase. *Science* **217,** 648–650.
6. Kerem, B. S., Goitein, R., Richler, C., Marcus, M., and Cedar, H. (1983) *In situ* nick-translation distinguishes between active and inactive X chromosomes. *Nature* **304,** 88–90.
7. Kerem, B. S., Goitein, R., Diamond, G., Cedar, H., and Marcus, M. (1984) Mapping of DNase I sensitive regions on mitotic chromosomes. *Cell* **38,** 493–499.
8. Dyer, K. A., Riley, D., and Gartler, S. M. (1985) Analysis of inactive X chromosome structure by *in situ* nick-translation. *Chromosoma* **92,** 209–213.
9. Hutchison, N., and Weintraub, H. (1985) Localization of DNase I-sensitive sequences to specific regions of interphase nuclei. *Cell* **43,** 471–482.
10. Kuo, M., and Plunkett, W. (1985) Nick-translation of metaphase chromosomes: *in vitro* labeling of nuclease-hypersensitive regions in chromosomes. *Proc. Natl. Acad. Sci. USA* **82,** 854–858.
11. Sperling, K., Kerem, B. S., Goitein, R., Kottusch, V., Cedar, H., and Marcus, M. (1985) DNase I sensitivity in facultative and constitutive heterochromatin. *Chromosoma* **93,** 38–42.
12. Ferrarro, M., and Prantera, G. (1988) Human NORs show correlation between transcriptional activity, DNase I sensitivity, and hypomethylation. *Cytogenet. Cell Genet.* **47,** 58–61.
13. De Graaf, A., van Hemert, F., Linnemans, W. A. M., Brakenhoff, G. J., de Jong, L., van Renswoude, J., and van Driel, R. (1990) Three-dimensional distribution of DNase I-sensitive chromatin regions in interphase nuclei of embryonal carcinoma cells. *Eur. J. Cell Biol.* **52,** 135–141.
14. Krystosek, A., and Puck, T. T. (1990) The spatial distribution of exposed nuclear DNA in normal cancer and reverse-transformed cells. *Proc. Natl. Acad. Sci. USA* **87,** 6560–6564.
15. Thiry, M. (1991) *In situ* nick-translation at the electron microscope level: a tool for studying the location of DNase I-sensitive regions within the cell. *J. Cytochem. Histochem.* **39,** 871–874.
16. Thiry, M. (1991) DNase I-sensitive sites within the nuclear architecture visualized by immunoelectron microscopy. *DNA Cell Biol.* **10,** 169–180.
17. Sugimoto, T., Takeyama, A., Xiao, C., Takano-Yamamoto, T., and Ichikawa, H. (1999) Electron microscopic demonstration of nick end-labeled DNA fragments during capsaicin-induced apoptosis of trigeminal primary neurons in neonatal rats. Brain Res. **818,** 147–152.

18. Roth, J., Bendayan, M., Carlmalm, E., Villiger, W., and Garavito, M. (1981) Enhancement of structural preservation and immunocytochemical staining in low temperature embedded pancreatic tissue. J. Histochem. Cytochem. **29,** 663–671.
19. Thiry, M., Schoonbroodt, S., and Goessens, G. (1991) Cytochemical distinction of various nucleolar components in insect cells. *Biol. Cell* **72,** 133–140.
20. Raska, I., and Dundr, M. (1993) Compartmentalization of the cell nucleus: case of the nucleolus, in *Chromosomes Today* (Summer, A. T., Chandley, A. C., eds.), Chapman and Hall, London, pp. 101–119.
21. Thiry, M. (1993) Differential location of nucleic acids within interchromatin granule clusters. *Eur. J. Cell Biol*. **62,** 259–269.
22. Thiry, M., and Puvion-Dutilleul, F. (1995) Differential distribution of single-stranded DNA, double-stranded DNA, and RNA in adenovirus-induced intranuclear regions of HeLa cells. *J. Histochem. Cytochem.* **43,** 749–759.
23. Olmedilla, A., Testillano, P., Raska, I., and Risueno, M. C. (1992) *In situ* nick-translation and anti-BrdU techniques as convenient tools to study the functional regions of chromatin in plants. *Electron Microscopy* **3,** 193–194.
24. Gross, D., and Garrard, W. (1988) Nuclease hypersensitive sites in chromatin. *Ann. Rev. Biochem.* **57,** 159–197.
25. Bendayan, M. (1984) Enzyme-gold electron microscopic cytochemistry: an new affinity approach for the ultrastructural localization of macromolecules. *J. Electron Microsc. Tech.* **1,** 349–372.
26. Cheniclet, C., Garzon, S., and Bendayan, M. (1995) *In situ* detection of nucleic acids by the nuclease-gold method, in *Visualization of Nucleic Acids* (Morel, G., ed.), CRC Press, Boca Raton, London, Tokyo, pp. 95–109.
27. Craigh, S. W., and Pollard, T. D. (1982) Actin-binding proteins. *Trends Biochem. Sci.* **7,** 88–92.
28. Geuskens, M., de Recondo, A., and Chavaillier, Ph. (1975) Autoradiographic demonstration of DNA replication in ultrathin sections of plastic-embedded tissues using an exogenous DNA polymerase. *Chromosoma* **52,** 175–188.

10

In Situ DNA Ligation as a Method for Labeling Apoptotic Cells in Tissue Sections

An Overview

Peter J. Hornsby and Vladimir V. Didenko

1. Introduction

In 1992 Gavrieli et al. published a seminal article showing that apoptotic cells could be detected by an *in situ* assay ***(1)***. The labeling method depends on the ability of terminal deoxyribonucleotidyl transferase to add nucleotides to breaks in DNA, and has generally been termed TUNEL (terminal dUTP nick end labeling), although ISEL (*in situ* end labeling) would be a more appropriate description. During the late stages of apoptosis, nucleases are activated that cleave DNA with the production of double-strand breaks. Terminal transferase is used in this *in situ* assay for apoptosis to add labeled nucleotides to the 3' ends of DNA molecules, thus providing a sensitive assay for detecting apoptotic cells in tissues. Since the publication of this method, this work has been cited in over 4,300 publications, attesting to the usefulness of the assay.

After the initial publication of the TUNEL method, it was recognized that the assay was very sensitive, but not as specific for apoptosis as is ideally desirable ***(2)***. Because the method is capable of labeling any free 3' end in DNA, other forms of damage to DNA, apart from apoptosis, produce positive signals. Over the years since the publication of this work, there have been various useful modifications to the TUNEL assay which have improved its specificity for apoptotic cells ***(3)***. Moreover, under uncomplicated circumstances the original TUNEL method gives unambiguous results. In particular, this is true of labeling in embryonic tissues where apoptosis is expected and other sources of DNA damage are unlikely. On the other hand, in pathological conditions it is by no means certain that the presence of DNA damage in a tissue can be reliably

From: *Methods in Molecular Biology, vol. 203:* In Situ *Detection of DNA Damage: Methods and Protocols*
Edited by: V. V. Didenko

interpreted as the occurrence of apoptosis. First, necrotic cells contain a variety of DNA strand breaks. Second, cells may have sublethal forms of DNA damage, giving rise to single-strand breaks that can be labeled. DNA damage in these cells could be repairable (although it could also be a precursor to apoptosis) and such cells need to be distinguished from actual apoptotic cells.

2. Biochemical Background and Principle of *In Situ* Ligation Method

With these observations in mind, we considered ways to improve the *in situ* detection of apoptosis. We thought of adapting the concept of *in situ* detection of DNA strand breaks by using a process that did not depend on terminal transferase end labeling. The distinctive feature of apoptosis is the presence of double-strand breaks, which may have either blunt or staggered ends. We wanted to label double-strand breaks in such a way that the double-stranded nature of the DNA ends would become an essential part of the labeling process—single-stranded DNA ends would not be labeled. We developed the idea that double-strand breaks could be labeled by ligation of a double-stranded DNA tag. This method is in essence an *in situ* adaptation of ligation methods used commonly in molecular biology, both during subcloning procedures and in analytical procedures, such as ligation-mediated PCR ***(4)***. In fact, at about the same time as we developed the *in situ* ligation method, a PCR-based method was developed for biochemical detection of double strand breaks in apoptotic cell DNA ***(5)***.

The biochemical literature on apoptosis suggested the involvement of a DNase I-type of endonuclease with restricted access to DNA in chromatin ***(6)***. This kind of nuclease would produce double-strand breaks with short (e.g. single-base) 3' overhangs. Our reasoning is as follows. Random cleavage by an endonuclease producing multiple single-strand nicks within internucleosomal DNA would not be expected to produce large numbers of single-base 3' overhangs, which are predicted only when the DNA is protected by bound protein ***(7–9)***. However, apoptotic cleavage of DNA has been shown to produce an abundance of DNA fragments not only of the intranucleosomal length (~140 bp) but also of the length of the intranucleosomal DNA plus linker DNA (~195 bp) ***(10)***. Thus it is predicted that the endonuclease involved in apoptosis does not initially have access to the entire internucleosomal region, but preferentially to the sites at the junction of the nucleosome and the internucleosomal region. This may arise from the higher order structure of chromatin in the nucleus ***(11)***. When DNA is bound to histones or other proteins in chromatin, it is partially protected from the action of endonucleases, which are able to cleave the DNA at approximately 10 bp intervals, the distance of a single helical turn of the DNA ***(7)***. Because of the helical twist of DNA, the two strands are accessible to endonucleases with production of staggered ends as well as some blunt ends.

Thus, DNase I cleavage of nucleosome-bound DNA gives rise to double strand cuts with 1, 2, or 3 bases of 3' overhang ***(8,9)***. In contrast, DNAse II cleavage of DNA in chromatin yields longer 3' overhangs of an average of 4 bases ***(7,9)***. The presence of single-base 3' overhangs in apoptotic cells thus is consistent with limited access of chromatin to a DNAse I-type apoptotic endonuclease.

It was reasonable to think that a method based on detection of single-base 3' overhangs would specifically label double-strand breaks of apoptotic cells and would not label double-strand breaks that happen to be present for other reasons. In particular, blunt-ended strand breaks could be present in necrotic cells. The presence of large numbers of accessible 3' ends in necrotic and autolytic tissue is predictable if, during necrosis, DNA is digested by a mixture of lysosomal nucleases ***(12,13)***. The destruction of DNA in necrosis is thought to be a late rather than an early event ***(14)***. In this case, the bulk of the destruction of the DNA may occur when the chromatin is in a more relaxed form, and the supposed greater variety of enzymes involved in destruction of the cells may give rise to a more random pattern of DNA fragmentation. Nevertheless, it has been noted that necrosis can give rise to a nucleosome-length DNA ladder ***(15,16)***. Some blunt ends in necrotic and autolytic cells could result from the combined action of endonucleases followed by exonucleases that flush staggered double-strand fragments. There would be a much lower level of 3' single-base overhangs, which, if produced, would be transient in the presence of this mixture of nucleases.

3. Probe Designs for *In Situ* Ligation

We set out to design a probe that could be ligated to double-strand breaks with single-base 3' overhangs. In doing so we took advantage of the known ability of *Taq* DNA polymerase to synthesize double-stranded DNA with single-base 3' overhangs in the polymerase chain reaction (PCR), an activity termed terminal transferase or "extendase" ***(17)***. This activity of *Taq* polymerase is the basis for use of the well-known T vectors in the cloning of PCR products ***(18)***. To make a PCR product that would be useful in *in situ* ligation we performed PCR using digoxigenin-labeled or fluorescent deoxyribonucleotide triphosphates (dNTPs) ***(19)***. The probe was then incubated with a deparaffinized or frozen section of tissue in a mix of buffer, T4 DNA ligase and ATP (required for the ligase reaction). The probe was allowed to become covalently attached to available sites on the section, and unattached probe was then washed away. The attached probe was detected by an antibody against digoxigenin or was directly observed by fluorescence microscopy.

Practical tests of the method showed that it did indeed label apoptotic cells specifically. As a positive control, we used rat thymus 24 h after administration of glucocorticoid, a model for apoptosis well established by previous

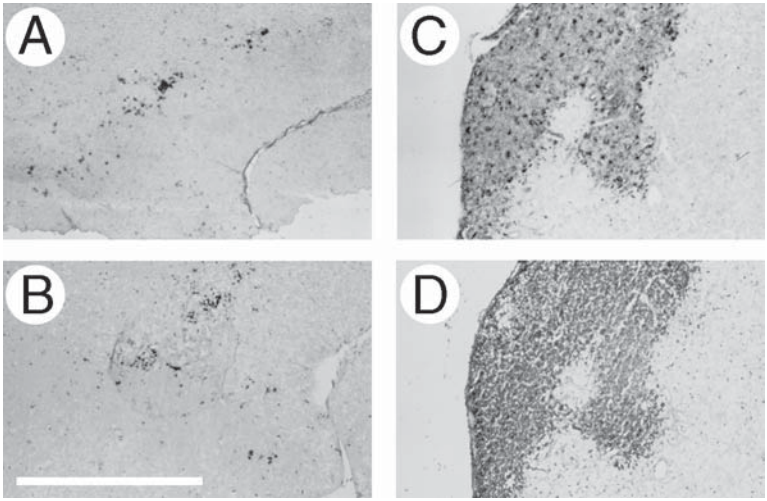

Fig. 1. Comparison of patterns of apoptotic cells, detected by the presence of different types of DNA ends, in control and glucocorticoid-treated thymus. Thymus from control **(A, B)** and glucocorticoid-treated **(C, D)** rats were fixed and processed as described in Figure 1. The figure shows the reaction products resulting from **(A, C)** ligation of *Taq* polymerase fragment, 15 minutes of alkaline phosphatase reaction; **(B, D)** TdT reaction, 7 min of alkaline phosphatase reaction. Bar, 2 mm. Reproduced with permission from ref. ***19***.

investigators ***(20)***. **Fig. 1** shows *in situ* ligation labeling in glucocorticoid-treated and control thymus. This series of experiments also showed that necrotic cells in a sample of Wilms' tumor were not labeled, thereby validating the specificity of the labeling for apoptotic cells.

As we gained more experience with *in situ* ligation, we realized that the major practical problems were to make sufficient amounts of the PCR product and to purify it away from unincorporated labeled dNTPs, which can produce increased background on the section. We thought that making a probe chemically rather than enzymatically might solve these problems. To that end, we thought about designing a double-stranded oligonucleotide that could be used to label double-strand breaks. We also realized that using oligonucleotides would give us the opportunity to design any kind of double-stranded DNA ends, both for apoptotic cell labeling and for labeling any types of double-strand breaks in other biological materials. In the first type of oligonucleotide that we designed we retained the single A 3' overhang, as found in the PCR products. As we thought about creating an oligonucleotide, we were aware that only a double-stranded oligonucleotide would be suitable. Single-stranded oligonucleotides could label many different kinds of DNA breaks, and labeling

Fig. 2. Configuration and sequence of biotin-labeled oligonucleotide probe for detection of double-strand breaks. **(A)** looped hairpin and **(B)** loopless hairpin. Both probes are designed so that the terminus of the stem has a characteristic structure, in this case, a single 3' A overhang. The loop **(A)** contains 5 deoxythymidine derivatives (t) labeled with biotin. The loopless probe **(B)** contains a single biotin positioned at the end of the hairpin opposite the ligated end. X in the sequence represents a biotinylated nucleotide (*see* text). Reproduced with permission from ref. ***22***.

would not depend on the presence of double-stranded ends on the section. To ensure that the oligonucleotides existed only in a double-stranded form we designed hairpin oligonucleotides that fold back on themselves; in accordance with the laws of thermodynamics, they exist in solution only in a double-stranded form ***(21)***. The hairpin oligonucleotides were modified with covalently attached biotin to enable detection with avidin conjugates (**Fig. 2A**). They proved to be specific and convenient for *in situ* ligation and thereby rapidly replaced the use of PCR products. As shown in **Fig. 3**, these oligonucleotides sensitively labeled apoptotic cells.

Hairpin probes are structurally uniform, stable in the assay environment, and easy to prepare in large quantities. However, the *in situ* labeling procedure still requires lengthy washing steps to remove unligated probe. The reason for the relative stickiness of the probe was unclear, as in theory the short nonattached oligonucleotides should be easily removed from the section. We reasoned that the cause of this stickiness was the single-stranded loop region. The oligonucleotide probes were synthesized with 20-base loops that contained five nucleotides modified by the attachment of biotin. The probes also had a

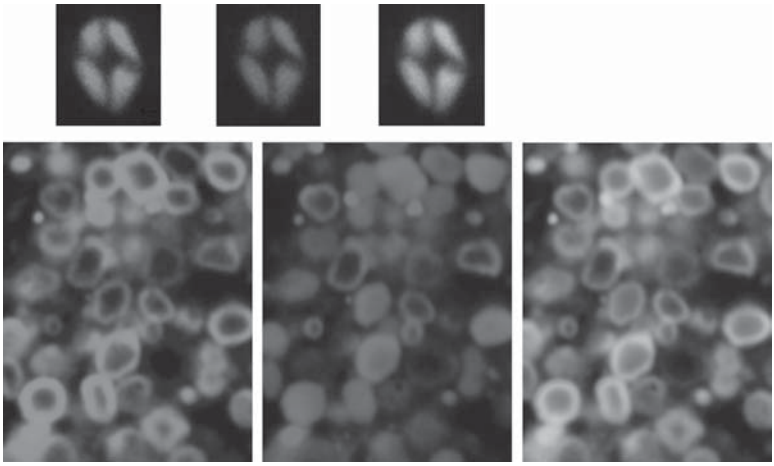

Fig. 3. Confocal microscope images of apoptotic nuclei successively labeled by ligation of a single A overhang hairpin oligonucleotide probe (green) and by terminal transferase (red). The computer-generated combined green and red images are also shown. Above, a single apoptotic nucleus in mouse kidney; below, dexamethasone-treated rat thymus. Reproduced with permission from ref. ***21***.

10 bp stem, with a short 3' overhang, which could be ligated to double-strand breaks in DNA. The placement of a nonradioactive label in the loop away from the stem of the hairpin was intended to prevent potential interference of the large biotin groups with the enzymatic linkage of the probe to the section. However, nonspecific binding could be caused by interactions between the negatively charged single-stranded loop of the probe and positively charged protein molecules, or by nonspecific hybridization to cellular RNA or single-stranded regions in cellular DNA, present in damaged or necrotic cells. In addition, the flexible loop structure could easily twist, preventing tagged nucleotides from being efficiently detected. The presence of several closely-positioned biotinylated nucleotides might also create steric hindrance problems.

With these issues in mind, we designed a new oligonucleotide probe (**Fig. 2B**) ***(22)***. In the new probe design, the reactive single-stranded loop was eliminated. This modification virtually eliminated nonspecific binding of the probe to tissue sections. In order to avoid steric hindrance problems and to create better conditions for the reaction between biotin and streptavidin in probe detection, the number of biotins was reduced from five to one. The single biotin was positioned at the end of the hairpin, at a maximal distance from the ligated end. The biotin was incorporated into the probe either by using amino modifier C6 deoxythymidine, with subsequent reaction with biotin bis-aminohexanoyl-N-

hydroxysuccinimide ester (Synthetic Genetics, San Diego, CA), or by chemical insertion of a biotin TEG phosphoramidite or biotinylated thymidine analogues (Glen Research, Sterling, VA) [performed by Serologicals Corp. (formerly Intergen), Gaithersburg, MD]. All types of labeling gave similar results. This new design substantially reduces the cost of the probe preparation, making *in situ* ligation a convenient and robust methodology to detect apoptosis and DNA damage in tissue sections.

The earlier probe designs can still be used for apoptosis detection, if their limitations are considered. The PCR-derived probes are the cheapest to prepare. The disadvantages of this type of probe include the difficulty of getting medium- and large-scale probe preparations, the unknown percentage of single-base overhangs, the presence of truncated products and the absence of uniformity in different probe preparations. In addition, the background can be a problem if the probe is not purified away from unincorporated labeled precursors and single-stranded DNA. Thorough control of the probe quality using PCR purification columns is needed. The High Pure PCR Product Purification Kit (Roche Molecular Biochemicals, Indianapolis, IN) gave good results in our experiments. Careful controls using sections with and without apoptotic cells are recommended because some tissues might still require extensive washing and additional blocking.

The looped hairpin probes can also be used if adequate washing of the section is done. However, the loopless hairpin proved to be the easiest to use, does not suffer from background problems, and provides a time- and cost-saving alternative to the other probe designs.

4. Conclusions

In situ ligation selectively labels a single type of DNA damage. At the basic biochemical level, the *in situ* ligation procedure detects double-strand DNA breaks of different configurations. Ends that can be detected include both blunt-ended breaks and those with one or two base 3' overhangs.

Blunt ends are abundant in apoptosis and probes with blunt ends give the strongest signal in *in situ* ligation. Although some blunt ends can be present in necrotic degradation, the probes with blunt ends can complement the overhang probes in detection of apoptotic cells in situations where apoptosis is the primary cellular response, or where both probes give the identical staining pattern and the stronger signal is preferred for detection purposes.

Overhangs longer than two bases are impractical to detect using this approach because of background problems and loss of ligation specificity of probes with longer 3' protruding ends. Breaks detected by this approach should have 5' phosphate groups on the DNA ends; the presence or absence of 3' hydroxyls does not influence the ligation reaction. Thus the combination of this tech-

nique with the TUNEL method in double-staining experiments can provide more information about the structure of the breaks.

The *in situ* ligation approach was first applied to detect apoptosis in fixed cells and tissues. However, double-strand breaks are not limited to apoptosis and can be produced by free radical oxidation, radiation exposure, and DNA recombination. The method has not yet been applied to the study of these processes.

There have been many exciting new developments in apoptotic DNA detection in recent years. The versatility and variety of these methods give greater power to the researcher wishing to search for and characterize apoptotic cells, and to the researcher wishing to distinguish different forms of DNA damage in tissues. The *in situ* ligation technique should play an important role in this panoply of new methods, to be used alongside both the well-established TUNEL technique as well as new methods described in this volume.

Acknowledgment

We are grateful to Dr. David Baskin for his support, encouragement, and advice. In his laboratory in the Neurosurgery Department at Baylor College of Medicine and the VA Houston Medical Center, he participated in the work that resulted in the development of loopless probes, our joint patent, and some of the publications cited in this chapter.

References

1. Gavrieli, Y., Sherman, Y., and Ben-Sasson, S. A. (1992) Identification of programmed cell death in situ via specific labeling of nuclear DNA fragmentation. *J. Cell Biol.* **119,** 493–501.
2. Charriaut-Marlangue, C., and Ben-Ari, Y. (1995) A cautionary note on the use of the TUNEL stain to determine apoptosis. *Neuroreport* **7,** 61–4.
3. Negoescu, A., Lorimier, P., Labat-Moleur, F., Drouet, C., Robert, C., Guillermet, C., Brambilla, C., and Brambilla, E. (1996) In situ apoptotic cell labeling by the TUNEL method: Improvement and evaluation on cell preparations. *J. Histochem. Cytochem.* **44,** 959–68.
4. Steigerwald, S. D., Pfeifer, G. P., and Riggs, A. D. (1990) Ligation-mediated PCR improves the sensitivity of methylation analysis by restriction enzymes and detection of specific DNA strand breaks. *Nucleic Acids Res.* **18,** 1435–1439.
5. Staley, K., Blaschke, A. J., and Chun, J. (1997) Apoptotic DNA fragmentation is detected by a semiquantitative ligation-mediated PCR of blunt DNA ends. *Cell Death Differ.* **4,** 66–75.
6. Walker, P. R., and Sikorska, M. (1994) Endonuclease activities, chromatin structure, and DNA degradation in apoptosis. *Biochem. Cell Biol.* **72,** 615–623.

7. Sollner-Webb, B., Melchior, W., Jr., and Felsenfeld, G. (1978) DNAase I, DNAase II and staphylococcal nuclease cut at different, yet symmetrically located, sites in the nucleosome core. *Cell* **14,** 611–27.
8. Lutter, L. C. (1979) Precise location of DNase I cutting sites in the nucleosome core determined by high resolution gel electrophoresis. *Nucleic Acids Res.* **6,** 41–56.
9. Cusick, M. E., Wassarman, P. M., and DePamphilis, M. L. (1989) Application of nucleases to visualizing chromatin organization at replication forks. *Meth. Enzymol.* **170,** 290–316.
10. Peitsch, M. C., Muller, C., and Tschopp, J. (1993) DNA fragmentation during apoptosis is caused by frequent single-strand cuts. *Nucleic Acids Res.* **21,** 4206–9.
11. Wolffe, A. P. (1995) *Chromatin: Structure and Function.* Academic Press, New York.
12. Holtzman, E. (1989) *Lysosomes.* Plenum Press, New York.
13. Van Dyck, J. M., and Wattiaux, R. (1968) Distribution intracellulaire de l'exonuclease acide dans le foie de rat. *Eur. J. Biochem.* **7,** 13–20.
14. Majno, G., and Joris, I. (1995) Apoptosis, oncosis, and necrosis. An overview of cell death. *Am. J. Pathol.* **146,** 3–15.
15. Campagne, M. V., Lucassen, P. J., Vermeulen, J. P., and Balazs, R. (1995) NMDA and kainate induce internucleosomal DNA cleavage associated with both apoptotic and necrotic cell death in the neonatal rat brain. *Eur. J. Neurosci.* **7,** 1627–1640.
16. Rink, A., Fung, K. M., Trojanowski, J. Q., Lee, V. M. Y., Neugebauer, E., and Mcintosh, T. K. (1995) Evidence of apoptotic cell death after experimental traumatic brain injury in the rat. *Am. J. Pathol.* **147,** 1575–1583.
17. Hu, G. (1993) DNA polymerase-catalyzed addition of nontemplated extra nucleotides to the 3' end of a DNA fragment. *DNA Cell Biol.* **12,** 763–770.
18. Marchuk, D., Drumm, M., Saulino, A., and Collins, F. S. (1991) Construction of T-vectors, a rapid and general system for direct cloning of unmodified PCR products. *Nucleic Acids Res.* **19,** 1154–1156.
19. Didenko, V. V., and Hornsby, P. J. (1996) Presence of double-strand breaks with single-base 3' overhangs in cells undergoing apoptosis but not necrosis. *J. Cell Biol.* **135,** 1369–1376.
20. Wyllie, A. H. (1980) Glucocorticoid-induced thymocyte apoptosis is associated with endogenous endonuclease activation. *Nature* **284,** 555–6.
21. Didenko, V. V., Tunstead, J. R., and Hornsby, P. J. (1998) Biotin-labeled hairpin oligonucleotides. Probes to detect double-strand breaks in DNA in apoptotic cells. *Am. J. Pathol.* **152,** 897–902.
22. Didenko, V. V., Boudreaux, D. J., and Baskin, D. S. (1999) Substantial background reduction in ligase-based apoptosis detection using newly designed hairpin oligonucleotide probes. *BioTechniques* **27,** 1130–1132.

11

Detection of Specific Double-Strand DNA Breaks and Apoptosis *In Situ* Using T4 DNA Ligase

Vladimir V. Didenko

1. Introduction

Specific DNA breaks underlie many morphological changes in normal and damaged cells. They can serve as important markers in cell and tissue research. Yet historically, the labeling of DNA breaks *in situ* was most often limited to the identification of apoptotic cells. Consequently, the major techniques for analysis of DNA cleavage in tissue sections were initially developed for the visualization of apoptotic death. These assays rely on enzymatic labeling of DNA breaks to detect the characteristic DNA fragmentation seen in apoptosis. One of two methods is typically employed: a) terminal transferase (TdT) digoxigenin dUTP nick end labeling (TUNEL), or b) the Klenow fragment of DNA polymerase I based *in situ* end labeling. In order to identify various pathological states *in situ* based on structural DNA changes, a technique to selectively detect the various types of DNA damage is required. However, due to the properties of the enzymes involved in these assays, multiple types of DNA breaks are labeled. The terminal transferase-based assay labels free 3' hydroxyl groups, which can be present in different types of breaks. As a result, it can detect stretches of single-stranded DNA (gaps) and also both single- and double-stranded breaks of various configurations (blunt-ended, 3' and 5' overhangs) ***(1)***. The Klenow polymerase-based assay in turn labels gaps and various 5' overhangs ***(2)***. This prevents the selective visualization of specific types of DNA breaks *in situ* using these approaches.

To address this issue, the *in situ* ligation technique was developed to label a particular type of DNA damage, namely, full double strand breaks, directly in fixed tissue sections ***(3,4,5)***. The technique uses double-stranded oligoprobes with specific ends, which are attached by T4 DNA ligase to the ends of DNA

From: *Methods in Molecular Biology, vol. 203:* In Situ *Detection of DNA Damage: Methods and Protocols*
Edited by: V. V. Didenko

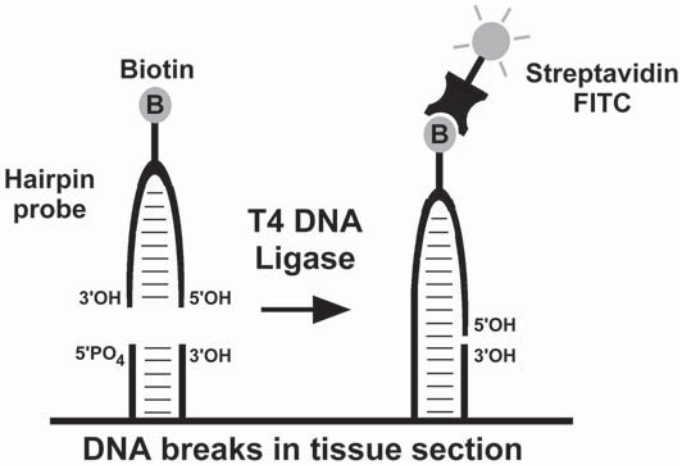

Fig. 1. Principle of *in situ* ligation assay. The assay detects double strand DNA breaks by ligation of hairpin oligonucleotide probes to the ends of the breaks directly in tissue sections. Due to the properties of T4 DNA ligase the probes can only be attached to the breaks with 5' phosphate groups. T4 DNA ligase needs a terminal 5' phosphate to create a phosphodiester bond between the 3' OH end of the probe and the free 5' end of cellular DNA.

breaks (**Fig. 1**). Though the PCR derived probes were introduced first ***(3)***, most often the hairpin-shaped oligonucleotides are used as probes ***(4,5)***. They have terminal 3' and 5'OH groups, which allow them to be ligated only to the double strand breaks in cellular DNA with 5'PO_4 at the end. This approach allows detection of blunt-ended breaks and breaks with single base 3' overhangs. Breaks with two base-long 3' overhangs as well as various breaks with 5' overhangs can also be detected.

Nevertheless, blunt-ended breaks and breaks with 3' single base extensions are the preferable targets for this technique. Though the 2 base-long 3' overhangs were successfully labeled using probes with 3'NN (random nucleotide extensions), higher levels of nonspecific background staining were observed ***(4)***. This nonspecific binding of the probe to sections probably occurred because of the "sticky" single-stranded part of the probe.

Probes with 5' overhangs can be designed to enable detection of 5' overhang breaks. However, in this case, binding to single-stranded DNA fragments will occur because the recessed 3' hydroxyl on the oligonucleotide would bind to 5' phosphates on the section, which could be at the end of a single-stranded DNA fragment as well as a double-strand break with a 5' overhang (**Fig. 2**). Thus, the detection of 5' overhangs would require dephosphorylation of the tissue sec-

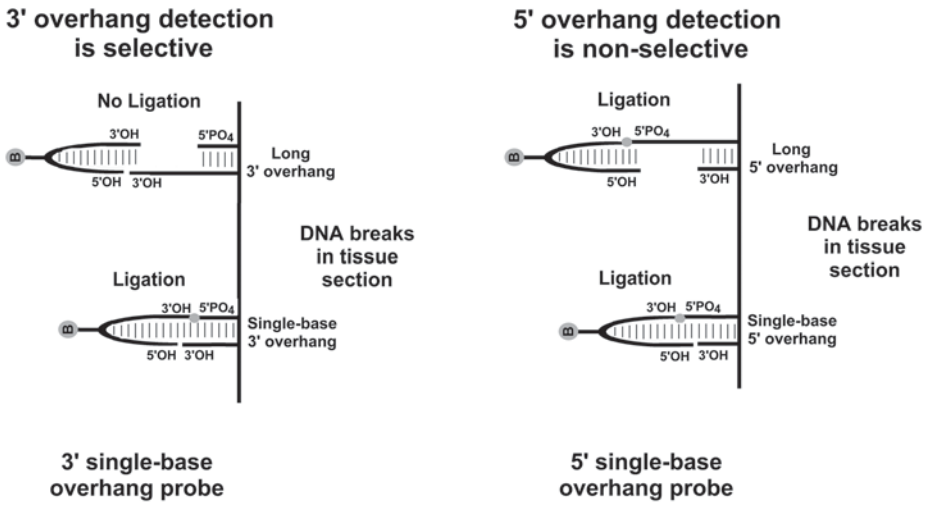

Fig. 2. Selective detection of 3'- and nonselective detection of 5'-overhangs using *in situ* ligation. Probes with 3' single base extensions are selectively ligated to the complimentary 3' single base overhangs in cellular DNA. Probes with 5' single base extensions are ligated nonspecifically to any 5' overhang or single-stranded DNA with terminal 5'PO_4 and a complimentary terminal nucleotide.

tion before ligation and the use of a 5' phosphorylated probe. The hairpin probes with 5' overhangs and 3'OH/5'OH ends applied to sections without these treatments will label various 5'PO_4 overhangs and single stranded DNA.

In situ ligation can be combined with TUNEL, allowing co-detection of free 3'OH groups *in situ*, and with immunohistochemical staining of cellular proteins.

The types of double-strand breaks which can be detected by *in situ* ligation occur in various cellular processes, the majority of which are related to cell damage and death. The basics of *in situ* ligation labeling of apoptotic cells were discussed in the previous chapter and rely on the fact that double-strand breaks produced by apoptotic endonucleases are either blunt-ended or have short 3' or 5' extensions.

Although a single apoptotic endonuclease has not been definitively identified, and might not exist, as various nucleases can perform the function in different tissues, the ends of the generated fragments almost exclusively were found to be of 3'OH/ 5' PO_4 configuration ***(6)***. Several candidate nucleases have been identified in apoptotic DNA cleavage. They include DNase I, DNase I-like nucleases (DNase Y, DNase γ, DNL1L, DNase X, DHP1/DNAS1L2, DNP2/DNAS1L3, (reviewed in ***7***) and caspase-activated deoxyribonuclease (DFF-40/CAD) ***(8)***. In a small number of cases, DNase II-like endonucleases

producing breaks with 3'PO_4/5'OH end configuration were implicated in apoptotic cleavage ***(9)***. In their action on chromatin, different endonucleases produce specific double strand breaks ***(10)***. These breaks can serve as molecular targets for *in situ* ligation.

DNase I and nucleases with a similar "double-hit" mechanism of DNA cleavage initially produce single-stranded cuts ***(11)***, however DNase I cleavage of chromatin results in double-strand breaks with terminal 3'OH/5'PO_4 groups, created when two single-stranded cuts superimpose ***(12)***. These breaks are either blunt-ended or have short 1–3 bases-long 3' overhangs, which are created due to unequal protection of two DNA strands wound around a nucleosomal histone core ***(10,12)***.

The other apoptotic nuclease—caspase-activated deoxyribonuclease (CAD, or DFF 40) ***(8,13)***—also produces 3'OH/5'PO_4 DNA cuts, which are either blunt-ended or have 5' single base overhangs ***(14)***. The enzyme is kept inactive by the binding of an inhibitor (ICAD, or DFF 45). Activation of the nuclease occurs when the inhibitor is cleaved by caspase-3 ***(8)***.

Although the majority of DNA breaks in many cases of apoptosis are blunt-ended with the 3'OH/5'PO_4 at the ends ***(15,16)***, the less frequent 3' single-base overhangs were shown to be more specific for apoptotic cleavage (compared to necrosis) and can serve as a convenient marker of apoptotic cells ***(3)***.

DNase II-type (3'PO_4/5'OH) double-strand breaks can be produced by acidic endonucleases. They were identified in a small number of cases of apoptosis ***(9,17)***. In principle, this type of break can be labeled by *in situ* ligation using 5' phosphorylated probes and the dephosphorylation of 3'PO_4 ends in the section.

It is important to mention that though *in situ* ligation can label apoptotic cells with high selectivity, the actual marker it detects is a 5' phosphorylated double-strand break. That is why this assay detects apoptosis when it is accompanied by internucleosomal DNA cleavage with the production of multiple double strand breaks. Blunt-ended DNA breaks as well as electrophoretic ladder-type DNA fragmentation can occur in necrosis ***(3,18)***, though with less frequency than in apoptosis.

Although in principle the *in situ* ligation assay can detect not only the breaks self-inflicted by the cell proceeding towards apoptosis, but also the breaks produced by the exogenous damaging agents, its current applications are limited to apoptosis detection.

Applications of *in situ* ligation to the investigation of the other sources of double-strand breakage in DNA are currently lacking. These other sources of double strand breaks include free radicals, ionizing radiation and various radiomimetic and chemotherapeutic agents, capable of inducing the breaks directly, or indirectly as a result of the damaged DNA repair, recombination and replication.

In addition, two physiological forms of intentional double-strand breakage, generating a small number of breaks, occur in lymphoid cell differentiation during V(D)J recombination and class switch recombination ***(19)***. However detection of these breaks, using the described approach, is problematic unless specialized methods of signal enhancement are used.

The quantitation of double-strand DNA breaks is yet another presently underused feature of the assay. *In situ* ligation places a single fluorophore at the end of each detectable break, which makes it a potentially quantifiable procedure, where the intensity of signal is directly proportional to the number of breaks.

The technique presented in this chapter is applicable to labeling of apoptotic cells in tissue sections in a fluorescent format (*see* **Note 1**) and can be combined with immunohistochemical detection of cellular proteins and with TUNEL. For the dual-detection of cellular proteins or TUNEL labeling, *in situ* ligation is performed first and is followed by immunohistochemistry or the terminal transferase assay. No changes in their regular protocols are necessary.

The described protocol was successfully used to detect apoptotic cells in various human, rat and bovine tissues including thymus, brain, heart and adrenal gland.

2. Materials

1. The 5–6 µm-thick sections cut from paraformaldehyde-fixed, paraffin-embedded tissue blocks onto ProbeOn™ Plus charged and precleaned slides (Fisher Scientific, Pittsburgh, Pa). Other slide brands can also be used if they retain tissue well.
2. Xylene
3. 80 and 96% Ethanol.
4. T4 DNA ligase 5 U/µL (Roche Molecular Biochemicals, Indianapolis, IN) (*see* **Note 2**).
5. 10 × reaction buffer for T4 DNA ligase: 660 m*M* Tris-HCl, 50 m*M* $MgCl_2$, 10 m*M* dithioerythritol, 10 m*M* ATP, pH 7.5 (20°C) (Roche Molecular Biochemicals, Indianapolis, IN) (*see* **Note 3**).
6. 30% (w/v) solution of PEG-8000 (Sigma, St. Louis, MO) in bidistilled water (*see* **Note 4**).
7. Proteinase K (Roche Molecular Biochemicals, Indianapolis, IN) 20 mg/mL stock solution in distilled water. Store at –20°C. In the reaction use 50 µg/mL solution in PBS, prepared from the stock. Do not reuse (*see* **Note 5**).
8. Oligonucleotide hairpin probe biotin-labeled (Synthetic Genetics, San Diego, CA) (*see* **Note 6**). The probes sequences:
   1. The probe with a 3' single dA overhang (for detection of double-strand breaks with 3'single T overhangs): 5' GCG CTA GAC GtC GTC TAG CGC A 3'
   2. The blunt-ended probe (for detection of blunt-ended DNA breaks): 5' GCG CTA GAC CtG GTC TAG CGC 3'. t represents biotinylated deoxythymidine or biotin-TEG spacer (Glen Research, Sterling, VA).

9. Phosphate-buffered saline (1× PBS): dissolve 9 g NaCl, 2.76 g $NaH_2PO_4 \cdot H_2O$, 5.56 g $Na_2HPO_4 \cdot 7H_2O$ in 800 mL of distilled water. Adjust to pH 7.4 with NaOH, and fill to 1 L with distilled water.
10. Sodium bicarbonate buffer: 50 m*M* $NaHCO_3$, 15 m*M* NaCl, pH 8.2.
11. Streptavidin-fluorescein conjugate or streptavidin-Texas Red conjugate (Molecular Probes, Eugene, OR) or TSA™ Fluorescence Systems (NEL701-TSA with fluorescein or NEL702-TSA with tetramethylrhodamine) (NEN™ Life Science Products, Boston, MA) (*see* **Note 7**).
12. Fluorescent microscope with appropriate filters and objectives.
13. Vectashield (Vector Laboratories, Burlingame, CA) antifading-counterstaining solution with DAPI (1 µg/mL). Store at 4°C in the dark. DAPI is a potential carcinogen.
14. 22 × 22 mm or 22 × 40 mm glass or plastic coverslips.

3. Method

1. Place the sections in a slide rack and dewax in xylene for 15 min, transfer to a fresh xylene bath for additional 5 min.
2. Rehydrate by passing through graded ethanol concentrations: 96% Ethanol—2 × 5 min; 80% Ethanol—5 min; water—2 × 5 min.
3. Digest section with Proteinase K. Use 100 µL of a 50 µg/mL solution per section. Incubate 15' at room temperature in a humidified chamber (*see* **Note 8**).
4. Rinse in distilled water for 4 × 2 min.
5. Apply 100 µL per section of the pre-incubation solution. Incubate for 15 min at room temperature (23°C). The pre-incubation solution consists of a 1 × T4 DNA ligase reaction buffer supplemented with PEG-8000 to the final concentration of 15%. It contains 66 m*M*-Tris HCl, pH 7.5, 5 m*M* $MgCl_2$, 1 m*M* dithioerythritol, 1 m*M* ATP, and 15% polyethylene glycol (*see* **Note 9**).
6. Aspirate the preincubation solution and apply the full ligase reaction mix with the hairpin probe (750 ng/µL stock) and T4 DNA ligase (*see* **Note 10**).
   In situ ligation labeling solution (20 µL per section):
   Prepare on ice in this order:
   5 µL—bidistilled water
   10 µL—PEG8000 (30% stock solution)
   2 µL—10× buffer for T4 DNA ligase
   1 µL—biotin labeled hairpin probe
   2 µL—T4 DNA ligase (5U/µL) (*see* **Note 2**)
   The total volume of the labeling solution can be scaled up to accommodate the bigger sections. Incubate for 18 h (overnight) at room temperature (23°C) (*see* **Note 11**) in a humidified chamber with a plastic coverslip.
7. Next day remove coverslips by gently immersing the slides vertically in a coplin jar containing water at room temperature. Then wash section 3 × 10 min in distilled water.
8. Dilute 2 µL of streptavidin-fluorescein or streptavidin-Texas Red conjugate in 1 mL of sodium bicarbonate buffer. Add 100 µL of this solution to the section. Incubate 45 min at room temperature in a covered humidified chamber (*see* **Note 7**).

9. Wash 3 × 10 min in distilled water.
10. Add Vectashield with DAPI and a coverslip.

4. Notes

1. *In situ* ligation-based labeling and detection in a nonfluorescent format can be performed using the ApopTag® Peroxidase *In Situ* Oligo Ligation kit [Serologicals Corp. (formerly Intergen), Gaithersburg, MD].
2. T4 DNA ligase in lower stock concentrations (1 U/μL) can also be used. The labeling reaction is only marginally less efficient at lower concentrations of ligase in labeling solution (125–250 U/mL). However the highly concentrated (5 U/μL) (Roche Molecular Biochemicals, Indianapolis, IN) ligase preparation gives the best signal.
3. ATP in ligase reaction buffer is easily destroyed in repetitive cycles of thawing-freezing. Aliquot the buffer in small 15–20 μL portions and store at –20°C. Use once.
4. 15% PEG-8000 in the ligation mix strongly stimulates the ligation reaction increasing the effective concentrations of the probe and ligase by volume exclusion ***(20)***. Use water of the highest quality for all solutions, which come in contact with T4 DNA ligase.
5. Proteinase K is a very stable enzyme, when stored at concentrations higher than 1 mg/mL. However autolysis of the enzyme occurs in aqueous solutions at low concentrations (~ 10 μg/mL) ***(21)***.
6. The probes contain a single internal biotin and can be synthesized by many commercial oligonucleotide producers. The biotin could be incorporated into the probe either by using an amino modifier C6 deoxyuridine with subsequent attachment of biotin bis-aminohexanoyl-N-hydroxysuccinimide ester, or by chemical insertion of a biotinTEG phosphoramidite directly into the oligonucleotide backbone. PAGE purification is advised. We primarily use the probe with a TEG linker. Dilute with bidistilled water to 750 ng/μL stock concentration. Store at –20°C. Direct fluorophore labeling (FITC, Texas Red, Alexa, etc.) instead of biotin is possible. However in our experiments, the directly labeled probes produced somewhat higher background staining compared to biotinylated probes.
7. TSA™ Fluorescence Systems (NEN™ Life Science Products, Boston, MA) significantly increase fluorescent signal. Use instead of streptavidin-fluorescein conjugates (at **step 8** in Method) if increase in fluorescence is needed. Follow instructions of the manufacturer. We found these systems advantageous in staining brain tissue.
8. Proteinase K digestion time may need adjustment depending on the tissue type. Hard tissues might require longer digestion. Times of 15–25 min are usually used. Insufficient digestion may result in the weaker signal. Overdigestion on the other hand results in signal disappearance and section disruption.
9. Pre-incubation with ligation buffer ensures even saturation of the section prior to addition of the enzyme and the probe, and was shown to increase the ligation efficiency. Prepare pre-incubation solution by adding 10 μL of the 10× ligase buffer (Roche Molecular Biochemicals, Indianapolis, IN) to 40 μL of bidistilled water and 50 μL of 30% PEG-8000.

10. A mock reaction is recommended as a regular control in order to rule out nonspecific background staining. In a mock reaction solution an equal volume of 50% glycerol in water is substituted for T4 DNA ligase.
11. Lowering of the temperature to 16°C reduces the signal; the temperature increase to 37°C completely eliminates the signal.

Acknowledgment

I am grateful to Dr. David Baskin for his support, encouragement and advice. In his laboratory in the Neurosurgery Department at Baylor College of Medicine and the VA Houston Medical Center we developed the loopless probes, which resulted in our joint patent and some of the publications cited in this chapter.

References

1. Walker, P. R., Carson, C., Leblanc, J., and Sikorska, M. (2002) Labeling DNA damage with terminal transferase: applicability, specificity and limitations, in *In Situ Detection of DNA Damage: Methods and Protocols* (Didenko, V. V. ed.) pp. 3–20.
2. Dierendonck, J. H. (2002) DNA damage detection using DNA polymerase I or its Klenow fragment: applicability, specificity, limitations, in *In Situ Detection of DNA Damage: Methods and Protocols* (Didenko, V. V. ed.) pp. 81–108.
3. Didenko, V. V., and Hornsby, P. J. (1996) Presence of double-strand breaks with single-base 3' overhangs in cells undergoing apoptosis but not necrosis. *J. Cell Biol.* **135,** 1369–1376.
4. Didenko, V. V., Tunstead, J. R., and Hornsby, P. J. (1998) Biotin-labeled hairpin oligonucleotides. Probes to detect double-strand breaks in DNA in apoptotic cells. *Am. J. Pathol.* **152,** 897–902.
5. Didenko, V. V., Boudreaux, D. J., and Baskin, D. S. (1999) Substantial background reduction in ligase-based apoptosis detection using newly designed hairpin oligonucleotide probes. *Biotechniques* **27,** 1130–1132.
6. Sikorska, M., and Walker, P. R. (1998) Endonuclease activities and apoptosis, in *When Cells Die* (Lockshin, R. A., Zakeri, Z., and Tilly, J. L., eds.), Wiley-Liss, New York, pp. 211–242.
7. Liu, Q. Y., Ribecco, M., Pandey, S., Walker, P. R., and Sikorska, M. (1999) Apoptosis-related functional features of the DNaseI-like family of nucleases. *Ann. N Y Acad. Sci.* **887,** 60–76.
8. Enari, M., Sakahira, H., Yokoyama, H., Okawa, K., Iwamatsu, A., and Nagata, S. (1998) A caspase-activated DNase that degrades DNA during apoptosis, and its inhibitor ICAD. *Nature* **391,** 43–50.
9. Barry, M. A. and Eastman, A. (1993) Identification of deoxyribonuclease II as an endonuclease involved in apoptosis. *Arch. Biochem. Biophys.* **300,** 440–450.
10. Sollner-Webb, B., Melchior, W., Jr., and Felsenfeld, G., (1978) DNAase I, DNAase II and staphylococcal nuclease cut at different, yet symmetrically located, sites in the nucleosome core. *Cell* **14,** 611–627.

11. Weir, F. A. (1993) Deoxyribonuclease I (EC 3.1.21.1) and II (EC 3.1.22.1), in *Enzymes of Molecular Biology* (Burrell, M. M. ed.), Humana, Totowa, NJ, pp. 7–16.
12. Lutter, L. C., (1979) Precise location of DNase I cutting sites in the nucleosome core determined by high resolution gel electrophoresis. *Nucleic Acids Res.* **6,** 41–56.
13. Liu, X., Zou, H., Slaughter, C., and Wang, X. (1997) DFF, a heterodimeric protein that functions downstream of caspase-3 to trigger DNA fragmentation during apoptosis. *Cell* **89,** 175–184.
14. Widlak, P., Li, P., Wang, X., and Garrard, W. T. (2000) Cleavage preferences of the apoptotic endonuclease DFF40 (caspase-activated DNase or nuclease) on naked DNA and chromatin substrates. *J Biol Chem.* **275,** 8226–8232.
15. Staley, K., Blaschke, A. J., and Chun, J. (1997) Apoptotic DNA fragmentation is detected by a semiquantitative ligation-mediated PCR of blunt DNA ends. *Cell Death Diff.* **4,** 66–75.
16. Alnemri E. S., and Litwack G. (1990) Activation of internucleosomal DNA cleavage in human CEM lymphocytes by glucocorticoid and novobiocin. Evidence for a non-Ca2(+)-requiring mechanism(s). *J. Biol. Chem.* **265,** 17,323–17,333.
17. Collins, M. K., Furlong, I. J., Malde, P., Ascaso, R., Oliver, J., and Lopez Rivas, A. (1996) An apoptotic endonuclease activated either by decreasing pH or by increasing calcium. *J. Cell Sci.* **109,** 2393–2399.
18. Dong, Z., Saikumar, P., Weinberg, J. M., and Venkatachalam, M. A. (1997) Internucleosomal DNA cleavage triggered by plasma membrane damage during necrotic cell death. Involvement of serine but not cysteine proteases. *Am. J. Pathol.* **151,** 1205–1213.
19. Lieber, M. R. (1998) Warner-Lambert/Parke-Davis Award Lecture. Pathological and physiological double-strand breaks: roles in cancer, aging, and the immune system. *Am J Pathol.* **153,** 1323–1332.
20. Maunders, M..J. (1993) DNA and RNA ligases (EC 6.5.1.1, EC 6.5.1.2, EC 6.5.1.3), in *Enzymes of Molecular Biology* (Burrell, M. M., ed.), Humana, Totowa, NJ, pp. 213–230.
21. Sweeney, P. J. and Walker, J. M. (1993) Proteinase K (EC 3.4.21.14), in *Enzymes of Molecular Biology* (Burrell, M. M., ed.), Humana, Totowa, NJ, pp. 305–311.

12

In Situ Detection of Double-Strand DNA Breaks with Terminal 5'OH Groups

Vladimir V. Didenko, Hop Ngo, and David S. Baskin

1. Introduction

DNA fragmentation is often used as a marker of programmed cell death in tissue sections. It is a sensitive indicator of apoptosis, particularly when utilized in combination with morphological verification. At least two types of DNA breaks are present in apoptotic cells: 1. Breaks with 3'OH and 5'PO_4 groups at the ends of the break, which can be generated by DNase I and DNase I-like nucleases; 2. Breaks with the inverted distribution of these chemical groups—3' PO_4/5'OH, produced by DNase II and DNase II-like nucleases ***(1–4)***.

Although in various cells enzymes other than the classical DNase I and II can generate these breaks, both of the original deoxyribonucleases were also directly implicated in apoptosis in at least some cells ***(2,5)***. Their role in apoptosis was intensively studied in determining the nature of the "executioner" nuclease responsible for apoptotic DNA fragmentation.

Several DNase II-like nucleases were identified in apoptotic cells ***(1,6,7)***. One example is NUC-1, the *C. elegans* apoptotic nuclease that is closely related to DNase II in both sequence and activity ***(8)***. Another important case is L-DNase II, which participates in caspase-independent cell clearance (LEI/L-DNase II pathway) ***(7)***. Beyond apoptosis DNase II was recently shown to be indispensable for definitive erythropoiesis in mouse fetal liver ***(9)***.

Analysis of the structure of breaks in apoptotic DNA fragmentation demonstrates that in many instances blunt-ends or short 3'overhangs are generated ***(10–12)***. TUNEL and *in situ* ligation are methods capable of detecting breaks with blunt-ends or short 3' overhangs in tissue sections ***(13,14)***. However, both of these techniques visualize breaks with 3'OH/5'PO_4 groups. They can not detect DNA fragmentation produced by nucleases generating 3'PO_4/5'OH

From: *Methods in Molecular Biology, vol. 203:* In Situ *Detection of DNA Damage: Methods and Protocols*
Edited by: V. V. Didenko

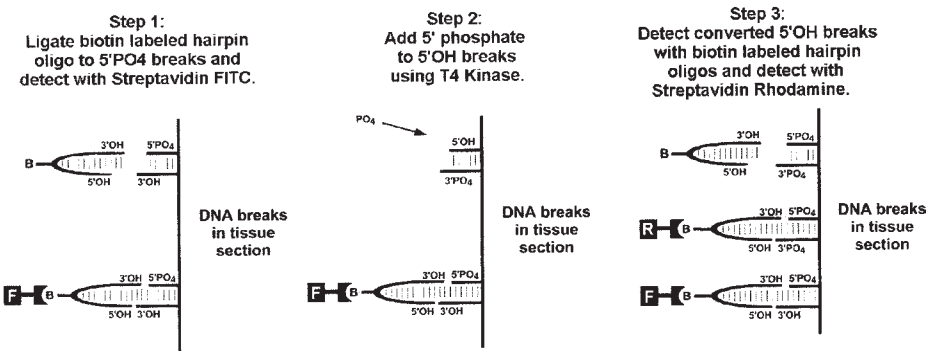

Fig. 1. Principle of the assay for *in situ* detection of double-strand DNA breaks with terminal 5'PO_4 and 5'OH groups. (Description in the text).

breaks, because the terminal deoxyribonucleotidyl transferase enzyme used in TUNEL does not react with 3' PO_4 ends and T4 DNA ligase in the ligation assay is unable to attach the probe to 5'OH ends in DNA ***(15,16)***.

Here we present a protocol developed in our laboratory for selective *in situ* labeling of double-strand DNA breaks with terminal 5'OH groups. The procedure is a modification of the standard *in situ* ligation approach ***(14)*** and allows fluorescent detection of 5' hydroxyl-bearing double strand breaks with blunt ends or short 1–2 base long 3' overhangs.

The assay is based on the conversion of 5' hydroxyls into 5' phosphates with the help of the enzyme T4 polynucleotide kinase and their subsequent detection by *in situ* ligation. The procedure is performed in three stages. In the first stage, the unlabeled hairpin oligonucleotides are ligated to the section, blocking available 5' phosphates, which may be present on the ends of DNA as a result of DNase I type nuclease activity. In the second stage, phosphate groups are added to the 5' OH ends by T4 polynucleotide kinase. In the third stage, an *in situ* ligation reaction is performed again using the hairpin probes.

The assay can be modified to simultaneously visualize both 5' phosphates and 5' hydroxyls using two different fluorophores. In this case, biotinylated hairpin probes (instead of unlabeled hairpins) are used in the first and third stages of the labeling reaction and visualized using different fluorophores (**Fig. 1**). This double-detection modification is described in the following protocol.

2. Materials

1. 5–6 μm-thick sections cut from paraformaldehyde-fixed, paraffin-embedded tissue blocks. Use slide brands which retain sections well such as ProbeOn™ Plus charged and precleaned slides (Fisher Scientific, Pittsburgh, Pa) or similar product.
2. Xylene.

3. 80 and 96% Ethanol.
4. T4 DNA ligase 5 U/µL (Roche Molecular Biochemicals, Indianapolis, IN) (*see* **Note 1**).
5. 10 × reaction buffer for T4 DNA ligase: 660 m*M* Tris-HCl, 50 m*M* $MgCl_2$, 10 m*M* dithioerythritol, 10 m*M* ATP, pH 7.5 (20°C) (Roche Molecular Biochemicals, Indianapolis, IN) (*see* **Note 2**).
6. T4 polynucleotide kinase 10 U/µL (New England Biolabs, Inc., Beverly, MA).
7. 10 × reaction buffer for T4 polynucleotide kinase: 700 m*M* Tris-HCl, 100 m*M* $MgCl_2$, 50 m*M* dithiothreitol, pH 7.6 (at 25°C) (New England Biolabs, Inc., Beverly, MA).
8. 100 m*M* ATP solution (Roche Molecular Biochemicals, Indianapolis, IN).
9. 30% (w/v) solution of PEG-8000 (Sigma, St. Louis, MO) in bidistilled water (*see* **Note 3**).
10. Proteinase K (Roche Molecular Biochemicals, Indianapolis, IN) 20 mg/mL stock solution in distilled water. Store at –20°C. In the reaction use 50 µg/mL solution in PBS, prepared from the stock. Do not reuse (*see* **Note 4**).
11. Oligonucleotide hairpin probe with biotin label (Synthetic Genetics, San Diego, CA) (*see* **Note 5**) and unlabeled oligo of the same sequence as the probe. The probes sequences:
    1. The probe with a 3' singe dA overhang (for detection of double-strand breaks with 3' single T overhangs): 5' GCG CTA GAC CtG GTC TAG CGC A 3'
    2. The blunt-ended probe (for detection of blunt-ended DNA breaks): 5' GCG CTA GAC CtG GTC TAG CGC 3'. t represents biotinylated deoxythymidine or biotin-TEG spacer (Glen Research, Sterling, VA).
12. Phosphate-buffered saline (1× PBS): dissolve 9 g NaCl, 2.76 g $NaH_2PO_4 \cdot H_2O$, 5.56 g $Na_2HPO_4 \cdot 7H_2O$ in 800 mL of distilled water. Adjust to pH 7.4 with NaOH, and fill to 1 L with distilled water.
13. TE buffer: 10 m*M* Tris-HCl, pH 7.5, 1 m*M* EDTA.
14. 10 m*M*, 30 m*M* and 100 m*M* EDTA solutions, pH 8.0.
15. Sodium bicarbonate buffer: 50 m*M* $NaHCO_3$, 15 m*M* NaCl, pH 8.2.
16. Streptavidin-fluorescein conjugate and streptavidin-Texas Red conjugate (Molecular Probes, Eugene, OR).
17. Fluorescent microscope with appropriate filters and objectives.
18. Vectashield (Vector Laboratories, Burlingame, CA) antifading-counterstaining solution with DAPI (1 µg/mL). Store at 4°C in the dark. DAPI is a potential carcinogen.
19. 22 × 22 mm or 22 × 40 mm glass or plastic coverslips. Plastic coverslips are preferable as they are easier to remove from the section.
20. DNase II 1500 U/mg (solid) (Sigma, St. Louis, MO) used in positive control reaction (*see* **Note 6**).

3. Method

1. Place the sections in a slide rack and dewax in xylene for 15 min, transfer to a fresh xylene bath for an additional 5 min.
2. Rehydrate by passing through graded ethanol concentrations: 96% Ethanol—2 × 5 min; 80% Ethanol—5 min; water—2 × 5 min.

3. Digest section with Proteinase K. Use 100 µL of a 50 µg/mL solution per section. Incubate 15' at room temperature in a humidified chamber
4. Rinse in distilled water for 4 × 2 min.
5. Apply 100 µL per section of the pre-incubation solution. Incubate for 15 min at room temperature (23°C). The pre-incubation solution consists of a 1× T4 DNA ligase reaction buffer supplemented with PEG-8000 and EDTA to the final concentrations of 15% and 1 m*M*, respectively (*see* **Note 7**). It contains 66 m*M* Tris-HCl, pH 7.5, 5 m*M* $MgCl_2$, 1 m*M* dithioerythritol, 1 m*M* ATP, 1 m*M* EDTA, 15% polyethylene glycol.
6. Aspirate the preincubation solution and apply the full ligase reaction mix with the hairpin probe (750 ng/µL stock) and T4 DNA ligase.
   In situ ligation labeling solution (20 µL per section):
   Prepare on ice in this order:
   3 µL—bidistilled water
   2 µL—10 m*M* EDTA
   10 µL—PEG8000 (30% stock solution)
   2 µL—10× buffer for T4 DNA ligase
   1 µL—biotin labeled hairpin probe
   2 µL—T4 DNA ligase (5U/µL) (*see* **Note 2**)
   The total volume of the labeling solution can be scaled up to accommodate bigger sections.
   Incubate for 18 h (overnight) at room temperature (23°C) in a humidified chamber with a plastic coverslip (*see* **Note 8**).
7. Remove coverslips the next day by gently immersing the slides vertically in a coplin jar containing TE buffer at room temperature. Then wash section 3 × 20 min in TE buffer.
8. Dilute 2 µL of streptavidin-fluorescein conjugate in 1 mL of TE buffer. Add 100 µL of this solution to the section. Incubate 45 min at room temperature in a covered humidified chamber.
9. Wash 3 × 10 min in TE buffer.
10. Add T4 polynucleotide kinase equlibration solution (100 µL/section):
    69 µL—water
    1 µL—EDTA (100 m*M*)
    20 µL—30% PEG
    10 µL—10× buffer for T4 polynucleotide kinase (*see* **Note 9**).
    Incubate 10 min at 37°C in a humidified chamber.
11. Aspirate equilibration solution and apply T4 polynucleotide kinase reaction solution (30 µL/section):
    16 µL—water
    1 µL—EDTA (30 m*M*)
    5 µL—30% PEG
    3 µL—10× buffer for T4 polynucleotide kinase
    1 µL—100 m*M* ATP
    4 µL (40 units)—T4 polynucleotide kinase
    Incubate 30 min at 37°C in humidified chamber (*see* **Note 10**).

12. Wash in TE buffer for 3 × 10 min.
13. Repeat steps 5–7.
14. Dilute 2 µL of streptavidin-rhodamine conjugate (*see* **Note 11**) in 1 mL of TE buffer. Add 100 µL of this solution to the section. Incubate 45 min at room temperature in a covered humidified chamber.
15. Wash 3 × 10 min in sodium bicarbonate buffer.
16. Cover section with an antifading solution (Vectashield with DAPI), coverslip and analyze the signal using a fluorescent microscope. Double-strand DNA breaks with 5'OH will fluoresce red, 5'PO_4 breaks—will fluoresce green (*see* **Note 12**).

4. Notes

1. The highly concentrated (5 U/µL) (Roche Molecular Biochemicals, Indianapolis, IN) ligase preparation gives the best signal.
2. ATP in the ligase reaction buffer is easily destroyed in repetitive cycles of thawing and freezing. Aliquot the buffer in small 15–20 µL portions and store at –20°C. Use once.
3. 15% PEG-8000 in the ligation mix stimulates the ligation reaction increasing the effective concentrations of the probe and ligase by volume exclusion.
4. Proteinase K is a very stable enzyme, when stored at concentrations higher than 1 mg/mL. However, autolysis of the enzyme occurs in aqueous solutions at low concentrations (~ 10 µg/mL) ***(17)***.
5. The probes contain a single internal biotin and can be synthesized by many commercial oligonucleotide producers. The biotin could be incorporated into the probe either by using an amino modifier C6 deoxyuridine with subsequent attachment of biotin bis-aminohexanoyl-N-hydroxysuccinimide ester, or by chemical insertion of a biotinTEG phosphoramidite directly into the oligonucleotide backbone. PAGE purification is advised. We primarily use the probe with a TEG linker. Dilute with bidistilled water to 750 ng/µL stock concentration. Store at –20°C. Direct fluorophore labeling (FITC, Texas Red, Alexa, etc.) instead of biotin is possible. Sometimes in our experiments the directly labeled probes produced somewhat higher background staining compared to biotinylated probes, but their usage can be advantageous in simultaneous detection of 5'PO_4 and 5'OH DNA breaks because they shorten the time of the procedure and thus lessen the probability of artifactual DNA damage.
6. DNase II treated sections can be used as positive controls. We use sections of normal bovine adrenals or rat heart because normal rat brain sections display high background levels after treatment with DNase II.

   Make the DNase II stock by diluting DNase II powder (Sigma, St. Louis, MO) in water to the concentration of 1 mg/mL, aliquot in small volumes and keep the stock at –20°C. To run a reaction, dilute the stock solution 1:1 with the DNase II reaction buffer. DNase II reaction buffer: 80 m*M* Potassium Acetate, 0.8 m*M* $MgCl_2$ (pH 4.2–5.5 at 23°C).

   To produce DNase II type breaks, incubate the tissue section with DNase II (100 µL of 0.5 mg/mL DNase II solution per tissue section) for 30 min at 37°C in humidified chamber.

7. The double-detection procedure is longer than regular *in situ* ligation. EDTA in a final concentration of 1 m*M* is added to the incubation, reaction and washing solutions as a precautionary measure to prevent activation of nonspecific nucleases, which could be present in these solutions or in commercial enzymatic preparations of T4 polynucleotide kinase. If present they could result in additional DNA cleavage, detectable in the second ligation reaction.
8. A mock ligase reaction is recommended as a regular control in order to rule out nonspecific background staining. In a mock reaction solution an equal volume of 50% glycerol in water is substituted for T4 DNA ligase. More details of a regular *in situ* ligation procedure are presented in Chapter 12 in this volume.
9. T4 polynucleotide kinase is fully active in 1×T4 DNA ligase buffer, which can be substituted for T4 polynucleotide kinase buffer. No need to add ATP in kinase reaction mix in this case, because 1× ligase buffer contains 1 m*M* ATP.
10. A mock kinase reaction is recommended as a regular control to make sure that the first ligation reaction blocks all detectable 5'PO_4 ends, which otherwise will be detected as 5'OH ends in the second ligation reaction. In the mock reaction, the first and the second ligations are performed without change, but an equal volume of 50% glycerol in water is substituted for T4 polynucleotide kinase. No signal from the second fluorophore should be observed. The negative controls are recommended for every new tissue type to ensure the absence of nonspecific staining. Commercially available T4 polynucleotide kinase may contain small amounts of nucleases. This can be tested by applying the kinase solution to the normal section without prior DNA damage for 60 min at 37°C and then performing the *in situ* ligation assay.
11. Rhodamine conjugates sometimes display more "stickiness" in the sections with considerable tissue damage showing more background staining. To reduce this effect fluorescein can be used instead as a second fluorophore, where the first ligation reaction is visualized by rhodamine.
12. If the first ligation reaction detects no 5'PO_4 breaks, it can be omitted and the procedure starts with T4 kinase treatment (perform Steps 1-4, 9-16 only).

Acknowledgment

The authors would like to thank Candace Minchew for her expert technical assistance.

References

1. Sikorska, M., and Walker, P. R. (1998) Endonuclease activities and apoptosis, in *When Cells Die* (Lockshin, R. A., Zakeri, Z., and Tilly, J. L., eds.), Wiley-Liss, New York, pp. 211–242.
2. Barry, M. A., and Eastman, A. (1993) Identification of deoxyribonuclease II as an endonuclease involved in apoptosis. *Arch. Biochem. Biophys.* **300,** 440–450.
3. Liu, Q. Y., Ribecco, M., Pandey, S., Walker, P. R., and Sikorska, M. (1999) Apoptosis-related functional features of the DNaseI-like family of nucleases. *Ann. N Y Acad. Sci.* **887,** 60–76.

4. Collins, M. K., Furlong, I. J., Malde, P., Ascaso, R., Oliver, J., and Lopez Rivas, A. (1996) An apoptotic endonuclease activated either by decreasing pH or by increasing calcium. *J. Cell Sci.* **109,** 2393–2399.
5. Oliveri, M., Daga, A., Cantoni, C., Lunardi, C., Millo, R., and Puccetti, A. (2001) DNase I mediates internucleosomal DNA degradation in human cells undergoing drug-induced apoptosis. *Eur J Immunol.* **31,** 743–751.
6. Counis, M. F., and Torriglia, A. (2000) DNases and apoptosis. *Biochem. Cell Biol*. **78,** 405–414.
7. Torriglia, A., Perani, P., Brossas, J. Y., Altairac, S., Zeggai, S., Martin, E., Treton, E., Courtois, Y., and Counis, M. F. (2000) A caspase-independent cell clearance program: the LEI/L-DNase II pathway. *Ann. N Y Acad. Sci.* **926,** 192–203.
8. Lyon, C. J., Evans, C. J., Bill, B. R., Otsuka, A. J., and Aguilera, R. J. (2000) The C. elegans apoptotic nuclease NUC-1 is related in sequence and activity to mammalian DNase II. *Gene* **252,** 147–154.
9. Kawane, K., Fukuyama, H., Kondoh, G., Takeda, J., Ohsawa, Y., Uchiyama, Y., and Nagata, S. (2001) Requirement of DNase II for definitive erythropoiesis in the mouse fetal liver. *Science* **292,** 1546–1549.
10. Alnemri, E. S., and Litwack, G. (1990) Activation of internucleosomal DNA cleavage in human CEM lymphocytes by glucocorticoid and novobiocin. Evidence for a non-Ca2(+)-requiring mechanism(s). *J. Biol. Chem.* **265,** 17,323–17,333.
11. Staley, K., Blaschke, A. J., and Chun, J. (1997) Apoptotic DNA fragmentation is detected by a semiquantitative ligation-mediated PCR of blunt DNA ends. *Cell Death Diff.* **4,** 66–75.
12. Didenko, V. V., and Hornsby, P. J. (1996) Presence of double-strand breaks with single-base 3' overhangs in cells undergoing apoptosis but not necrosis. *J. Cell Biol.* **135,** 1369–1376.
13. Walker, P. R., Carson, C., Leblanc, J., and Sikorska, M. (2001) Labeling DNA damage with terminal transferase: applicability, specificity and limitations, in *In Situ Detection of DNA Damage: Methods and Protocols* (Didenko, V. V., ed.) pp. 3–20.
14. Didenko, V. V. (2001) Detection of specific double-strand DNA breaks and apoptosis *in situ* using T4 DNA ligase, in *In Situ Detection of DNA Damage: Methods and Protocols* (Didenko, V. V., ed.) pp. 143–152.
15. Grosse, F. and Manns A. (1993) Terminal Deoxyribonucleotidyl Transferase (EC 2.7.7.31), in *Enzymes of Molecular Biology* (Burrell, M. M., ed.), Humana, Totowa, NJ, pp. 95–105.
16. Maunders, M. J. (1993) DNA and RNA Ligases (EC 6.5.1.1, EC 6.5.1.2,and EC 6.5.1.3), in *Enzymes of Molecular Biology* (Burrell, M. M., ed.), Humana, Totowa, NJ, pp. 213–230.
17. Sweeney, P. J. and Walker, J. M. (1993) Proteinase K (EC 3.4.21.14), in *Enzymes of Molecular Biology* (Burrell, M. M., ed.), Humana, Totowa, NJ, pp. 305–311.

13

The Comet Assay

Principles, Applications, and Limitations

Andrew R. Collins

1. Introduction

Over the past decade, the comet assay, or single cell gel electrophoresis (SCGE) has become one of the standard methods for assessing DNA damage, with applications in genototoxicity testing, human biomonitoring and molecular epidemiology, ecotoxicology, as well as fundamental research in DNA damage and repair. The assay attracts adherents by its simplicity, sensitivity, versatility, speed and economy, and the number of publications it spawns rises each year. It is sometimes used without too much thought as to how it works or what sort of information it provides; the fact that it is so successful at demonstrating DNA damage is enough to justify its use. This is a shame, as it is capable of subtle manipulation to tell us not just how much damage is present in cells, but what form it takes. Although it is essentially a method for measuring DNA breaks, the introduction of lesion-specific endonucleases allows detection of, for example, UV-induced pyrimidine dimers, oxidized bases and alkylation damage.

The purpose of this introductory review chapter is to clear up some misconceptions about the comet assay and to show how its special features can best be exploited.

2. How the Comet Assay Works and What It Measures

2.1. Background

In the 1970s, Peter Cook and colleagues ***(1)*** developed an approach to investigating nuclear structure based on the lysis of cells with non-ionic detergent

From: *Methods in Molecular Biology, vol. 203:* In Situ *Detection of DNA Damage: Methods and Protocols*
Edited by: V. V. Didenko

and high molarity sodium chloride. This treatment removes membranes, cytoplasm and nucleoplasm, and disrupts nucleosomes (almost all histones being solubilized by the high salt). What is left is the nucleoid, consisting of a nuclear matrix or scaffold composed of RNA and proteins, together with the DNA, which is negatively supercoiled as a consequence of the turns made by the double helix around the histones of the nucleosome. The survival of the supercoils implies that free rotation of the DNA is not possible; Cook et al. proposed a model with the DNA attached at intervals to the matrix so that it is effectively arranged as a series of loops, rather than as a linear molecule. When the negative supercoiling was unwound by adding the intercalating agent ethidium bromide, the loops expanded out from the nucleoid core to form a 'halo'. A similar effect was seen when ionizing radiation was used to relax the loops—one single-strand break being sufficient to relax the supercoiling in that loop.

The comet assay, too, in its most commonly used form, involves lysis with detergent and high salt—after embedding cells in agarose so that the DNA is immobilized for subsequent electrophoresis. The first demonstration of "comets" (though they did not use the word) was by Östling and Johanson ***(2)***, who describe the tails in terms of DNA with relaxed supercoiling and refer to the nucleoid model of Cook et al. Essentially, the comet tail seems to be simply a halo of relaxed loops pulled to one side by the electrophoretic field. Östling and Johanson employed a pH of less than 10. It needs to be clearly understood that although the most common variant now employed is *alkaline* SCGE, a high pH is not essential to detect single strand breaks.

2.2. Common Comet Assay Variants.

2.2.1. Alkaline Single Cell Gel Electrophoresis

The procedure of Östling and Johanson was not widely adopted. A few years later, two research groups independently developed procedures involving treatment at high pH. Singh et al. ***(3)*** lysed cells at pH 10 with 2.5 *M* NaCl, Triton X-100 and sarkosyl for 1 h, following this with a treatment with alkali (0.3 *M* NaOH) and electrophoresis at the resulting high pH (>13). Olive et al. ***(4)*** simply lysed cells in weak alkali (0.03 *M* NaOH) for 1 h before electrophoresis. Thus the idea has grown up that the comet assay is in the same category as alkaline unwinding, alkaline elution or alkaline sucrose sedimentation, where separation of two DNA strands around a break by alkaline denaturation is essential to reveal the break. For the reasons stated in **Section 2.1**, I believe this to be a profound misunderstanding. The use of alkali makes comet tails more pronounced and improves the resolving power of the assay ***(5)***, but does not affect the sensitivity (i.e., the lowest dose of damage detected). Östling and Johanson ***(2)*** detected the effect of ionizing radiation from a fraction of a Gy

up to 3 Gy; Singh et al. ***(3)*** reported tails increasing in length over the range 0.25 to 2 Gy.

2.2.2. Neutral Single Cell Gel Electrophoresis

Following the example of Östling & Johanson ***(2)***, we demonstrated the ability of a neutral procedure to detect low levels of DNA breaks ***(5)***. We later used a variant in which, after a period of alkaline treatment, conditions were restored to neutral for the electrophoresis ***(6)***. This modification decreased the sensitivity and extended the useful range of the assay, but it was clear (from the kind of damaging agent used) that we were still detecting single strand breaks.

A radically different kind of neutral comet assay was developed earlier by Olive et al. ***(7)*** to facilitate detection of double strand breaks without interference from single strand breaks. Their procedure employs extended treatment of lysed cells in agarose at 50°C, and under these conditions it is likely that the nuclear matrix is disrupted so that we are truly looking at the behavior of double-stranded pieces of DNA (or the free ends of these fragments).

2.2.3. Use of Lesion-Specific Enzymes

Measuring DNA strand breaks gives limited information. Breaks may represent the direct effect of some damaging agent, but they are generally quickly rejoined. They may in fact be apurinic/apyrimidinic sites (i.e., AP-sites, or base-less sugars), which are alkali-labile and therefore appear as breaks. Or they may be intermediates in cellular repair, since both nucleotide and base excision repair processes cut out damage and replace it with sound nucleotides.

To make the assay more specific as well as more sensitive, we introduced the extra step of digesting the nucleoids with an enzyme that recognizes a particular kind of damage and creates a break. Thus, endonuclease III is used to detect oxidized pyrimidines ***(8)***, formamidopyrimidine DNA glycosylase (FPG) to detect the major purine oxidation product 8-oxoguanine as well as other altered purines ***(9)***, T4 endonuclease V to recognize UV-induced cyclobutane pyrimidine dimers ***(10)***, and Alk A incises DNA at 3-methyladenines ***(10a)***. In each case, the increased DNA break frequency increases tail intensity.

Oxidized bases are readily detected with endonuclease III or FPG in cells that have been treated with H_2O_2, or with photosensitizer plus visible light. They are also present in significant numbers in normal human lymphocytes (*see* **Subheading 4.3.4**).

2.3. Some Less Common Variants

2.3.1. Bromodeoxyuridine Labeling to Detect Replicating DNA

DNA breaks associated with replicating DNA would be expected to give rise to comet tails. However, it is normally impossible to distinguish S-phase

from non-S-phase cells in this way—perhaps because the amount of DNA taking part in replication at any one time is exceedingly small, or because the replication apparatus stabilizes the replicating fork in some way so that the break does not behave as a normal damage break. If cells are labeled during replication with bromodeoxyuridine (BUdR), which is then visualized with anti-BUdR antibody, labeled comet tails are seen; maturation of replicating DNA during a post BUdR-labeling chase results in 'retreat' of the labeled material into the head ***(11)***.

2.3.2. Detecting Intermediates in DNA Repair

The breaks that occur as intermediates in nucleotide excision repair of UV-induced damage or bulky adducts are normally short-lived—at least in proliferating cells. Incubation of UV-irradiated cells with DNA synthesis inhibitors hydroxyurea, cytosine arabinoside or aphidicolin blocks repair patch synthesis and causes incision breaks to accumulate, and this provides a sensitive way to detect the effects of the damaging treatment ***(12)***. (In non-dividing cells such as peripheral lymphocytes, incision breaks accumulate without inhibitors, as the rate of religation is limited by the poor supply of deoxyribonucleoside triphosphates ***(13)***.)

2.3.3. FISH Comets

The appearance of a comet reflects damage in the cellular DNA overall. It would be extremely informative to locate specific chromosomes, or regions of chromosomes, classes of DNA or specific genes within the comet. Fluorescent *in situ* hybridization (FISH), using probes of cDNA or oligonucleotides to recognize the sequences of interest is the normal approach to this, but hybridization to DNA with the fine structure of comets in a slide-mounted agarose matrix that melts at normal hybridization temperatures presents technical difficulties. These have been solved, and it is possible to identify DNA of a particular chromosome, telomeric DNA, centromeric DNA and single copy genes ***(14–16)***. Little by way of useful information has emerged so far (though the pictures are pretty), but the approach is promising. For example, it is possible to measure gene-specific repair rates after low doses of DNA-damaging agent (A.R. Collins, E. Horváthová and M. Dušinská, in preparation).

2.4. Does the Comet Assay Detect Apoptosis?

When almost all the DNA is in the tail of a comet, the head is reduced in size, and the image has fancifully been referred to as a 'hedgehog' comet. For some reason, the idea has grown that hedgehog comets represent apoptotic cells. It is possible, of course, that some of these relatively severely damaged cells will subsequently go through programmed cell death, but they cannot be described as apoptotic, for two reasons:

- Apoptosis is irreversible, but cells with damage revealed as 'hedgehog' comets can repair their damage so that hedgehogs are no longer seen. (The explanation is not that the damaged cells die and disappear from the experiment, as the density of comets in the gel indicates that all cells are still present.)
- Apoptosis is characterized by fragmentation of DNA to the size of nucleosome oligomers. Such small pieces of DNA would certainly disappear during lysis or electrophoresis; the 'ghosts' of comets that are sometimes seen, with a few percent of normal DNA fluorescence, may represent a residue of high MW DNA in apoptotic cells.

Singh ***(17)*** recently described a visualization method for apoptotic cells in which cells were embedded in agarose and lysed as for the normal comet assay, and then—instead of electrophoresis—the DNA was precipitated with ethanol. Cells treated with an agent known to induce apoptosis appeared with a halo of granular DNA and a hazy outer boundary—as one would expect from diffusing small fragments.

2.5. Are AP Sites Seen as DNA Breaks in the Comet Assay?

AP sites are alkali-labile—but are the pH and treatment time commonly used for alkaline SCGE enough to convert some or all of them to breaks? It seems likely that the methods employing strong alkali (0.3 *M* NaOH) convert more AP sites to breaks than do the methods employing only 0.03 *M* NaOH, and this may account in part for the apparently lower sensitivity of the mild alkali methods, but pH is not the only variable, and a direct comparison of methods is difficult.

It should be possible to use AP endonucleases to clear up this question; under specific conditions of pH, and after treatment of cells with an agent known to induce base loss from DNA, does digestion of nucleoids with AP endonuclease increase the yield of breaks? However, AP endonucleases are often associated with glycosylases that remove particular damaged bases, providing AP substrate, and there is also the possibility of non-specific contaminating nuclease activity, so attempts to give decisive answers often leave a suspicion of ambiguity. Experiments with methyl methanesulphonate-treated *Vicia faba* root tip cells indicated that there certainly are some AP endonuclease-sensitive sites that are not converted to breaks under strongly alkaline conditions (0.3 *M* NaOH) ***(6)***.

3. Quantitation

3.1. Visualizing Comets

DNA is visualized by fluorescence microscopy after staining with a DNA-binding dye. Ethidium bromide (EB) is probably most commonly used, followed

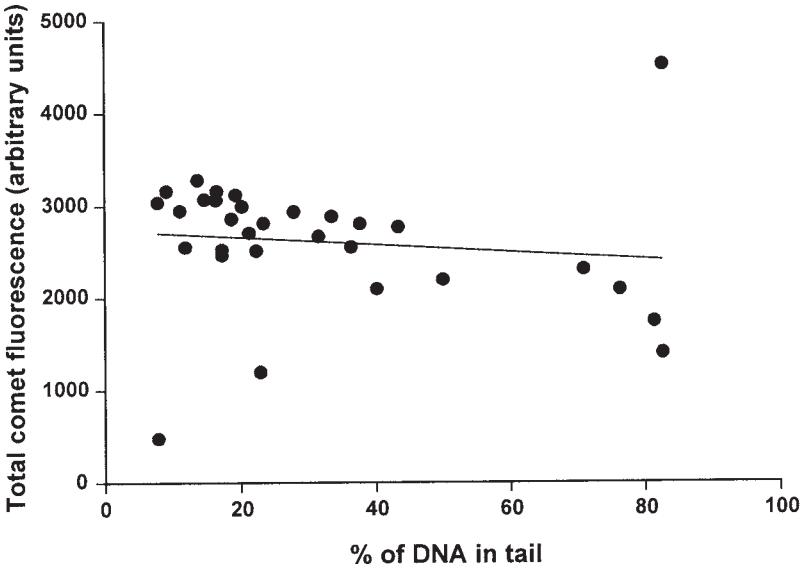

Fig. 1. Relationship between total DAPI fluorescence and % of DNA in the tail. Typical results, with comets from H_2O_2-treated lymphocytes.

by 4,6-diamidino-2-phenylindole (DAPI). EB is an intercalating dye which binds more efficiently to double-stranded DNA than to single-stranded DNA. DAPI binds to the major groove and fluorescence should therefore be dependent on double-stranded structure. DNA strand separation occurs during alkaline treatment, and even if intact, supercoiled loops in the head renature readily on neutralization, at least the DNA in the tail should be thoroughly single-stranded. Staining with acridine range (AO) confirms this. AO gives red fluorescence with single-stranded nucleic acid and yellow/green fluorescence with double-stranded DNA. We found ***(5)*** that AO staining produced red comet tails and predominantly yellow/green heads. So what can we make of the EB and DAPI fluorescence? It should, at least, be less intense with single-stranded DNA compared with double-stranded DNA, so the higher the proportion of DNA in the tail, the less the total fluorescence detected in the whole comet should be. We measured this, with DAPI staining, and found little decrease in total fluorescence (**Fig. 1**). Perhaps there is a fortuitous compensation, self-quenching of fluorescence in the densely-packed DNA of the head detracting from the more efficient staining of double-stranded DNA. Whatever the reason, it allows us to obtain additional information from the comets. Total fluorescence reflects DNA content, and a cell in G_2 should give rise to a comet with more fluorescence than a cell in G_1. Thus levels of damage in individual

comets from a cell population can be related to cell cycle phase ***(18)***. In effect, comets are sorted according to DNA content in the same way as in flow cytometry.

3.2. Measuring Comets: Image Analysis

There are numerous software packages to choose from which will compute fluorescence parameters for comets selected by the operator. The most important parameters are tail length, relative fluorescence intensity of head and tail (normally expressed as % of DNA in tail), and tail moment. Tail length, in my experience, is not very useful, as it increases only while tails are first becoming established, at relatively low damage levels. Subsequently, the tail increases in intensity but not in length as the dose of damage increases. Tail length is also sensitive to the background or threshold setting of the image analysis program, as the end of the tail is defined by a certain excess of fluorescence over background. Relative tail intensity is the most useful parameter, as it bears a linear relationship to break frequency (*see* below), is relatively unaffected by threshold settings, and allows discrimination of damage over the widest possible range (in theory, from 0%–100% DNA in tail). It also gives a very clear indication of what the comets actually looked like. In contrast the third parameter, tail moment (essentially the product of tail length and tail intensity) is not linear with respect to dose, and does not give any idea of the comet's appearance. It is hard to understand why this method of quantitation is so popular.

Analysis of 50 comets per slide is recommended.

3.3. Measuring Comets: Visual Scoring

It is possible to compute DNA damage from comets without sophisticated image analysis programs. The human eye is easily trained to discriminate degrees of damage according to comet appearance (**Fig. 2**). We find that 5 classes, from 0 (no tail) to 4 (almost all DNA in tail) give sufficient resolution. If 100 comets are scored, and each comet assigned a value of 0–4 according to its class, the total score for the sample gel will be between 0–400 'arbitrary units'. Visual scoring is rapid as well as simple, and should appeal to those exploring the usefulness of the technique without wanting to invest in expensive analytical equipment.

3.4. Selection of Comets

This is an issue for both computer-based analysis and visual scoring. Comets must be selected without bias and must represent the whole gel, so it is necessary to scan the gel in a systematic way. The edges, as well as areas around air bubbles, should be avoided, as they often display comets with anomalously high levels of damage. Analysis of overlapping comets is impossible, at least

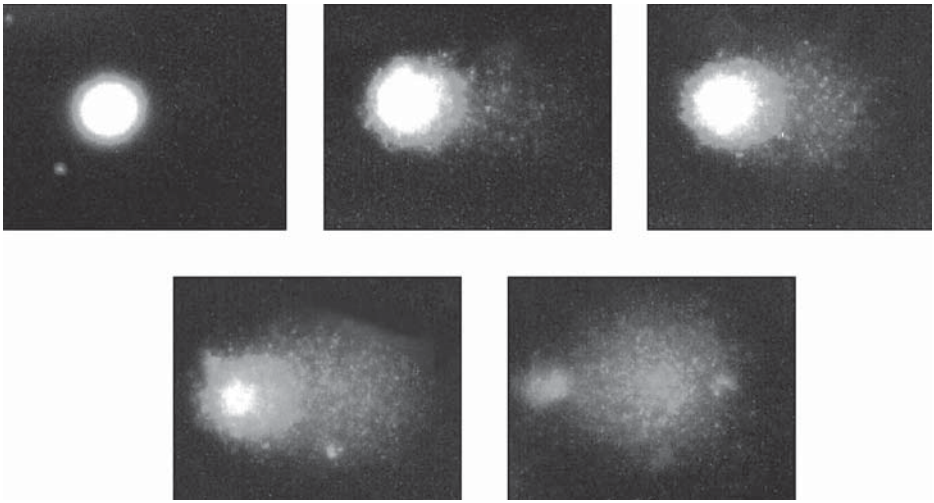

Fig. 2. Images of comets (from lymphocytes), stained with DAPI. They represent, in sequence, our classes 0–4, and are representative examples used for visual scoring.

with computer analysis, but the most likely comets to overlap are those with big tails. If too many large overlapping comets are rejected, there may be a significant bias towards undamaged, tail-less comets. It is important not to have gels too densely packed with cells.

3.5. Calibration

The usual method of calibration is to irradiate samples of cells with gamma- or X-rays to induce known numbers of single-strand breaks in DNA. The breaks tend to be rapidly repaired, so cells should be irradiated on ice—preferably already embedded in agarose to minimize post-irradiation handling.

Comets show a linear increase in % DNA in tail (or in visual score) over a range of 0–8 Gy, which corresponds to DNA damage up to about 2.5 breaks per 10^9 daltons. It is important to keep this figure in mind when considering the behavior of DNA under SCGE conditions: it corresponds to a 'fragment' length of about 160 μm—far longer than the comet tail itself—and so it is clearly nonsense to represent the tail as made up of DNA fragments migrating according to their size. This point was recognized by Östling and Johanson ***(2)*** who stated that ". . . the molecular weight of DNA is . . . certainly many magnitudes higher than the molecular weight of DNA used in conventional electrophoretic separations and any comparison with separation of DNA of 10^9 daltons or less is not relevant."

When the same comet slides are checked by computer image analysis and by visual scoring, the correspondence is excellent ***(19)***.

4. Applications

4.1. Genotoxicity Testing

The comet assay has achieved the status of a standard test in the battery of tests used to assess the safety of novel pharmaceuticals or other chemicals. It is readily applied to in vivo experiments; tissues that can be disaggregated to single cell suspensions, as well as white blood cells, provide the material. The assay is normally used in its simple form to measure strand breaks; increased sensitivity, as well as additional information on mechanisms of action, would accrue from including repair endonucleases to measure specific types of lesion.

Genotoxicity is also assessed in cell culture systems, on their own or in conjunction with the microsomal 'S9' fraction from liver which provides enzymes to metabolize chemicals to more reactive forms.

Chemoprotection is the other side of the coin: the comet assay is eminently suitable for assessing the ability of phytochemicals, for example, to protect cells against genotoxic insult.

4.2. Ecological Monitoring

Suitable organisms can be used in combination with the comet assay as biosensors for contamination of the environment with genotoxins. This work is at an early stage, but promising results have been reported with marine organisms such as mussels, with earthworms and even mice.

4.3. Human Studies

The comet assay is ideally suited for human investigations, since it requires no prelabeling with radioactivity, or other harmful procedures, and can be applied to easily obtainable cells (normally white blood cells).

4.3.1. Biomonitoring

Applications include monitoring occupational exposure to genotoxic chemicals or radiation ***(20)***; assessment of oxidative stress associated with various human diseases ***(21)***; and detection of DNA damage associated with smoking ***(22)***. In general, though significant differences are seen between exposed and control groups of subjects, there is a wide inter-individual range of damage levels within any group—as well as intra-individual variability resulting from changes in diet, stress or infection—and attempts to assess individual risk of diseases such as cancer from comet assay results would be premature and unjustifiable.

4.3.2. Nutritional Studies

The comet assay is ideal for investigating nutrient/micronutrient effects at the level of DNA damage in humans. Diets differing in lipid content lead to changes in oxidative DNA damage in lymphocytes—polyunsaturated fatty acids apparently causing an increase ***(23)***. On the other hand, the protective effects of in vivo supplements of antioxidants, or of foods rich in antioxidants, are very readily demonstrated in lymphocytes as either a decrease in endogenous base oxidation (measured with endonuclease III or FPG) or a decreased sensitivity to H_2O_2-induced damage in vitro ***(24,25)***.

4.3.3. Diagnosis

In a few cases, it may be possible to use the comet assay as an aid to diagnosis. The Nijmegen breakage syndrome is an autosomal recessive condition associated with genetic instability and cancer proneness. Heterozygote carriers are identifiable by an abnormally high level of strand breakage in lymphocyte comets ***(26)***.

4.3.4. Assessing Background Levels of Damage

Oxidative base damage in DNA is a possible factor in cancer etiology, and yet we do not know how much damage is present. Estimates of the content of 8-oxoguanine in human DNA vary over 3–4 orders of magnitude. High values provided by GC-MS and HPLC + electrochemical detection are affected by the serious artefact of oxidation of guanine during sample preparation: limiting the possibilities for oxidation has brought estimates down. The comet assay—used in a quantitative way, with FPG—suggests that the frequency of 8 oxoguanine is only about 0.5 per 10^6 guanines—several times less than the lowest of the HPLC estimates ***(27)***

4.4. Measuring DNA Repair

Surprisingly, we know very little about the variation in capacity for DNA repair between individuals, even though this is likely to be an important determinant of individual susceptibility to cancer. To date, a suitably robust and sensitive assay has not been available, but the comet assay has the potential to fill this gap.

4.4.1. Cellular Repair

Theoretically, a sound approach to measuring repair capacity is to inflict DNA damage on cells and to monitor the speed with which they remove the lesions. Thus, lymphocytes can be treated with ionizing radiation, or H_2O_2, and rejoining of breaks followed; or, after treatment with base-damaging chemicals, and incubation, the remaining lesions can be assayed by use of an

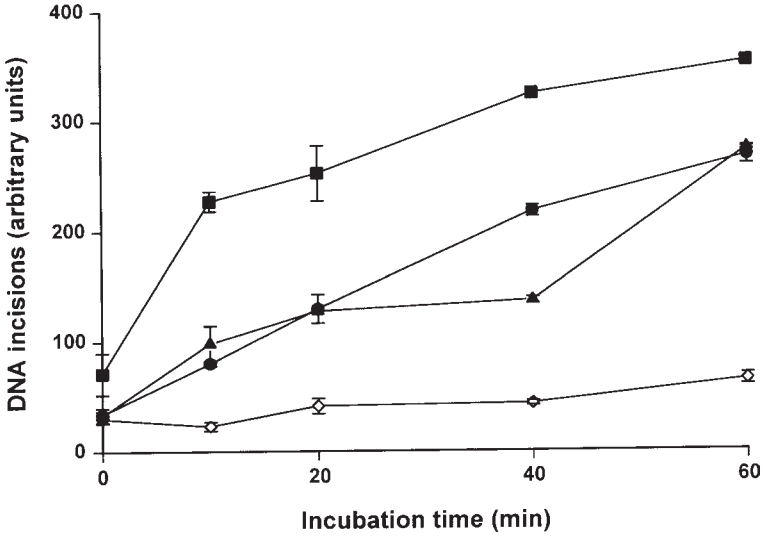

Fig. 3. DNA repair activity of extract from lymphocytes from three subjects (solid symbols) given substrate of gel embedded nucleoids from cells treated with Ro 19–8022 (Hoffmann-La Roche) and visible light to induce 8-oxoguanine. Open symbol: substrate incubated without extract.

appropriate endonuclease on the gel. We have found strand break rejoining after H_2O_2-treatment of lymphocytes to be very slow, and it seems that sudden exposure of cells freshly isolated from blood to atmospheric oxygen causes substantial additional damage, which seriously compromises the analysis.

4.4.2. An In Vitro Repair Assay

As an alternative, the repair activity of a cell extract can be assessed in an in vitro assay ***(28)*** which is the converse of the normal enzyme-linked comet assay. A simple extract is prepared from cells, such as lymphocytes, by freezing, thawing, adding Triton X-100, and centrifuging to remove cell debris. A damaged DNA substrate is prepared in the form of gel-embedded nucleoids from (cultured) cells treated with whichever damaging agent is appropriate for the repair being measured—for instance, UV radiation, or photosensitizer plus visible light to induce base oxidation. The substrate is then presented to the extract, and the rate at which breaks accumulate indicates the capacity of the extract to incise at damage sites. Incision is normally regarded as the rate-limiting step of repair.

Fig. 3 illustrates the use of this approach to measure the repair capacity of lymphocyte extract given DNA containing oxidized bases.

4.5. Practical Considerations for the Use of the Comet Assay in Human Population Studies and in Animal Trials

The comet assay is eminently suited for use in molecular epidemiology and animal experiments, but care must be taken to ensure its reliability and to make it truly quantitative.

4.5.1. Study Design

Human studies should be designed according to standard epidemiological considerations. Power calculations are required to establish the size of groups to be studied; a pilot study may be necessary to estimate the range of intra- and inter-individual variation in the kind of damage being measured.

4.5.2. Standardization of the Comet Assay

Standards should be included in the analysis; for example, lymphocytes prepared from several individuals can be pooled and frozen as aliquots, to be thawed as needed. The standard should give a similar measure of damage each time, and deviation or drift gives warning that some aspect of the assay has changed.

4.5.3. Storage of Lymphocytes

Samples of lymphocytes from a trial can be frozen and stored in liquid nitrogen for months. However, the cells must be suspended in medium that will preserve viability (for human lymphocytes, 90% fetal calf serum/10% dimethyl sulphoxide is recommended), and they must be frozen slowly—at 1°C/min or less; this is achieved by placing vials of the suspended cells in a styrofoam box in a –80°C freezer overnight before transferring them for long-term storage in liquid nitrogen.

4.5.4. Checking Cell 'Viability'

Integrity of cells—whether used fresh or thawed—can be checked by trypan blue staining (so-called viability test) and should be >90%. Excessive background damage is associated with poor quality cells; however, we have found that even with 50% of cells showing membrane damage (i.e. allowing entry of the dye), acceptably low background damage levels are seen.

4.5.5. Storage of Gels After Electrophoresis

It is often impracticable to score slides immediately after performing the comet assay. If the gels are prepared on ordinary glass slides (rather than fully frosted ones), they can be dried and stored indefinitely. Dried gels are easier to score than fresh ones, as all comets are in the same plane and there is no need for constant refocusing.

4.5.6. Statistical Analysis

This can be carried out at different levels. For instance, a single gel might be analyzed in terms of the levels of damage recorded in different comets, and the way in which they are distributed; or we might be interested in the CV for replicate determinations of the same sample. But when we are analyzing differences between groups in human or animal experiments, or effects of treatment, all we are interested in is the overall mean comet score for each individual (whether it is expressed as % DNA in tail, or arbitrary units by visual examination).

4.5.7. Assay Saturation

DNA break frequency is linearly related to % tail DNA—up to a certain level. Saturation obviously occurs once all the DNA is in the tail, and a deviation from linearity is seen as this level of damage is approached. Particular care is needed when the sites revealed with lesion-specific endonucleases are `superimposed on already high levels of strand breakage; there is a tendency for the damaged bases to be underestimated.

5. Conclusions

The comet assay, in various guises, is now well established as a sensitive method for detecting strand breaks in the DNA of single cells. Once calibrated, it can be used in a quantitative way. Lesions other than strand breaks can be detected with the inclusion of a step in which nucleoid DNA is incubated with a lesion-specific endonuclease. The comet assay promises to provide answers to important questions concerning, for example, background levels of DNA damage in normal cells, the variation in DNA repair capacity within human populations, and the regulation of DNA repair at the molecular level within the nucleus.

Acknowledgments

The author is supported by the Scottish Executive Rural Affairs Department. The data in **Fig. 1** were obtained by Dr. Umit Türkoğlu, and the repair experiment (**Fig. 3**) was performed by Vikki Harrington.

References

1. Cook, P. R., Brazell, I. A. and Jost, E. (1976) Characterization of nuclear structures containing superhelical DNA. *J. Cell Sci.* **22,** 303–324.
2. Östling, O. and Johanson, K. J. (1984) Microelectrophoretic study of radiation-induced DNA damages in individual mammalian cells. *Biochem. Biophys. Res. Commun.* **123,** 291–298.
3. Singh, N. P., McCoy, M. T., Tice, R. R. and Schneider, E. L. (1988) A simple technique for quantitation of low levels of DNA damage in individual cells. *Exper. Cell Res.* **175,** 184–191.

4. Olive, P. L., Banáth, J. P. and Durand, R. E. (1990) Heterogeneity in radiation-induced DNA damage and repair in tumor and normal cells measured using the 'comet' assay. *Rad. Res.* **122,** 86–94.
5. Collins, A. R., Dobson, V. L., Dušinská, M., Kennedy, G. and Štětina, R. (1997) The comet assay: what can it really tell us? *Mut. Res.* **375,** 183–193.
6. Angelis, K. J., Dušinská, M. and Collins, A. R. (1999) Single cell gel electrophoresis; detection of DNA damage at different levels of sensitivity. *Electrophoresis* **20,** 1923–1933.
7. Olive, P. L., Wlodek, D. and Banáth, J. P. (1991) DNA double-strand breaks measured in individual cells subjected to gel electrophoresis. *Cancer Res.* **51,** 4671–4676.
8. Collins, A. R., Duthie, S. J. and Dobson, V. L. (1993) Direct enzymic detection of endogenous oxidative base damage in human lymphocyte DNA. *Carcinogenesis* **14,** 1733–1735.
9. Dušinská, M. and Collins, A. (1996) Detection of oxidised purines and UV-induced photoproducts in DNA of single cells, by inclusion of lesion-specific enzymes in the comet assay. *Alternatives to Laboratory Animals* **24,** 405–411.
10. Collins, A. R., Mitchell, D. L., Zunino, A., de Wit, J. and Busch, D. (1997) UV-sensitive rodent mutant cell lines of complementation groups 6 and 8 differ phenotypically from their human counterparts. *Env. Mol. Mutagenesis* **29,** 152–160.

10a. Collins, A. R., Dušinská, M., and Horská, A. (2001) Detection of alkylation damage in human lymphocyte DNA with the comet assay. *Acta Biochemica Polonica* **48,** 611–614.

11. McGlynn, A. P., Wasson, G., O'Connor, J., McKelvey-Martin, V. J. and Downes, C. S. (1999) The bromodeoxyuridine comet assay: Detection of maturation of recently replicated DNA in individual cells. *Cancer Res.* **59,** 5912–5916.
12. Gedik, C. M., Ewen, S. W. B. and Collins, A. R. (1992) Single-cell gel electrophoresis applied to the analysis of UV-C damage and its repair in human cells. *Intl. J. Rad. Biol.* **62,** 313–320.
13. Green, M. H. L., Waugh, A. P. W., Lowe, J. E., Harcourt, S. A., Cole, J. and Arlett, C. F. (1994) Effect of deoxyribonucleosides on the hypersensitivity of human peripheral blood lymphocytes to UV-B and UV-C irradiation. *Mut. Res.* **315,** 25–32.
14. Santos, S. J., Singh, N. P. and Natarajan, A. T. (1997) Fluorescence in situ hybridization with comets. *Exper. Cell Res.* **232,** 407–411.
15. McKelvey-Martin, V. J., Ho, E. T. S., McKeown, S. R., McCarthy, P. J., Rajab, N. F. and Downes, C. S. (1998) Emerging applications of the single cell gel electrophoresis (Comet) assay.I.Management of invasive transitional cell human bladder carcinoma. II. Fluorescent in situ hybridization Comets for the identification of damaged and repaired DNA sequences in individual cells. *Mutagenesis* **13,** 1–8.
16. Rapp, A., Bock, C., Dittmar, H. and Greulich, K. O. (1999) Comet-fish used to detect UV-A sensitive regions in the whole human genome and on chromosome 8. *Neoplasma* **46,** 99–101.
17. Singh, N. P. (2000) A simple method for accurate estimation of apoptotic cells. *Exper. Cell Res.* **256,** 328–337.

18. Olive, P. L. and Banáth, J. P. (1993) Induction and rejoining of radiation-induced DNA single-strand breaks—tail moment as a function of position in the cell-cycle. *Mut. Res.* **294,** 275–283.
19. Collins, A., Dušinská, M., Franklin, M., Somorovská, M., Petrovská, H., Duthie, S., Fillion, L., Panayiotidis, M., Rašlová, K. and Vaughan, N. (1997) Comet assay in human biomonitoring studies: reliability, validation, and applications. *Env. Mol. Mutagenesis* **30,** 139–146.
20. Somorovská, M., Szabová, E., Vodička, P., Tulinská, J., Barancoková, M., Fábry, R., Líšková, A., Riegerová, Z., Petrovská, H., Kubová, J., Rausová, K., Dušinská, M. and Collins, A. (1999) Biomonitoring of genotoxic risk in workers in a rubber factory: comparison of the Comet assay with cytogenetic methods and immunology. *Mut. Res.* **445,** 181–192.
21. Collins, A. R., Rašlová, K., Somorovská, M., Petrovská, H., Ondrušová, A., Vohnout, B., Fábry, R. and Dušinská, M. (1998) DNA damage in diabetes: correlation with a clinical marker. *Free Radical Biol. Med.* **25,** 373–377.
22. Betti, C., Davini, T., Giannessi, L., Loprieno, N. and Barale, R. (1994) Microgel electrophoresis assay (comet test) and SCE analysis in human lymphocytes from 100 normal subjects. *Mut. Res.* **307,** 323–333.
23. Jenkinson, A. M., Collins, A. R., Duthie, S. J., Wahle, K. W. J. and Duthie, G. G. (1999) The effect of increased intakes of polyunsaturated fatty acids and vitamin E on DNA damage in human lymphocytes. *FASEB J.* **13,** 2138–2142.
24. Pool-Zobel, B. L., Bub, A., Muller, H., Wollowski, I. and Rechkemmer, G. (1997) Consumption of vegetables reduces genetic damage in humans: first results of a human intervention trial with carotenoid-rich foods. *Carcinogenesis* **18,** 1847–1850.
25. Duthie, S. J., Ma, A., Ross, M. A. and Collins, A. R. (1996) Antioxidant supplementation decreases oxidative DNA damage in human lymphocytes. *Cancer Res.* **56,** 1291–1295.
26. Novotná, B. (2000) Increased DNA fragmentation detected by comet assay in peripheral blood of heterozygotes for a frameshift mutation in the DNA repair protein nibrin. *DNA Repair Workshop, Smolenice, Slovakia, October 2000, Abstracts* p.33.
27. Collins, A., Cadet, J., Epe, B. and Gedik, C. (1997) Problems in the measurement of 8-oxoguanine in human DNA. Report of a workshop, DNA Oxidation, held in Aberdeen, UK, 19–21 January, 1997. *Carcinogenesis* **18,** 1833–1836.
28. Collins, A. R., Dušinská, M., Horváthová, E., Munro, E., Savio, M. and Štětina, R. (2001) Inter-individual differences in repair of base oxidation, measured in vitro with the comet assay. *Mutagenesis* **16,** 297–301.

14

The Comet Assay

An Overview of Techniques

Peggy L. Olive

1. Introduction

The comet assay is a gel electrophoresis method that is used to visualize and measure DNA strand breaks in individual cells using microscopy. In its simplest form, cells are embedded in agarose on a microscope slide, immersed in a lysis solution to remove lipids and proteins, and exposed to a weak electric field to attract broken, negatively-charged DNA towards the anode. After electrophoresis, DNA is stained using a fluorescent dye, and viewed using a fluorescence microscope. Individual images can then be digitized and analyzed for informative properties such as the distance the DNA has migrated and the percent of DNA that has migrated. These features give an indication of the number of strand breaks present in the cell.

The original method described by Ostling and Johanson ***(1)*** has been modified in several significant ways to improve reproducibility and sensitivity, and to provide objective ways of measuring DNA damage ***(2)***. Different approaches have been devised to expand the range of DNA damage types that can be detected with this technique (**Fig. 1**). In addition to DNA single-strand breaks, the comet assay can be used to measure DNA double-strand breaks, damage to DNA bases, DNA inter-strand crosslinks, and apoptotic fragments (for reviews see ***(3–6)***). Use of antibodies to detect DNA adducts ***(7,8)*** or fluorescence *in situ* hybridization to label specific DNA sequences ***(9,10)*** extend the applications even further.

The popularity of the method is largely due to its ability to measure DNA damage in virtually any population of monodispersed cells. A drop of blood, an early embryo ***(11)*** or a fine needle aspirate biopsy of a tumor ***(12)*** provide

From: *Methods in Molecular Biology, vol. 203:* In Situ *Detection of DNA Damage: Methods and Protocols*
Edited by: V. V. Didenko

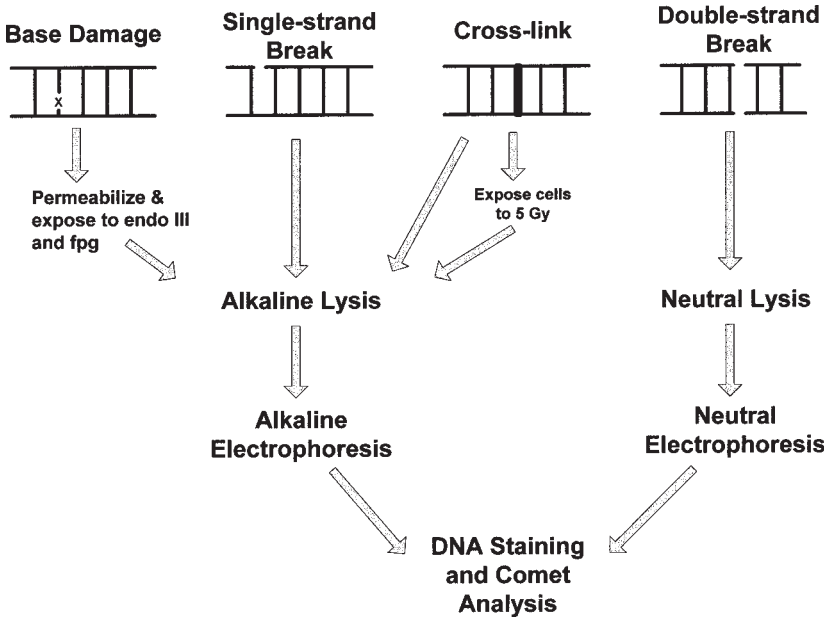

Fig. 1. Indication of the types of DNA damage (and their repair) that can be detected using various adaptations of the comet assay.

enough cells for analysis. A unique feature of this method is that it describes the response of individual cells, so that information can be obtained on heterogeneity in DNA damage or repair within a population of cells. Subpopulations that respond differently to treatment can then be identified. Examples from our work are cells in different phases of the cell cycle ***(13)***, cells with different ploidy ***(14)***, cell populations with different abilities to activate a toxic drug ***(15)*** or cells that lack specific drug targets ***(16)***. **Fig. 2** illustrates heterogeneity in response using the alkaline method for 5 cells showing various degrees of DNA damage. Comet 4 shows the most damage with little DNA remaining in the comet head. This is the typical appearance for an apoptotic cell in this assay since most of the DNA is highly fragmented. Comets 1 and 3 show similar levels of damage, but more than comets 2 and 5. In fact, this population is a mixture of cells that had been exposed to either 2 Gy or 6 Gy X-rays.

Application of this single cell gel electrophoresis method in genetic toxicology has stimulated the need to standardize the procedures so that different laboratories can more easily intercompare their data. Standardized methods for lysis and electrophoresis are possible, and recommended procedures for comet preparation have been published ***(17,18)***. However, image analysis methods

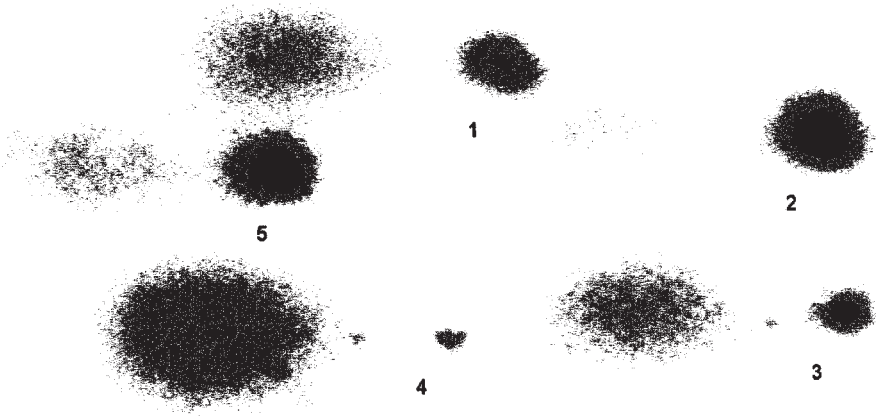

Fig. 2. Digitized comet images of TK6 human lymphoblast cells exposed to either 2 Gy or 6 Gy X-rays, mixed together, and analyzed using the alkaline comet assay. A single field (at higher density than normal) is shown. The field width is 370 microns. Individual comets are numbered clockwise, starting at the top.

vary considerably from one lab to another, and results with different systems have not been rigorously intercompared. Depending on the question or requirement, the relative importance of sensitivity, speed of analysis, automatic data collection, or ability to detect a wide spectrum of damage may influence the choice of image analysis system.

Fig. 3 is a computerized analysis cells exposed to ionizing radiation. Tissue from the mouse cerebrum was rinsed, dissected and finely chopped. Cells were filtered and centrifuged before exposure, on ice, to X-irradiation. Cells were then embedded in agarose, and slides were submersed in lysis solution. Average DNA content shows a small decline with radiation dose, as previously observed ***(19)***. This 30% drop in fluorescence is believed to be due to incomplete renaturation of the damaged DNA duplex, a conclusion supported by observations of DNA in solution, where calf thymus DNA denatured by heat, then renatured, shows a 50% drop in fluorescence ***(20)***. Two measures of DNA damage, mean tail moment and percent DNA in tail, increase in proportion to dose over this range (for these electrophoresis conditions), however, the signal to noise ratio is higher for tail moment than for percentage of DNA in tail. This is not surprising since tail moment includes a measure of both tail length and percentage of DNA in the tail. Tail length shows a plateau above about 2 Gy and is therefore a useful endpoint only for low damage levels. The plateau simply reflects the fact that maximum DNA migration distance is largely dependent on

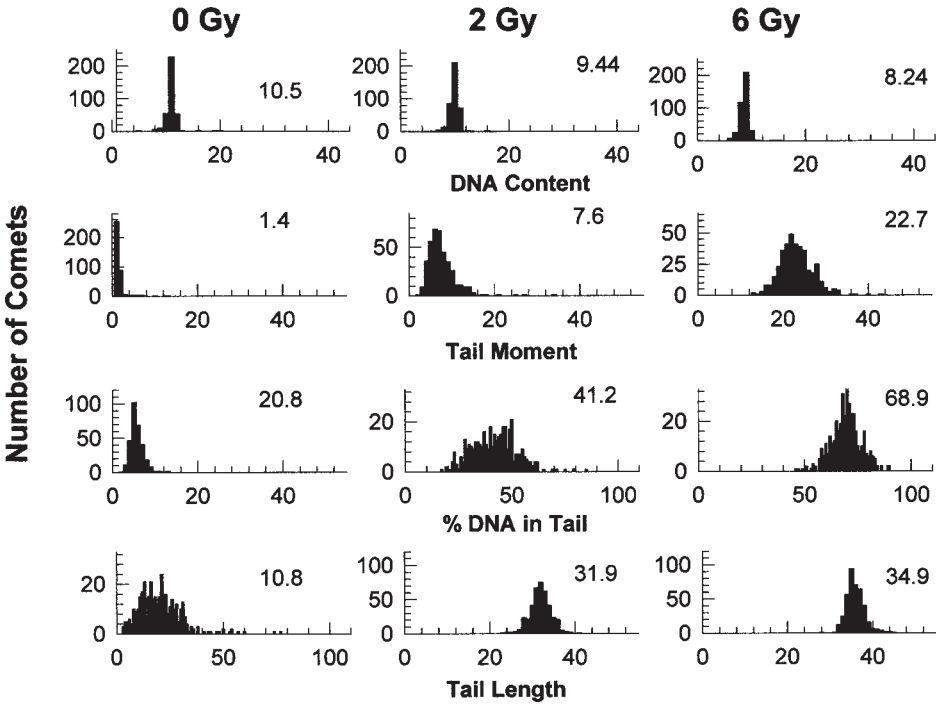

Fig. 3. Single cells were obtained from the cerebrum of a C3H mouse, then exposed to X-rays and examined for DNA damage using the alkaline comet assay using an overnight lysis. Approximately 400 images were analyzed for 4 comet features. A tail length of 40 using our software corresponds to a tail length of 160 microns. Exposure to 1 Gy X-rays produces about 1000 single-strand breaks per cell. Values in each panel are the mean values for the distributions.

electrophoresis voltage and time, not DNA size. Even small fragments in apoptotic cells migrate the same distance as much larger fragments in cells exposed to radiation doses that produce only 2000 breaks/cell (**Fig. 2**). All of the responses shown in Figure 3 are relatively homogeneous for X-irradiation, and can be adequately described by a normal distribution. Therefore mean values of each feature are good approximations of the overall response of these populations. However, when cells show a wide range in responses to a DNA damaging agent, the mean values become less reliable and less useful as descriptors of response. In this situation, information on the range of responses (e.g., variance divided by mean) is helpful, and analysis of tail moment histograms can be used to identify the percentage of cells that respond (or fail to respond) to a drug ***(21)***.

2. Materials

2.1. Single Cell Preparation

1. Approximately 10,000 single cells for each slide (trypan blue excluding cells are preferable).
2. Enzymes for tissue disaggregation: trypsin (1.5 mg/mL, Difco Laboratories, Detroit, MI), collagenase (0.25 mg/mL, Sigma C-9891) and DNAse (0.6 mg/mL, Sigma DN-25). Enzymes are prepared as individual frozen stocks in phosphate buffered saline (PBS) without calcium or magnesium, and thawed and mixed immediately before use.
3. Nylon mesh to filter cell suspensions (20–30 micron pore Nitex screening fabric) is obtained from B & SH Thompson, Toronto, ON, Canada, and is cut to fit 25 mm Gelman syringe-type filter holders (Fisher Scientific).

2.2. Microscope Slides

1. For alkaline lysis, single end frosted slides are appropriate for most applications.
2. For detection of double-strand breaks using high temperature lysis, fully frosted slides (Fisher Scientific) are generally necessary to keep the agarose firmly attached to the slide.
3. To reduce the possibility of detachment of the agarose during the procedure, slides are pre-coated with 50–100 µL liquid agarose and the agarose is allowed to dry to a thin film. For overnight lysis, scoring the edges of the pre-coated slide with a diamond-tipped pen provides even stronger attachment (*see* **Note 1**).

2.3. Agarose

1. Low gelling temperature agarose (e.g., Sigma type VII, Owl Scientific or equivalent).
2. Once dissolved, the agarose is kept in a water bath at 40°C, and it is made fresh daily.

2.4. Lysis Solutions

1. Lysis solution A for detection of single-strand breaks, crosslinks, and base damage: 1.2 *M* NaCl, 0.3 *M* NaOH, 0.1% sarkosyl and 100 m*M* Na_2EDTA (pH 13.3). This solution is freshly prepared for each experiment and equilibrated at ≈5°C in a refrigerator or cold room. Typical lysis chambers are 1.5 L Pyrex glass storage containers with fitted covers, and we use 200 mL of lysis solution for up to 10 slides.
2. Lysis solution B for detection of double-strand breaks: 30 m*M* Na_2EDTA and 0.5% SDS, pH 8.0. This solution can be kept for several weeks and stored at room temperature.
3. Lysis Solution C for permeabilizing cells before base damage detection with endonuclease III (endo III) and formamidopyrimidine glycosylase (fpg): 2.5 *M* NaCl, 10 m*M* Tris, 100 m*M* Na_2EDTA and 1% TX-100 (pH 10.0). This solution is freshly prepared for each experiment.

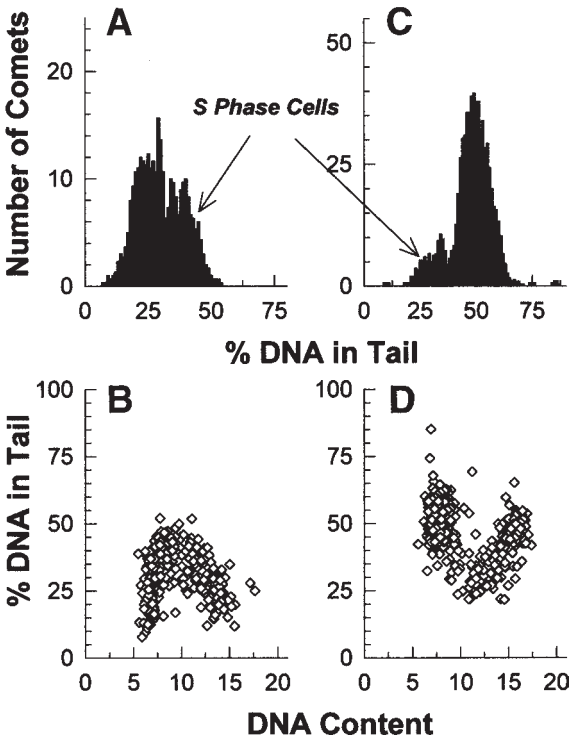

Fig. 4. Analysis of DNA damage in irradiated cells as a function of DNA content. The percentage of DNA in the tail was measured for V79 cells exposed to 1.5 Gy at 4°C, and analyzed for damage using the alkaline comet assay **(A,B)** or HT144 melanoma cells exposed to 25 Gy and analyzed using the neutral method **(C,D)**. Although X-rays produces the same amount of damage independent of DNA content, for technical reasons S phase cells appear to be more sensitive to damage using the alkaline method and less damage using the neutral method (*see* **Note 13**).

2.5. Electrophoresis Equipment and Solutions

1. A horizontal bed gel electrophoresis chamber with a power source that can supply a constant voltage (≈20 V for a large chamber). The size of chamber is not critical, with the obvious caveat that larger chambers accommodate more slides. The chamber bed should be level. If slides are pre-equilibrated in electrophoresis solution before transfer to the chamber containing fresh electrophoresis solution, a re-circulation pump is not necessary.
2. Electrophoresis solution A for alkaline assay: 0.03 *M* NaOH and 2 m*M* Na_2EDTA, pH 12.3, equilibrated at room temperature. Re-use of this solution beyond the day of preparation is not recommended, except to rinse and equilibrate slides before electrophoresis.

3. Electrophoresis solution B for neutral assay (TBE buffer): 90 m*M* Tris, 90 m*M* boric acid, 2 m*M* Na_2EDTA, pH 8.5. This buffer can be reused several times.

2.6. DNA Staining and Image Analysis

1. Propidium iodide (or ethidium bromide from Sigma Chemical Co., St. Louis MO) dissolved in 0.1 *M* NaCl at a concentration of 2.5 µg/mL. As this stain tends to bind to the glass container, it should be made fresh daily. Propidium iodide is mutagenic and should be handled with caution. SYBR gold (Molecular Probes, Eugene, OR), a less mutagenic dye, can be diluted 1:10,000 in TBE. Silver staining kits for comet assay are available from R&D Systems (Minneapolis, MN).
2. Epifluorescence microscope equipped with 50–100 watt mercury arc lamp and power supply.
3. For propidium iodide-stained DNA, a green light (546 nm) fluorescent filter set including excitation, reflector and emission filters. SYBR gold shows an excitation peak at 488 nm (blue light), with an emission peak at 520 nm.
4. Depending on light intensity and camera sensitivity, a neutral density filter in the excitation path may also be necessary to minimize comet bleaching.
5. Good quality microscope objectives suitable for fluorescence images.
6. Black & white camera suitable for collecting comet images in "real time". This can be an image intensified camera or a high sensitivity integrating camera.
7. Software, preferably operating on the images in real time, not on stored images.

3. Methods

3.1. Single Cell Preparation

1. Prepare a single cell suspension. When using tissues from animals, chop the tissue (≈50 mg) with scalpels in a small amount of ice-cold solution of PBS containing 20 m*M* Na_2EDTA and 2% DMSO. At this point, tissue may also be digested by adding enzymes such as trypsin and collagenase, typically for 30 min at 37°C with agitation. Enzymes provide a higher cell recovery but the decision to use enzymes may depend on whether DNA repair during enzyme digestion could compromise results (*see* **Note 2**).
2. Filter the solution through 30 micron pore nylon mesh.
3. Centrifuge at 800 *g* and resuspend the single cells in PBS.
4. Count the cells using a Coulter counter or hemocytometer, and dilute accordingly in cold PBS (e.g., so that 0.4 mL contains 10,000 cells).
5. If the goal of the experiment is to determine whether DNA interstrand crosslinks are present, a sample of the cells can also be exposed, on ice, to X-rays to produce a known number of single-strand breaks (i.e., exposure to 5 Gy should produce approximately 5000 strand breaks/diploid cell). If many fewer X-ray strand breaks are observed than expected, this is taken as an indication of the presence of crosslinks that prevent DNA from unwinding.

3.2. Mixing Cells with Agarose

1. Prepare 1% low gelling temperature agarose in distilled water (*see* **Note 3**).
2. Mix 0.4 mL cell suspension with 1.2 mL agarose and rapidly pipette 1.2 mL onto the surface of the pre-coated slide (*see* **Note 4**).
3. Allow the agarose to gel for 3 minutes, either at room temperature or in a cold room. Consistency in technique is important.

3.3. Lysis for Detection of Single-Strand Breaks and Crosslinks

1. After gelling, submerse slides horizontally in a covered container with the alkaline lysis solution (*see* **Note 5**). Since fluorescent lights in combination with alkali treatment of DNA can create DNA breaks ***(22)***, it is important to protect slides from room light during alkaline lysis, rinse and electrophoresis.
2. After lysis at 5°C for 18–24 h, carefully submerse slides in rinse buffer (identical in composition to the electrophoresis buffer A).
3. Transfer slides to a second rinse container after 30 min. Discard rinse buffer after use.
4. After another 30 min rinse, transfer slides to the gel electrophoresis chamber that is pre-filled with the required amount of freshly made electrophoresis solution A.

3.4. Lysis for Detection of Double-Strand Breaks (see Note 6)

1. Place slides in lysis solution B that has been equilibrated in a 50°C incubator.
2. After lysis at 50°C for 4 h, remove slides to the room temperature rinse solution (identical to the electrophoresis solution B).
3. After 4 h or an overnight rinse, transfer slides to the gel electrophoresis chamber that is pre-filled with the required amount of electrophoresis solution B.

3.5. Lysis for Detection of Base Damage (see Note 7)

1. Mix single cells with low gelling temperature agarose dissolved in PBS to produce a final agarose concentration of 0.75%, and spread 150 µL on an agarose pre-coated microscope slide.
2. Cover slides with a coverslip and allow agarose to gel for approximately 3 min. at about 8°C.
3. In preparation for enzyme treatment, remove the coverslip and carefully submerse slides for 1 h in lysis buffer C at 4°C.
4. To rinse slides after permeabilization, carefully submerse slides 2–3 × for a total of 1 h in 10 m*M* Tris-HCl, pH 7.5, 1 m*M* Na_2EDTA and 100 m*M* KCl.
5. Incubate slides with 50 µL Tris buffer (for measurement of strand breaks only) or Tris buffer containing endonuclease III and formamidopyrimidine-DNA glycosylase (dilute enzyme to the appropriate concentration according to methods recommended by the supplier, or determine optimum concentration). Cover the enzyme solution with a coverslip and incubate samples for 20 min at 37°C.
6. After enzyme treatment, remove the coverslips and rinse slides briefly in 1 *M* KCl at room temperature.
7. Place slides in lysis buffer A for 45 min.
8. Place slides in electrophoresis buffer A for 45 min.

3.6. Electrophoresis and DNA Staining

1. Fill electrophoresis tank with a specified volume of electrophoresis buffer chosen so that the level of buffer is about 2–3 mm above the agarose on the slide.
2. Adjust voltage for 0.6 V/cm for 25 min (*see* **Note 8**). Between runs, the buffer in the electrophoresis chamber should be stirred to redistribute ions.
3. After electrophoresis, rinse slides by submersing in a large volume of distilled water or neutralizing solution.
4. Stain DNA by submersing slides in 2.5 µg/mL propidium iodide for 15–30 min (*see* **Note 9**).
5. Rinse slides briefly in distilled water, and place slides in a humidified, covered box and store in a cold room. Slides can also be dried for storage or transport (*see* **Note 10**).

3.7. Comet Analysis

1. Examine comet images with green light excitation if DNA is stained with propidium iodide or blue light excitation if stained with SYBR green.
2. The light intensity must be adjusted for even illumination across the field (*see* **Note 11**).
3. Collect and analyze comet images for several useful features (*see* **Note 12**). Remember that cells actively replicating their DNA show anomalous migration in agarose (*see* **Note 13** and **Fig. 4**)
4. Avoid analyzing images at edges of slides, overlapping images, debris and cell doublets. If using a visual scoring method, code the slides first so they can be read in a blinded fashion.

3.8. Statistical Analysis

1. When the average amount of DNA damage is required, determine the mean and standard deviation from 3 or more independent experiments. Generally 50 comets per point is adequate.
2. When heterogeneity within a sample is examined, the ratio of the mean/variance can be a useful measure of variability. Curve fitting programs can be used to define the proportion of cells that are sensitive or resistant to treatment. The goodness of fit will improve as more comets are collected, and analysis of 400–800 comets per slide is not atypical. A normal distribution of values about the mean(s) is assumed for each population ***(23)***. Alternatively, non-parametric methods may also be used.
3. ANOVA and paired t-tests can be used for data analysis. It is generally useful to have positive and negative controls.

4. Notes

1. One of the major complaints of those new to the method is that the agarose detaches from the slide at some point during the procedure. Precoating with agarose, scoring the edges of the slide, and maintaining the slides horizontally at all

times, prevents most problems. The use of GelBond polyester film (BioWhittaker Molecular Applications, Rockland, ME) greatly improves attachment of agarose. Since this material produces a high background when used with propidium iodide, SYBR green is a more appropriate stain with GelBond ***(24)***.

2. Preparation of a single cell suspension from tissues may introduce significant DNA damage, either by tissue mincing or enzyme digestion. Freezing/thawing procedures can also introduce breaks ***(25)*** and should be avoided if possible. Although trypan blue excluding cells are likely to show the lowest background damage, even membrane damaged cells or nuclei, if collected appropriately, may be adequate for many studies ***(26)***. If studying tissues, efforts should be made to remove as much blood as possible from a tissue, by draining, rinsing or perfusing the tissue before mincing. This is particularly important when a mechanical disaggregation method is used since white cells can constitute a variable but significant proportion of cells recovered from many tissues using this method. Cell sorting procedures or magnetic bead cell separation, based on antibody labeling of cell surface markers ***(27,28)***, may also be useful in removing "contaminating" white blood cells.
3. Careful preparation of the agarose, and adequate mixing with the cells are critical since small differences in the percentage of agarose can influence comet tail length. It is important to ensure that the agarose is completely dissolved. A microwave oven is used at low power to produce minimal bubbling and evaporation during the 1–2 min required to dissolve the agarose. The homogeneity of pore structure within the agarose is also dependent on the temperature during gelling ***(29)***. Therefore, this step should be performed in a way that can be reproduced easily (i.e., it is important to maintain a constant time and temperature of gelling before placing the slides in lysis solution).
4. The slide preparation method originally described by Singh et al. ***(30)*** uses 3 layers of agarose, generally no more than 250 µL in total. The first layer is used to precoat the slide to enhance attachment, the second layer contains the cells in 75 µL 0.5% LGT agarose, and the third layer of 1% agarose, also 75 µL, covers the second layer ***(30)***. The advantage is that all of the cells are in a thin layer protected by an overlay of agarose, and the overall thickness of the gel is small. The disadvantage is that preparing the slides is more time consuming and technically more difficult since coverslips must be placed and removed for each step. Although the method we describe is simpler, slides are covered by 1.2 mL agarose to avoid manually spreading the agarose, and this thicker gel may necessitate purchase of a long working distance objective for the microscope.
5. Many different alkaline lysis solutions have been described in the literature, often leading to some confusion about which method is best to use. All alkaline methods include NaOH (0.03–0.3 *M*) and NaCl (1–2.5 *M*), with or without Triton X-100, sodium sarcosine, Tris, EDTA, DMSO, and proteinase K. The addition of the radical scavenger, DMSO, is necessary when red blood cells are present since lysis of red cells in alkali appears to produce reactive species that damage neighboring nucleated cells. DMSO can be included in the agarose (2%) or lysis solu-

tion (up to 10%). Proteinase K added to the lysis solution (0.5–1 mg/mL) may reveal DNA-protein crosslinks for those chemicals where detergents and alkali are not adequate for this purpose. Since a higher pH lysis solution (> 13) has been found to be more sensitive for detecting DNA damage by many agents (some types of base damage are alkali-labile), our recommended general purpose alkaline lysis solution contains 0.3 *M* NaOH. A one hour lysis is probably adequate for most studies, however, the longer lysis at 5°C allows more time for DNA unwinding, and therefore increases sensitivity for detecting breaks (usually by a factor of 2 or so for lysis times greater than 6 h). An important point to appreciate is that once DNA is denatured in alkali, it should not be allowed to renature before electrophoresis. This leads to partial reannealing of the strands, probably causing tangling around agarose fibers and inability to migrate efficiently during subsequent electrophoresis.

6. Several extra steps are required for the measurement of oxidative base damage, as originally described by Collins et al. ***(31,32)***. Initial permeabilization, and treatment with enzymes requires extra care to avoid losing the gel during preparation and electrophoresis. Although endonuclease III is commercially available from Trevigen Inc. (Gaithersburg, MD), the efficiency of enzymes for this application needs to be high and may require independent purification ***(33,34)***. It is important to optimize the concentration of enzymes to obtain maximum numbers of breaks at sites of base damage. It should also be noted that the presence of large numbers of strand breaks can reduce sensitivity for detecting base damage by this method ***(31,35)***. The use of external references ***(31)***, or comparisons with HPCL using electrochemical detection ***(36)*** is required for accurate quantitation of lesions.
7. DNA double-strand breaks are produced much less frequently than single-strand breaks, and only by a few selected agents (e.g., ionizing radiation, topoisomerase inhibitors, bleomycin, carcinostatin). Most of these agents produce several times more single-strand breaks than double-strand breaks. When slides are first placed in the neutral lysis solution, single-strand breaks cause loss of DNA supercoiling. This allows DNA to relax and diffuse to a greater extent than if single-strand breaks were not present. The result is the presence of small tails on the comets which might be falsely attributed to double-strand breaks. Once all of the DNA supercoils have been relaxed (about 2000 single-strand breaks or 2 Gy will relax most supercoils), then only double-strand breaks will increase the amount of DNA able to migrate. Therefore the slope of the initial part of the dose response curve in the neutral assay is steep and should not be interpreted as a measure of double-strand break induction ***(37)***. In fact, Ostling and Johanson used a neutral lysis buffer to measure radiation-induced single-strand breaks, and this explains why their dose- response relationship appeared to plateau above 2 Gy ***(1)***. Neutral lysis and electrophoresis can also be used to detect apoptotic cells ***(38)*** and may be more appropriate than the alkali lysis methods especially if average DNA fragment size is small (< 50kb).
8. The choices of voltage and time of electrophoresis are largely arbitrary, and are chosen primarily to give an appropriate comet size for image analysis. A typical

voltage for an electrophoresis chamber is determined by measuring the perpendicular distance in cm between the positive and negative electrodes in the electrophoresis chamber, and multiplying this distance by 0.6. With this voltage, electrophoresis for 20–25 min provides a useful image.

9. The original paper describing the single cell gel electrophoresis method employed the DNA and RNA stain, acridine orange, that shows a high background fluorescence. Since then, a variety of DNA stains have been used including those commonly applied in flow cytometry, propidium iodide and ethidium bromide, which are economic to use and have a much lower background than acridine orange. YOYO-1 (Molecular Probes, Eugene, OR), another intercalating DNA dye, binds to DNA with higher efficiency but does not necessarily improve resolution ***(2)***. SYBR-green 1 and SYBR-gold (Molecular Probes) also have higher affinity for double-stranded DNA than propidium iodide ***(39)***. SYBR-gold shows a 1000 fold enhancement of fluorescence upon binding to DNA versus only 50 fold for propidium iodide. However these dyes are subject to photobleaching, as are the UV-excited DNA binding dyes, DAPI and Hoechst 33342. In our experience, we have not seen a significant improvement of any of the newer stains over propidium iodide using image analysis methods, although, in theory, a dye that binds with high efficiency to single-stranded DNA should increase sensitivity in the alkaline method. The use of silver staining ***(40)*** or other non-fluorescent methods for detecting DNA are also possible, although as with any stain, DNA binding should be confirmed to be stoichiometric if one wishes to measure tail moment or percent in tail ***(24)***. In other words, cells in G2 phase should bind twice as much stain as cells in G1 phase. Finally, alkali treatment degrades RNA so that it does not contribute to the staining intensity in the comet. For the neutral method, RNAse treatment of slides (40 µg/mL for 2 h) after electrophoresis and before PI staining did not change the dose-response relationship for ionizing radiation.
10. Slides can be dried after electrophoresis and staining, and viewed even months later ***(41)***. Before viewing, slides are re-hydrated in water, and we pipette up to 1 mL agarose onto the slide to reduce background fluorescence. Generally, only a small amount of comet shrinkage occurs, and the percentage of DNA in the comet tail remains fairly constant. Dipping slides in ethanol before drying will reduce the possibility of microbial contamination, but re-staining will be necessary. Drying agarose on fully frosted slides can lead to problems in measuring damage when comets dry partially in and out of the grooves on these slides.
11. The intensity and duration of illumination should not produce noticeable bleaching of the image. Therefore the camera should be sufficiently sensitive that a long integration time is not required. Alternatively an image intensified camera that allows real time image capture is appropriate. In either case, it is important that the image not be saturated, that is, that the intensity of fluorescence in any part of the image not exceed the dynamic range of the camera. For example, as one increases the camera gain or integrating time, the tail will appear more substantial, but at some point, the intensity in the head will saturate, and measuring

an accurate tail moment or percent DNA in tail will no longer be possible. [Notes provided for NIH image software for comet analysis recommend saturating the nucleus, but this means that total DNA and tail moment cannot be accurately described.] Once a camera gain has been chosen, it should be kept constant for that experiment. Many comet image analysis programs are commercially available, and often the camera, computer and software can be purchased as a package. Given the issues described above, it is highly recommended that the camera/software "linearity" be experimentally verified for the standard measurement conditions. For example, one should not observe a decrease in DNA content as DNA damage increases, except in the extreme situation of an apoptotic or necrotic cell.

12. Useful features of the comet image include the total image intensity (DNA content), comet length or tail length, head diameter/tail length, percentage of DNA in the comet tail, and tail moment ***(42)***. We define tail moment as percentage of DNA in the tail multiplied by the distance between the means of the head and tail distributions. The length of the comet image or comet tail is a function of electrophoresis voltage and time. However, as more DNA enters the tail, average tail length will increase until it eventually plateaus for cells with more than about 2000 breaks. Actually, maximum tail length is relatively invariant for a specific voltage/time of electrophoresis, and it is the increase in amount of DNA in the tail makes the tail length appear, to the camera, to gradually increase with damage. Therefore tail length is a qualitative indicator of damage at low damage levels only, and tail length measurements are highly dependent on the image analysis system. In contrast, the percentage of DNA in the tail is a robust endpoint, much less dependent on electrophoresis voltage or time and therefore easier to compare between different laboratories. However, this endpoint is less sensitive for detecting changes at low damage levels because it does not take into account the distribution of DNA damage in the tail. In Figure 3, the percentage DNA in tail increases only 2 fold over the range of 0–2 Gy, but tail length increases 3 fold, and tail moment increases more than 5 fold over the same range (because it is a measure of both length and percentage in tail). In addition to the commercial and "home-built" image analysis systems for comet analysis, captured comet images can also be analyzed with NIH image software by using a macro program available on the Internet ***(43)***. However, speed of analysis becomes a limitation if images must be saved and then recalled for analysis by a different program. Systems that allow rapid on-screen image analysis make it possible to identify and analyze 600 or more comets per hour. A visual scoring system is also acceptable in some instances, but coded slides should be used to avoid bias. Pooling results from separate experiments to generate DNA damage histograms is generally not recommended since outliers may come from a single experiment.
13. Cells in S phase contain replication bubbles and forks that respond differently than non-replicating DNA during gel electrophoresis (**Fig. 4**). Under alkaline conditions, replication forks act as single-strand breaks, and denature and unwind. This promotes migration so that untreated S phase DNA can display the

equivalent of up to 2000 single-strand breaks ***(13)***. Therefore, under alkaline conditions, S phase cells are most easily identified in populations with minimal damage. Conversely, when lysis and electrophoresis occur under neutral conditions, the replication bubbles *inhibit* DNA migration, and S phase DNA migrates 2–3 times more slowly ***(44)***. Therefore, for comparison of DNA damage between different samples containing S phase cells, it is important to ensure that the S phase fraction is constant, or to adjust for these differences (e.g., by omitting S phase cells from analysis or using synchronous cells).

References

1. Ostling, O. and Johanson, K. J. (1984) Microelectrophoretic study of radiation-induced DNA damages in individual mammalian cells. *Biochem. Biophys. Res. Commun.* **123,** 291–298.
2. Singh, N. P., Stephens, R. E., and Schneider, E. L. (1994) Modifications of alkaline microgel electrophoresis for sensitive detection of DNA damage. *Int. J. Radiat. Biol.* **66,** 23–28.
3. Fairbairn, D. W., Olive, P. L., and O'Neill, K. L. (1995) The comet assay: A comprehensive review. *Mutat. Res.* **339,** 37–59.
4. McKelvey-Martin, V. J., Green, M. H., Schmezer, P., Pool-Zobel, B. L., De Meo, M. P., and Collins, A. (1993) The single cell gel electrophoresis assay (comet assay): a European review. *Mutat. Res.* **288,** 47–63.
5. Tice, R. R. and Strauss, G. H. (1995) The single cell gel electrophoresis/comet assay: a potential tool for detecting radiation-induced DNA damage in humans. *Stem Cells* **13,** 207–214.
6. Olive P. L. (1999) DNA damage and repair in individual cells: applications of the comet assay in radiobiology. *Int. J. Radiat. Biol.* **75,** 395–405.
7. Sauvaigo, S., Serres, C., Signorini, N., Emonet, N., Richard, M. J., and Cadet, J. (1998) Use of the single-cell gel electrophoresis assay for the immunofluorescent detection of specific DNA damage. *Anal. Biochem.* **259,** 1–7.
8. Olive, P. L. and Banáth, J. P. (1992) Growth fraction measured using the comet assay. *Cell Prolif.* **25,** 447–457.
9. McKelvey-Martin, V. J., Ho, E. T., McKeown, S. R., Johnston, S. R., McCarthy, P. J., Rajab, N. F., and Downes, C. S. (1998) Emerging applications of the single cell gel electrophoresis (Comet) assay. I. Management of invasive transitional cell human bladder carcinoma. II. Fluorescent in situ hybridization Comets for the identification of damaged and repaired DNA sequences in individual cells. *Mutagenesis* **13,** 1–8.
10. Santos, S. J., Singh, N. P., and Natarajan, A. T. (1997) Fluorescence in situ hybridization with comets. *Exp. Cell Res.* **232,** 407–411.
11. Takahashi, M., Saka, N., Takahashi, H., Kanai, Y., Schultz, R. M., and Okano, A. (1999) Assessment of DNA damage in individual hamster embryos by comet assay. *Mol. Reprod. Dev.* **54,** 1–7.
12. Olive, P. L., Trotter, T., Banáth, J. P., Jackson, S. M., and Le Riche, J. (1996) Heterogeneity in human tumour hypoxic fraction using the comet assay. *Br. J. Cancer* **74,** S191–S195

13. Olive, P. L. and Banáth, J. P. (1993) Induction and rejoining of radiation-induced DNA single-strand breaks: "tail moment" as a function of position in the cell cycle. *Mutat. Res.* **294,** 275–283.
14. Zheng, H. and Olive, P. L. (1997) Influence of oxygen on radiation-induced DNA damage in testicular cells of C3H mice. *Int. J. Radiat. Biol.* **71,** 275–282.
15. Olive, P. L. (1995) Use of the comet assay to detect hypoxic cells in murine tumours and normal tissues exposed to bioreductive drugs. *Acta Oncol.* **34,** 301–305.
16. Olive, P. L., Banáth, J. P., and Durand, R. E. (1990) Detection of etoposide resistance by measuring DNA damage in individual chinese hamster cells. *J. Natl. Cancer Inst.* **82,** 779–783.
17. Tice, R. R., Agurell, E., Anderson, D., Burlinson, B., Hartmann, A., Kobayashi, H., Miyamae, Y., Rojas, E., Ryu, J. C., and Sasaki, Y. F. (2000) Single cell gel/comet assay: guidelines for in vitro and in vivo genetic toxicology testing. *Environ. Mol. Mutagen* **35,** 206–221.
18. Albertini, R. J., Anderson, D., Douglas, G. R., Hagmar, L., Hemminki, K., Merlo, F., Natarajan, A. T., Norppa, H., Shuker, D. E., Tice, R., Waters, M. D., and Aitio, A. (2000) IPCS guidelines for the monitoring of genotoxic effects of carcinogens in humans. International Programme on Chemical Safety. *Mutat. Res.* **463,** 111–172.
19. Olive, P. L., Banáth, J. P., and Fjell, C. D. (1994) DNA strand breakage and DNA structure influence staining with propidium iodide using the alkaline comet assay. *Cytometry* **16,** 305–312.
20. LePecq, J. B. and Paoletti, C. (1967) A fluorescent complex between ethidium bromide and nucleic acids. Physical-chemical characterization. *J. Mol. Biol.* **27,** 87–106.
21. Olive, P. L., Banáth, J. P., and Durand, R. E. (1997) Detection of subpopulations resistant to DNA-damaging agents in spheroids and murine tumours. *Mutat. Res.* **375,** 157–165.
22. Bradley, M. O., Erickson, L. C., and Kohn, K. W. (1978) Non-enzymatic DNA strand breaks induced in mammalian cells by fluorescent light. *Biochim. Biophys. Acta* **520,** 11–20.
23. Olive, P. L., Durand, R. E., LeRiche, J. C., Olivotto, I. A., and Jackson, S. M. (1993) Gel electrophoresis of individual cells to quantify hypoxic fraction in human breast cancers. *Cancer Res.* **53,** 733–736.
24. McNamee, J. P., McLean, J. R., Ferrarotto, C. L., and Bellier, P. V. (2000) Comet assay: rapid processing of multiple samples. *Mutat. Res.* **466,** 63–69.
25. Fairbairn, D. W., Reyes, W. A., Van Grigsby, R., and O'Neill, K. L. (1994) Laser scanning microscopic analysis of DNA damage in frozen tissues. *Cancer Lett.* **76,** 127–132.
26. Singh, N. P. (1998) A rapid method for the preparation of single-cell suspensions from solid tissues. *Cytometry* **31,** 229–232.
27. Vijayalaxmi, Strauss, G. H., and Tice, R. R. (1993) An analysis of gamma-ray-induced DNA damage in human blood leukocytes, lymphocytes and granulocytes. *Mutat. Res.* **292,** 123–128.
28. Myllyperkio, M. H. and Vilpo, J. A. (1999) Increased DNA single-strand break joining activity in UV-irradiated CD34+ versus CD34– bone marrow cells. *Mutat. Res.* **425,** 169–176.

29. Kusukawa, N., Ostrovsky, M. V., and Garner, M. M. (1999) Effect of gelation conditions on the gel structure and resolving power of agarose-based DNA sequencing gels. *Electrophoresis* **20,** 1455–1461.
30. Singh, N. P., McCoy, M. T., Tice, R. R., and Schneider, E. L. (1988) A simple technique for quantitation of low levels of DNA damage in individual cells. *Exp. Cell Res.* **175,** 184–191.
31. Collins, A. R., Dusinska, M., Gedik, C. M., and Stetina, R. (1996) Oxidative damage to DNA: do we have a reliable biomarker? *Environ. Health Perspect.* **104 Suppl 3,** 465–469.
32. Collins, A. R., Duthie, S. J., and Dobson, V. L. (1993) Direct enzymic detection of endogenous oxidative base damage in human lymphocyte DNA. *Carcinogen.* **14,** 1733–1735.
33. Boiteux, S., O'Connor, T. R., Lederer, F., Gouyette, A., and Laval, J. (1990) Homogeneous Escherichia coli FPG protein. A DNA glycosylase which excises imidazole ring-opened purines and nicks DNA at apurinic/apyrimidinic sites. *J. Biol. Chem.* **265,** 3916–3922.
34. Asahara, H., Wistort, P. M., Bank, J. F., Bakerian, R. H., and Cunningham, R. P. (1989) Purification and characterization of Escherichia coli endonuclease III from the cloned nth gene. *Biochemistry* **28,** 4444–4449.
35. Banath, J. P., Wallace, S. S., Thompson, J., and Olive, P. L. (1999) Radiation-induced DNA base damage detected in individual aerobic and hypoxic cells with endonuclease III and formamidopyrimidine-glycosylase. *Radiat. Res.* **151,** 550–558.
36. Pouget, J. P., Ravanat, J. L., Douki, T., Richard, M. J., and Cadet, J. (1999) Measurement of DNA base damage in cells exposed to low doses of gamma-radiation: comparison between the HPLC-EC and comet assays. *Int. J. Radiat. Biol.* **75,** 51–58.
37. Olive, P. L. and Johnston, P. J. (1997) DNA damage from oxidants: influence of lesion complexity and chromatin organization. *Oncol. Res.* **9,** 287–294.
38. Olive, P. L., Frazer, G., and Banáth, J. P. (1993) Radiation-induced apoptosis measured in TK6 human B lymphoblast cells using the comet assay. *Radiat. Res.* **136,** 130–136.
39. Ward, T. H. and Marples, B. (2000) Technical report: SYBR Green I and the improved sensitivity of the single-cell electrophoresis assay. *Int. J. Radiat. Biol.* **76,** 61–65.
40. Cerda, H., Delincee, H., Haine, H., and Rupp, H. (1997) The DNA 'comet assay' as a rapid screening technique to control irradiated food. *Mutat. Res.* **375,** 167–181.
41. Woods, J. A., O'Leary, K. A., McCarthy, R. P., and O'Brien, N. M. (1999) Preservation of comet assay slides: comparison with fresh slides. *Mutat. Res.* **429,** 181–187.
42. Olive, P. L., Banáth, J. P., and Durand, R. E. (1990) Heterogeneity in radiation-induced DNA damage and repair in tumor and normal cells measured using the "comet" assay. *Radiat. Res.* **122,** 86–94.
43. Helma, C. and Uhl, M. (2000) A public domain image-analysis program for the single-cell gel-electrophoresis (comet) assay. *Mutat. Res.* **466,** 9–15.
44. Olive, P. L. and Banáth, J. P. (1993) Detection of DNA double-strand breaks through the cell cycle after exposure to X-rays, bleomycin, etoposide and 125IdUrd. *Int. J. Radiat. Biol.* **64,** 349–358.

15

Ultrasensitive Detection of DNA Damage by the Combination of the Comet and TUNEL Assays

Andrei L. Kindzelskii and Howard R. Petty

1. Introduction

The assessment of cellular DNA damage is crucial in many areas of biology including immunology, developmental biology, aging, cancer, and environmental science. A variety of experimental techniques including alkaline sucrose gradient centrifugation, alkaline elution, nucleoid sedimentation, viscoelastic measurements of DNA, alkaline unwinding, and gel electrophoresis ***(1–4)*** have been developed to detect DNA damage in large cell populations. However, these methods can only detect the average amount of DNA damage over millions of cells. These approaches do not reveal the heterogeneity of DNA damage within a sample; some cells may experience extensive damage whereas others may display no damage at all. Moreover, one might want to analyze the amount of DNA damage in variety of cell subpopulations within a sample. In more specialized applications (e.g., a specific target cell undergoing immunologic recognition and destruction) the extent of DNA damage in a particular cell may be required. Furthermore, there are some clinical experiments where the amount of sample is severely limited (e.g., biopsy material) and therefore large-scale assays are impossible. Thus, there are many biological circumstances that require the use of small cell samples. To extract DNA damage information from these samples, techniques that rely upon the evaluation of DNA damage at the level of single cells is required. The single cell gel electrophoresis (SCGE) or "comet" assay is the most widely applied method for the detection of DNA damage in single cells. In this approach damaged DNA in individual cells is electrophoresed away from a nucleus into an agarose gel followed by staining.

From: *Methods in Molecular Biology, vol. 203:* In Situ *Detection of DNA Damage: Methods and Protocols*
Edited by: V. V. Didenko

1.1. Overview of Microscopic Methods and Strategies to Detect DNA Damage

The analysis of DNA damage in single cells was first reported in the studies of Rydberg and Johanson *(5)*. In this technique DNA damage was detected by: 1) lysing cells embedded in agarose on slides, 2) promoting partial DNA unwinding, and 3) staining DNA with a dye. This method was improved by the subsequent addition of an in situ agarose gel electrophoresis step *(6)* to allow easier discrimination between damaged and undamaged DNA. This approach was further refined by Singh et al. *(7)* who included exposure to alkaline/high salt conditions, which allowed a direct correlation between electrophoretic migration distance and the extent of DNA damage. This comet assay is a convenient method for the visualization of DNA damage within single cells and is now widely employed *(8)*.

In addition to the SCGE assay, DNA strand breaks in single cells can also be detected by directly labeling the break using terminal deoxynucleotidyl transferase (TdT) and radioactive dAMP or biotin-dUTP *(9,10)*. Recently, a convenient protocol to directly tag 3'-hydroxyl groups of DNA has become available *(11,12)*. In this method, 3'-hydroxyl groups are labeled with biotinilated-dUTP or fluoresceinated-dUTP via TdT. The tagged 3'-hydroxyl is then visualized by standard fluorescence techniques. This procedure, termed TdT-mediated fluorescein-dUTP nick end labeling (TUNEL) is now widely employed to detect DNA fragmentation *(13)*.

In this chapter we discuss modifications of the SCGE assay to increase the microscopic contrast of damaged DNA and, hence, its sensitivity. Two approaches are employed: 1) the use of TdT-mediated fluorescein-dUTP nick end labeling and 2) optical occultation of the nucleus or "comet head" to improve the sensitivity of the SCGE assay. By specifically labeling 3'-hydroxyls of strand breaks in the comet tail, the contrast is improved in comparison to less specific intercalating dyes relative to the background. Moreover, the contrast of the tail is improved by passing an opaque disk into a field-conjugated plane near the lamp. By occluding a comet's head, the tail appears brighter since the ICCD (intensified charge-coupled device) camera can operate at maximal gain. This latter approach is somewhat analogous to other optical methods wherein the sun's disk is occluded to image its corona. These modifications of the comet assay are reported below.

2. Materials

1. Hanks Balanced Salt Solution (HBSS) is obtained from BRL-Gibco (Grand Island, NY).
2. Lysing Solution: Ingredients per 1000 mL: 2.5 *M* NaCl—146.1 g, 100 m*M* EDTA—37.2 g, 10 m*M* Trizma base—1.2 g. Add ingredients to about 700 mL dH_2O, and begin stirring the mixture. Add ~8 g NaOH pellets and allow the mix-

ture to dissolve (about 20 min). Adjust the pH to 10.0 using concentrated HCl or NaOH. Add dH_2O to 890 mL (the Triton X-100 and DMSO will increase the volume to the correct amount), store at room temperature.

3. Final lysing solution: Add fresh 1% Triton X-100 and 10% DMSO to the lysing solution above. This should be refrigerated for at least 30 min prior to slide addition (*see* **Note 1**).
4. APO-DIRECT™ kit (PharMingen, San Diego, CA).
5. 0.5% agarose (normal melting temperature) from Sigma Chemical Co. (St. Louis, MO).
6. 0.5% low melting temperature agarose (Sigma Chemical Co., St. Louis, MO).
7. The staining solution is prepared from the APO-DIRECT™ kit as follows: 60 µL of reaction buffer, 4.5 µL of TdT enzyme solution, 48 µL of FITC-dUTP, and distilled water 192 µL (*see* **Note 2**).
8. 1% paraformaldehyde in PBS.
9. 70% ethanol.
10. Platinum electrodes (0.1–0.4 mm in diameter).
11. Fluorescence Microscope. Stained samples are examined using an axiovert fluorescence microscope (Carl Zeiss, New York, NY) with mercury illumination (HB0 100). A 100 W lamp is recommended since it produces four times the output of an HBO 50 lamp (*see* **Note 3**). Fluorescence emission is detected using a fluorescein filter set (*see* **Note 4**). Since the fluorescence intensities are low compared to a typical epi-fluorescence sample, sensitive detectors are required. An intensified charge-coupled device (ICCD) camera is required. Dage-MTI, Inc. (Michigan City, IN) and Hamamatsu Photonics, Inc. (Bridgewater, NJ) ICCD cameras can be used in this application. Images were captured using a Scion SG-7 video card (Vay-Tek, Fairfield, IA) and a Dell 410 workstation. Imaging was managed with ScionImage software and stored as TIFF files.
12. Nuclear Occlusion. To provide enhanced contrast of the comet tail, the "head" of the comet can be occluded. By occluding the head of the comet, the "tail" becomes the brightest object in the field of view. This allows the ICCD to operate at maximal gain; hence, the contrast with respect to the background and the number of grey levels of the tail are enhanced. For example, this strategy has been used to detect small amounts of cytoplasmic components leaking from bright tumor cell targets ***(14)***. To occlude the head of the comet, a special adapter for the fluorescence light source was obtained from Zeiss, Inc. A small opaque disk was cut from aluminum foil then attached to a glass slide. An aluminum slider to contain the glass slide and fit into the port of the Zeiss special adapter was constructed in the machine shop. A schematic illustration of the method is shown in **Fig. 1**. With the slider inserted into the field-conjugated plane in the adapter, a shadow in the shape of the disk appears over the sample. The position of the comet head can be adjusted by translation of the stage whereas the position of the shadow can be adjusted by the slider. **Fig. 2**, panels A and B, illustrate the microscopic appearance of a comet using the modified SCGE assay in the presence and absence of an optical occlusion of the comet head.

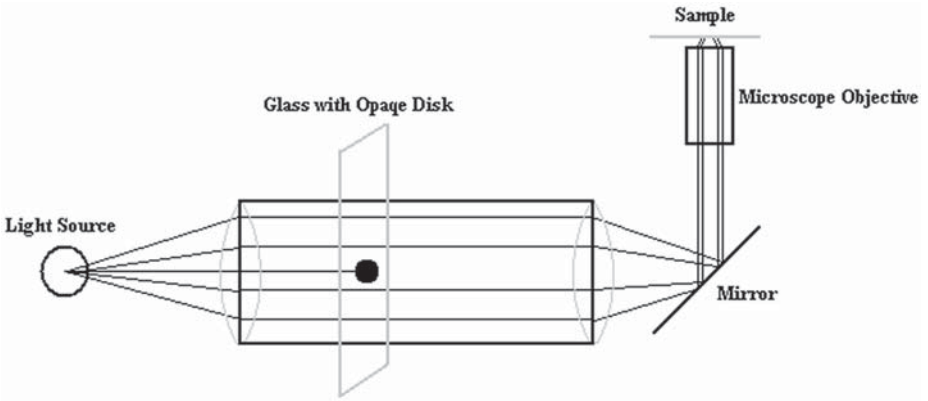

Fig. 1. Schematic illustration of the illumination system.

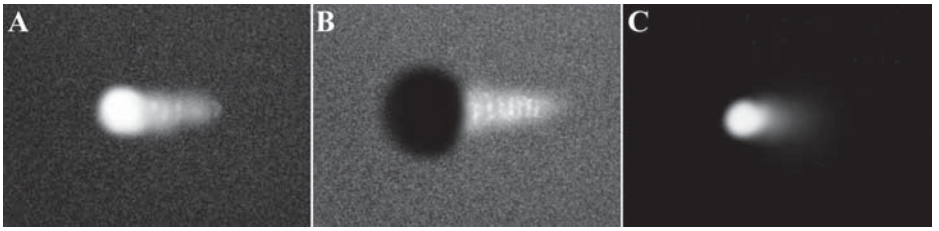

Fig. 2. Images of representative data. All cells were exposed to 30 μ*M* H_2O_2 for 60 min at room temperature. Panels **A** and **B** show the same cell without and with occultation of the comet head, respectively. Note that the detection of bands within the tail improves with occultation. Panel **C** shows a different cell using the conventional comet assay. (×890)

3. Methods

3.1. Modified SCGE Assay

1. Warm container with 0.5% agarose (normal melting temperature) to 50°C in a water bath.
2. Cover microscope slides with thin layer of warm 0.5% agarose (normal melting temperature).
3. Resuspend cells ($1.0–5.0 \times 10^3$) in 25 μL of 0.5% low melting temperature agarose at 37°C.
4. Place cell suspension (in low melting temperature agarose) atop the first (normal) agarose layer on the microscope slide.
5. Immediately cover this "sandwich" with a No. 1 coverglass.
6. Cool to 4°C to promote agarose solidification.

7. Prepare coverglass with thin layer of 0.5% agarose (low melting temperature) as described above (**Subheading 3.1**, **Steps 1–2**).
8. Carefully replace standard coverglass with the one covered with low melting temperature agarose.
9. Dip the "sandwich" into the alkaline lysing buffer for 1 h at 4°C.
10. Attach platinum electrodes (0.1–0.4 mm in diameter) to the microscope slide at opposite sides of the "sandwich."
11. Apply electric field (25V) for 20 min using Grass SD9 power supply unit.
12. Carefully remove coverslip and rinse cell layer with ice-cold 70% ethanol.
13. Rinse twice with of Wash Buffer (blue cap), provided in APO-DIRECT™ kit.
14. Incubate slides with 100 µL Staining Solution (**Subheading 2**, **Step 7**) for 60 min at 37°C.
15. Wash "sandwich" with Rinse Buffer (provided with kit, red cap) at room temperature.
16. Add 1 mL of PI/RNase A solution (amber bottle) to the top of the "sandwich" for 30 min at room temperature.
17. Cover "sandwich" with new coverslip.
18. Proceed with fluorescence microscopy.

3.2. Microscopy of DNA Damage

1. The samples are now placed in a fluorescence microscope, as described under **Subheading 2.3**. Optical filters appropriate for fluorescein are employed. If the sample is only labeled with FITC-dUTP, a long-pass emission filter will increase the intensity of the fluorescence emission. Since the comet tails can be rather long, observations are of fluorochrome-stained DNA are made using a 25× objective.
2. In some cases, observations are being made of a cell previously imaged in during the experiment (for example, given a specific treatment using a micropipette). To locate the same cell before and after staining for DNA damage, it is important to record the position of the cell(s) using the vernier calibration points for both the x and y axes of the microscope stage. It is also useful to record a "before" picture on the computer to assist in locating the "after" image of DNA damage.
3. In many cases, it will not be necessary to individually identify each cell. Thus, it is only important to obtain an appropriate statistical sample, which has been described for the conventional comet assay. In general, the comets of 25–50 cells should be evaluated in any particular experiment on every day. When evaluating microscope slides, it is important to avoid counting the same cell twice. Hence, do not retrace your steps in an experiment. These experiments can also be conducted "blind." That is, the person reading the comets does not know which particular experiment is currently being read.
4. To obtain the highest level of sensitivity, TUNEL labeling should be combined with occlusion of the nucleus, as described in **Subheading 2**, item 11. A comet is selected then centered in the field of view. The slider is then inserted into the back focal plane of the microscope. The slider and/or the x- and y-translation knobs are adjusted to occlude the image of the comet head. **Fig. 2A** and **B** show micrographs of the same comet in the absence and presence of the occultation

slider. As this illustrates, the comet tail is longer and its component bands are much better resolved in the presence of occultation. **Fig. 2C** shows a comet from a different cell treated in exactly the same way as the cell show in panel B.

3.3. Evaluation of DNA Damage

1. Several methods are available to evaluate the extent of DNA damage. One key variable used in most of these analyses is the length of the comets' tails, which is roughly proportional to the amount of DNA damage. This can be performed by manually measuring of the comet tail length. It may be performed on black and white prints or as displayed on video or computer screens. The general rule for the measurement is to find length between center of the comet head and the visible end of the "tail".
2. A second group includes automated methods of comet evaluation. This may be computer software or software/hardware systems.

4. Notes

1. The purpose of the DMSO in the lysing solution is to scavenge radicals generated by the iron released from hemoglobin when blood or animal tissues are used. It is not needed for other solutions or where the slides will be kept in lysing buffer for a brief time only.
2. The staining solution must be used within 24 h of preparation. Therefore, prepare only enough solution for use during a single day.
3. Carefully follow the manufacturer's guidelines. Never look directly at the high intensity source; its intensity and ultraviolet component can cause blindness. Similarly, always insure that the filters are in place before looking into the microscope.

   Carl Zeiss, Inc. now produces an adjustable HBO100 lamp, which is very stable. The ability to adjust its intensity is useful in prolonging the lifetime of the bulb and in preventing photobleaching of the sample.
4. We have found that the AF filter series available from Omega Optical offers superior performance in these experiments.

Acknowledgment

This research has been supported by NIH grant CA74120.

References

1. Freeman, S. E., Blackett, A. D., Monteleone, D. C., Setlow, R. B., Sutherland, B. M., and Sutherland, J. C. (1986) Quantitation of radiation, chemical-, or enzyme-induced single-strand breaks in nonradioactive DNA by alkaline gel electrophoresis: application to pyrimidine dimers. *Anal. Biochem.* **158,** 119–129.
2. Kohn, K. W., Erickson, L. C., Ewig, R. A., and Friedman, C. A. (1976) Fractionation of DNA from mammalian cells by alkaline elution. *Biochemistry* **15,** 4629–4637.
3. Lipetz, P. D., Brash, D. E., Joseph, L. B., Jewett, H. D., Lisle, D. R., Lantry, L. E., Hart, R. W., and Stephens, R. E. (1982) Determination of DNA superhelicity and

extremelly low levels of strand breaks in low numbers of nonradiolabeled cells by DNA-4',6-diamino-2-phenylindole fluorescence in nucleoid gradients. *Anal. Biochem.* **121,** 339–348.

4. Uhlenhopp, E. L. (1976) Viscoelastic analysis of high molecular weight, alkali-denatured DNA from mouse 3T3 cells. *Biophys. J.* **15,** 233–238.
5. Ryberg, B., and Johanson, K. J. (1978) Estimation of DNA strand breaks in single mammalian cells, in: *DNA Repair Mechanisms* (Hanawalt, P. C., Friedberg, E. C., and Fox, C. F., eds.) Academic Press, NY, pp. 465–468.
6. Osstling, O., and Johanson, K. J. (1984) Microelectrophoretic study of radiation-induced DNA damage in individual mammalian cells. *Biochem. Biophys. Res. Comm.* **123,** 291–298.
7. Singh, N. P., McCoy, M. T., Tice, R. R., and Schneider, E. L. (1988) A simple technique for quantitation of low levels of DNA damage in individual cells. *Exp. Cell Res.* **175,** 184–191.
8. McKelvey-Martin, V. J., Green, M. H. L., Schmezer, P., Pool-Zobel, B. L., De Meo, M. P., and Collins, A. (1993) The single cell electrophoresis assay (comet assay): A European review. *Mutation Res.* **288,** 47–63.
9. Modak, S. P., and Bollum, F. J. (1972) Detection and measurement of single-strand breaks in nuclear DNA in fixed lens sections. *Exp. Cell Res.* **75,** 307–313.
10. Dawson, B. A. and Lough, J. (1988) Immunocytochemical localization of transient DNA strand breaks in differentiating myotubes using in situ nick-translation. *Develop. Biol.* **127,** 362–367.
11. Li, X., Traganos, F., Melamed, M. R., and Darzynkiewicz, Z. (1995) Single-step procedure for labeling DNA strand breaks with fluorescein- or BODIPY-conjugated deoxynucleotides: Detection of apoptosis and bromodeoxyuridine incorporation. *Cytometry* **20,** 172–180.
12. Gavrieli, Y., Sherman, Y., and Ben-Sasson, S. A. (1992) Identification of programmed cell death in situ via specific labeling of nuclear DNA fragmentation. *J. Cell Biol.* **119,** 493–501.
13. Kindzelskii, A. L. and Petty, H. R. (1999) Ultrasensitive detection of hydrogen peroxide-mediated DNA damage after single cell gel electrophoresis using occultation microscopy and TUNEL labeling. *Mutation Res.* **426,** 11–22.
14. Kindzelskii, A. L. and Petty, H. R. (1999) Early membrane rupture events during neutrophil-mediated antibody-dependent tumor cell cytolysis. *J. Immunol.* **162,** 3188–3192.

16

Application of FISH to Detect DNA Damage

DNA Breakage Detection-FISH (DBD-FISH)

José Luis Fernández and Jaime Gosálvez

1. Introduction

Chromatin structure can affect the level of induced DNA damage and/or repair, and so these effects may vary within different DNA sequence areas of a cell, as well as between different cell types. DBD-FISH is a procedure that allows both intragenomic and intercellular heterogeneity in DNA breakage induction and repair to be assayed ***(1)***. Thus, besides whole cellular DNA, the behavior of different specific DNA sequence areas may be simultaneously analyzed within a specific cell. Cells contained within a very thin inert agarose layer on a glass slide are briefly incubated in an alkaline unwinding solution that transforms DNA breaks ***(2,3)*** into single-stranded DNA (ssDNA) motifs. These motifs are initiated from the end of the DNA breaks, serving as targets for hybridization of DNA probes. DNA melting is then stopped and proteins are removed with subsequent incubations in neutralizing and lysing solutions, to yield DNA in a residual nucleus-like structure, known as the nucleoid. After washing and dehydration in increasing ethanol baths, the microgel containing the nucleoids collapses and dries, thereby allowing DNA probes to be hybridized and detected, as in current FISH procedures ***(4)***. As DNA breaks increase within a specific nuclear target area, the alkali produces more ssDNA in the region and more DNA probe hybridizes, giving rise to a more intense and/or widely distributed FISH signal, which can be captured and quantified with a digital image analysis system. The specific DNA probe determines the chromatin area to be analyzed. In summary, DBD-FISH integrates the microgel techniques habitually employed in the "nuclear halo" ***(5,6)*** or "comet tail" tests

From: *Methods in Molecular Biology, vol. 203:* In Situ *Detection of DNA Damage: Methods and Protocols*
Edited by: V. V. Didenko

(7,8), the alkaline unwinding assays for the detection of DNA breaks currently used in radiobiological studies *(9,10)*, and FISH *(11)*.

2. Materials

2.1. Reagents and Technical Equipment

1. Normal melting point agarose.
2. Low melting point agarose.
3. Epifluorescence microscope with appropriate filters and objectives.
4. High-sensitivity CCD camera coupled to a computer.
5. Image analysis software (Visilog 5.1, Noesis Vision Inc., Ville St-Laurent, Quebec, Canada).

2.2. Solutions

2.2.1. Slide Preparation

1. Alkaline unwinding solution: 0.03 *M* NaOH, 1 *M* NaCl, pH 12.2. Make fresh and keep cold at 4°C. It is used at 7°C.
2. Neutralizing and lysing solution 1: 0.4 *M* Tris-HCl, 0.8 *M* DTT, 1% SDS, 0.05 *M* EDTA, pH 7.5. Store at 4°C and use at room temperature in a hood. DTT is an irritant, with an unpleasant odor and is neurotoxic. SDS is an irritant and is harmful if swallowed.
3. Neutralizing and lysing solution 2: 0.4 *M* Tris-HCl, 2 *M* NaCl, 1% SDS. Store at 4°C and use at room temperature.
4. Neutralizing solution: 0.4 *M* Tris-HCl, pH 7.5. Store at 4°C and use at room temperature.
5. Isotonic saline solution: 0.9% NaCl. Store at 4°C.
6. TBE buffer: 0.09 *M* Tris-borate, 0.002 *M* EDTA, pH 7.5. Store at room temperature.

Wear gloves and mask when preparing and using these solutions.

2.2.2. FISH

1. DNA probes for FISH directly labeled with fluorochromes or with hapten (e.g., biotin or digoxigenin).

   An increasing variety of human DNA probes are available from, for example, Serologicals Corp. (formerly Intergen) Gaithersburg, MD; Vysis Inc., Downer's Grove, IL; Roche Molecular Biochemicals, Indianapolis, IN. They include whole genome probes, chromosome-specific classical satellite DNA probes, chromosome-specific alphoid and pancentromeric DNA probes, chromosome specific "painting" probes, cosmid or YAC probes, telomeric probes, and oligonucleotide probes. All are supplied with their specific hybridization buffer. Suppliers provide information on preparation, incubation, washing and detection conditions.

   A small number of examples of human DNA probes in hybridization buffer are presented (**Figs. 1** and **2**):

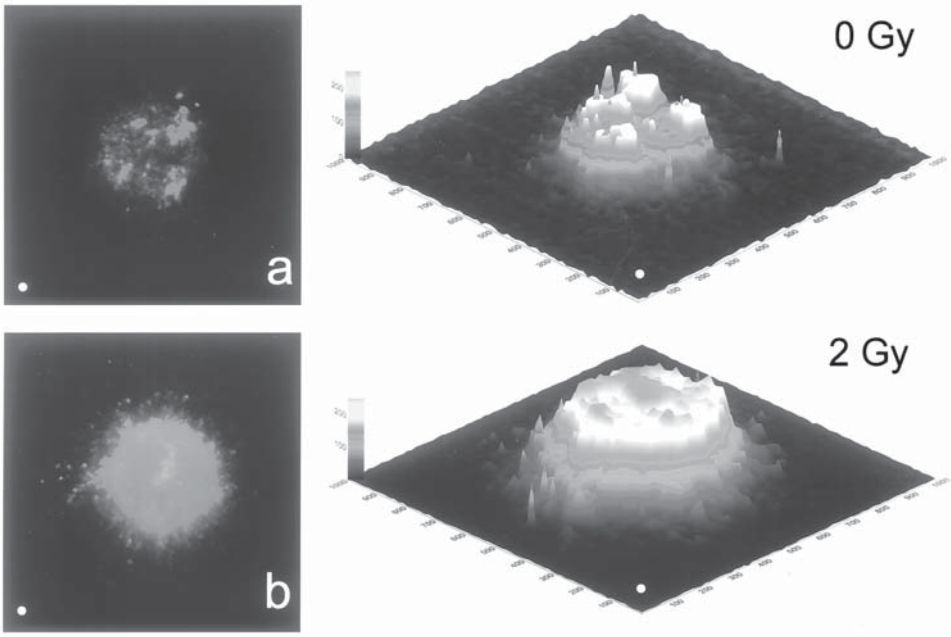

Fig. 1. Human blood leukocytes processed for DBD-FISH. Cells were first lysed and then exposed to the alkaline unwinding solution for 2.5 min at 7°C. **(A)** Unirradiated cell. **(B)** Leukocyte exposed to 2Gy of X-rays. A pseudo-3D representation of the fluorescence intensity of each pixel, following a color code, is presented alongside the original image.

- Chromosome-specific classical or alpha satellite DNA probes (0.5 ng/µL final concentration) in 65% formamide/2×SSC, 10% dextran sulfate, 100 m*M* calcium phosphate, pH 7.0 (1×SSC is 0.015 *M* NaCitrate, 0.15 *M* NaCl, pH 7.0).
- Whole genome (4.3 ng/µL final concentration), or Pancentromeric: all alphoids (0.5 ng/µL final concentration) DNA probes, in 50% formamide/2×SSC, 10% dextran sulfate, 100 m*M* calcium phosphate, pH 7.0.

Formamide is a potential carcinogen. It should be used in a deionized form.

2. DNA probe washing solutions. All should be freshly prepared and used at specific temperatures, depending on the stringency of the probe washings, as described in the methods (*see* **Subheading 3.2.2., Step 2**).
3. Blocking solution: 5% BSA, 4×SSC, 0.1% Triton X-100. Store in aliquots at –20°C.
4. Detection reagent, e.g. streptavidin-Cy3 (Sigma, St. Louis, MO) for biotin-labeled probes, freshly diluted (1:200) in antibody detection buffer (1% BSA, 4×SSC, 0.1% Triton X-100), and (if both biotin and digoxigenin labeled probes were incubated in the same slide)/or anti-digoxigenin-FITC (Roche Molecular Biochemicals, Indianapolis, IN) (1:100) in the same buffer. The antibody detection buffer is stored in aliquots at –20°C.

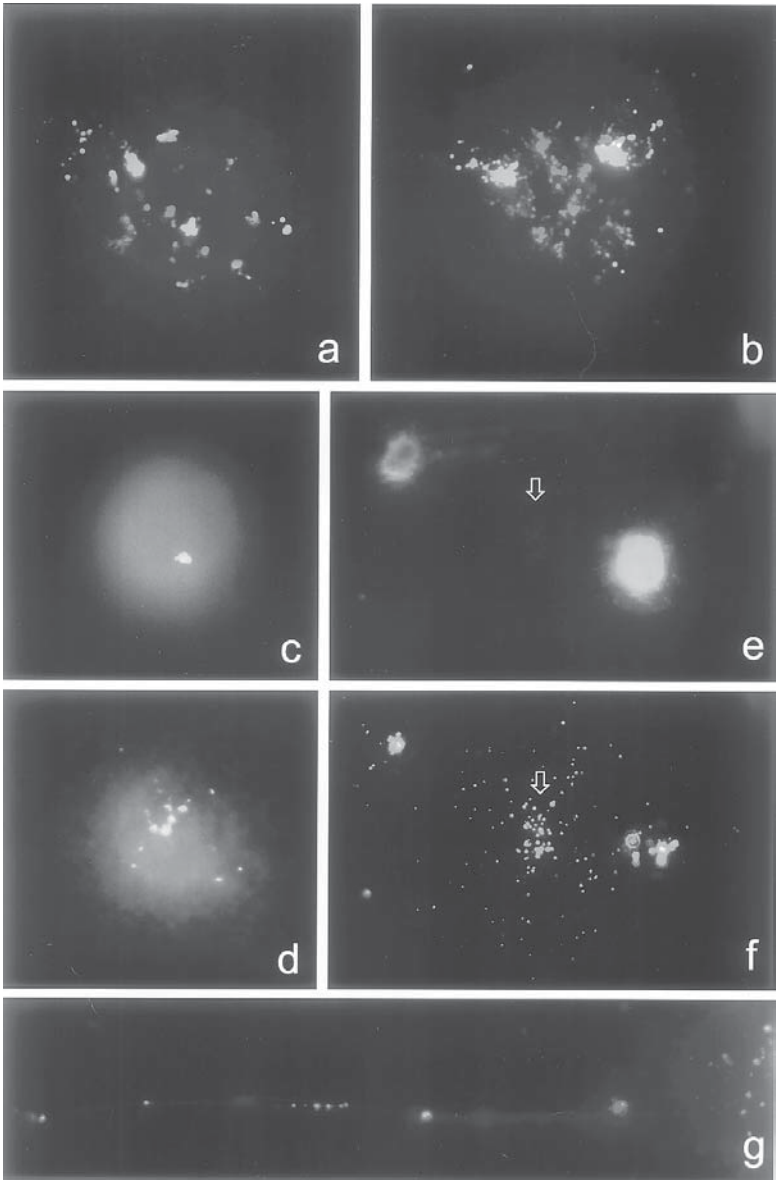

Fig. 2. Human blood leukocytes processed for DBD-FISH. **(A** and **B)** cells initially lysed and then exposed to the alkaline unwinding solution for 2.5 min at 7°C. **(A)** Untreated control. **(B)** Cell exposed to 2Gy of X-rays. A sequential hybridization of two different probes within each cell is shown. Cy3-red signal corresponds to a pancentromeric probe (all alphoid sequences), whereas FITC-green signal belongs to the 5bp classical satellite DNA of chromosome 1 (D1Z1 locus). DAPI counterstaining

5. Antibody washing solution: 4×SSC, 0.1% Triton X-100, pH 7.0. Store at 4°C.
6. Counterstaining-Antifading solution: DAPI (1 µg/mL) in Vectashield (Vector Laboratories, Burlingame, CA). Store at 4°C in the dark. DAPI is a potential carcinogen.

3. Methods

3.1. Slide Preparation

3.1.1. Coating of Slides

1. A coplin jar with 0.65% standard normal melting point agarose in water is kept in a water bath at 70°C after preheating in the microwave.
2. Standard glass microscope slides are immersed vertically for 2 sec and then immediately deposited horizontally on a cold metallic plate to solidify the agarose layer.
3. The slides are incubated at 80°C until the agarose layer is completely dry, giving rise to a thin film that is firmly attached to the slides. The coated slides can be used immediately or stored in a tightly closed box at room temperature for several months (*see* **Note 2**).

3.1.2. Microgel Embedding of Cell Suspension

1. 1% low melting point agarose in water is prepared by microwave heating and kept at 37°C within a glass tube, in a water bath.
2. Cells in suspension, like human leukocytes or isolated lymphocytes or granulocytes, in buffy coat, or cells in culture medium, are gently mixed using a micropipette with the low melting point agarose solution at 37°C, to arrive at a final concentration of 0.7%.

Fig. 2. *(continued)* is blue. Taking into account the relative size of target DNA, the background signal of D1Z1 is stronger than that of all alphoid sequences **(A)**. **(C** and **D)** Leukocytes unexposed **(C)** and irradiated with 10Gy of X-rays **(D)**, first treated with the alkaline unwinding solution for 5 min at 22°C, and then lysed. The specific alpha satellite DNA sequences of chromosome X (DXZ1 locus) are assayed. Under these conditions, a faint background signal **(C)** is detected in about 60% of cells, whereas all cells appear labeled after 10Gy **(D)**, showing highly dispersed spots. More restricted unwinding conditions reduce both the cells with background signal as well as the dispersed spots in the irradiated cells. **(E** and **F)** Apoptotic nucleus. DAPI fluorescence **(E)** shows very residual staining compared with the adjacent nucleus (arrow). Only fragments containing the specific 5bp classical satellite DNA sequences of chromosome 1 are detected after hybridization with the specific probe **(F)**. **(G)** An extended fiber shows the spot-like appearance of the DBD-FISH signals, in this case resulting from DNA breaks within the D1Z1 locus. Probably, these spots correspond to unwound ssDNA motifs that curl up and tangle.

3. 50 µL of the cell-agarose suspension are pipetted onto the coated surface of a glass slide and covered with a 24 × 60 mm glass cover slip, taking care to avoid trapping any bubbles.
4. The slide is cooled at 4°C for 5 min to allow the agarose to solidify.
5. Cell density can be checked by phase-contrast microscopy (*see* **Notes 3–6**).

3.1.3. Alkaline Unwinding

1. The alkaline unwinding solution is freshly prepared, kept at 4°C, and then transferred to a tray on ice, until the temperature stabilizes at 7°C.
2. The cover slip is removed and the slide immediately immersed horizontally in the tray with the alkaline unwinding solution for 2.5 min at 7°C. During this incubation, the tray is covered with a sheet of aluminum foil to avoid light-induced DNA damage ***(10)*** (*see* **Notes 7–9**).

3.1.4. Neutralization and Lysis

1. The slide is horizontally immersed in a tray with abundant neutralizing and lysing solution 1 at room temperature, and left for 20 min.
2. The slide is horizontally immersed in abundant neutralizing and lysing solution 2 at room temperature, for 10 min (*see* **Notes 10**, **11**).

3.1.5. Washing and Dehydration

1. The slide is removed and left horizontally on a box with abundant TBE buffer for 15 min at room temperature.
2. The slide is sequentially transferred to 70%, 90% and 100% ethanol baths, 2 min each, at room temperature.
3. After the 100% ethanol bath step, the slide is left to dry horizontally at room temperature or at 37°C for 10–15 min. This causes the agarose layer to flatten, turning into a very thin film with the nucleoids inside. After drying, the slides can be used immediately for hybridization or may be stored at room temperature in darkness for at least a month.

3.2. FISH

3.2.1. DNA Probe Hybridization

Denatured or single-stranded DNA probes, either directly labeled with fluorochromes or hapten-labeled, are incubated on dried slides. All types of probe are susceptible to being hybridized.

1. Double-stranded DNA probe is denatured at 70°C for 8 min in an Eppendorf tube, with its specific hybridization buffer, in a water bath, and is then immediately put on ice for 2–3 min.
2. 15 µL of probe solution are distributed on the slide from a pipette and are covered with a cover slip (10 × 60 mm). At least two probes or probe combinations may

be hybridized on the same slide, as long as their hybridization, incubation and washing conditions are the same.

3. The slide with the probe is incubated overnight, in darkness, in a moist chamber, lined with two sheets of wet filter paper. We incubate all probes at 37°C, except whole genome and telomeric probes, which are kept at room temperature (*see* **Note 12**).

3.2.2. DNA Probe Washings

1. The glass cover slip is removed by gently immersing the slides vertically in a coplin jar containing isotonic saline solution at room temperature.
2. Unbound DNA probe is washed out by incubation in coplin jars containing formamide/SSC solutions and then in SSC solutions, with gentle agitation, their stringency being that appropriate for the chosen probe.
   - Specific human alphoid satellite DNA probes: two washes in 60% formamide/2×SSC, pH 7, 42°C, 5 min each, followed by two washes in 2×SSC, pH 7, 37°C 3 min each.
   - Specific human classical satellite DNA probes: two washes in 50% formamide/2×SSC, pH 7, 42°C, 5 min each, followed by two washes in 2×SSC, pH 7, 37°C, 3 min each.
   - Human pancentromeric probe: two washes in 50% formamide/2×SSC, pH 7, 37°C, 5 min each followed by two washes in 2×SSC, pH 7, 37°C, 3 min each.
   - Whole genome probe: similar to the latter, but with all solutions at room temperature.
3. After probe washings, the slide is briefly transferred to a coplin jar containing antibody washing solution.
4. The slide is removed from the antibody washing solution and excess fluid is briefly blotted from the edge. Slides incubated with directly fluorescent-labeled probes are directly counterstained, whereas those with hapten-labeled probes are subjected to the detection steps (*see* **Notes 13–15**).

3.2.3. DNA Probe Detection

1. 90 µL of blocking solution are pipetted onto the slide and then covered with a plastic cover slip, incubating for 5 min at 37°C in a moist chamber.
2. The cover slip is carefully removed and the slide tilted briefly to allow excess fluid to drain.
3. 90 µL of detection reagent solution (streptavidin-Cy3 for biotin-labeled probes and/or anti-digoxigenin-FITC for digoxigenin-labeled probes) are applied to the slide, placing a plastic cover slip on top of the solution, and then incubated for 30 min in a humidified chamber at 37°C.
4. The cover slip is pulled off and the slides are gently agitated in three volumes of antibody washing solution at room temperature, 2 min each.
5. The slides are removed from the antibody washing solution and the excess fluid is blotted from the edge (*see* **Note 16**).

3.2.4. Nucleoid Counterstaining and Microscope Visualization

1. 20 μL of Counterstaining-Antifading solution is distributed from a pipette over the slide and covered with a 24 × 60 mm glass cover slip, avoiding trapping air bubbles.
2. DAPI-stained nucleoids are visualized under an epifluorescence microscope using 10×, 40× and 100× objectives and a specific "blue" fluorescence filter. DBD-FISH signal is observed under 40× or 100× objectives, but using the appropriate fluorescence filter for the fluorochrome ("red" filter for Cy3, "green" filter for FITC).

3.3. Image Capture

Fluorescent images are captured and digitized using a high-sensitivity CCD camera, such as the Ultrapix-1600 (Astrocam, Microphotonics Inc., Allentown, PA), which has a 1536 × 1024 pixel spatial resolution format and distinguishes more than 16000 grey level values.

1. Images are acquired using an intermediate resolution level (e.g. 3 × 3 binning factor).
2. The exposure time for image capture is determined by taking the highest and lowest signal intensities of the whole experiment into account. The highest signal intensity should be captured without grey level saturation within its field and the lowest signal intensity should be clearly discriminated. Always use the same objective (100×) and zoom magnification (1.5×) with the microscope. All subsequent images are taken at the same resolution level and exposure time.
3. Two calibration steps are necessary before fluorescent images can be captured:
   - A reference image from the current black level is obtained, corresponding to the electronic noise detected by the CCD camera under the specific conditions of image acquisition.
   - A flatfield image is captured from a dark area of the glass slide, without a FISH signal. This image must be acquired using the same filter, objective and magnification as are the DBD-FISH signals. It is a reference image of illumination variation within the visualization field in the sample due to the autofluorescence microscope optics, CCD sensitivity or external sources. Each glass slide should have its own flatfield image.
4. A sequence of 25–150 randomly selected images from DBD-FISH signals per experiment point is captured.
5. The black level and flatfield calibration images previously taken are subtracted from the images of the sequence, thus correcting them for background noise and illumination variation.
6. The sequence of images is saved in a file in the format of the camera (.apf).
7. A new sequence of images from a different experimental point is then captured, corrected for black level and flatfield images, saved, and so on.
8. Each sequence of images to be analyzed is exported from .apf into .img files (imager 2), in our case, since our digital image analysis system cannot operate

with the file type of the camera. The transformation does not modify the grey levels, and each image appears separately and numbered (*see* **Notes 17**, **18**).

3.4. Digital Image Analysis

The images captured with the CCD camera are analyzed using image analysis software. We have designed two semiautomatic routines that can run within an open system such as Visilog 5.1 (Noesis). One routine is dedicated to the analysis of the large extended DBD-FISH signals from the whole genome probe, while the other analyzes spot-like signals typical of those obtained with the rest of the probes. The main difference between the two routines is that the latter incorporates a "top-hat" transformation to highlight the spots.

The main steps in the digital image analysis are:

1. Selection of the area of interest within the whole image. This is usually a rectangle selected by the operator in the region containing the specific signal to be analyzed, and includes surrounding background fluorescence.
2. Thresholding to obtain a binary image. A fixed grey level of segmentation is chosen so the DBD-FISH signal is separated from the background. Higher grey levels correspond to DBD-FISH fluorescence, while lower grey levels correspond to background fluorescence.
3. The mean grey level from the background is automatically subtracted from the grey level corresponding to each pixel from the DBD-FISH signal.
4. Three main variables are measured for each DBD-FISH signal image, and are exported as .txt files to an Excel spreadsheet for statistical analysis.
   - Surface area (A): number of pixels. DNA breaks relax the DNA loops of the nucleoids, thus increasing the surface of the signal (**Fig. 1**, **Fig. 2A,B**; **C,D**).
   - Mean Fluorescence Intensity (MFI): average pixel grey level.
   - Whole Fluorescence Intensity (WFI= A × MFI): This is the sum of the grey levels from all pixels comprising the DBD-FISH signal. It should correspond to the entire quantity of hybridized probe, and therefore be the most informative variable in the analysis (**Fig. 1**).

   (*see* **Notes 19–21**).

4. Notes

1. Time considerations: DBD-FISH is a simple procedure. Slide preparation may take less than 1.5 h. DNA probes are incubated overnight and then washed in under 20 min. If probes are not directly fluorescent-labeled, detection is performed in around 45 min. A group of 50 images can be captured and stored in 10 or 20 min (assuming 0.5 s or 2 s camera exposure per image, respectively for Cy3 signals) and processed in 25 min, although this time may be shortened by the use of more powerful computers.
2. Slide preparation is carried out to promote the firm attachment of the low melting point agarose layer to the slide. In our experience, a layer of dried normal melting point agarose is simple and rapid, avoiding the loss of the low melting point

agarose layer in subsequent incubations. Standard glass slides may be used, and so the more expensive fully frosted glass slides or polystyrene slides employed in other protocols are not necessary.

3. Only one layer of low melting point agarose with the cells inside is necessary. Other protocols for microgel preparation include an additional low melting point agarose layer extended over the layer with cells once it has solidified and the cover slip has been removed. This microgel is thicker and probably modifies the time for diffusion of the unwinding solution to more deeply located cells.
4. Virtually any cell type may be assayed if a single cell suspension is generated. It is important to mix the cell suspension with the liquid agarose when the latter has stabilized at 37°C, to avoid cell damage by heat.
5. Cell density within the agarose matrix should be not excessively high in order to avoid the overlapping of DBD-FISH signals, and not too broadly spread, to facilitate rapid signal capture. When using human leukocytes in buffy coat, i.e., after 1 h sedimentation in vertical heparinized blood in a 5 mL tube, we extract 0.6 mL directly without further dilution, for mixing with the agarose, in order to achieve an appropriate cell density consistently. The cell concentration in buffy coat from a normal healthy subject is usually 6000–12000 leukocytes/μL, most of them being granulocytes polymorphonuclear neutrophils and lymphocytes. These specific cell types may be separated by centrifugation in Polymorphprep or Lymphoprep (Nycomed, Oslo, Norway) and the cell layer washed and diluted in plasma from the same individual or in culture medium.
6. Cells can be exposed to the DNA-damaging agent either before mixing with the liquid agarose, in suspension or monolayer, or when included within the microgel monolayer. We prefer to expose the cells to X-rays when they are in the gel on the microscope slide. To avoid DNA repair, a cold plate is placed under the slide, taking care not to freeze the agarose layer as this disrupts the gel and damages the cells. Only a fraction of each slide is exposed to the X-rays. An area is always left unexposed, either by protecting it or by keeping it out of the irradiated field, in order to act as an unirradiated control. At least three doses may be applied on a single slide, in addition to the unirradiated area. If cooled cells are exposed to X-rays in suspension, mixing with agarose at 37°C could provide enough time at the appropriate temperature to initiate the repair of induced DNA damage, given that single-strand breaks are quickly repaired.
7. The ssDNA produced by the alkali may arise by single-strand breaks, double-strand breaks, alkali-labile sites (i.e. DNA lesions or modifications that turn into strand breaks by alkaline treatment) ***(12)***, and chromosome telomeric ends. Except in the case of telomeres, all of them can either be spontaneous or induced by exposure to DNA-damaging agents or through internal cellular processes such as excision repair, apoptosis or the action of topoisomerases.
8. Unwinding begins on both sides of each break and proceeds along the DNA helix (**Fig. 2G**). The rate of production or length of ssDNA produced from a break of origin will be dependent on the time, temperature and ionic strength of the alkaline unwinding solution ***(10)***. These variables may be manipulated for each

experimental situation (**Fig. 2A,B**; **C,D**). When analyzing the DNA breakage level exclusively induced within a specific DNA region, it is important to restrict the length of the ssDNA extended from the break as far as possible. This reduces the possibility of ssDNA being generated from DNA breaks relatively close to the probed sequence, as these could extend into the probed area with the consequence that DBD-FISH would not be absolutely restricted to the specific area. We prefer an incubation time of 2.5 min at 7°C since shorter times do not allow the alkali to diffuse homogeneously to all cells within the gel matrix ***(13)***.

9. DNA breaks or other possible lesions capable of being transformed into DNA breaks that could be produced by experimental manipulations after neutralizing the alkali do not affect the DBD-FISH results since they are not transformed into ssDNA that is susceptible to hybridization.
10. The unwinding incubation preceding the lysis steps probably detects only those DNA breaks induced initially (e.g. by ionizing radiation) if performed immediately after exposure, so as to avoid possible additional DNA breaks by manipulation before the unwinding step. Nevertheless, it is also possible to perform the lysing incubation before the alkali treatment. In this case, after incubation in lysing solutions 1 and 2, nucleoids are washed by horizontally immersing the slide in abundant isotonic saline solution (0.9% NaCl) for 15 min at room temperature. It is then transferred to the alkaline unwinding solution, followed by an incubation in abundant neutralizing solution (0.4 *M* Tris-HCl, pH 7.5) for 10 min at room temperature. After a brief wash in TBE buffer, the slide is dehydrated. Carrying out this experimental variant increases the background DBD-FISH signal. Furthermore, the recognition of multifragmented apoptotic nuclei is not as easy because of the extensive dispersion of the spotted labeled DNA fragments within the gel (**Fig. 2E,F**). This technical variant is of great value for the analysis of DNA lesions that may be hidden by the chromatin organization, such as the constitutive alkali-labile sites from human mature sperm DNA ***(14)***.
11. Though lysing solution 2 is sufficient for effective protein extraction in most cell types, it is totally ineffective in sperm cells. We recommend the routine use of both lysing solutions. DTT breaks disulfide bonds, so SDS and the high salt solutions remove nearly all the proteins ***(15)***. Lysing solution 1 is probably sufficient, but the appearance of nucleoid fibers is cleaner and tighter when using the lysing solution 2 afterwards, allowing a better discrimination of the "core" and "halo" of the nucleoid.
12. During probe incubation it is not advisable to apply cover slip sealant along the perimeter of the glass cover slip. Removal of the rubber cement after the incubation period could damage the microgel.
13. Incubation in DNA probe washing solutions at high temperature can destroy or damage the microgel or nucleoids. It is recommended not to exceed 42°C in the washing solutions. When necessary, increasing the formamide concentration and/or decreasing the ionic strength can decrease the washing temperature while maintaining high stringency (e.g. chromosome-specific "painting" probes should be washed twice in 50% formamide/1×SSC, pH 7, 5 min each, 42°C, and twice in 1×SSC, pH 7, 42°C, 3 min each).

14. Several probes with different haptens or fluorochromes can be simultaneously hybridized, washed and detected, if their hybridization buffer and washing conditions are similar. If the hybridization buffer and/or the DNA probe washings are different, the probe with most stringent hybridization and washing conditions can be hybridized first. After the specific washings, the slide with the microgel film is immersed in increasing ethanol baths (70%, 90%, 100%, 2 min each) and then air-dried. The new DNA probe with less stringent hybridization and washing conditions is then hybridized and washed. Once the final wash is finished, the detection step may be initiated with a mixture of the different fluorochrome-conjugated antibodies to each different hapten-labeled DNA probe, if necessary.
15. Do not allow the slide surface to dry after washing the probe, since this will cause non-specific binding of the detection reagent, resulting in high background fluorescence.
16. No amplification of the signal is necessary, even when using small cosmid probes. Though the alkali incubation lyses the cell, extensive protein removal in lysing steps greatly improves the accessibility of DNA probes and detection reagents to the target, resulting in intense signals.
17. CCD camera technology is progressing rapidly, with products offering more advanced features. Nevertheless, it is not necessary to use megapixel images. They require an excessive amount of RAM and magnetic storage, and increase the processing time ***(16)***.
18. If it is necessary to transform images from one file format to another, it is important to ensure that the range of grey levels is maintained after the transformation.
19. Interslide and interexperimental variation is evident in DBD-FISH results, as in all DNA unwinding techniques ***(2)***. In each X-ray-irradiated slide, it is important to preserve an unirradiated area to provide a control signal to which that of the exposed area is compared (**Fig. 1**, **Fig. 2A,B**; **C,D**). It is also desirable to incubate two different probes on the same slide. This aids the more accurate evaluation of the relative differences in labeling between the different targets, in a similarly processed cell population. If the probes are labeled with the same fluorochrome, they may be hybridized in separate areas of the slide, including both unirradiated and irradiated regions. Moreover, if differentially labeled, they may be simultaneously or sequentially hybridized in the same area, and then the same cell measured with different filters to establish the fluorescence ratio between the signals (**Fig. 2A,B**).
20. Replicating structures behave as DNA strand breaks when denatured in alkaline assays ***(17)***. Thus, cells in S-phase could appear with strong labeling after DBD-FISH.
21. Extensive DNA breakage could lead to the generation of very small DNA fragments that would spread within the agarose matrix and dissolve in the incubation solutions, thereby decreasing the target available for probe hybridization and the subsequent fluorescent signal. In fact, apoptotic nuclei sometimes appear as small but widely distributed, faintly labeled residual spots (**Fig. 2E,F**).

Acknowledgments

This work has been supported by the Consejo de Seguridad Nuclear (CSN), Spain, and the European Atomic Energy Community (Fifth Framework Programme, FIGH-CT1999–00009, TELORAD). We thank V. Goyanes for helpful comments, J. Ramiro-Díaz, F. Vázquez-Gundín, M. T. Rivero, B. Ferreiro, and S. Dorado for technical assistance, and P. Mason for improving the English style.

References

1. Fernández, J. L., Goyanes, V., Ramiro-Diaz, J., and Gosálvez, J. (1998) Application of FISH for *in situ* detection and quantification of DNA breaks. *Cytogenet. Cell Genet.* **82,** 251–256.
2. Bunch, R. T., Gewirtz, D. A., and Povirk, L.F (1992) A combined alkaline unwinding/Southern blotting assay for measuring low levels of cellular DNA breakage within specific genomic regions. *Oncol. Res*. **4,** 7–15.
3. Bunch, R. T., Gewirtz, D. A., and Povirk, L. F. (1995) Ionizing radiation-induced DNA strand breakage and rejoining in specific genomic regions as determined by an alkaline unwinding/Southern blotting method. *Int. J. Radiat. Biol*. **68,** 553–562.
4. Verma, R. S., and Babu, A. (ed.) (1995*) Human chromosomes. Principles and techniques.* 2nd ed. McGraw-Hill. Inc.
5. Roti, Roti, J. L., and Wright, W. D. (1987) Visualization of DNA loops in nucleoids from HeLa cells: assays for DNA damage and repair. *Cytometry* **8,** 461–467
6. Smith, P. J., and Sykes, H. R. (1992) Simultaneous measurement of cell cycle phase position and ionizing radiation-induced DNA strand breakage in single human tumour cells using laser scanning confocal imaging. *Int. J. Radiat. Biol.* **61,** 553–560.
7. McKelvey-Martin, V. J., Green, M. H. L., Schmezer, P., Pool-Zobel, B. L., De Méo, M. P., and Collins, A. (1993) The single gel cell electrophoresis (comet assay): a European review. *Mutation Res.* **288,** 47–63.
8. Fairbain, D. W., Olive, P. L., and O'Neill, K. L. (1995) The comet assay: a comprehensive review. *Mutation Res.* **339,** 37–59.
9. Ahnström, G., and Erixon, K. (1973) Radiation-induced single-strand breaks in DNA determined by rate of alkaline strand separation and hydroxylapatite chromatography: an alternative to velocity sedimentation. *Int. J. Radiat. Biol.* **36,** 197–199.
10. Rydberg, B. (1975) The rate of strand separation in alkali of DNA of irradiated mammalian cells. *Radiat. Res*. **61,** 274–287.
11. Santos, S. J., Singh, N. P., and Natarajan, A. T. (1997) Fluorescence in situ hybridization with comets. *Exp. Cell Res.* **232,** 407–411.
12. Von Sonntag, C. (1987) *The chemical basis of radiation biology*. Taylor and Francis Ltd., London, UK.

13. Vázquez-Gundín, F., Gosálvez, J., de la Torre, J., and Fernández, J. L. (2000) DNA breakage detection-FISH (DBD-FISH): effect of unwinding time. *Mutation Res*. **453,** 83–88.
14. Fernández, J. L., Vázquez-Gundín, F., Delgado, A., Goyanes, V. J., Ramiro-Díaz, J., de la Torre, J., and Gosálvez, J. (2000) DNA breakage detection-FISH (DBD-FISH) in human spermatozoa: technical variants evidence different structural features. *Mutation Res*. **453,** 77–82.
15. Olive, P. L., and Banáth, J. P. (1993) Detection of DNA double strand breaks through the cell cycle after exposure to X-rays, bleomycin, etoposide and 125IdUrd. *Int. J Radiat. Biol.* **64,** 349–358.
16. Ballard, S. G., and Ward, D. C. (1993) Fluorescence in situ hybridization using digital imaging microscopy. *J Histochem. Cytochem.* **41,** 1755–1759.
17. Olive, P. L., Chan, A. P. S., and Cu, C. S. (1988) Comparison between the DNA precipitation and alkali unwinding assays for detecting DNA strand breaks and cross-links. *Cancer Res*. **48,** 6444–6449.

17

Simultaneous *In Situ* Detection of DNA Fragmentation and RNA/DNA Oxidative Damage Using TUNEL Assay and Immunohistochemical Labeling for 8-Hydroxy-2'-Deoxyguanosine (8-OHdG)

Alexander E. Kalyuzhny

1. Introduction

Analysis of DNA fragmentation using Terminal deoxynucleotidyl Transferase (TdT)-mediated nick end-labeling (TUNEL) is a very sensitive technique for in situ detection of various types of DNA breaks in cells undergoing apoptosis and/or necrosis ***(1–6)***. TUNEL technique is widely used, for instance, to study mechanisms underlying early development and morphogenesis ***(7–14)***, aging ***(15–24)***, cancer ***(25,5,25–35)*** and neurodegenerative diseases ***(36,20,21,36–44)***. TUNEL detects the DNA fragmentation, which represents the end point of DNA degradation in apoptosis but does not depict primary stimuli that caused irreversible disruption to the integrity of DNA. Oxidative stress is one of such primary stimuli and there is a great deal of research aimed at unraveling the molecular mechanisms underlying oxidative damage to DNA by so-called reactive oxygen species (ROS) and oxygen radicals. Oxidative damage has been implicated in a wide variety of neurodegenerative disorders including Alzheimer's dementia, amyotrophic lateral sclerosis, Huntington's disease and Parkinson's disease ***(45–55)***. Formation of 8-hydroxy-2'-deoxyguanosine (8-OHdG) is the most common modification of DNA caused by oxidative stress. Therefore, immunohistochemical quantification of 8-OHdG would be a valuable tool in determining the extent of oxidative DNA damage caused by ROS. On the other hand, methods analyzing the oxidative damage to the DNA, are not sufficient alone either, since they do not reveal whether oxidative stress will result in apoptosis and cell death or not. Thus, it appears that limitations of each individual

From: *Methods in Molecular Biology, vol. 203:* In Situ *Detection of DNA Damage: Methods and Protocols*
Edited by: V. V. Didenko

assay may be overcome if both techniques are combined in a single assay that is applied to the same cytological of histological specimen.

Here we describe two protocols to be used either on cultured cells or tissue sections. These protocols are based on double-staining immunohistochemistry that allows detection of both fragmentation and oxidative damage to DNA/RNA in the same specimen. Since oxidative damage to the DNA appears to precede DNA fragmentation ***(5,15)***, the sequential application of both detection techniques allows in situ monitoring of the ratio of cells representing the early phase (8-OHdG-immunoreactive cells) to cells in the late phase (TUNEL-positive) of the cell death process within the specific anatomical region. On the other hand, it also appears that oxidative damage does not necessarily cause cell death ***(2)*** and hence quantification of double-labeled, TUNEL-positive and 8-OHdG-immunoreactive, cells allows to establish a threshold of cellular sensitivity to oxidative stimuli at which DNA oxidation will induce irreversible DNA damage resulting in cell death.

Our protocol combines TUNEL assay and immunohistochemical labeling for 8-OHdG in both cultured cells and tissue sections. First, cells and tissues are stained with antibodies against 8-OHdG and after that TUNEL assay is employed on the same specimens. This double-staining technique can be easily optimized for the majority of cells and tissues, and may be further combined with other molecular techniques.

2. Materials

1. Primary culture of rat dorsal root ganglia (DRG) neurons from 3-day-old Sprague-Dawley rats.
2. DRG dissociation reagent: solution of 10 mg/mL of collagenase/dispase (Roche Molecular Biochemicals, Indianapolis, IN) in Hank' Balanced Salt Solution (HBSS; Gibco BRL, Grand Island, NY).
3. DRG culture medium (all reagents except NGF are from Sigma, St. Louis, MO): Ham's medium (F-12; Gibco BRL, Grand Island, NY) supplemented with 5% heat-inactivated horse serum and 5% fetal bovine serum, 50 ng/mL nerve growth factor (R & D Systems, Minneapolis, MN), 4.4 m*M* glucose, 2 m*M* L-glutamine, penicillin (50 µg/mL) and streptomycin (50 µg/mL).
4. Fixative: 4% paraformaldehyde in phosphate-buffered saline (PBS). Wear mask and gloves and use the hood when preparing paraformaldehyde fixative.
   a. Solution A, PBS: Fill 1 L beaker with 900 mL of distilled water and dissolve 0.23 g of NaH_2PO_4 (anhydrous), 1.15 g Na_2HPO_4 (anhydrous) and 9 g NaCl. Adjust pH to 7.4 using 1 *M* NaOH and/or 1 *M* HCl;
   b. Solution B, 8% paraformaldehyde: Dissolve 8 g of paraformaldehyde powder (Sigma, St. Louis, MO) in 100 mL of deionized water using heating stir plate. Heat this solution during stirring. Turn the heat off after temperature reaches 56–58°C and add 1–2 drops of 1 *M* NaOH to clear solution. Continue stirring

for another 20–30 min and then filter this solution using regular filter paper (for example Whatman #1);

Avoid overheating of the paraformaldehyde solution by using thermometer to monitor the temperature. If accidentally heated above 58°C, discard it and prepare a new paraformaldehyde solution;

c. Fixing solution: 4% paraformaldehyde—made by mixing 1 part of Solution A with 1 part of Solution B. Store at 4°C. Avoid using this fixative after being stored longer than three weeks.

5. Cell culture tools and accessories: Multi-well (4 or 8 wells) chamber slides and sterile 35 mm Petri dishes (Nalge Nunc International, Rochester, NY), 70% alcohol (Fisher Scientific, Pittsburgh, Pa), Pasteur pipettes, scissors and forceps for microdissection of DRG neurons, dissecting microscope, sterile hood, cell culture incubator.
6. Oxidative stress reagent: prepare 1 mM solution of H_2O_2 by adding 0.5 µL of 30% H_2O_2 (Sigma, St. Louis, MO) to 8.8 mL of Hank's Balanced Salt Solution (HBSS; Gibco BRL, Grand Island, NY). Prepare 10 µ*M* solution of H_2O_2 by adding 100 µL of 1 m*M* H_2O_2 solution to 9.9 mL of HBSS. Store at 4°C. Volume of each reagent should be sufficient to stimulate cells in 2 multi-well chamber slides.
7. Dilution buffer: PBS containing 1% bovine serum albumin, 1% normal donkey serum, 0.3% Triton X-100 (v/v) and 0.01% sodium azide.
8. Primary, anti-8-OHdG antibodies: Make working dilution of 5 µg/mL of mouse monoclonal anti-8-OHdG antibodies (QED Bioscience Inc., San Diego, CA) in dilution buffer. This antibody solution may be used to stain DRG neurons and tissue sections. May be stored at 4°C for at least 3 months.
9. Fluorescent secondary antibodies for 8-OHdG detection: Donkey anti-mouse conjugated with fluorescein isothiocyanate (FITC; Jackson ImmunoResearch Laboratories, West Grove, PA). Make 1:100 working dilution with antibody dilution buffer. May be stored at 4°C for at least 1 month.
10. Fluorescent detection reagent for TUNEL: Make 1:100 working dilution of Streptavidin conjugated with cyanine 3.18 (Cy3; Jackson Immunoresearch Laboratories, West Grove, PA) with dilution buffer. May be stored at 4°C for at least 1 month.
11. Mounting medium for fluorescent labels: ProLong antifade kit (Molecular Probes, Eugene, OR). This medium minimizes loss of fluorescence by FITC and Cy3 due to photobleaching during examination under the fluorescence microscope.
12. TUNEL assay: TACS 2 TdT DAB kit (Trevigen, Gaitherburg, MD.).
13. Chromogenic system for 8-OHdG detection: HRP-AEC Cell and Tissue Staining kit (CTS 002; R&D Systems, Inc., Minneapolis, MN);
14. Chromogenic system for TUNEL detection: HRP-DAB Cell and Tissue Staining kit (CTS 003; R&D Systems, Inc., Minneapolis, MN) combined with DAB enhancer (CTS010; R&D Systems, Inc., Minneapolis, MN);
15. Mounting medium for chromogenic labels: Aqueous mounting medium (CTS011; R&D Systems, Inc., Minneapolis, MN).

16. Pen to label slides: SHUR/MARK pen (Fisher Scientific, Pittsburgh, Pa).
17. Wax-like pen to outline tissue sections: ImmEdge pen (Vector Laboratories, Burlingame, CA). Used to create a hydrophobic barrier around the tissue section to retain incubation reagents.
18. Humidity incubation chamber for cell and tissue staining: Staining tray of 5-slide capacity with humidity cover (Signet Laboratories, Dedham, MA).
19. Microscopy: Bright field/fluorescence microscope (Provis; Olympus, Melville, NY) equipped with cooled CCD color digital camera (Spot; Diagnostic Instruments, Sterling Heights, MI) and fluorescence filter set to visualize FITC (460–490 nm excitation and 510–550 nm emission) and Cy3 (541–551 nm excitation and 572–607 nm emission).

3. Methods

Unless otherwise stated, all procedures are performed at room temperature. If protocol calls for incubation at room temperature, reagents stored at 4°C should be adjusted to room temperature before they added to cell and tissue samples. Since AEC (3-amino-9-ethylcarbazole) and DAB (3,3'Diaminobenzidine) are potential carcinogens wear gloves to avoid contact of these reagents with skin. It is recommended to perform each staining experiment at least in duplicate in case some of samples dry out during the incubation and cannot be used to complete experiment.

3.1 Double-Staining of Cultured Cells

1. These studies were conducted on rat neonatal dorsal root ganglia (DRG) neurons in a sterile hood (*see* **Note 1**). Culture cells in the 37°C/CO_2 for 2–3 d and then use them for double-staining experiments.
2. Transfer chamber slides with cells from the 37°C/CO_2 humidified incubator into the sterile hood. Wait for approximately 20 min to allow temperature of the culture medium in the chamber slide to decrease from 37°C to ambient.
3. Using a sterile pipet, gently remove the culture medium from each well: position the tip of the pipette into the corner of the well to avoid disturbing cells. Collect a removed culture medium into a sterile tube. This culture medium will be reused later.
4. Add oxidative stress reagents into designated wells. Add plain HBSS into at least one of the wells that will serve as a control group (*see* **Note 2**). Return the chamber slide into the 37°C/CO_2 humidified incubator and incubate for 30 min.
5. Transfer the chamber slides into a sterile hood from the CO_2 incubator, discard oxidative stress reagents and rinse each well three times with sterile HBSS. Discard HBSS and add culture medium that has been collected in Step 3. Return cells into the 37°C/CO_2 humidified incubator and incubate for 18–24 h (*see* **Note 3**).
6. Remove the chamber slides from the incubator, discard the culture medium and add 4% paraformaldehyde into each well. Fix for 10 min and then wash 3 × 15 min with PBS.

7. Using the Slide Separator provided with chamber slides lift the upper chamber from slide.
8. Place slides horizontally into humidity chamber, add anti-8-OHdG antibodies and incubate 3 h. Alternatively, cells may be incubated overnight at 4°C.
9. Wash slides 3 × 15 min in PBS and incubate with anti-mouse FITC-conjugated antibodies for 1 h.
10. Wash 3 × 15 min in PBS and start TUNEL assay.
11. Rinse slides with DNase-free water and permeabilize cells for 30 min with CytoPore reagent provided with TUNEL kit.
12. Rinse slides with DNase-free water and then transfer them into a Coplin jar containing TdT labeling buffer: follow up dilution recommendations provided with TUNEL kit. Incubate for 5 min.
13. Prepare TdT labeling mixture. Calculate the volume of TdT mixture: 150 µL is required to cover the entire area of the slide occupied by the cells. Combine TdT labeling components (TdT dNTP mix, 50× Mn2+, TdT enzyme and TdT labeling buffer) as recommended in the TUNEL kit insert (*see* **Note 4**). Apply TdT labeling mixture and cover it accurately with 22 × 60 mm coverslip. Do not press the coverslip to avoid squeezing of the labeling mixture. Place the slide horizontally into a humid chamber and incubate at 37°C for 1 h.
14. Transfer slides with coverslips into a Coplin jar containing TdT Stop Buffer: follow up dilution recommendations provided in TUNEL kit protocol. Keep slide in stop buffer for 2 min and then pull them slowly out to get rid of coverslips. If coverslips are sticking to the slide, lift them gently using sharp fine forceps. Transfer uncovered slides with tissues into another Coplin jar filled with Stop Buffer and incubate for 5 min.
15. Wash slides in PBS for 5 min.
16. Place slides horizontally into humidity chamber, apply 3–5 drops of Streptavidin-Cy3 solution and incubate for 1 h.
17. Stop the reaction by rinsing slides with PBS and then wash them 3 × 10 min with PBS in a Coplin jar.
18. Mount under coverslips using mounting medium for fluorescent labels. After slides are dry, they can be examined under the fluorescence microscope (*see* **Note 5**). **Fig. 1** illustrates the results of TUNEL/8-OHdG double-labeling in DRG neurons.

3.2 Double-Staining of Paraffin-Embedded Tissue Sections

Immunofluorescence protocol utilizing two-color labeling is more convenient than the chromogenic one: it is shorter and results in unambiguous separation of colors (*see* **Note 6**). However, on tissue sections of human brain immunofluorescent histochemistry may not be used in most cases due to strong autofluorescence of lipofuscin (age pigment)—granules of various size are distributed in the neuropile and inside the neurons. Lipofuscin granules were reported to appear at 9 years of age and accumulate progressively with the advancement of age ***(56)***. Abundant distribution of lipofuscin in Alzheimer's

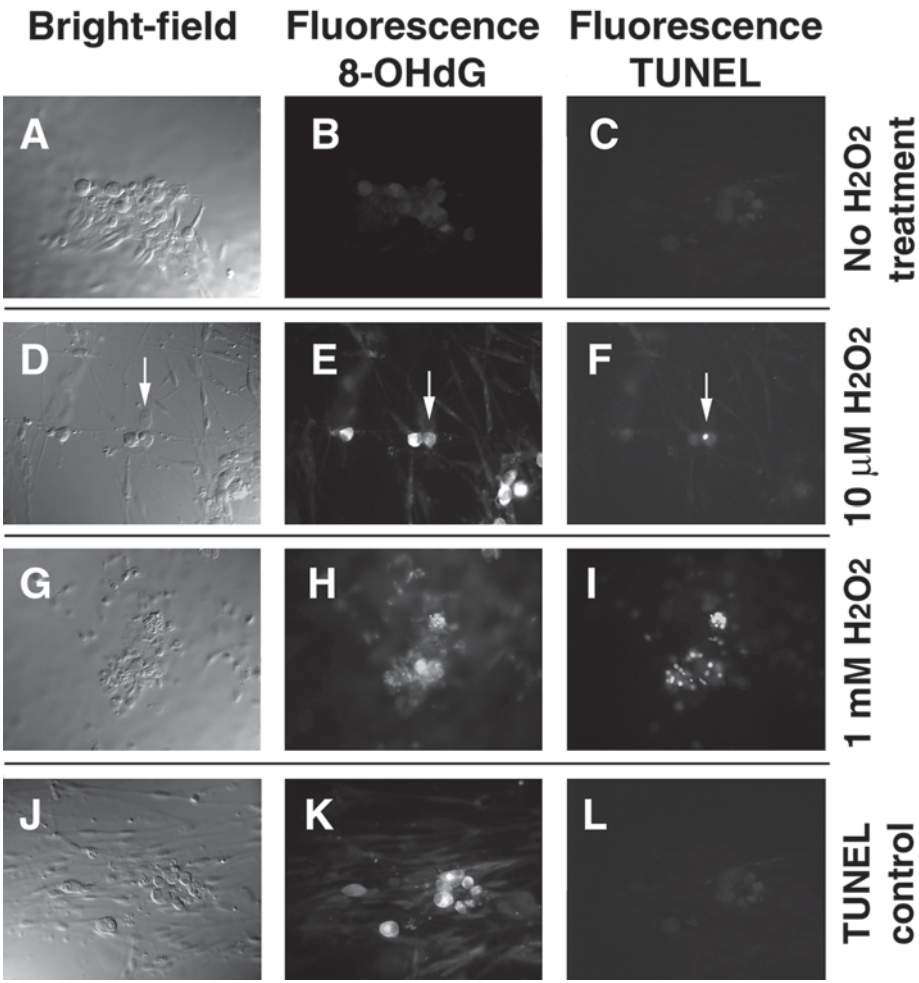

Fig. 1. Double-labeling for 8-OHdG and TUNEL in cultured rat DRG neurons. **A, D, G, J:** overview of DRG neurons using bright-field illumination. **B, E, H, K:** immunofluorescent detection of 8-OHdG-immunoreactivity. **C, F, I, L:** detection of DNA fragmentation using TUNEL assay with fluorescent label. **A, B, C:** in control group cells did not express 8-OHdG-immunoreactivity and were TUNEL negative. **D, E, F:** 10 μ*M* of H_2O_2 induced substantial oxidative damage, but DNA fragmentation appeared to be a rare event—arrow depicts only one out of many 8-OHdG-immunoreactive cell which was also TUNEL-positive. **G, H, I:** in concentration 1 m*M* H_2O_2 induced both, severe oxidative damage and DNA fragmentation. **J, K, L:** specificity of TUNEL reaction has been demonstrated by excluding TdT enzyme from the TdT labeling mixture. Cells were treated with 1 m*M* of H_2O_2 and suffered sever oxidative damage, but were TUNEL-negative.

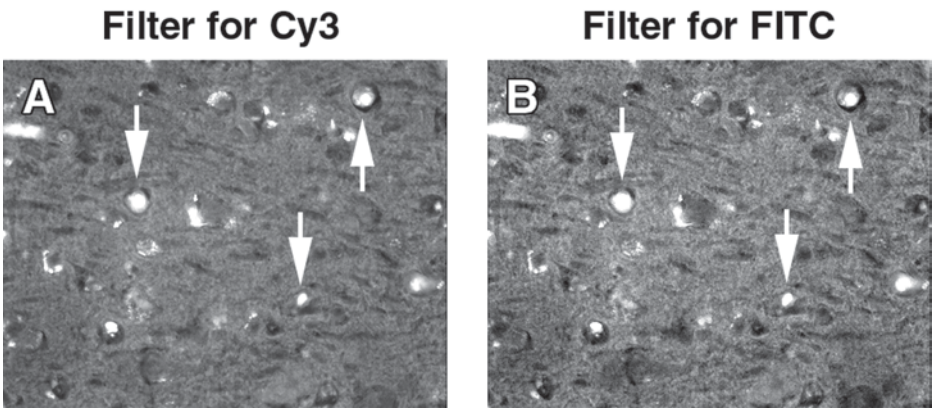

Fig. 2. Autofluorescence of Alzheimer's brain tissue. Strong autofluoresescence is observed using filters to visualize Cy3 **(A)** and FITC **(B)**. Arrows depict some profiles that may be erroneously considered as double-labeled structures should fluorescent labels be used for 8-OHdG immunohistochemistry and TUNEL assay.

brain (***(57)***; **Fig. 2**) leaves no other choice than to use chromogenic rather than fluorescent detection systems for immunohistochemical studies. Using Alzheimer's brain tissue sections as a model, we have developed a protocol that employs two chromogenic labels on the same tissue sample. This technique results in a good contrast and reliable separation of colors and may be used as a routine immunohistochemical procedure to study DNA fragmentation (*see* **Note 7**) and oxidative damage to RNA and DNA within the same cells.

1. Label slides using SHUR/MARK pen.
2. On the slide outline the tissue section with ImmEdge pen and let it dry for 5 min.
3. Deparaffinize the sections by incubating slides at room temperature in a glass Coplin jar as follows:
   a. Xylenes—two baths, 10 min each;
   b. 100% ethanol—two baths, 10 min each;
   c. 95% ethanol—two baths, 10 min each;
   d. 70% ethanol—two baths, 10 min each.
4. Wash slides (2×5 min) in PBS.
5. Wash slides in DNase-free water for 5 min.
6. Treat tissue sections with Proteinase K solution (*see* **Notes 8**, **9**). Calculate the volume of working Protein K solution: 50 µL is required to treat 2×1 cm^2 tissue area. Dilute Proteinase K concentrate with DNase-free water using the ratio recommended in the TUNEL kit data sheet. Apply 50 µL of Proteinase K solution onto tissue sections and cover them accurately with coverslips of appropriate size. Do not press the coverslips to avoid squeezing of Proteinase K solution. Place the slide into a humid chamber and incubate 30 min.

7. Transfer slides with coverslips into a Coplin jar containing DNase-free water. Keep slides in water for 2 min and then pull them slowly out to remove coverslips. Transfer uncovered slides with tissues into another Coplin jar with DNase-free water.
8. Remove slides from the Coplin jar, shake excess water, place them horizontally and add 3–5 drops of H_2O_2 blocking reagent from Cell and Tissue Staining kit. Incubate 10 min in a humid chamber.
9. Rinse slides in DNase-free water for 5 min.
10. Transfer slides into a Coplin jar containing TdT labeling buffer: follow up dilution recommendations in TUNEL kit protocol. Incubate for 5 min.
11. Prepare TdT labeling mixture. Calculate the volume of TdT mixture: 50 µL is required to label 2×1 cm^2 of tissue area. Combine TdT labeling components (TdT dNTP mix, 50× Mn2+, TdT enzyme and TdT labeling buffer) as recommended in the TUNEL kit protocol. Apply 50 µL of TdT labeling mixture onto tissue sections and cover them accurately with coverslips of appropriate size. Do not press the coverslips to avoid leakage of the labeling mixture. Place the slide horizontally into a humid chamber and incubate 1 h at 37°C.
12. Transfer slides with coverslips into a Coplin jar containing TdT stop buffer: follow up dilution recommendations provided in TUNEL kit protocol. Keep slide in stop buffer for 2 min and then pull them slowly out to get rid of coverslips. Transfer uncovered slides with tissues into another Coplin jar with stop buffer and incubate for 5 min.
13. Wash slides in PBS for 5 min.
14. Place slides horizontally into a humid chamber and apply 3–5 drops of Streptavidin-HRP solution from Cell and Tissue staining kit. Incubate 30 min.
15. Wash slides 2×5 min in PBS.
16. Place slides horizontally on a white paper towel and apply mixture of DAB (from Cell and Tissue Staining kit, CTS003) with DAB enhancer to cover entire tissue section. Monitor the development of dark-blue color under the microscope using 4× or 10× power lens. Usually it takes from 3–10 min to get strong blue-black labeling of nuclei in apoptotic and/or necrotic cells.
17. Discard DAB mixture by draining it from the slides into a beaker.
18. Wash slides in PBS for 20 min at room temperature.
19. Place slides horizontally and add 3–5 drops of H_2O_2 blocking reagent from Cell and Tissue Staining kit. Incubate 10 min in a humid chamber at room temperature.
20. Rinse slides in PBS and run avidin-biotin block using reagents from Cell and Tissue Staining kit. Place slides horizontally into a humid chamber and add 3–5 drops of avidin blocking solution and incubate for 15 min. Rinse slides in PBS, place them horizontally and add 3–5 drops of biotin blocking solution and incubate 15 min. Wash slides in PBS for 20 min.
21. Place slides into the humid chamber and apply 80–150 µL of anti-8-OHdG antibodies per slide (*see* **Notes 10**, **11**). Incubate 16–24 h at 4°C.
22. Wash slides 3×15 min in PBS.
23. Repeat step 14.

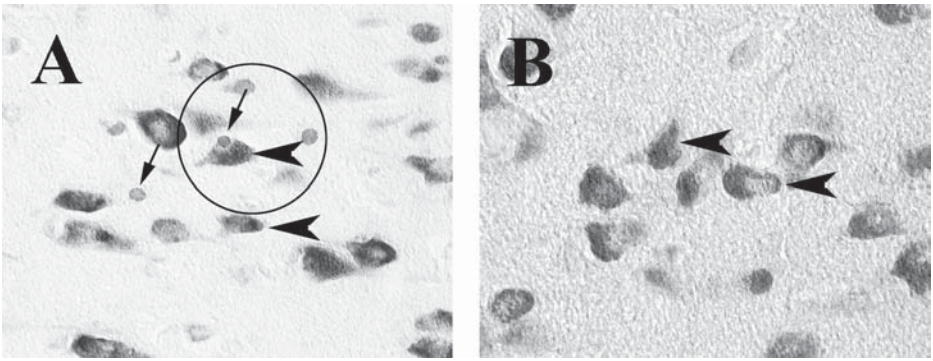

Fig. 3. 8-OHdG and TUNEL double-labeling in Alzheimer's brain. **(A)** TUNEL-positive nuclei are depicted by arrows. Arrowheads point to some 8-OHdG-immunoreactivity which appeared to be confined to neuronal cytoplasm. A double-labeled neuron is outlined by black circle. **(B)** No TUNEL-positive profiles observed in adjacent tissue section that has been stained only using anti-8-OHdG antibodies.

24. Repeat step 15.
25. Place slides horizontally and apply AEC solution from Cell and Tissue Staining kit (CTS002) to cover entire tissue section. Monitor the development of red color under the microscope using 4× or 10× lens. It may take from 1–3 min to get distinct labeling.
26. Repeat step 18.
27. Mount tissues using aqueous mounting medium and let them dry.
28. Use bright-field microscope equipped with digital color cooled CCD camera to examine and collect images of tissue sections double-labeled for TUNEL and 8-OhdG. **Fig. 3** illustrates the results of such a double-labeling.

4. Notes

1. Isolation of DRG neurons and set-up of culturing conditions represent a modification of the technique described by Usachev et al., ***(58)*** and includes these steps. Decapitate 3-day old Sprague-Dawley rats. Use 70% alcohol to sterilize decapitated rats and surgical instruments (scissors and forceps). Under dissection microscope dissect DRGs from the thoracic and lumbar segments of the spinal cord and treat them with collagenase/dispase digestion solution for 30 min in the 37°C/CO_2 incubator. Dissociate cells by triturating DRGs through large, medium and small diameter flame constricted pipets: 50–60×/per pipet. Stop digestion by adding 10 mL of sterile HBSS into cell suspension and centrifuge it at 500 × *g* for 10 min. Discard supernatant and resuspend in the same volume of HBSS and centrifuge again. Resuspend the pellet in 5 mL of F-12 medium and fill the wells of sterile chamber slides with DRG cell suspension.

2. It is recommended to employ different types of controls to be sure that TUNEL assay depicts apoptotic/necrotic cells rather than non-specific cell and tissue binding sites. Three types of TUNEL controls may be employed: (a) reaction-specific, (b) tissue specific and (c) positive control.
   a. *Reaction-specific* control answers the question whether components of the TdT mixture interact properly. This is done by incubating specimens with TdT mixture that does not contain Terminal deoxynucleotidyl Transferase (TdT enzyme). No specific nuclei labeling should occur. Some tissues (i.e., postmortem tissues stored for a long time in formalin fixative) may express a non-specific background due to non-specific binding of streptavidin-HRP and non-specific adsorption of DAB chromogen. However, the pattern of such a background (cytolpasmic and/or extracellular) is different from TUNEL reaction (nuclei staining).
   b. *Tissue-specific* control addresses the issue of TUNEL assay selectivity. This is done by comparing labeling in normal tissues vs. that one in tissues undergoing apoptotis or necrosis. To run a tissue-specific control it is recommended to include normal cells and tissues with specimens undergoing apoptosis. Even though normal specimens may contain cells with TUNEL-positive nuclei (due to naturally occurring apoptosis), their number is expected to be much lower in comparison with pathological samples.
   c. *Positive control* is done to assure the researcher that TUNEL assay is both reaction-and tissue-specific. This is done by "converting" normal tissue into an apoptotic-like by treating specimens with nuclease. Such treatment will cause DNA break and result in increased number of cells with TUNEL-positive nuclei. Nuclease may be purchased either as a part of the TUNEL kit or separately.
3. Do not allow cell and tissue samples to dry during the incubation and washing steps. Cell or/and tissues samples that were found dry should be excluded from experiment. Also watch for partial drying of tissue section margins: this may result in strong and not necessarily specific labeling for TUNEL and for 8-OHdG. Since partial drying may be overlooked (i.e. when staining a large number of slides) during the staining procedure, it is recommended to interpret "marginal" results cautiously. It appears that labeling in the central part of the tissue will be more specific than that one on the tissue edges.
4. TUNEL kit manufactured by Travigen contains Streptavidin-HRP and DAB chromogen which may be used to obtain strong monochrome (red-brown color) labeling of nuclei. However, it appears that staining using analogous reagents from R&D Systems' Cell and Tissue Staining kit in combination with R&D Systems' DAB enhancer (dark-blue color) works better when combined with AEC (red color) chromogen, due to better separation of colors. It is also possible to use analogous reagents purchased separately from different vendors. However using kits saves a lot of time, since requires little or no optimization to multiple reagents.
5. When manipulating digital images, adjust brightness and contrast simultaneously on "control" and "experimental" samples to avoid biased and inaccurate interpretation of cell and tissue staining.

6. A double-staining technique described in this article may be used as a powerful research tool to study mechanisms underlying pre- and post- implantation development, cancer, aging, toxicity and neurodegenerative disorders. It appears that this technique can be used for qualitative and quantitative measurement of cytotoxicity and hence can help to *monitor pollution* using cultured cells as a model. Being optimized for double- or single-staining, this technique, if necessary, may be used to study only DNA/RNA oxidative damage (8-OHdG labeling) or to analyze cells and tissues undergoing apoptosis and/or necrosis (TUNEL assay).
7. In addition to TUNEL labeling, apoptosis should be also confirmed by morphological criteria including membrane blebbing, shrinkage of cells and the formation of apoptotic bodies.
8. In some cases treatment of tissue samples with Proteinase K for 30 min may case tissue damage. If signs of tissue damage including detached (floating) tissue fragments and/or holes of irregular size are observed in tissue section, reduce the time of treatment with Proteinase K to 10–20 min. It is not recommended to use Proteinase K on cytological samples since cells are more sensitive to digestive damage produced by this enzyme. The alternative to Proteinase K pretreatment may be permeabilization of cells with 0.1–0.3% detergent Triton X-100 for 20 min.
9. To enhance 8-OHdG labeling cells and tissues may be treated with proteinase K (10 μg/mL in PBS) from 10–30 min in a humid chamber at 37°C, but refer to **Note 8**.
10. The specificity of labeling for 8-OHdG is determined by two factors: (a) specificity of 8-OHdG antibodies and (b) specificity of immunohistochemical reagents. In addition, the specificity of staining may be evaluated using (c) negative control.
    a. The purpose of determining the specificity of anti-8-OHdG antibodies is to confirm whether cell and tissue staining resulted from the interaction of antibodies with specific target (8-OHdG) or caused by their cross-reaction with irrelevant antigens. The efficient way to study the specificity is to employ a so-called absorption control: mix anti-8-OHdG antibodies (taken in working dilution, i.e. 5 μg/mL) with purified 8OHdG (Sigma, St Louis, MO) taken in concentration 10 μg/mL. Mix well and incubate either 5 h at room temperature as described by Nunomura et al., ***(59)*** or overnight at 4°C. Since these antibodies recognize RNA-derived 8-OHG as well, it is also recommended to employ absorption control by pre-incubating antibodies with 8-OHG. It is expected that cell and tissue labeling will be decreased when using absorption control mixtures since soluble antigens occupy binding sites on anti-8-OHdG antibodies and thus reduce or abolish their capacity to interact with cellular antigens.
    b. The analysis of the specificity of immunohistochemical reagents needs to be done to demonstrate that such reagents as anti-mouse secondary antibodies (fluorescent or biotinylated), streptavidin-HRP and AEC chromogen do not bind to cells and tissues per se. The simplest way to answer this question is to incubate specimens by substituting antibody diluent for anti-8-OHdG antibody

solution: lack of labeling will be indicative for the specificity of immunohistochemical reagents. However, if non-specific labeling is observed, additional steps are required to minimize it. Frequently a high non-specific background is caused by free aldehyde groups present in tissues that are fixed with paraformaldehyde or glutaraldehyde: free aldehyde groups are capable of reacting with secondary antibodies and "crosslinking" them to the tissue. Free aldehyde groups may be blocked for instance by incubating specimens before applying primary, anti-8-OHdG, antibodies with 0.5 mg/mL of sodium borohydrate ($NaBH_4$) for 10–20 min at room temperature. Another way to neutralize free aldehyde groups is to incubate samples in 10% normal either horse or swine or donkey serum for 5–30 min at room temperature before applying primary antibodies.

c. *Negative control* constitutes a specimen with intentionally destroyed antigen. Since anti-8-OHdG antibodies target DNA and/or RNA, their degradation is expected to result in reduced or abolished cell and tissue labeling. DNA and RNA may be degraded by pretreatment of specimen with PBS containing either 10 U/μL of DNase I or 10 U/μL S1 DNase or 5 μg/μL of RNase from 30–60 min in a humid chamber at 37°C. The much more robust effect may be obtained by combining all three enzymes in one mixture.

11. The advantage of combining TUNEL with antibodies manufactured by QED Bioscience Inc. is interaction of these antibodies with RNA-derived 8-OHG present in the cytoplasm. 8-OHG labeling in the cytoplasm does not attenuate visualization of TUNEL-positive nuclei within the same cell.

References

1. Ansari, B., Coates, P. J., Greenstein, B. D., and Hall, P. A. (1993) In situ end-labeling detects DNA strand breaks in apoptosis and other physiological and pathological states. *J. Pathol.* **170,** 1–8.
2. Allen, R. T., Hunter, W. J., **3rd,** and Agrawal, D. K. (1997) Morphological and biochemical characterization and analysis of apoptosis. *J. Pharmacol. Toxicol. Methods* **37,** 215–228.
3. Heatwole, V. M. (1999) TUNEL assay for apoptotic cells. *Methods Mol. Biol.* **115,** 141–148.
4. Takashi, E. and Ashraf, M. (2000) Pathologic assessment of myocardial cell necrosis and apoptosis after ischemia and reperfusion with molecular and morphological markers. *J. Mol. Cell Cardiol.* **32,** 209–224.
5. Mangili, F., Cigala, C., and Santambrogio, G. (1999) Staining apoptosis in paraffin sections. Advantages and limits. *Anal. Quant. Cytol. Histol.* **21,** 273–276.
6. van Lookeren Campagne, M., Lucassen, P. J., Vermeulen, J. P., and Balazs, R. (1995) NMDA and kainate induce internucleosomal DNA cleavage associated with both apoptotic and necrotic cell death in the neonatal rat brain. *Eur. J. Neurosci.* **7,** 1627–1640.
7. Liu, L. and Keefe, D. L. (2000) Cytoplasm mediates both development and oxidation-induced apoptotic cell death in mouse zygotes. *Biol. Reprod.* **62,** 1828–1834.

8. Marin-Teva, J. L., Cuadros, M. A., Calvente, R., Almendros, A., and Navascues, J. (1999) Naturally occurring cell death and migration of microglial precursors in the quail retina during normal development. *J. Comp. Neurol.* **412,** 255–275.
9. Bessert, D. A. and Skoff, R. P. (1999) High-resolution in situ hybridization and TUNEL staining with free-floating brain sections. *J. Histochem. Cytochem.* **47,** 693–702.
10. Maciejewska, B., Lipowska, M., Kowianski, P., Domaradzka-Pytel, B., and Morys, J. (1998) Postnatal development of the rat striatum—a study using in situ DNA end labeling technique. *Acta. Neurobiol. Exp. (Warsz)* **58,** 23–28.
11. Simonati, A., Rosso, T., and Rizzuto, N. (1997) DNA fragmentation in normal development of the human central nervous system: a morphological study during corticogenesis. *Neuropathol. Appl. Neurobiol.* **23,** 203–211.
12. Fekete, D. M., Homburger, S. A., Waring, M. T., Riedl, A. E., and Garcia, L. F. (1997) Involvement of programmed cell death in morphogenesis of the vertebrate inner ear. *Development* **124,** 2451–2461.
13. Vaahtokari, A., Aberg, T., and Thesleff, I. (1996) Apoptosis in the developing tooth: association with an embryonic signaling center and suppression by EGF and FGF-4. *Development* **122,** 121–129.
14. Hensey, C. and Gautier, J. (1998) Programmed cell death during Xenopus development: a spatio-temporal analysis. *Dev. Biol.* **203,** 36–48.
15. Asai, K., Kudej, R. K., Shen, Y. T., Yang, G. P., Takagi, G., Kudej, A. B., Geng, Y. J., Sato, N., Nazareno, J. B., Vatner, D. E., Natividad, F., Bishop, S. P., and Vatner, S. F. (2000) Peripheral vascular endothelial dysfunction and apoptosis in old monkeys. *Arterioscler. Thromb. Vasc. Biol.* **20,** 1493–1499.
16. Borras, D., Pumarola, M., and Ferrer, I. (2000) Neuronal nuclear DNA fragmentation in the aged canine brain: apoptosis or nuclear DNA fragility? *Acta. Neuropathol. (Berl)* **99,** 402–408.
17. Savory, J., Rao, J. K., Huang, Y., Letada, P. R., and Herman, M. M. (1999) Age-related hippocampal changes in Bcl-2:Bax ratio, oxidative stress, redox-active iron and apoptosis associated with aluminum-induced neurodegeneration: increased susceptibility with aging. *Neurotoxicology* **20,** 805–817.
18. Aggarwal, S., Gollapudi, S., and Gupta, S. (1999) Increased TNF-alpha-induced apoptosis in lymphocytes from aged humans: changes in TNF-alpha receptor expression and activation of caspases. *J. Immunol.* **162,** 2154–2161.
19. Harocopos, G. J., Alvares, K. M., Kolker, A. E., and Beebe, D. C. (1998) Human age-related cataract and lens epithelial cell death. *Invest. Ophthalmol. Vis. Sci.* **39,** 2696–2706.
20. Li, W. P., Chan, W. Y., Lai, H. W., and Yew, D. T. (1997) Terminal dUTP nick end labeling (TUNEL) positive cells in the different regions of the brain in normal aging and Alzheimer patients. *J. Mol. Neurosci.* **8,** 75–82.
21. Troncoso, J. C., Sukhov, R. R., Kawas, C. H., and Koliatsos, V. E. (1996) In situ labeling of dying cortical neurons in normal aging and in Alzheimer's disease: correlations with senile plaques and disease progression. *J. Neuropathol. Exp. Neurol.* **55,** 1134–1142.

22. Aggarwal, S. and Gupta, S. (1998) Increased apoptosis of T cell subsets in aging humans: altered expression of Fas (CD95), Fas ligand, Bcl-2, and Bax. *J. Immunol.* **160,** 1627–1637.
23. Usami, S., Takumi, Y., Fujita, S., Shinkawa, H., and Hosokawa, M. (1997) Cell death in the inner ear associated with aging is apoptosis? *Brain Res.* **747,** 147–150.
24. Kiatipattanasakul, W., Nakamura, S., Hossain, M. M., Nakayama, H., Uchino, T., Shumiya, S., Goto, N., and Doi, K. (1996) Apoptosis in the aged dog brain. *Acta. Neuropathol. (Berl)* **92,** 242–248.
25. Foster, J. R. (2000) Cell death and cell proliferation in the control of normal and neoplastic tissue growth. *Toxicol. Pathol.* **28,** 441–446.
26. Kohji, T., Hayashi, M., Shioda, K., Minagawa, M., Morimatsu, Y., Tamagawa, K., and Oda, M. (1998) Cerebellar neurodegeneration in human hereditary DNA repair disorders. *Neurosci. Lett.* **243,** 133–136.
27. Sugawa, M., Ikeda, S., Kushima, Y., Takashima, Y., and Cynshi, O. (1997) Oxidized low density lipoprotein caused CNS neuron cell death. *Brain Res.* **761,** 165–172.
28. Heesters, M. A., Koudstaal, J., Go, K. G., and Molenaar, W. M. (1999) Analysis of proliferation and apoptosis in brain gliomas: prognostic and clinical value. *J. Neurooncol.* **44,** 255–266.
29. Mundle, S. D., Gao, X. Z., Khan, S., Gregory, S. A., Preisler, H. D., and Raza, A. (1995) Two in situ labeling techniques reveal different patterns of DNA fragmentation during spontaneous apoptosis in vivo and induced apoptosis in vitro. *Anticancer. Res.* **15,** 1895–1904.
30. Bodis, S., Siziopikou, K. P., Schnitt, S. J., Harris, J. R., and Fisher, D. E. (1996) Extensive apoptosis in ductal carcinoma in situ of the breast. *Cancer* **77,** 1831–1835.
31. Chia, S. J., Tang, W. Y., Elnatan, J., Yap, W. M., Goh, H. S., and Smith, D. R. (2000) Prostate tumours from an Asian population: examination of bax, bcl-2, p53 and ras and identification of bax as a prognostic marker. *Br. J. Cancer* **83,** 761–768.
32. Yamasaki, F., Tokunaga, O., and Sugimori, H. (1997) Apoptotic index in ovarian carcinoma: correlation with clinicopathologic factors and prognosis. *Gynecol. Oncol.* **66,** 439–448.
33. Kiyozuka, Y., Akamatsu, T., Singh, Y., Ichiyoshi, H., Senzaki, H., and Tsubura, A. (1999) Optimal prefixation of cells to demonstrate apoptosis by the TUNEL method. *Acta. Cytol.* **43,** 393–399.
34. Zhang, X. and Takenaka, I. (2000) Cell proliferation and apoptosis with BCL-2 expression in renal cell carcinoma. *Urology* **56,** 510–515.
35. Hindermann, W., Berndt, A., Wunderlich, H., Katenkamp, D., and Kosmehl, H. (1997) Quantitative evaluation of apoptosis and proliferation in renal cell carcinoma. Correlation to tumor subtype, cytological grade according to thoenes-classification and the occurrence of metastasis. *Pathol. Res. Pract.* **193,** 1–7.
36. Thomas, L. B., Gates, D. J., Richfield, E. K., O'Brien, T. F., Schweitzer, J. B., and Steindler, D. A. (1995) DNA end labeling (TUNEL) in Huntington's disease and other neuropathological conditions. *Exp. Neurol.* **133,** 265–272.
37. Jellinger, K. A. (2000) Cell death mechanisms in Parkinson's disease. *J. Neural. Transm.* **107,** 1–29.

38. He, Y., Lee, T., and Leong, S. K. (2000) 6–Hydroxydopamine induced apoptosis of dopaminergic cells in the rat substantia nigra. *Brain Res.* **858,** 163–166.
39. Kingsbury, A. E., Mardsen, C. D., and Foster, O. J. (1998) DNA fragmentation in human substantia nigra: apoptosis or perimortem effect? *Mov. Disord.* **13,** 877–884.
40. Kitt, C. A. and Wilcox, B. J. (1995) Preliminary evidence for neurodegenerative changes in the substantia nigra of Rett syndrome. *Neuropediatrics* **26,** 114–118.
41. Anderson, A. J., Stoltzner, S., Lai, F., Su, J., and Nixon, R. A. (2000) Morphological and biochemical assessment of DNA damage and apoptosis in Down syndrome and Alzheimer disease, and effect of postmortem tissue archival on TUNEL. *Neurobiol. Aging.* **21,** 511–524.
42. Ekegren, T., Grundstrom, E., Lindholm, D., and Aquilonius, S. M. (1999) Upregulation of Bax protein and increased DNA degradation in ALS spinal cord motor neurons. *Acta. Neurol. Scand.* **100,** 317–321.
43. Kerrigan, L. A., Zack, D. J., Quigley, H. A., Smith, S. D., and Pease, M. E. (1997) TUNEL-positive ganglion cells in human primary open-angle glaucoma. *Arch. Ophthalmol.* **115,** 1031–1035.
44. Smale, G., Nichols, N. R., Brady, D. R., Finch, C. E., and Horton, W. E., Jr. (1995) Evidence for apoptotic cell death in Alzheimer's disease. *Exp. Neurol.* **133,** 225–230.
45. Davies, K. J. (1995) Oxidative stress: the paradox of aerobic life. *Biochem. Soc. Symp.* **61,** 1–31.
46. Facchinetti, F., Dawson, V. L., and Dawson, T. M. (1998) Free radicals as mediators of neuronal injury. *Cell. Mol. Neurobiol.* **18,** 667–682.
47. Jenner, P. and Olanow, C. W. (1998) Understanding cell death in Parkinson's disease. *Ann. Neurol.* **44,** S72–84.
48. Nunomura, A., Perry, G., Pappolla, M. A., Wade, R., Hirai, K., Chiba, S., and Smith, M. A. (1999) RNA oxidation is a prominent feature of vulnerable neurons in Alzheimer's disease. *J. Neurosci.* **19,** 1959–1964.
49. Mecocci, P., MacGarvey, U., and Beal, M. F. (1994) Oxidative damage to mitochondrial DNA is increased in Alzheimer's disease. *Ann. Neurol.* **36,** 747–751.
50. Mecocci, P., Polidori, M. C., Ingegni, T., Cherubini, A., Chionne, F., Cecchetti, R., and Senin, U. (1998) Oxidative damage to DNA in lymphocytes from AD patients. *Neurology* **51,** 1014–1017.
51. Zhang, J., Perry, G., Smith, M. A., Robertson, D., Olson, S. J., Graham, D. G., and Montine, T. J. (1999) Parkinson's disease is associated with oxidative damage to cytoplasmic DNA and RNA in substantia nigra neurons. *Am. J. Pathol.* **154,** 1423–1429.
52. Browne, S. E., Bowling, A. C., MacGarvey, U., Baik, M. J., Berger, S. C., Muqit, M. M., Bird, E. D., and Beal, M. F. (1997) Oxidative damage and metabolic dysfunction in Huntington's disease: selective vulnerability of the basal ganglia. *Ann. Neurol.* **41,** 646–653.
53. Polidori, M. C., Mecocci, P., Browne, S. E., Senin, U., and Beal, M. F. (1999) Oxidative damage to mitochondrial DNA in Huntington's disease parietal cortex. *Neurosci. Lett.* **272,** 53–56.

54. Ferrante, R. J., Browne, S. E., Shinobu, L. A., Bowling, A. C., Baik, M. J., MacGarvey, U., Kowall, N. W., Brown, R. H., Jr., and Beal, M. F. (1997) Evidence of increased oxidative damage in both sporadic and familial amyotrophic lateral sclerosis. *J. Neurochem.* **69,** 2064–2074.
55. Bogdanov, M., Brown, R. H., Matson, W., Smart, R., Hayden, D., O'Donnell, H., Flint Beal, M., and Cudkowicz, M. (2000) Increased oxidative damage to DNA in ALS patients [In Process Citation]. *Free Radic. Biol. Med.* **29,** 652–658.
56. Goyal, V. K. (1982) Lipofuscin pigment accumulation in human brain during aging. *Exp. Gerontol.* **17,** 481–487.
57. Stojanovic, A., Roher, A. E., and Ball, M. J. (1994) Quantitative analysis of lipofuscin and neurofibrillary tangles in the hippocampal neurons of Alzheimer disease brains. *Dementia* **5,** 229–233.
58. Usachev, Y. M., Khammanivong, A., Campbell, C., and Thayer, S. A. (2000) Particle-mediated gene transfer to rat neurons in primary culture. *Pflugers Arch.* **439,** 730–738.
59. Nunomura, A., et al. (1999) RNA oxidation is a prominent feature of vulnerable neurons in Alzheimer's disease. *J. Neurosci.* **19,** 1959–1964.

18

The *In Situ* Detection of Apurinic/Apyrimidinic Sites and DNA Breaks Bearing Extension Blocking Termini

Philip K. Liu, Jiankun Cui, Niki Moore, and Dongya Huang

1. Introduction

Stroke is a major cause of disability in the United States affecting approximately 500,000 people per year at a rate of one person every minute. Stroke induces a decrease in ATP, an increase in the expression of immediate early genes, and causes oxidative damage to DNA, RNA, protein and lipid. One determinant of recovery is the ability of the affected brain cells to repair themselves. Very little is known about oxidative damage to DNA and RNA in the brain. Tissue culture studies indicate that the presence of oxidative lesions in DNA and RNA can terminate or change coding properties during translation, transcription, and replication. The molecular lesions can be detected using gas chromatography/mass spectrometry ***(1–5)***, high-pressure liquid chromatography with electrochemical detection or with salicylate treatment ***(5–11)***, and immunohistochemistry ***(12–17)***. Recently, a nucleic acid probe has been generated that binds to an abnormal guanine base, 8-hydroxyguanine (oh8G) (**Fig. 1**) ***(18)***. In addition, nucleic acids without a base (apurinic/apyrimidinic sites, AP sites) can be detected using a biotin-containing aldehyde-reactive probe ***(19,20)***. AP sites are generated by a breakage in the glycosylic bond between the base and ribose. Other types of DNA/RNA lesions are DNA single-stranded breaks (SSBs), which involve the breakage of bonds that create a phosphate terminus (3'-PO_4: with a phosphomonoester bond to 3'-ribose, **Fig. 1**), or a 3'-phosphoglycolate terminus (3'-PG, a breakage on the ribose/deoxyribose, **Fig. 1**). Some of these lesions can also be detected by the inability of the DNA to serve as a template for polymerase chain reaction ***(21,22)***. Several laboratories have detected modified bases in the brain after brain injury ***(5,16,23,24)***. However, with the exception of immunohistochemical assays using antibodies,

From: *Methods in Molecular Biology, vol. 203:* In Situ *Detection of DNA Damage: Methods and Protocols*
Edited by: V. V. Didenko

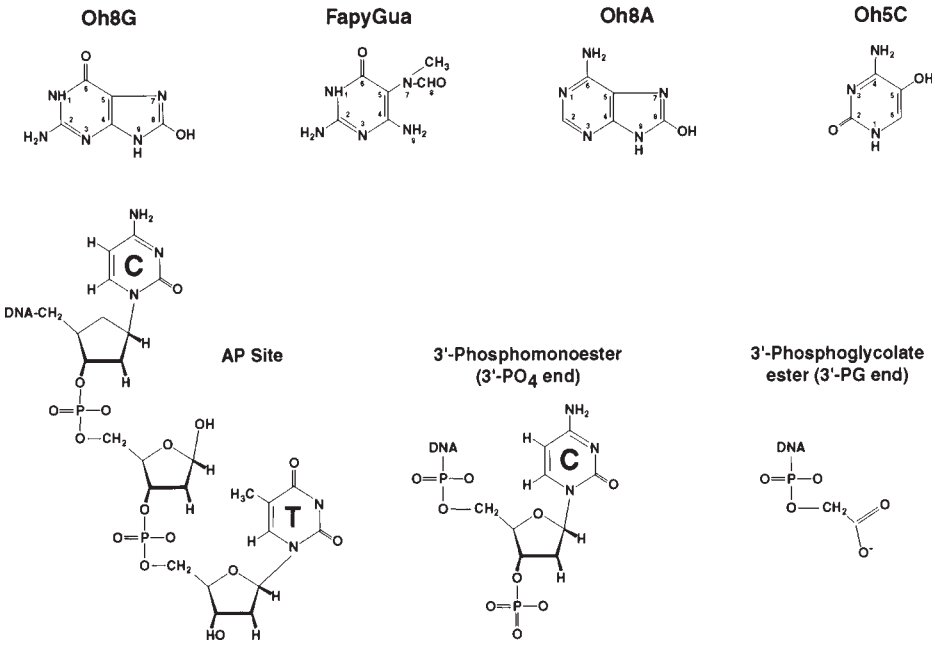

Fig. 1. Oxidative DNA damage found in brain after cerebral oxidative stress (Reproduced with permission from ***24a***. Abnormal DNA bases: 8-hydroxyguanine (oh8G), 2,6 diamino-4-hydroxy-5-N-methylformamidopyrimidine (FapyGua), 8-hydroxyadenine (oh8A), 5'-hydroxycytosine (oh5C). AP site (deoxyribose without base is shown between cytosine and thymine); Two strand breaks (3'-phosphate and 3'-phosphoglycolate) are present at the ends of the broken DNA strands.

none of these assays definitively locate the lesions in the tissue. In addition, monoclonal antibodies used in immunohistochemical assays do not distinguish oxidative lesions in DNA from those in RNA. To study the effect of DNA lesions in the brain, we have developed *in situ* assays for the detection of oxidative DNA lesions in the brain.

Fig. 1 shows seven nucleic acid lesions that have been detected in the brain. Apurinic/apyrimidinic sites permit trans-lesional synthesis by RNA or DNA polymerases ***(25,26)***. Therefore, AP sites may allow aberrant transcription ***(27)***. In addition, DNA SSB with a 3'-PO_4 or a 3'-PG terminus can support neither terminal extension by polymerases, nor ligation by DNA ligase. These DNA polymerase-blocking lesions are not detectable by common assays. To determine whether cell nuclei contain these lesions, we have developed assays using a combination of lesion-specific nucleases and the Klenow fragment of DNA polymerase I. Two lesion-specific nucleases that have been used are those that

Table 1
***E. Coli* AP Endonucleases (Class II)**

Name	Endonuclease IV	Exonuclease III
Size (Kda)	31.5	30.9
Activities	AP endonuclease 3'phosphodiesterase 3'phosphomonoesterase	3'phosphomonoesterase AP endonuclease 3'phosphodiesterase 3'–5'exonuclease RNase H
Cofactor	Mg^{++} (EDTA sensitive)	Mg^{++} (EDTA sensitive)

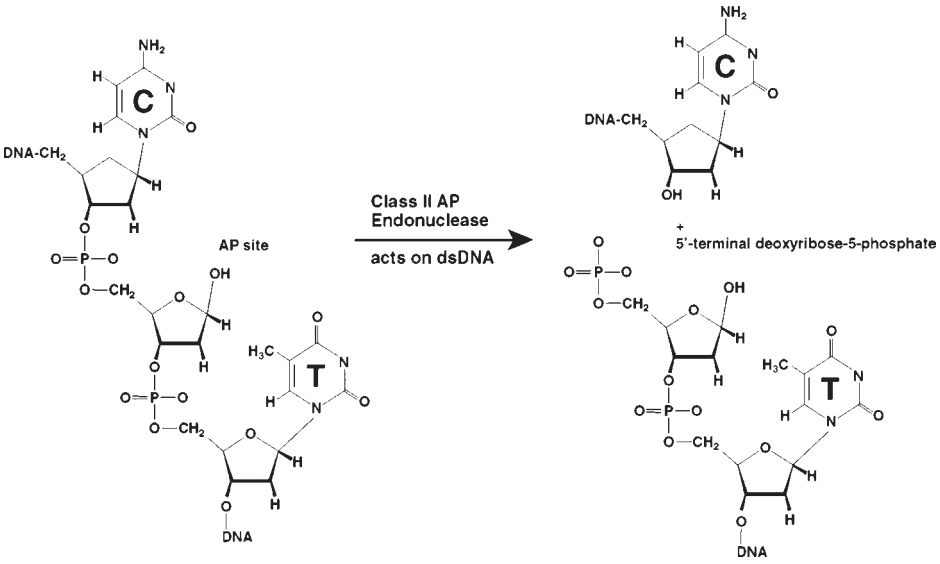

Fig. 2. The first step of AP site removal by Class II AP endonuclease. A DNA fragment with a 3'OH end is generated from DNA with an AP site using AP endonuclease. The 3'OH end that is generated can be labeled as described in the text.

remove both AP sites and SSBs with a 3'-PO_4 or a 3'-PG terminus ***(28,29)***. These AP endonucleases (class II, **Table 1**) are E. coli exonuclease III (Exo-III) and endonuclease IV (Endo-IV). This method has allowed us to demonstrate the presence of these two types of SSBs and AP sites in genomic DNA, both of which can have adverse biological consequences ***(27,30–32)***. **Fig. 2** shows the reaction catalyzed by AP endonuclease. A normal 3'-OH end is specifically generated after *in situ* treatment of DNA with E. coli AP endonuclease. This 3'-OH end can be labeled using a Klenow fragment of DNA

polymerase I in the presence of digoxigenin-11-2'-deoxy-uridine-5'-triphosphate (dig-dUTP) in the dNTP reaction mix. The incorporated dig-dUTP is detected using alkaline phosphatase- or fluorescein-conjugated antibodies against digoxigenin. In this chapter we will describe the method that detects specific sensitive sites in DNA using class II AP endonucleases.

We typically use four 20-µm-thick sections from each rat brain (*see* **Note 1**). The samples are dried in a low vacuum at room temperature (23°C) for 2–16 h. They are then treated with proteinase K (0.02 mg/mL) at 37°C for 15 min, followed by six one-minute washes in sterile H_2O. The sections are incubated with E. coli Exo-III (40 U/50 µL/slide) or Endo-IV (4 U/50 µL/slide) in a humidified chamber at 37°C for 3 h and subsequently washed three times with phosphate-buffered saline (PBS). The samples are then labeled by incorporating dig-dUTP/dNTP into the 3'-OH ends using the Klenow fragment of DNA polymerase-I (0.15 U/50 µL/slide) at 37°C for 1 h. After washing the tissue sections with PBS, the slides are incubated with anti-digoxigenin antibody conjugated to FITC (green fluorescence) under dim light at room temperature for 1 h. To identify nuclear DNA, the sample is stained with propidium iodide, which binds to nuclear DNA and fluoresces red. Control tissue samples include brain sections from sham-operated animals treated with the same endonuclease, or from animals exposed to cerebral ischemia not treated with AP endonuclease (negative controls, *see* **Note 2**).

This technique works well in frozen tissue sections. High background fluorescence is usually observed with paraffin-embedded tissue sections. The negative controls should exhibit no significant incorporation of dig-dUTP. These types of DNA lesions in tissue after brain injury depend on Exo-III or Endo-IV enzymes to create 3'-OH ends for labeling by the Klenow fragment of DNA polymerase I, and are different from DNA damage resulting from apoptotic DNA fragmentation ***(17,30)***.

2. Materials

All enzymes were tested before use for optimal concentration (*see* **Note 3**), time of incubation (*see* **Note 4**), and temperature (*see* **Note 5**).

1. AP endonucleases (Exo-III or Endo IV, Trevigen, Gaithersburg, MD).
2. Proteinase K (Qiagen, Valencia, CA).
3. Digoxigenin-11–2'-deoxy-uridine-5'-triphosphate (Roche Molecular Biochemicals, Indianapolis, IN).
4. DNase I (10 U/µL) (Roche Molecular Biochemicals, Indianapolis, IN).
5. Klenow fragment of DNA polymerase-I (Roche Molecular Biochemicals, Indianapolis, IN).
6. Anti-GFAP-Texas Red (Sigma Chem Co. St Louis, MO).
7. Poly-L-lysine-coated slides (Fisher Scientific, Pittsburgh, PA).

8. The anti-dig-Fluorescein was from ApopTag® Fluorescein kit [Serologicals Corp. (formerly Intergen), Gaithersburg, MD].
9. Freshly prepared fixatives contain 4% paraformaldehyde in 0.1 *M* PBS (pH 7.4).
10. DNase I working buffer: 30 m*M* Tris-HCl (pH 7.2), 140 m*M* cacodylate, 4 m*M* $MgCl_2$, 0.1 m*M* dithiothreitol.
11. Phosphate buffered saline (PBS): 0.1 *M*, pH 7.4; each liter contains 8 g NaCl, 1.3 g dibasic phosphate, 0.2 g monobasic phosphate).
12. *E. coli* Endo IV buffer (10× working concentration): 50 m*M* Tris-HCl (pH 8.0), 5 m*M* $MgCl_2$ and 1 m*M* dithiothreitol.
13. dig-dUTP-dNTP mix: 1 m*M* each of dATP, dCTP and dGTP with 0.65 m*M* dTTP and 0.35 m*M* digoxigenin-11-dUTP.
14. Working mix for post labeling using dig-dUTP (for 10 samples): 50 µL of 0.1 *M* Tris-HCl (pH 8.3), 50 µL of 0.5 *M* KCl, 50 µL of $MgCl_2$ (25 m*M*), 5 µL of dig-dUTP/dNTP mix, 0.75 µL of the Klenow fragment of DNA polymerase I (2 U/µL), 4.25 µL of dithiothreitol (100 m*M*), add 340 µL H_2O to a total of 500 µL.

3. Methods

3.1. Tissue Preparation (Retrograde Perfusion)

The volume of fixative and the time of fixation are for a 250 g rat. For a 20–25 g mouse, use one-tenth the volume for the rat. Solution should be freshly prepared (within 24 h).

1. Anesthetize the animal by intraperitoneal injection with general anesthesia of choice (e.g., nembutol 80 mg/kg, i.p.); use slightly more than the usual surgical dose for very deep anesthesia. Secure the limbs of the animal.
2. Fill pump tubing with saline before opening the abdominal cavity or the chest cavity.
3. Insert the cannula into the base of the left ventricle of the heart.
4. Start perfusion with saline as soon as the right atrium is opened to allow outflow.
5. Perfuse with 300 mL of saline (at 40 mL/min) to clear the blood from the vasculature (in the mouse: 40 mL saline at 5 mL/min).
6. Change to 4% paraformaldehyde in phosphate buffered saline (PBS). Spasm of the limbs shortly after paraformaldehyde perfusion is expected in a good perfusion. Remove the brain and place in a 4% paraformaldehyde solution for 4–6 h.
7. Change to 20% sucrose in 4% paraformaldehyde and store at 4°C overnight.
8. Prepare frozen sections (20 micrometer [µm]-thick) and mount on poly-L-lysine coated slides.

3.2 Frozen Tissue Section

1. Cut 10–15 µm thick frozen sections in a cryostat.
2. Collect free-floating sections in cold PBS.
3. Mount sections onto subbed poly-L-lysine-coated slides as soon as possible after cutting. Air dry sections for about 10–15 min and then store them at –70°C.

4. Frozen tissue sections stored in this condition are suitable for AP site detection for up to 3 months.

3.3. Detection of Sensitive Sites to DNA Repair Enzymes

1. Let sections dry overnight under vacuum at room temperature before the experiment.
2. Protein digestion: Incubate sections in proteinase K (20 µg/mL in PBS) for 15 min at 37°C.
3. Wash sections in sterilized double-distilled water (ddH_2O) 6 × 1 min.
4. Add AP endonuclease (Exo-III [40U/50 µL], or Endo-IV [4U/50 µL]). Incubate for 3 h at 37°C. Negative and positive testers should always be included to assist with the interpretation of data (*see* **Note 2**).
5. Wash in PBS, 3 × 5 min.
6. Incubate in the working mix for post labeling using dig-dUTP (50 µL/reaction), 1 h at 37°C (*see* **Note 6**).
7. Repeat Step 5
8. Incubate 1 h with 2% normal goat serum + 1% bovine serum albumin (BSA) in PBS at room temperature (50 µL/slide). For double staining, prepare antibody (e.g., antibody against glial fibrillary acidic protein (GFAP, *see* **Note 7**).
9. Add primary anti-GFAP antibody (rabbit, 1:80, Sigma Chem, code G9269) with 1% normal goat serum +1% BSA + PBS, 50 µL/slide.
10. Incubate 1 h at room temperature or overnight at 4°C.
11. Wash in PBS with 0.1% Triton X-100, 3 × 5 min.
12. Add working strength antibody solution that detects dig-dUTP: Anti-dig-Fluorescein (ApopTag®) 16 µL, and blocking solution 38 µL (54 µL/slide).
13. Incubate 1 h at RT under dim light.
14. Repeat Step 11.
15. GFAP is detected by adding secondary antibody (Goat anti-Rabbit IgG Texas Red (1:800), Jackson ImmunoResearch Laboratories, Inc), 50 µL/slide.
16. Repeat Step 11.
17. Mount on a cover slip.
18. Observe signals under microscope with a fluorescent light source or store at –20°C (*see* **Note 8**).

4. Notes

1. The final concentration of AP endonuclease in the reaction mix needs to be adjusted for thicker tissue sections. The incubation of 50 µm sections in the free-floating protocol requires additional AP endonuclease compared to the 20 µm thick sections. To determine the suitable concentration, *see* **Note 3**.
2. On separate slides, include negative and positive controls. Negative controls are samples without one of the following: AP endonuclease, Klenow fragment of DNA polymerase I, dig-dUTP, or the secondary antibody. To make sure that all solutions work properly, we also make positive controls. Positive controls are made by treating normal brain tissue section with DNase I (20 U/100 µL in DNase I buffer) for 10 min at 37°C, followed by five one-minute washes in

water. The positive control sections are passed through graded ethanol concentrations (one min in each of the following: 50%, 75%, 90% and 100% ethanol), and then air-dried. The positive controls are stored at –20°C. We generally make 10 positive control slides and use at least one in each experiment. In the event that none of the testing samples gives a positive signal, positive controls are needed to determine if all solutions work properly. If the positive control does not produce a signal, use a new set of working solutions and enzymes.

3. We recommend a test for a suitable working concentration for each new enzyme (AP endonuclease and Klenow fragment of DNA polymerase I) that you purchase from commercial sources, because the enzymes may not be uniform in activity and often contain non-specific DNases. Excessive amounts of AP endonuclease or Klenow fragment of DNA polymerase I may give the reaction a positive signal due to contaminating nucleases. The objective of this testing is to demonstrate the lowest concentration that will give a positive signal in positive samples from a previous testing (e.g. ischemic brain samples) and give no signal in non-ischemic samples. In the case of EXO III, four positive samples are treated with four concentrations of enzyme (40, 20, 10, 5 U per 50 µL) in a given incubation time (20 µm-thick tissue section, 4 h at 37°C).
4. We recommend a test for a suitable incubation time for the each new enzyme (AP endonuclease and Klenow fragment of DNA polymerase I) that you purchase. Once the concentration of the enzyme in each new lot is determined, the optimal incubation time is determined by incubating a positive control section with the enzyme for different time periods (0.5 h, 1 h, 2 h, 4 h, and 6 h at 37°C). The shortest incubation time that gives a positive signal is considered optimal.
5. We recommend a test for a suitable temperature be preformed for each new enzyme (AP endonuclease and Klenow fragment of DNA polymerase I) to get the best results. The temperatures of 23°C (room temperature), 30°C and 37°C are tested for the lowest temperature that works for the reaction.
6. We recommend preparing enough dig-dUTP/dNTP mix for at least 10 reactions.
7. For a given antibody, determine the lowest dilution that gives a positive signal on a slide treated with the primary antibody. Without the primary antibody, the dilution should not give any positive signal.
8. Depending on the initial signal strength, the fluorescent signal is visible for approximately two weeks.

Acknowledgments

Research is supported by grants from NINDS (NS34810) and American Heart Association (9640202N). PKL is an Established Investigator of American Heart Association. We thank Mr. T. Arora for assisting the preparation of this manuscript.

References

1. Aruoma, O. I., Halliwell, B., Gajewski, E. and Dizdaroglu, M. (1989) Damage to the bases in DNA induced by hydrogen peroxide and ferric ion chelates. *J. Biol. Chem*. **264,** 20,509–20,512.

2. Aruoma, O. I., Halliwell, B. and Dizdaroglu, M. (1989) Iron ion-dependent modification of bases in DNA by the superoxide radical-generating system hypoxanthine/xanthine oxidase. *J. Biol. Chem*. **264,** 13,024–13,028.
3. Dizdaroglu, M. (1992) Oxidative damage to DNA in mammalian chromatin. *Mut. Res.* **275,** 331–342.
4. Kasprzak, K. S., Diwan, B. A., Rice, J. M., Misra, M., Riggs, C. W., Olinski, R. and Dizdaroglu, M. (1992) Nickel (II)-mediated oxidative DNA base damage in renal and hepatic chromatin of pregnant rats and their fetuses. Possible relevance to carcinogenesis. *Chem. Res. Toxicol.* **5,** 809–815.
5. Liu, P. K., Hsu, C. Y., Dizdaroglu, M., Floyd, R. A., Kow, Y. W., Karakaya, A., Rabow, L. E., Cui, J. K. (1996) Damage, repair and mutagenesis in nuclear genes after mouse forebrain ischemia-reperfusion. *J. Neurosci.* **16,** 6795–6806.
6. Mecocci, P., MacGarvey, U., Kaufman, A. E., Koontz, D., Shoffner, J. M., Wallace, D. C., and Beal, M. F. (1993) Oxidative damage to mitochondrial DNA shows marked age-dependent increases in human brain. *Ann. Neurol*. **34,** 609–616.
7. Helbrock, H. J., Beckman, K. B., Shigenaga, M. K., Walter, P. B., Woodall, A. A., Yeo, H. C. and Ames, B. N. (1998) DNA oxidative matters: The HPLC-electrochemical detection assay of 8-oxo-deoxyguanosine and 8-oxo-guanine. *Proc. Natl. Acad. Sci. USA* **95,** 288–293.
8. Floyd, R. A., Watson, J. J., and Wong, P. K. (1984) Sensitive assay of hydroxyl free radical formation utilizing high pressure liquid chromatography with electrochemical detection of phenol and salicylate hydroxylation products. *J. Biochem. Biophys. Methods* **10,** 221–235.
9. Grootveld, M., and Halliwell, B. (1986) Aromatic hydroxylation as a potential measure of hydroxyl-radical formation *in vivo*. *Biochemistry* **237,** 499–504.
10. Althaus, J. S., Andrus, P. K., Williams, C. M., Von-voigtlander, P. F., Cazers, A. R., and Hall, E. D. (1993) The use of salicylate hydroxylation to detect hydroxyl radical generation in ischemic and traumatic brain injury. Reversal by tirilazad mesylate (U-74006F). *Mol. Chem. Neuropathol.* **20,** 147–162.
11. Hall, E. D., Andrus P. K., and Yonkers, P. A. (1993) Brain hydroxyl radical generation in acute experimental head injury. *J. Neurochem*. **60,** 588–594.
12. Schulz, J. B., Mathews, R. T., Jenkins, B. G., Ferrante, R. J., Siwek, D., Henshaw, D. R., Cipolloni, P. B., Mecocci, P., Kowall, N. W., Rosen, B. R. and Beal, M. F. (1995) Blockade of neuronal nitric oxide synthase protects against excitotoxicity *in vivo*. *J. Neurosci*. **15,** 8419–8429.
13. Park, E-M., Shigenaga, M. K., Degan, P., Korn, T. S., Kitzler, J. W., Wehr, C. M., Kolachana, P. and Ames, B. N. (1992) Assay of excised oxidative DNA lesions: Isolation of 8-oxoguanine and its nucleoside derivatives from biological fluids with a monoclonal antibody column. *Proc. Natl. Acad. Sci. USA* **89,** 3375–3379.
14. Nunomura, A., Perry, G., Pappolla, M. A., Wade, R., Hirai, K., Chiba, S., Smith, M. A. (1999) RNA oxidation is a prominent feature of vulnerable neurons in Alzheimer's disease. *J. Neurosci.* **19,** 1959–1964.
15. Won, M. H., Kang, T. C., Jeon, G. S., Lee, J. C., Kim, D. Y., Choi, E. M., Lee, K. H., Choi, C. D., Chung, M. H. and Cho, S. S. (1999) Immunohistochemical detec-

tion of oxidative DNA damage induced by ischemia-reperfusion insults in gerbil hippocampus *in vivo*. *Brain Res*. **836,** 70–78.
16. Cui, J. K., Holmes, E. H., Liu, P. K. (1999) Oxidative Damage to the c-fos gene and reduction of its transcription after focal cerebral ischemia. *J. Neurochem.* **73,** 1164–1174.
17. Cui, J. K., Holmes, E. H., Cao, S. T., Greene, T. G., and Liu, P. K. (2000) Oxidative DNA damage precedes DNA fragmentation after experimental stroke in rat brain. *FASEB J.* **14,** 955–967.
18. Rink, S. M., Shen, J. C. and Loeb, L. A. (1998) Creation of RNA molecules that recognize the oxidative lesion 7,8-dihydro-8-hydroxy-2'-deoxyguanosine (8-oxodG) in DNA. *Proc. Natl. Acad. Sci. USA* **95,** 11,619–11,624.
19. Lan, J., Hanshall, D. C., Simon, R. P., Chen, J. (2000) Formation of the base modification 8-hydroxyl-2'-deoxyguanosine and DNA fragmentation following seizures induced by systemic Kainic acid in the rat. *J. Neurochem.* **74,** 302–309.
20. Atamna, H., Cheung, I. and Ames, B. (2000) A method for detecting abasic sites in living cells: Age-dependent changes in base excision repair. *Proc. Natl. Acad. Sci. USA* **97,** 686–691.
21. Englander, E. W., Greeley, G. H. Jr., Wang, G., Perez-Polo, J. R., and Lee, H. M. (1999) Hypoxia-induced mitochondrial and nuclear DNA damage in the rat brain. *J. Neurosci. Res.* **58,** 262–269.
22. Yakes, F. M. and van Houten, B. (1997) Mitochondrial DNA damage is more extensive and persists longer than nuclear DNA damage in human cells following oxidative stress. *Proc. Natl. Acad. Sci. USA* **94,** 514–519.
23. Nouspikel, T. and Hanawalt, P. C. (2000) Terminally differentiated human neurons repair transcribed genes but display attenuated global DNA repair and modulation of repair gene expression. *Molec. Cell. Biol.* **20,** 1562–1570.
24. Lin, L., Cao, S., Yu, L., Cui, J., Hamilton, W. J. and Liu, P. K. (2000) Up-regulation of base excision repair activity for 8–2'deoxyhroxyl guanosine in the mouse brain after forebrain ischemia-reperfusion. *J. Neurochem.* **74,** 1098–1105.

24a. Liu, P. K., Grossman, R. G., Hsu, C. Y., and Robertson, C. S. (2001) Ischemic injury and faulty gene transcripts in the brain, *Trends Neurosci.* **24,** 581–588.

25. Zou, W. and Doetsch, P. W. (1993) Effects of abasic sites and DNA single-strand breaks on prokaryotic RNA polymerases. *Proc. Natl. Acad. Sci. USA* **90,** 6601–6605.
26. Loeb, L. A., Preston, B. D. (1986) Mutagenesis by apurinic/apyrimidinic sites. *Annu. Rev. Genet.* **20,** 201–230.
27. Cui, J. K. and Liu, P. K. (2001) Neuronal NOS inhibitor that reduces oxidative DNA lesions and neuronal sensitivity increases the expression of intact c-fos transcripts after brain injure. *J. Biomedical Sci.* **8,** 336–341.
28. Krokan, H. E., Standal, R. and Slupphaug, G. (1997) DNA glycosylases in the base excision repair of DNA. *Biochem. J.* **325,** 1–16.
29. Wilson, D. M., Engelward, B. P. and Samson, L. (1998) Prokaryotic base excision repair, in *DNA Damage and Repair, volume I, DNA Repair in Prokaryotes and*

Lower Eukaryotes (Nickoloff, J. A. and Hoekstra, M. F., eds.) Humana, Totowa, NJ, pp. 29–64.
30. Huang, D., Shenoy, A., Huang, W., Cao, S., Cui, J. and Liu, P. K. (2000) *In situ* detection of AP sites and DNA single stranded breaks with 3'-phosphate terminus in cerebral ischemia-reperfusion. *FASEB J.* **14,** 407–417.
31. Cui, J. K. and Liu, P. K. (2001) Expression of aberrant messenger RNA during oxidative stress in the mouse brain: transcription activators from nuclear genes that are damaged. Submitted.
32. Fujimura, M. Fujimura, M., Morita-Fujimura, Y., Kawase, M., and Chan, P. H. (1999) Early decrease of apurinic/apyrimidinic endonuclease expression after transient focal cerebral ischemia in mice. *J. Cereb. Blood Flow Metab.* **19,** 495–501.
33. Wilson, S. H. and Singhal, R. K. (1998) Mammalian DNA repair and the cellular DNA polymerases, in *DNA Damage and Repair, volume II, DNA Repair in Higher Eukaryotes* (Nickoloff, J. A. and Hoekstra, M. F., eds.) Humana Press, Totowa, NJ, pp. 161–180.

19

Markers of Poly (ADP-Ribose) Polymerase Activity as Correlates of DNA Damage

Yinong Zhou, Shi Liang, and Lawrence R. Williams

1. Introduction

Poly (ADP-ribose) polymerase (PARP-1; EC 2.4.2.30) is a predominantly nuclear enzyme long presumed to function in the identification and repair of DNA strand nicks and breaks (for recent reviews *see*: ***1–3***). PARP is comprised of a N-terminal DNA-binding domain, a central automodification domain (site of auto poly-ADP-ribosylation), and a C-terminal catalytic domain. In its traditional role, PARP-1 is believed to be activated following single or double strand DNA breakage induced by a variety of stressors such as UV radiation, and oxidative stressors such as hydrogen peroxide, and the superoxide, hyroxyl, and peroxynitrite free radicals ***(4–6)***. In response, PARP is known to polyribosylate itself and a variety of other (predominantly nuclear) proteins. Nicotinamide adenine dinucleotide (NAD^+) is the substrate for the reaction, and intracellular stores of NAD^+ are consumed as the polymers of ADP-ribose (PAR) are formed by activated PARP ***(7)***.

Ischemia-reperfusion injury has been shown to cause extensive DNA injury in several models of focal cerebral stroke. The TUNEL procedure (*see* Part I, this volume), identifies numerous positive cells, mostly neurons in the core and penumbra of cortical infarcts. ***(8–13)***. Our model of choice for studying DNA injury following cerebral ischemia-reperfusion is the 3-vessel permanent middle cerebral artery occlusion (MCAO) paradigm ***(14)***. In this model, after 90 min of ischemia and 10 min of carotid reperfusion, extensive DNA injury can be identified in the area at risk using both TUNEL and ligase oligonucleotide methods, even at this very early time period (Didenko, personal communication).

Methods using isotopically-labeled NAD^+ have been described for the tissue localization of PARP using an *in situ* enzymatic procedure (PARIS)

From: *Methods in Molecular Biology, vol. 203:* In Situ *Detection of DNA Damage: Methods and Protocols*
Edited by: V. V. Didenko

(15,16). Pieper et al. *(17)* improved the resolution of this these techniques using custom-ordered P^{33}-labeled NAD^+. Zhang *(18)* developed a method for synthesis of biotinylated NAD as a non-isotopic PARP substrate for Western blot analysis of ADP-ribosylated proteins.

In this chapter, two techniques are described for the non-isotopic localization of PAR in rat brain using histochemical methodologies and commercially available reagents. Sites of active PAR synthesis can be identified by incubating fresh tissue with biotinylated substrate (NAD^+), and after fixation, localizing the incorporation of the labeled substrate into PAR using avidin conjugates. Changes in PAR can be visualized using traditional immunohistochemical techniques with specific polyclonal antibodies to PAR. We have applied these techniques to study the changes in PAR in our focal cerebral ischemia model. After 10 min of reperfusion following 90 min ischemia, PARP enzyme activity is increased as seen with the PARIS method (**Fig. 1**) and the number of PAR-positive cells is increased as identified by PAR immunohistochemistry (**Fig. 2**). The increases in both of these markers correlates well with the incidence of DNA damage identified by the direct marking methods.

Recently, the understanding of the roles PARP plays in genomic homeostasis and response to stress has become more complex. At least four other gene products have been identified that posses poly(ADP-ribosyl)ation enzyme activity *(3)*. These include PARP-2 *(19)*, PARP-3 *(20)*, VARP *(21)*, and tankyrase *(22)*. Recently, PARP-1 has been shown to exist in a short form (sPARP-1) that does not require DNA strand breaks for activation *(2)*. In an *in vivo* study, Pieper et al., *(17)* found that constitutive PARP activity was low in some tissues, such as brain, but was surprisingly high in other tissues, particularly kidney and pancreas. Intriguingly, the levels of activity in these peripheral tissues did not correlate with extent or incidence of DNA damage. However, in ischemic brain the PARIS activity correlates very well with the incidence of DNA damage.

2. Materials

2.1. *PAR* In Situ *Assay (PARIS)*

1. Biotinylated NAD (6-biotin-17 nicotinamide-adenine-dinucleotide). Activity measurement for NAD requiring enzyme. Trevigen, Inc., Gaithersburg, MD 20877 U.S.A.
2. PARIS buffer: 56 m*M* HEPES ph 7.5, 28 m*M* KCl, 28 m*M* NaCl, 5 m*M* $MgCl_2$, 0.01% Digitonin, 2 m*M* DTT and 1 m*M* novobiocin.
3. !0% Trichloroacetic acid. A reagent for stopping reaction.
4. Avidin Peroxidase Complex: A complex of peroxidase enzyme and avidin VECTASTAIN ABC-Peroxidase Kits, Vector laboratory, Inc., Burlingame, CA 94010, U.S.A.

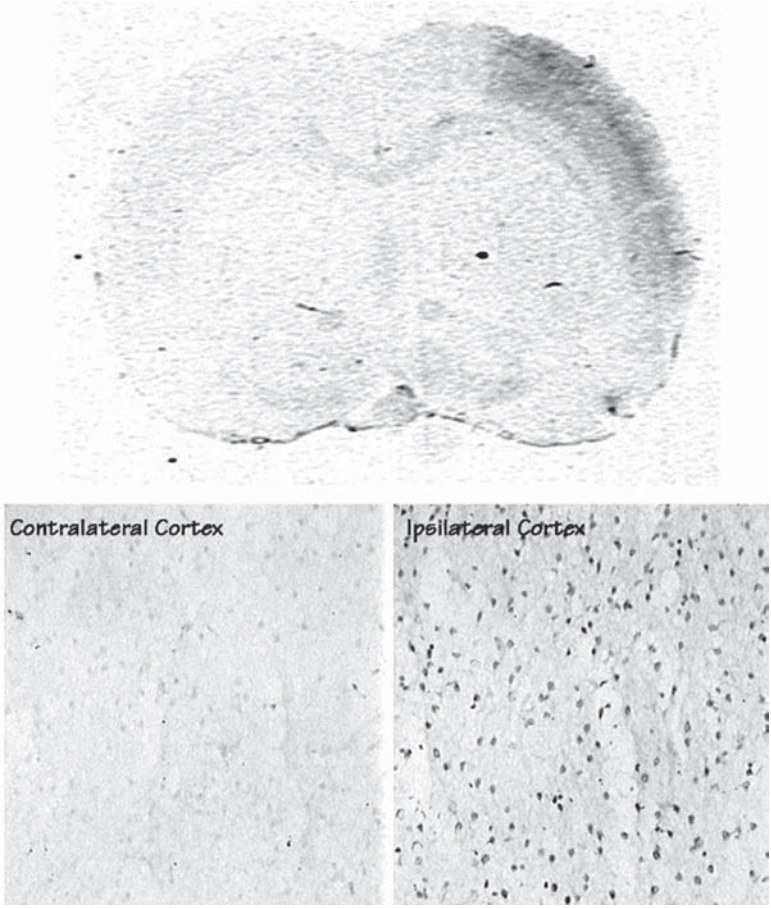

Fig. 1. These micrographs illustrate the activation of PARP using the PARIS assay following 90 min ischemia and 10 min reperfusion in Long Evans rats using the distal MCA, 3 vessel occlusion paradigm. The area at-risk following the ischemia is clearly demarcated in the right hemisphere by the histochemical method. At higher power, a distinct nuclear localization of constituative PARP activity can be resolved in the normal cortex, contralateral to the ischemia.

5. Chromogen: DAB-4-HCl (3,3' Diaminobenzidine tetrahydrochloride) dissolved in PBS, pH 7.4. Vector laboratory, Inc., Burlingame, CA 94010, U.S.A.
6. PARP inhibitors: 3-aminobenzamide.
7. Rinsing buffer: PBS, pH 7.4.
8. Histological staining dishes.
9. Wash bottle.
10. Pasteur pipets.
11. Shaker table or similar device.

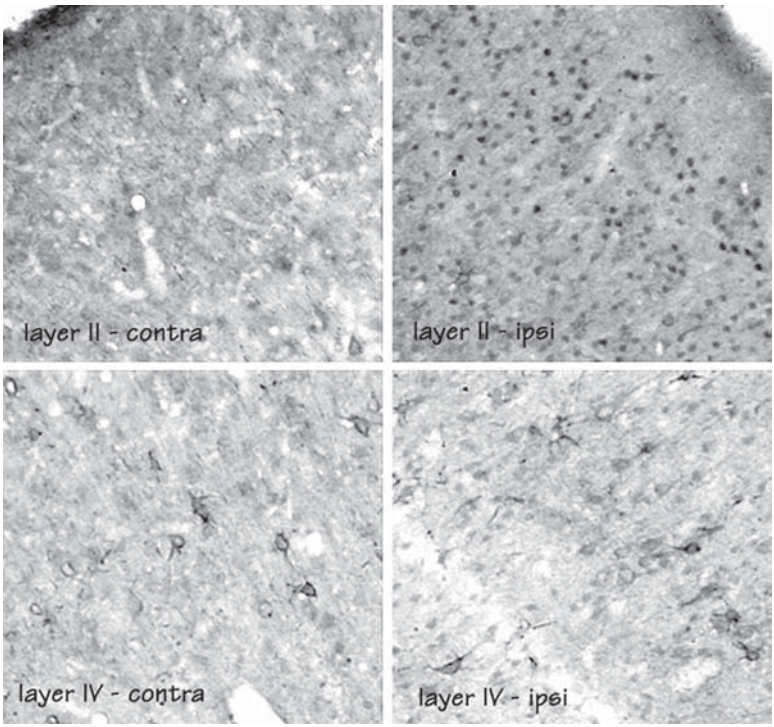

Fig. 2. These micrographs illustrate the immunohistochemical staining patterns characteristic of normal brain (contralateral to a focal ischemia/reperfusion) and the increased accumulation of PAR following 90 min ischemia and 10 min reperfusion in Long Evans rats using the distal MCA, 3 vessel occlusion paradigm. In layer II, few cells are labeled in the non-ischemic contralateral cortex. In the larger cells and neurons of layer IV, perinuclear staining is evident [*see also* ***(23)***]. Following ischemia/reperfusion, an increase in nuclear staining of PAR is clearly evident in the outer layers of the cortex, and subtle increase in density and number of positive profiles is found in layer IV.

12. Incubation chamber capable of retaining moisture (plastic or metal box with tight-fitting lid).

2.2. PAR Immunohistochemistry

1. Primary Antibodies: Polyclonal rabbit antibody against polyADP-ribose (PAR), 96-10 Aparptosis Inc., Sillery, Quebec, Canada, or monoclonal mouse antibody against polyADP-ribose (PAR) from Trevigen, Inc., Gaithersburg, MD 20877 U.S.A. 1:1000 working dilution is optimal for both of these antibodies.
2. Biotinylated Secondary Antibody: A biotinylated antibody against a species immunoglobulin that matches the host species of the primary antibody, Vector laboratory, Inc., Burlingame, CA 94010, U.S.A.

3. Avidin Peroxidase Complex: A complex of peroxidase enzyme and avidin. VECTASTAIN ABC-Peroxidase Kits, Vector laboratory, Inc., Burlingame, CA 94010, U.S.A.
4. Pre-blocking Agent: A reagent solution that serves to block nonspecific antigenic sites found on tissue. Contains normal serum from the host species providing the secondary antibody. 10% normal serum in PBS, pH 7.4. If using frozen tissue sections, the reagent should contain 0.3% Triton X-100.
5. Rinsing Buffers: PBS, pH 7.4.
6. Chromogen: DAB-4-HCl (3,3' Diaminobenzidine tetrahydrochloride) dissolved in PBS buffer, pH 7.4. Vector laboratory, Inc., Burlingame, CA 94010, U.S.A.
7. Substrate reagent: Hydrogen Peroxide.
8. Dehydration reagents: Ethanol baths of increasing concentration: 70, 80, 95 and 100% ethanol and xylene baths.
9. Histological staining dishes.
10. Wash bottle.
11. Pasteur pipets.
12. Incubation wells (such as tissue culture slides fitted with wells).
13. Camel's hair brush.
14. Glass microscope slides.
15. Coverslips, 24 × 50 mm.
16. Shaker table or similar device.
17. Slide warmer.
18. Microtome.

3. Methods

3.1 PAR In Situ *Assay (PARIS)*

3.1.1 Tissue Preparation

1. Long Evans rats are subjected to permanent distal middle cerebral artery occlusion plus 90 min bilateral common carotid arterial occlusion followed by 10 min reperfusion. The rats are killed humanely, and brains are fresh frozen on dry ice for 20 min, and stored at –80°C.
2. Mount frozen 20 µm cryostat sections onto polylysine-coated slides.

3.1.2 PARIS Assay

1. All procedures are performed at room temperature.
2. Sections are equilibrated to room temperature and then pre-incubated with PARIS buffer for 15 min in a staining jar.
3. Slides are then transferred to PARIS buffer containing 4 µ*M* biotinylated NAD and incubated for 30 minutes. *See* **Notes 1** and **2**.
4. For a specific control, 30 µ*M* 3-amino-benzamide is added to the buffer to inhibit PARP activity.
5. Stop the reaction by transferring the slides to 10% trichloroacetic acid solution and incubate for 10 min.

6. Wash 3× in PBS, each time for 5 min.
7. Place the sections into VECTASTAIN ABC reagent for 60 min.
8. Wash 3× in PBS, each time for 5 min.
9. Demonstrate peroxidase with freshly prepared chromogen/substrate reagent, DAB/H_2O_2. DAB concentration is 50 mg in 100 mL of 0.001% H_2O_2. Incubate for about 5 min until tissue turns a light caramel color.
10. Wash 3× in PBS, each time for 5 min.
11. Rinse sections in deionized tap water, air dry and coverslip.

The results of a PARIS localization indicating PARP activation following focal cerebral ischemia/reperfusion are shown in **Fig. 1**.

3.2. PAR Immunohistochemistry

3.2.1. Tissue Preparation

1. Long Evans rats are subjected to permanent distal MCAO plus 90 min bilateral common carotid arterial occlusion followed by 10 min reperfusion.
2. Under deep anesthesia, animals are perfused intracardially with PBS until the effluent runs clear (about 3 min). The perfusate is changed to 4% paraformaldehyde, and perfusion continued until the neck musculature is fairly firm, about 8 min or 150–200 mL. *See* **Note 3**.
3. Remove the brain from the rat and immerse in 4% paraformaldehyde fixative within a 25 mL scintillation vial. Store at 4°C, e.g., in a refrigerator.
4. After about 6 h post-fixation, change the solution to 30% sucrose and let sit at 4°C until the brain sinks to the bottom of the vial, about 2 d. This step cyroprotects the brain to reduce the incidence of ice crystal formation upon freezing.
5. Block the brain with a razor blade and freeze in dry ice-cooled isopentane.
6. Cut sections for free floating incubation using a sliding microtome. Standard section thickness is 30 µm.
7. Collect sections with a soft brush and place in incubation wells containing PBS.

3.2.2. Protocol for Immunostaining (Free Floating Method)

1. Use a shaker table or similar devices to mildly agitate sections during incubations and washes. We recommend that tissue sections be placed in a minimum of 300 µL of diluted antibody for 4 small sections or 2 large sections. Greater volumes should be used for wash buffers and preincubation reagents.
2. Wash 3× in PBS, each time for 5 min.
3. Incubate tissues with a pre-blocking agent containing 0.3% Triton X-100 for 60 min in room temperature. No Wash.
4. Incubate the sections with primary antibody for 48–72 h at 4°C. *See* **Note 4**.
5. Wash 3× in PBS, each time for 5 min.
6. Incubate with secondary antibody for 60 min in room temperature.
7. Wash 3× in PBS, each time for 5 min.
8. Incubate with avidin-biotin complex for 60 min.

9. Wash 3× in PBS, each time for 5 min.
10. Demonstrate peroxidase with freshly prepared chromogen/substrate reagent, DAB/H_2O_2. DAB concentration is 50 mg in 100 mL of 0.001% H_2O_2. Incubate for about 5 min until tissue turns a light caramel color.
11. Terminate reaction by transferring tissue into PBS.
12. Mount sections on gelatinized slides and dry for 12 h on a slide warmer.
13. Dehydrate sections with increasing ethanol concentrations followed by xylene as in conventional histology.
14. Coverslip.

The results of a PAR immunolocalization indicating novel PAR accumulation following focal cerebral ischemia/reperfusion are shown in **Fig. 2**.

4. Notes

1. The PARIS assay was first described by Pieper et al. ***(17)***, using ^{33}P-labeled NAD. This substrate is available from New England Nuclear by custom order. Biotynylated-NAD is now available from Trevigen and the methods reported here are applicable to the biotinylated substrate. Lower concentrations of substrate gave less intense reaction product.
2. Make fresh dilutions of substrate.
3. We have found that paraformaldehyde perfusion fixation to be the preferred method for PAR immunohistochemistry of the rat brain. We tested alternative methods using 20 µm cryostat sections of fresh frozen brain. On slide fixation with acetone, methanol, or paraformaldehyde gave inferior staining than sections from perfused brain. We did find that acetone fixation was preferred for optimal demonstration of PAR immunohistochemistry in other tissues, particularly paw.
4. Antibody specificity is tested by using a negative control serum and/or absorbed primary antiserum on adjacent sections. Any staining which occurs using the negative control is due to nonspecific background and helps differentiate specific positive staining from nonspecific background staining on the specimens under investigation. In addition, the primary antibody may be pretreated for 12 h with the same antigen used to generate the antibody. For LP-96–10, we applied 7.6 µL PAR of 73.5 ng/µL to 1 mL 1:1000 primary antibody, and incubate for 1 h at 37°C. Structures that are stained using untreated antiserum, but unstained with pretreated antiserum, are considered "specific" localizations by present standards.

Acknowledgment

We want to thank Jie Zhang, Ph.D., Guilford Pharmaceuticals Inc., for motivating our study of PARP histology in models of focal ischemia.

References

1. D'Amours, D., Desnoyers, S., D'Silva, I., et al. (1999) Poly(ADP-ribosyl)ation reactions in the regulation of nuclear functions. *Biochem. J.* 342 (Pt 2), 249–268.

2. Sallmann, F. R., Vodenicharov, M. D., Wang, Z. Q., et al. (2000) Characterization of sPARP-1—An alternative product of PARP-1 gene with poly(ADP-ribose) polymerase activity independent of DNA strand breaks. *J. Biol. Chem.* **275,** 15,504–15,511.
3. Shall, S. and de Murcia, G. (2000) Poly(ADP-ribose) polymerase-1: what have we learned from the deficient mouse model? *Mutation Research-Dna Repair* **460,** 1–15.
4. Pieper, A. A., Verma, A., Zhang, J., et al. (1999) Poly (ADP-ribose) polymerase, nitric oxide and cell death. *Trends Pharmacol. Sci.* **20,** 171–181.
5. Zhang, J., Pieper, A., and Snyder, S. H. (1995) Poly(ADP-ribose) synthetase activation: an early indicator of neurotoxic DNA damage. *J. Neurochem.* **65,** 1411–1414.
6. Zhang, J., Dawson, V. L., Dawson, T. M., et al. (1994) Nitric oxide activation of poly(ADP-ribose) synthetase in neurotoxicity. *Science* **263,** 687–689.
7. Le Rhun, Y., Kirkland, J. B., and Shah, G. M. (1998) Cellular responses to DNA damage in the absence of poly(ADP-ribose) polymerase. *Biochem. Biophys. Res. Commun.* **245,** 1–10.
8. Charriaut-Marlangue, C., Margaill, I., Plotkine, M., et al. (1995) Early endonuclease activation following reversible focal ischemia in the rat brain. *J. Cereb. Blood Flow Metab.* **15,** 385–388.
9. Chen, J., Jin, K., Chen, M., et al. (1997) Early detection of DNA strand breaks in the brain after transient focal ischemia: implications for the role of DNA damage in apoptosis and neuronal cell death. *J. Neurochem.* **69,** 232–245.
10. Li, Y., Chopp, M., Jiang, N., et al. (1995) Temporal profile of in situ DNA fragmentation after transient middle cerebral artery occlusion in the rat. *J. Cereb. Blood Flow Metab.* **15,** 389–397.
11. Linnik, M. D., Miller, J. A., Sprinkle-Cavallo, J., et al. (1995) Apoptotic DNA fragmentation in the rat cerebral cortex induced by permanent middle cerebral artery occlusion. *Mol. Brain Res.* **32,** 116–124.
12. Du, C., Hu, R., Csernansky, C. A., et al. (1996) Very delayed infarction after mild focal cerebral ischemia: A role for apoptosis? *J. Cereb. Blood Flow Metab.* **16,** 195–201.
13. Love, S., Barber, R., and Wilcock, G. K. (1998) *Apoptosis* and expression of DNA repair proteins in ischaemic *brain* injury in man. *Neuroreport* **9,** 955–959.
14. Takahashi, K., Pieper, A. A., Croul, S. E., et al. (1999) Post-treatment with an inhibitor of poly(ADP-ribose) polymerase attenuates cerebral damage in focal ischemia. *Brain Res.* **829,** 46–54.
15. Payne, J. F. and Bal, A. K. (1976) Cytological detection of poly (ADP-ribose) polymerase. *Exp. Cell Res.* **99,** 428–432.
16. Oikawa, A., Ital, Y., Okuyama, H., et al. (1969) Studies on polymer of adenosine diphosphate ribose. VI. Radioautographic demonstration of incorporation of NAD into nuclear macromolecule. *Exp. Cell Res.* **57,** 154–156.
17. Pieper, A. A., Blackshaw, S., Clements, E. E., et al. (2000) Poly(ADP-ribosyl)ation basally activated by DNA strand breaks reflects glutamate-nitric oxide neurotransmission. *Proc. Natl. Acad. Sci. USA* **97,** 1845–1850.

18. Zhang, J. (1997) Use of biotinylated NAD to label and purify ADP-ribosylated proteins. M*ethods Enzymol.* **280,** 255–265.
19. Ame, J. C., Rolli, V., Schreiber, V., et al. (1999) PARP-2, a novel mammalian DNA damage-dependent poly(ADP-ribose) polymerase. *J. Biol. Chem.* **274,** 17,860–17,868.
20. Johansson, M. (1999) A human poly(ADP-ribose) polymerase gene family (ADPRTL): cDNA cloning of two novel poly(ADP-ribose) polymerase homologues. *Genomics* **57,** 442–445.
21. Kickhoefer, V. A., Siva, A. C., Kedersha, N. L., et al. (1999) The 193-kD vault protein, VPARP, is a novel Poly(ADP-ribose) polymerase. *J. Cell Biol.* **146,** 917–928.
22. Smith, S., Giriat, I., Schmitt, A., et al. (1998) Tankyrase, a poly(ADP-ribose) polymerase at human telomeres. *Science* **282,** 1484–1487.
23. Endres, M., Wang, Z. Q., Namura, S., et al. (1997) Ischemic brain injury is mediated by the activation of poly(ADP-ribose)polymerase. *J. Cereb. Blood Flow Metab.* **17,** 1143–1151.

20

Ultrasound Imaging of Apoptosis

DNA-Damage Effects Visualized

Gregory J. Czarnota, Michael C. Kolios, John W. Hunt, and Michael D. Sherar

1. Introduction

1.1. High Frequency Ultrasound Imaging of Apoptosis

This chapter presents a new method for the detection of DNA damage that leads to the physiological process of apoptosis which is a normal programmed cell-death response to sufficiently toxic levels of DNA damage. The high-frequency ultrasonic detection of programmed cell death has been demonstrated in vitro, *in situ*, and in vivo using a variety of different apoptosis inducing methods ***(1,2)***. This method provides a useful image based adjunct for the detection of programmed cell death in a laboratory setting as well as being a powerful potential clinical tool which can be used to monitor tumour responses to treatment. Typical low-frequency medical ultrasound imaging devices operate at 1–10 MHz, provide mainly low resolution structural information, and predominantly are used in obstetrics and cardiology. In contrast, high-frequency ultrasound imaging devices operate at 30–50 MHz and offer increased resolution as well as the emerging capability to detect cells and tissues in different physiological states including those undergoing programmed cell death, or apoptosis ***(1–4)***. Data collected to date indicates that this capability of high-frequency ultrasound is based on interactions of high-frequency ultrasound waves with the chromosomal nuclear material in cells, which undergoes structural changes of condensation and subsequent fragmentation with the process of programmed cell death ***(1–2,4)***. We have demonstrated this process experimentally in vitro, *in situ*, and in vivo using a number of different systems in which apoptosis is induced with physiological stimuli, chemothera-

From: *Methods in Molecular Biology, vol. 203:* In Situ *Detection of DNA Damage: Methods and Protocols*
Edited by: V. V. Didenko

peutic drugs, radiation, or photodynamic therapy. The ultrasound-based approach to detecting apoptosis has a number of potential applications which range from embryological studies of development where apoptosis plays an important role, to assessing organ viability for the purposes of transplantation, again a situation where the presence of programmed cell death is correlated to clinical outcome ***(5)***.

In particular, our aspiration is for this method to be used in a number of clinically relevant scenarios poised to improve modern cancer medicine. For instance, such apoptosis-detecting technology can readily be used in laboratory the aid of anti-neoplastic drug discovery or design. It also has an emerging role in the clinic as a method to follow the effects of chemotherapeutic drug regimes as a predictor of eventual treatment outcome and to assure treatment efficacy well in advance temporally of more traditional clinical assays. It can also be used to investigate and guide experimental radiotherapeutic procedures by providing visual maps of treatment effects—not possible by any other non-invasive radiological method. In this chapter, we highlight the history of using ultrasound in biological imaging. We then describe the experimental systems and protocols for monitoring apoptosis in vitro and in vivo using high-frequency ultrasound imaging. Lastly, we conclude with a discussion of the limits and limitations of this technology and highlight future developments in progress geared to overcoming the present day limitations of this technology and simultaneously designed to increase the versatility of this already powerful imaging approach to detecting programmed cell death.

1.2. Background

1.2.1. Apoptosis

The process of apoptosis has become central to the understanding of the development of normal tissues, the carcinogenic process and the response of tumors to anti-cancer agents ***(6–11)***. It is a complex multi-step process which can be elicited by a number of factors which include normal developmental stimuli, the withdrawal of cell survival factors, mitochondrial damage, and DNA damage. From a physical viewpoint the changes inside the cell which occur during apoptosis alter a number of different sub-cellular organelles consequently changing the structure and physico-chemical properties of the cell. The most striking of changes take place in the cell's nucleus. There, the chromatin, undergoes post-translational modifications at the level of the nucleosome ***(12,13)***, its fundamental subunit, which results in increased condensation—similar to the manner in which chromosomes condense during mitosis. Subsequent to this phenomenon, a number of different enzymatic processes are typically activated involving caspaces which cleave the cellular nuclear material into fragments ***(6–11)***. The cell's outer

membrane also changes morphology becoming blebbed in appearance. Further, the cell may begin to extrude intra-cellular components in plasma-membrane delimited granules which avoid the stimulation of an inflammatory response in vivo. Traditional procedures for detecting and monitoring apoptosis and apoptotic changes rely on tissue biopsy and histological assays ***(14)*** which are specialized, invasive and time consuming. The result is that spatial maps of apoptosis in tissues cannot easily be produced. The ultrasound methods that we have developed for the detection of apoptosis represent the only non-invasive radiological method, to our knowledge, capable of detecting this important physiological process. The ultrasound imaging process is rapid, taking only minutes, is non-invasive, and can readily produce real-time spatial maps of apoptosis in addition to providing more quantitative radio-frequency ultrasound data for more detailed analyses discussed further in the following sections.

1.2.2. Ultrasound Imaging

The use of high frequency ultrasound for analyzing tissues has followed two paths that now converge consisting of origins separately based on acoustical microscopy and conventional ultrasound technology (reviewed in ***15***). The use of ultrasound transmission methods for microscopy, analogous to conventional optical microscopes, dates back to 1955 based on a concept proposed by Sokolov in 1936 ***(16)***. Further improvements in resolution were achieved Dunn and Fry in 1959 ***(17)*** but it was not until 1971 with the development of the scanning laser acoustic microscope operating at 100 MHz ***(18)*** and the later development of the scanning acoustic microscope that significant improvements in resolution were made. In 1978, resolution equal to that of an optical microscope was achieved with a scanning acoustical microscope operating at 3.1 GHz. Although these instruments provide very high resolution images they are restricted to use with micron-thin specimens and cannot be used for imaging in vivo (reviewed in ***15***).

Parallel to these developments, the use of ultrasound for medical imaging was under development. The main difference compared with acoustic microscopy is that short-pulse/high-bandwidth transducers were used to allow non-invasive imaging at depth in living specimens. The technique involves exciting a piezoelectric plate with a high voltage electrical signal. In response to the electrical pulse, the transducer transmits a short ultrasound pulse through the coupling medium into the specimen. The ultrasound is scattered due to acoustic impedance variations in the sample analogous to the scattering of electromagnetic radiation at electrical impedance interfaces. The reflection coefficient at an acoustic boundary is given by a relationship dependent on the characteristic impedance of the first medium and second medium, respectively. A fraction of the scattered ultrasound will return towards the transducer being

transformed into an electrical signal. This backscatter signal therefore varies in time according to scattering events at different depths in the specimen. An image of the internal structure of the specimen can then be made by measuring the amplitude of the backscatter signal as a function of time and representing the brightness value on a screen. This is one line in the image. A 2-D image, called a B-Mode image, is formed by scanning the transducer perpendicular to the direction of travel of the ultrasound. The B-scan image is therefore a result of scattering from acoustic impedance (density and speed of sound) variations in the specimen (reviewed in ***15***).

Pulse-echo B-Mode imaging dates back to the First World War when Langevin and Chilowski developed an underwater imaging system to detect submarines ***(19)***. The first laboratory pulse-echo system was developed by Wild and Reid who in 1952 ***(20)*** realized the potential of this technique for imaging the internal structure of biological specimens. Today, pulse-echo scanners operating in the 1–10 MHz range are widely used for monitoring pregnancies, diagnosing disease deep in the body and planning therapy. As with scanning-line acoustical microscopy and scanning acoustical microscopy, the lateral resolution of the a pulse-echo ultrasound system is determined by the ultrasound wavelength. In pulse-echo ultrasound the axial resolution (in the direction of beam propagation) is also determined by the wavelength and the number of waves in the short ultrasound pulse. Short pulses can only be produced by transducers with a large bandwidth and therefore transducer design is critical in the development of a pulse-echo system.

The extension of pulse-echo imaging to high frequencies allowing much higher resolution than achievable with conventional medical ultrasound scanners, required the development of high-frequency, high-bandwidth transducers. Those used in the scanning acoustical microscopies had low bandwidth and so could only produce long pulses. High-bandwidth, high-frequency transducers were first developed by Sherar et al. ***(21)*** who used a piezoelectric polymer to build 100 MHz pulse-echo transducers. These were used in the development of the first 100 MHz B-scan ultrasound microscope with a lateral resolution and an axial resolution, both of approximately 40 μm.

The ultrasound backscatter microscope was first applied to the imaging of intact multicellular spheroids. These images demonstrated very high contrast between cells in different physiological states. The necrotic core and viable rim were clearly distinguished ***(4,22)***. This contrast was hypothesized to be largely due to differences in acoustic impedance in the cell's nucleus between viable and necrotic cells. Further experiments in spheroids to investigate the effect of hypoxic cell cytotoxins, of interest as an adjunct to radiation therapy, demonstrated that changes in cell morphology in response to stress could be detected in high frequency ultrasound images. We have now discovered, as

is described in this chapter, that the morphological changes due to programmed-cell death or apoptosis and other changes in the cell's nucleus can be detected with high frequency ultrasound imaging and ultrasound spectroscopy. The work described here also represents a revolution in ultrasound imaging in terms of ultrasound no longer only providing structural information but being able to detect the functional or physiological states of cells and tissues akin to other modalities such as functional-magnetic resonance imaging or positron-emission tomography. Although not described here in full detail, we have been able to detect and differentiate viable, coagulated necrotic, mitotic, and apoptotic samples ***(1,2)***. We also have emerging data that this method is sensitive to phases of the cell cycle in addition to the nuclear changes induced by changes in gene expression.

In addition to in vitro systems, the ultrasound backscatter microscope has been used extensively in the routine clinical examination of living ocular tissue ***(3)*** and now has found relatively widespread use in academic ophthalmology centers. The microscopes are used to help in the diagnosis and staging of glaucoma as well as anterior segment tumors in the eye. In addition, the use of high frequency ultrasound to monitor coagulation therapy in the eye has been demonstrated. Further work has recently extended the applications of high frequency ultrasound imaging to skin, vascular (using catheter-based, high-frequency ultrasound probes) and cartilage studies. More recently we have extended our apoptosis imaging to in vivo studies of patients undergoing radiation therapy and chemotherapy based on the hypothesis that it may be possible to monitor response to treatment using ultrasound based on the importance of apoptosis as a cell death mechanism in treated tissues ***(1,2)***.

1.2.3. Analysis of Ultrasound Backscatter Signals

Ultrasound transducers detect primarily backscattered ultrasound due to geometric constraints and the fact that the transducer is both a generator and receiver of ultrasound. High-frequency ultrasound transducers are also broadband in nature. For instance, a transducer may have a characteristic frequency at 40 MHz at which it is most sensitive but it may also be able to generate and detect ultrasound from 20–60 MHz with appreciable efficiency. Spectral analysis provides more information in comparison to ultrasound images which are fundamentally representations of backscattered ultrasound amplitude. Spectral analysis characterizes the changes in ultrasound amplitude over a range of frequencies and changes in spectral patterns may reflect important underlying physical changes in a tissue. Mathematical analysis of spectral profiles of ultrasound can yield important parameters including effective ultrasound scatterer size, scatterer concentration and tissue attenuation properties ***(23–25)***. Such analyses have indicated the potential of such spectral analyses to be used in the

study of neoplastic lesions. Although to date most of our spectroscopic analyses have been Fourier transform based it is possible to carry out more sophisticated studies used wavelet analyses.

It has also been demonstrated that ultrasound backscatter signals are related to the spatial organization of individual scatterers of ultrasound. In particular, the greater the randomness or disorganization of individual scatters the greater the ultrasound backscatter signal that is theorized to occur. This is of special relevance to the case of apoptosis given that the major scatterer of ultrasound is believed to be the DNA in the cell's nucleus. Hence as apoptosis occurs the randomness of the system increases as both the number of apoptotic DNA fragments increases and as their positions in the cell become less organized and distal from a central nucleus ***(26)***.

2. Materials

2.1. High-frequency Ultrasound Imaging Device

For the purposes of our experiments we have used a prototype ultrasound imager or its commercial analog, a VisualSonics V40 (VisualSonics, Toronto, Canada; *see* **Fig. 1** and caption for more information). Although a number of different ultrasound research centres are developing modern user-friendly high-frequency ultrasound devices this company is the only commercial producer of such instrumentation at this point in time. This instrument operates in a user-selectable range from 20–60 MHz, and is able to produce images 8 mm by 8 mm in size at a scan rate up to 5 Hz. It operates in B-mode and as well is able to collect Doppler ultrasound information. Additionally, it features a 500 MHz digitization board in order to collect radio-frequency data. Alternatively, software controls permit such data to be collected using an external digital oscilloscope operating in the same frequency range.

2.2. Apoptosis

We have used a number of different experimental systems in which apoptosis has been induced using a variety of methods. These are explained in detail below and provided in the methods section only as examples. The reader is free to induce apoptosis using the materials and biological reagents they are most familiar with. Any experimental system in which apoptosis may be induced is potentially applicable to examination using ultrasound imaging providing a suitable volume of cellular material (approx 2 mm by 2 mm) can be produced for imaging purposes. The model systems which are discussed below include acute myeloid leukemia cells (AML-5) in which apoptosis is induced with cisplatinum, and rat brain tissue in which apoptosis is induced with photodynamic therapy. Materials for these models include:

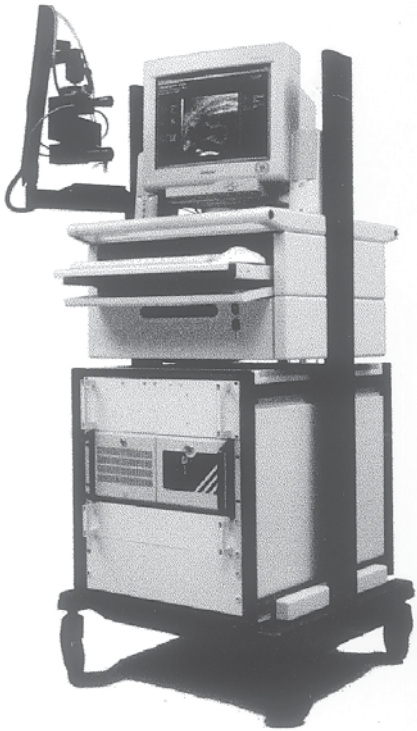

Fig. 1. High-Frequency Ultrasound Biomicroscope. This instrument features proprietary wide-band front-end signal processing and an adjustable center frequency from 25–60 MHz to allow selection of resolution for optimal penetration. The device features analog to digital conversion with 8 bits at 500 MHz and has 3D micropositioning capability. The transducer is coupled to a mobile positioning arm shown at the left of the instrument. It is coupled with a Windows NT (Microsoft, Redmond Washington) operating system, is network ready, and features CD image archiving capability. Instrument information may be obtained from Dr. Stuart Foster, VisualSonics, Sunnybrook and Women's College Health Sciences Centre, S-658, 2075 Bayview Avenue, Toronto, Ontario M4N 3M5, e-mail: info@visualsonics.com.

2.2.1. Apoptosis in Cells

1. AML-3 cells (Acute Myeloid Leukemia Cells). Available from the Ontario Cancer Institute of Canada, 610 University Avenue, Toronto, Canada M5G 2M9.
2. Cisplatinum: the stock solution available at a concentration of 1 mg/mL should be stored in the dark (Sigma-Aldrich, St Louis, MO).
3. α-Minimal media—for growing cells (Sigma-Aldrich).
4. Cell lysis buffer for cytometry: 0.2% Triton X-100 in isotonic phosphate-buffered-saline-citrate, 0.1 mg/mL RNase, 0.05 mg/mL propidium iodide.

5. DNase I—for digesting nuclear material (Sigma-Aldrich).
6. Triton X-100—for permeabilizing cells (Sigma-Aldrich).
7. Cochicine—for arresting cells in metaphase of mitosis (Sigma-Aldrich).
8. EDTA—for terminating DNAse and RNAse reactions (Sigma-Aldrich).
9. Terminal-deoxynucleotidyl transferase—for labeling free ends of DNA (Promega, Madison WI).
10. Fluorescein-12-dUTP—for labeling free ends of DNA (Promega).
11. Propidium Iodide—0.05 mg/mL, for staining cells (Promega).
12. RNAse A—used in DNA labeling (Promega).
13. Proteinase K—used in DNA labeling (Promega)
14. Phosphate buffered saline: 0.8% NaCl, 0.01 *M* phosphate buffer pH 7.4
15. Phosphate buffered saline citrate: 0.8% NaCl, 0.01 *M* phosphate buffer pH 7.4, 8.8% citrate (w/v).

2.2.2. Apoptosis in Tissues

1. Male Fisher rats.
2. Photofrin II (QLT, Canada).
3. 632 nm Laser (QLT) set such that optical power irradiance as 100 mW/cm^2.
4. Ketamine for anaesthesia purposes . (Sigma-Aldrich).

2.3. Analysis of Ultrasound Backscatter Signals

Analysis of backscatter signals can be carried out using a variety of standard numerical analysis packages on the computing platform of one's choice. These are left to the individual researcher. Our preference is to use Matlab (The Mathworks Inc., Natick, MA) running on a 500 MHz Windows NT or UNIX based computer system.

3. Methods

3.1. Apoptosis in Cells

For the purpose of ultrasound imaging of cells from an in vitro system adequate numbers of cells are required to provide a sample of packed cells approx 1 cm^3 in volume. Any cell line may be used. To date we have worked with leukemia, melanoma and breast cancer cell cultures. If it is a cell line that does not grow in liquid suspension culture then once confluent, cells must by trypsinized to remove them from the growth surface. For the purposes of our experiments, all cells were prepared for ultrasound imaging using an acute myeloid leukemia cell culture system (AML-5) growing in suspension, an ideal model for studying apoptosis. For any experimental time point or condition, experiments are typically completed in quadruplicate.

1. For each experiment, approx 1×10^6 cells are grown at 37°C in 300 mL alpha minimal-media always from frozen stock samples.

2. To induce apoptosis, expose cells to cisplatinum at 10 μg/mL for a specific time. This drug is a DNA intercalater that causes a p53-dependent apoptosis in this cell line ***(27)***. For example, in our previous studies ***(1,2)*** cells have been treated with cisplatinum for 0, 6, 12, 24, and 48 h.
3. To confirm the presence of apoptosis examine the 24 h sample using corroborative methods including light-microscopy, standard DNA gel-electrophoresis showing DNA laddering, and trypan-blue staining. We usually confirm that approx 95% of the cells undergo apoptosis at the 24 h time point.
4. Cells are then washed in phosphate-buffered saline (PBS) and counted using a light microscope to ensure equal numbers of cells and subsequently pelleted in flat bottom cryo-tubes at 800 *g* on a desktop swinging bucket centrifuge. This results in a 1 cm^3 cell pellet which is sufficiently large enough to readily image.
5. Immerse cell pellets in a PBS bath and then visualize using high-frequency ultrasound.

Representative results are shown in **Fig. 2** and discussed in **Note 1**.

3.2. Other Forms of DNA Configurations

We have also been interested in the effects of other, non-apoptotic, DNA configurations on ultrasound backscatter. The preparative methods are essentially identical to that above with the exception that different drug agents are used to arrest cells in metaphase of mitosis. For instance, in order to arrest cells in mitosis, effectively enriching the mitotic fraction in the cell population, cells are treated with colchicine at a concentration of 0.1 μg/mL for 0, 6, 12, 24, and 48 h. By inhibiting microtubule formation this drug arrests dividing cells at the G2/M checkpoint of the cell cycle, corresponding to metaphase of mitosis ***(28)***. In this cell culture system the maximal enrichment of the mitotic population is an increase to approx 30%. It is possible to investigate, in this manner, not only mitotic cells but populations of cells trapped in other phases of the cell cycle. To help characterize the effects of the drugs, we use flow cytometry using nuclei from approximately 3×10^5 cells.

1. To obtain nuclei, lyse cells after resuspension in 1 mL isotonic buffer (0.2% Triton X-100 in PBS-citrate, 0.1 mg/mL RNase A, 0.05 mg/mL propidium iodide).
2. Strain this suspension is through a fine gauze mesh to remove cell debris.
3. Incubate material at 4°C in the dark for 30 min.
4. Analyze samples on a flow cytometer (Becton-Dickenson, Franklin Lakes, NJ). A cell cycle analysis program, CellFIT 2.01.2 (SOBR), is used to quantify cells with respect to different cell cycle phases.

3.3. Effects of DNA Condensation

We also are in the process of investigating the effects of DNA condensation on ultrasound backscatter using experiments designed to specifically perturb DNA configuration.

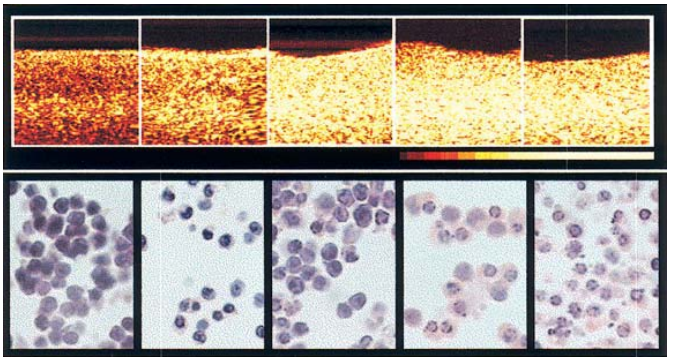

Fig. 2.

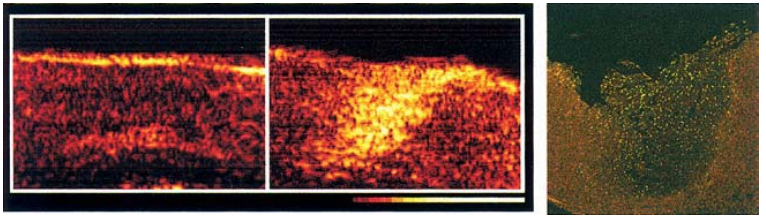

Fig. 3.

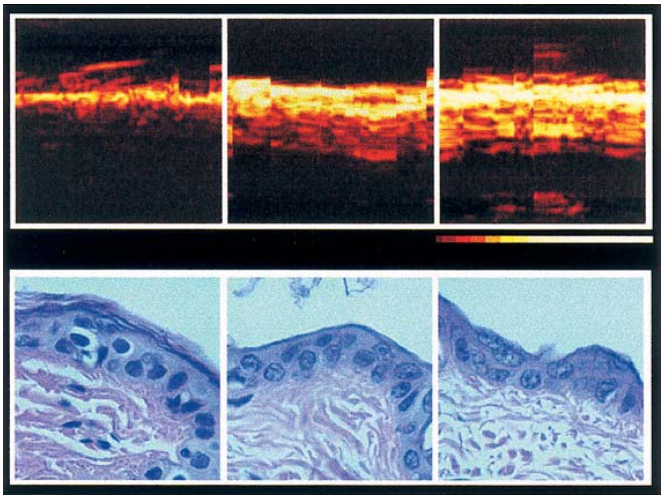

Fig. 4.

Fig. 2. Ultrasound Imaging of Apoptosis and Correlative Histology. Top panels present results of ultrasound imaging of apoptotic cells. Each panel is a representative ultrasound scan of a pellet of AML cells. The bottom of each ultrasound scan is at the bottom of each frame. Pellets are immersed in buffered saline. From left to right, panels correspond to cells treated with cisplatinum for 0, 6, 12, 24 and 48 h, the point at which apoptosis is maximized. A bar at the bottom right of the figure indicates the color map used in this image, the left of the bar indicating the color that corresponds to pixel values of 0 and the right giving the color that corresponds to a pixel value of 256. The speckle pattern is characteristic of all ultrasound images and does not correspond to individual cells but rather represents constructive and destructive interference effects from the collective of cells in the sample. Bottom panels correspond to standard hematoxylin and eosin stained samples of AML cells at the same time points. At 0 and 24 h, histological analysis indicated that 1.6, and 87% of all cells showed nuclear fragmentation, respectively. By 6 h of drug exposure 72% of the cells exhibited prominent nuclear condensation changing from a nuclear diameter 70% of the cellular diameter before addition of the drug, to a diameter 40% of the cellular diameter at 6 h. Additionally, after the 6 h time point, 95% of all cells exhibited nuclear condensation or fragmentation. The field of view in each panel is approx 50 μm. Top panels reprinted from ***(2)***, by permission of the publisher Churchill Livingstone.

Fig. 3. Ultrasound Imaging of Apoptosis in Response to Photodynamic Therapy. Representative ultrasound image of photodynamic therapy treated brain tissue examined *ex vivo*. The left panel corresponds to non-irradiated control tissue contralateral to the treated tissue shown in the central panel. The cone-shaped yellow area of increased ultrasound backscatter corresponds to the treated region. The tissue shown was freshly excised 24 h after therapy and is not fixed. The contrast is equivalent to that obtained with samples fixed for histology. The color map indicated by the bar below the right panel is the same as for **Fig. 1**. Panel width is 4 mm. The right-most panel presents representative results of fluorescence microscopy assays for apoptosis. Images are composed of intact cells stained with red propidium iodide. In this same assay apoptotic cells are stained using a fluorescein dye coupled to an enzymatic assay which stains the DNA-ends of fragmented DNA in apoptotic cells green. The wedge of green staining cells is the same region which results in increased ultrasound backscatter as illustrated in the panel to the left. The left two panels are reprinted from ***(2)***, by permission of the publisher Churchill Livingstone.

Fig. 4. Imaging of Apoptosis in vivo. Top panels present the results of ultrasound imaging whereas the bottom panels illustrate corresponding representative histological results. From left to right panels correspond to rat skin imaged in vivo 24 h after exposure to 0, 8.5, and 17 J/cm^2 of activating laser light. Any discontinuities in the images are a result of motions in the living animal caused by its respiration. The color map shown below the right panel is the same as used in all other figures. The most prominent increase in the top panels occurs at the epidermal surface with increasing dose. The epidermal layer is easily visualized in the left panel—it is the bright line at the top of the skin. An increase in the lower dermal region also occurs. Corresponding histology shows prominent apoptotic cells with condensed and fragmented nuclei in

1. Prepare pellets of mitotically-enriched cells as described above for apoptotic cells and gently resuspended in 1 mL of PBS. It is possible to also use cells trapped in different phases of the cell-cycle at this stage.
2. As controls, treat samples with only DNase I at concentrations of 5,413 U/mL and 10,826 U/mL and only Triton X-100 at a concentration of 0.1% (w/v).
3. In order to permeabilize cells and permit DNase I to enter the cells, expose samples to both DNase I and Triton X-100 at the concentrations given above.
4. Permit digestions to proceed for 30 min at 37°C and terminate by adding EDTA to a final concentration of 15 m*M*. It is reasonable to assess all samples histologically at this point.

Representative results are discussed in **Note 2**.

3.4. Apoptosis in Tissues

We have induced apoptosis in tissues before *(2)*, using a process known as photodynamic therapy. This has been applied to brain tissue experimentally as a method of potentially treating brain neoplasms and rat skin tissue in vivo.

3.4.1. Rat Brain Tissue

1. Treat male Fisher rats with 12.5 mg/kg of Photofrin II (QLT) by intraperitoneal injection. Keep animals in a dark environment for 24 h prior to irradiation.
2. Anesthetize animals using ketamine injected intraperitoneally at a dose of 2–4 mg/kg.
3. Create a 5.5 mm craniotomy in each side of the rat's skull avoiding mechanical stress to the underlying cortex using a mechanical surgical drill.
4. Treat this area for 30 sec using a red laser light with a wavelength of 632 nm and a spot size of 3 mm in diameter. This spot size is selected in order to be readily visualized in the 4 mm scan width of the ultrasound microscope next to an untreated region.
5. Several treatment irradiances can be employed including 1, 3, 5, and 17 J/cm^2. To minimize post-therapy cerebral swelling and still show a sufficient response to therapy, 3 J/cm^2 was the condition selected for further study in our previous work. The optical power irradiance at the dural surface should be 100 mW/cm^2.
6. Sacrifice animals at a desired time point. In our previous work *(2)*, animals were sacrificed at 3 time points: 1.5, 3, and 24 h after the above photodynamic therapy. The first two time points were chosen to survey early treatment effects. The last time was chosen since earlier experimentation seemed to suggest an accumulation of cells arrested in relatively early stages of apoptosis 8 h post apoptosis

Fig. 4. *(continued)* the epidermal region in both the 8.5 and 17 J/cm^2 samples. A disruption of the cellularity in the dermal region below also occurs with dose. The field of view in the ultrasound images is 2 mm. The field of view in the histology images in approx 100 μm per panel. Reprinted from *(2)*, by permission of the publisher Churchill Livingstone.

inducing therapy ***(29)***. Equivalent results were obtained whether the rat brains were formalin fixed prior to ultrasound imaging in order to minimize degradation effects, or imaged ultrasonically prior to fixation ***(2)***.

Representative results are shown in **Fig. 3** and discussed in **Note 3**.

3.4.2. In Vivo Rat Skin Experiments

In rat skin experiments, skin from the dorsal posterior of the animal is shaved. A 1 cm diameter area is exposed to 0, 8.5, or 17/cm^2 with an irradiance of 100 mW/cm^2. Animals are kept in a dark environment before and after treatment. Living animals are imaged in a sedated state 24 h after treatment using the same anaesthesia as described above. Skin biopsies are always obtained and submitted for histological analyses when completing this type of experiment.

The reader is referred to **Note 4** and **Fig. 4** for discussion and representative results.

3.4.3. Pathological Analysis

For general pathological analysis, rat brains and skin tissue are sectioned and haematoxylin and eosin stained. To specifically assess for the effects of apoptosis, an enzymatic method is used [which with terminal-deoxynucleotidyl-transferase labeled the 3'-OH ends of fragmented DNA with fluorescein-12-dUTP (Promega, Apoptosis Detection Kit)]. Since ultrasound analyses of the 24 h post-therapy specimens were most consistent with the highest levels of putative apoptosis, this specimen was subjected to the apoptosis labeling assay.

1. As a positive control treat a photodynamic therapy-untreated rat brain section with proteinase-K and DNase I, at a concentration of 1 μg/mL and incubate at room temperature for 10 min prior to staining sections. This method results in about 70–80% positive green-staining cells in a control section, but may stain control cells more intensely that apoptotic cells.
2. As a negative control, contralateral sections of the PDT-treated rat brain are used. Sections of the PDT-exposed rat brain are also stained in this fashion.
3. Counterstain all sections with propidium iodide (0.05 mg/mL), which stains both apoptotic and non-apoptotic cells red throughout the cytoplasm.
4. Visualize slides of sections immediately after staining.
5. Carry out microscopy as above using a standard fluorescein filter set (520 ± 20 nm) and an appropriate filter (>620 nm, which permits the red staining of propidium iodide to be visualized separate from fluorescein staining) to detect propidium iodide staining, respectively. Images of red and green fluorescence are captured separately and combined to form composites. In order to analyze the fluorescence levels within cells in the sections, use a computerized approach is used to crop cells after automatic contouring and to quantitatively determine separate

levels of red staining and green staining within each cell. These integrated values are then corrected by normalization for slightly different red and green fluorescent background staining values. Aldus Photostyler (Aldus Corporation) is an image analysis software package with this capability.

3.5. Light Microscopy and Analysis

To confirm and investigate the morphology of cells at each experimental condition, ultrasonically imaged and duplicate non-imaged samples are saved for haematoxylin and eosin staining by fixing 12 h in 10% (w/v) formalin in buffered saline. These cells are then embedded in paraffin and processed as histological sections. No histological differences due to ultrasound imaging have been observed. Images of pellet cryosections are often obtained to confirm that no differences in packing are present ***(1)***. We carry out light and fluorescence microscopy using a Zeiss Axioscope 20 (Carl Zeiss, Germany) coupled to a color SONY CCD (Sony Corporation, Japan) camera. Images are recorded digitally on a IBM PC using the Northern Eclipse Image Analysis Software 1.1 (EMPIX Imaging Inc., Mississauga, ON, Canada).

3.6. Analyzing Ultrasound Backscatter Signals Associated with Apoptosis

All cell samples and animal tissue samples are imaged at room temperature using either a custom built high-frequency ultrasound instrument operating at 40 MHz ***(1,2,21)*** which is a prototype to a commercially available instrument (VisualSonics V40 Toronto, Canada, *see* **Fig. 1** and caption) which we have been currently been using. The focal depth of these instruments typically is 9 mm, axial resolution 38 μm, and their lateral resolution, limited by the ultrasound beam width, is 55 μm. During imaging sessions the ultrasound probe is positioned such that the focal zone is the same depth in each imaged specimen. All images are digitally recorded and a physical hard-copy is simultaneously produced. In this system, centrifuged samples of cells grown in vitro are imaged under phosphate-buffered saline (*see* **Fig. 2**). Tissues may be imaged under saline or using gel, and living animals are imaged using high viscosity ultrasound gel (ATL Inc., Reedsville PA) over areas of skin (*see* **Figs. 3** and **4**). We find that use of this specific gel is optimal as it minimizes bubble formation and is highly viscous.

1. Prepare cells or tissue specimens as described in preceding sections. Immerse cell or *ex vivo* samples in phosphate-buffered-saline.
2. Obtain radiofrequency-signal from a standard reference for purposes of inter-experiment calibration. We use a highly polished and flat quartz standard.
3. Scan samples with instrument settings (such as focal depth, ultrasound frequency, signal gating, and signal bias settings) unchanged throughout the experiment. Store images digitally.

4. Assess ultrasound backscatter amplitude. The ultrasound backscatter amplitude for each specimen or time-point can be assessed in two manners (*see* steps 5 and 6).
5. In the first method, transform pixel intensities from images to relative ultrasound backscatter amplitudes by multiplying the inverse of the transfer function of the electronics of the ultrasound imaging instrument. This corresponds directly to the degree of ultrasound backscatter amplitude. For each sample, make measurements using 32 images, each 64×64 pixels in size, cropped from the focal band of images.
6. In the second method A-scans, the individual line scans which are processed to produce two-dimensional ultrasound images are obtained and assessed. Such A-scans are also independent of the instrument's image processing and amplification processes. In short, in A-scan analyses by detecting subtle shifts it the frequency content of the signal one can make inferences about changes in the underlying structure that causes these shifts. The frequency content of the backscattered signal from cells and tissues depends on the attenuation of the intervening tissue and physical characteristics of the ultrasound scatterers in the tissue. Typically 30–50 A scans should obtained per sample, each from a distinct location separated by one beamwidth. We hypothesize that the changes in the ultrasound backscatter signal and its frequency content are due to changes in a) nuclear size, b) acoustic properties, and c) the scatterer organization.
7. To assess A-scans, a Hamming function of length L is applied to each scan and the Fourier transform of the section is taken. Square and divide the resulting spectrum by a normalizing spectrum (the spectrum derived from a pulse reflected from a standard quartz reflector). This step is required to compensate for the spectrum of the original pulse and the system transfer function of the ultrasound imager. This power spectrum is expressed in dB (or dBr, referring to the fact that the spectrum is normalized) and is evaluated over the frequency band providing good signal-to-noise ratios.
8. To characterize the curves generated, linear regression is applied. Results of the regression that are analyzed are the slope of the best fit (in dBr/MHz), the intercept (in dBr, extrapolation to 0 frequency), and the mid-band fit (dBr value of the linear fit at the center frequency of the transducer). These values permit the effective scatterer size to be calculated and compared amongst specimens.

Note 5 and **Fig. 5** display and discuss the nuances of quantification of ultrasound data. The reader is also referred to **Notes 6–9** which deal with the technical limits and practical limitations of the method as well as future advancements geared at improving the technique.

4. Notes

4.1. Apoptosis in Cells

1. **Figure 2** presents a representative result for the detection of apoptosis using a cell-culture system. Centrifuged cells visualized using a high-frequency ultrasound

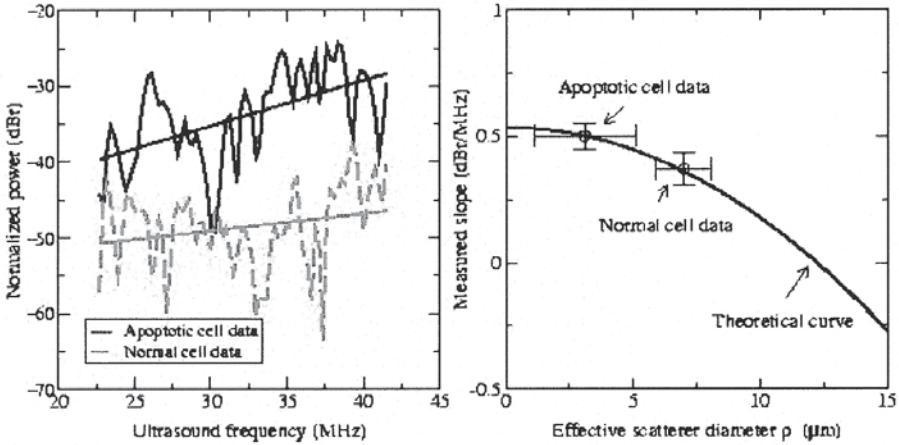

Fig. 5. Radiofrequency Analysis of Apoptotic Cells Normalized radio-frequency analysis spectra of normal (dotted line) and apoptotic cells (solid line) and best linear fits. The spectrum slope and normalized power change in the two cell populations. The intercept and slope of each line correspond to primary ultrasound backscatter characteristics for each analyzed sample. In the right panel measured slopes which are shown superimposed on a theoretical curve produce reasonable estimates of experimentally measured nuclear fragment scatterer size and concur with the reduction in scatterer size.

device operating at 40 MHz (**Fig. 1**) and thus permitting higher resolution imaging in comparison to conventional ultrasound devices operating at much lower frequencies are shown. Individual cells cannot be resolved at the operating wavelength of this instrument but we demonstrate in this study that changes in ensembles of cells can result in significant changes in ultrasound images. The results presented in **Fig. 2** indicate that apoptotic cells scatter ultrasound at a level approx 6× that observed with non-apoptotic cells. The degree of scattering also exhibits an approximate linear relation to the progression of apoptosis in terms of nuclear condensation and fragmentation. In addition, we now have established our detection limit to be, so far, at best 5% apoptosis, determined in a carefully controlled titration experiment. The ultrasound backscatter amplitude begins to increase as the cells' nuclei condense approximately 2–3-fold in diameter over that of nuclei in non-apoptotic cells. The backscatter signal then continues to increase to 6× that obtained for normal cells with subsequent apoptotic nuclear fragmentation. Changes in cell morphology that are observable include changes in the nuclear membrane, nuclear condensation and nuclear fragmentation (*see* **ref. *2*** and **Fig. 2**—this chapter).

2. Arrest of cells in mitosis also results in an increase in ultrasound backscatter. Whereas the ultrasound images of the apoptotic cells indicated a 6-fold increase in backscatter in comparison to normal cells, the mitotic cells exhibited only an

approximate 3-fold increase in ultrasound backscatter amplitude ***(2)***. This is in good agreement with the ultrasound levels observed at the 6 h time point after treatment with cisplatinum where the apoptotic fraction of cells exhibits primarily nuclear condensation. We have also carried out further series of experiments in which we have established that nuclear condensation is both necessary and sufficient for increases in ultrasound backscatter. These experiments enzymatically disrupted DNA condensation (using DNase) in mitotic cells reducing the ultrasound signal to that of non-mitotic cells.

4.2. Apoptosis in Tissues

3. **Figure 3** illustrates the use of ultrasound imaging at high frequencies to detect apoptosis that occurred *ex vivo* in an animal system which involved photodynamic therapy. This type of therapy has been demonstrated to induce apoptosis in several tissues ***(30,31)***. In our study, photodynamic therapy using Photofrin II, a haematoporphyrin derivative, was applied in a rat model system. After an investigation of dose and time effects, tissue responses were monitored at three separate time points. Ultrasound backscatter images obtained at the 24 h time point at the site of therapy and in the non-irradiated contralateral side of an unfixed freshly-excised brain are shown. Backscatter amplitude measurements indicate that the 24 h post-photodynamic therapy brain exhibited a 3.7 ± 2.0 fold increase in ultrasound backscatter in comparison to a control sample. A specific staining procedure, a TdT assay, was is used to detect apoptosis. Free DNA ends produced by apoptotic chromosome fragments are labeled with a green fluorescent stain and a propidium iodide counterstain was used to mark cytoplasm red. Computerized analysis indicated that approx 40% of the cells in this area are apoptotic (**Fig. 3**).
4. To demonstrate the feasibility of detecting apoptosis in vivo additional experiments were carried out in which a photosensitized rat had areas of its skin exposed to activating laser light. **Fig. 4** indicates that increases in dose of activating light correlated with increases observed in ultrasound backscatter. Histological analyses revealed increasing levels of apoptosis with the dose of activating light.

4.3. Analysis of Ultrasound Backscatter Signals Associated with Apoptosis

5. In theoretical models it is assumed that structures that scatter ultrasound are weak isotropic scatterers randomly distributed in the tissue and that fluctuations in acoustic impedance can be modeled as a Gaussian spatial autocorrelation function. This permits calculable parameters to be related to the physical attributes of the scatterers. One can then derive, based on the measured values from the linear regression of the power spectrum as outlined above, values for the effective scatterer diameter and concentration. For cells undergoing apoptosis, assuming on the basis of experimental evidence that the nucleus is primarily responsible for the scattering, one would expect that the effective scatterer diameter would decrease (since there is nuclear fragmentation) as cells undergo apoptosis. Representative results

consistent with this theory are presented in **Fig. 5** where a decrease in the effective scatterer diameter by a factor of 2 is demonstrated with apoptosis.

4.4. Limits, Limitations and Future Developments

6. One of the most significant current limitations to this technique for detecting apoptosis in response to DNA damage is borne out of the fact that in the process of forming ultrasound images valuable radio-frequency information is lost. For instance, pyknosis due to nuclear condensation and apoptosis can both result in increases in ultrasound backscatter and have similar appearances in terms of speckle, the effect of constructive and destructive coherent interference, in ultrasound images. This can be misleading and confusing as different physiological states of cells can potentially have similar appearances. However, the radio-frequency spectra, the spatial frequency dependent ultrasound backscatter information associated with the two types of samples would be very different. But the interpretation of such data is often very complex. To this end, we are devising a method which combines real-time analyses of spectral data with ultrasound image display in order to differentiate better the sub-cellular processes which are being detected. It is now possible to calculate scatterer sizes which can be used to infer whether a sample is apoptotic with fragmented nuclear fragments or in another physiological state with different sized scatterers of ultrasound.
7. Another compounding factor to facile image acquisition and interpretation arises in the case of the clinical imaging of tumors. Attenuation from different tissues in the ultrasound path to the target lesion can result in different intensities from the same tumor tissue being generated. In the absence of different overlying tissues the intensity from the lesion would be otherwise homogeneous. Moreover, specular reflections at interfaces between different tissues such as blood vessel walls can compound image complexity since such reflections are angle dependent.
8. Another limit to interpreting images of cells, tissues, and tumors, in terms of modern ultrasound knowledge, is due a paucity of data regarding the very nature of the cellular and sub-cellular agents of ultrasound backscatter. Simply stated, this means that although we have detected a powerful and useful phenomenon in terms of ultrasound image formation we are still wrestling with arriving at an explanation in regards to the physical processes which are significant to the effect taking place. To date, physicists and imaging scientists have tended to explain ultrasound image formation as the result of backscatter from interfaces between regions with different attenuation properties in a biological sample as modulated by the tissue properties of acoustical attenuation. What is recognized from extensive theoretical studies is that the degree of randomization or the entropy of scattering agents plays an important role in the backscatter of high-frequency ultrasound. Namely, the more randomly positioned the scatterers of ultrasound are within a sample, the greater the backscatter is observed ***(26)***. However, the identity of the scatters remains mostly a mystery—researchers have not been able to pinpoint the features inside cells responsible for ultrasound backscatter.

We have also begun to tackle this problem using modern biochemistry and molecular biology methods which facilitate the chemical and enzymatic dissection of cellular components thus permitting the effects of different biological components on ultrasound backscatter to be delineated. To this end we have begun to conduct experiments some of which are outlined in this chapter above which point to the chromatin-bound DNA in the cell's nucleus as the chief scattering agent in the cell. Other structures currently under investigation and being characterized for their ultrasonic properties include RNA, histones, chromosome fibres, the multi-lamellar endoplasmic reticulum, as well as a representative protein and lipid samples from cells. We hope to be able one day to understand how each of the these components contributes to ultrasound backscatter and then to expand this model to tissues.

9. From a technological perspective, due to the imaging wavelengths which are being used, we are limited to a relatively short penetration depth typically of 1–2 cm at 30–40 MHz which appears to be the optimal frequency range for detecting apoptosis. Technological advances are being made in an effort to overcome this limitation in at least two manners. In the first, developers of ultrasound instrumentation have been developing newer electronic circuitry to permit an increased penetration depth, almost doubling it in the newest generation of instruments (**Fig. 1**). Additionally, collaborators in the ultrasound field have developed miniature transducers that fit onto the end of 27 gauge needles thus permitting intracavitary or even interstitial imaging and spectroscopy in the frequency range compatible with detecting the cellular features associated with apoptosis (Foster et al., unpublished results). Such developments should permit imaging to be carried out at high frequencies of any internal human organ or neoplasms seated deeply inside healthy tissue expanding the versatility of the imaging technique which is currently limited to superficial lesions.

Acknowledgments

I am most grateful to Dr. Stuart Foster and his laboratory for use of their high-frequency ultrasound imaging device. I also thank VisualSonics for access to ultrasound imaging devices in development. I thank Allan Fernandes, Yew Meng Heng, Arthur Worthington, Kasia Harasiewicz, Brian Starkowski and Karen Hahn for technical assistance. I am indebted to Dr. Brent Zanke, Dr. Richard Tsang, Dr. Woodrow Wells, Dr. Wilfred Levin, and Dr. Ian Quirt for helpful discussions. Most importantly, I thank Julie Beaulieu for her understanding and loving support. This chapter is dedicated to all those who want to change the world—GJC. This work was supported by research awards to GJC from the Faculty of Medicine, University of Toronto with funds in part from the Medical Research Council of Canada. This research was supported by grants awarded to the authors from the MRC Canada, NSERC, the University of Toronto, Ryerson Polytechnic University and Canadian Foundation for Innovation.

References

1. Czarnota, G. J., Kolios, M. C., Vaziri, H., Benchimol, S., Ottensmeyer, F. P., Sherar, M. D., and Hunt. J. W. (1997) Ultrasound biomicroscopy of viable, dead and apoptotic cells. *Ultrasound Med. & Biol.* **23,** 961–965.
2. Czarnota, G. J., Kolios, M. C., Abraham, J., Portnoy, M., Ottensmeyer, F. P., Hunt, J.W, and Sherar M. D. (2000) Ultrasound imaging of apoptosis. *British J. Cancer* **81,** 520–527.
3. Pavlin, C. J., Sherar, M. D., and Foster, F. S. (1990) Subsurface ultrasound microscopic imaging of the intact eye. *Opthamology* **97,** 244–250.
4. Sherar, M. D., Noss, M. B., and Foster, F. S. (1987) Ultrasound backscatter microscopy images the internal structure of living tumour spheroids. *Nature* **330,** 493–495.
5. Wood, K. Transplantation biology: recent advances. 5th basic sciences symposium of the Transplantation Society (1998). *Molecular Medicine Today*. **4,** 56–57.
6. Berry, M. A., Behnke, C. A., and Eastman, A. (1990) Activation of programmed cell death (apoptosis) by cisplatin, other anti-cancer drugs, toxins and hyperthermia. *Biochem. Pharmacol* **90,** 2353–2362.
7. Meterissian, S. H. (1990) Apoptosis: its role in the progression of and chemotherapy for carcinoma. *J. Am. College of Surgeons* **184,** 658–666.
8. Lowe, S. W., Boris, S., McClatchey, A., Remington, L., Ruley, H. E., and Jacks, T. (1994) p53 status and the efficacy of cancer chemotherapy. *Science* **266,** 807–810.
9. Luo, Y., Chang, C. K., and Kessel, D. (1996) Rapid induction of apoptosis by photodynamic therapy. *Photochem. Photobiol.* **63,** 528–534.
10. Fisher, A. M. R., Danenberg, K., Banerjee, D., Bertino, J. R., Danenberg, P., and Gomer, C. J. (1997) Increased photosensitivity in HL60 cells expressing wild-type p53. *Photochem.Photobiol.* **66,** 265–270.
11. Thatte, U., and Dahanikar, S. (1997) Apoptosis: clinical relevance and pharmacological manipulation. *Drugs* **54,** 511–532.
12. Allegra, C. et al. (1997) The condensation of chromatin in apoptotic thymocytes shows a specific structural change. *J. Biol. Chem.* **272(16),** 10,817–10,822.
13. Czarnota, G.J, and Ottensmeyer, F. P. (1996) Structural states of the nucleosome (1996) *J. Biol. Chem.* **271,** 3677–3683.
14. Gaurieli, Y., Sherman, Y., and Ben-Sasson, S. A. (1992) Identification of programmed cell death *in situ* via specific labeling of nuclear DNA fragmentation. *J. Cell. Biol.* **119,** 493–501.
15. Sherar, M. D. (1990) Ultrasound backscatter microscopy and its application to biological studies. Ph.D. Thesis, University of Toronto, 1990.
16. Sokolov, S. J. Means for Indicating Flaws in Materials, USSR Patent No. 49 (1936), British Patent No. 477139 (1937), and U. S. Patent No. 2164125 (1939).
17. Dunn, F., and Fry, W. J. (1959) Ultrasonic absorption microscope. *J. Acoust. Soc. Am.* **31,** 632–633.
18. Korpel, A., Kessler, L. W., and Palermo, P. R. . (1971) An acoustic microscope operating at 100 MHz. *Nature* **232,** 110.

19. Langevin, P., and Chilowski, M. C. Procedes et appareils pour la production de signauz sous-marins direges et pour la localisation a distance d'obstacles sous-marins. French Patent 502913 (1916).
20. Wild, J. J., and Reid, J. M. (1952) Application of echo-ranging techniques to the determination of the structure of biological tissues. *Science* **115,** 226–230.
21. Sherar, M. D., Starkowski, B. G., taylor, B., and Foster, S. F. (1989) A 100 MHz B-scan ultrasound backscatter microscope. *Ultrasonic Imaging* **11,** 95–105.
22. Bérubé, L. R., Harasiewicz, K., and Foster, F. S. (1992) Use of a high frequency ultrasound microscope to image the action of 2–nitroimidazoles in multicellular spheroids. *Br. J. Cancer.* **65,** 633–640.
23. Ursea, R., Coleman, D. J., Silverman, R. H., Lizzi, F. L., Daly, S. M., and Harrison, W. (1998) Correlation of high-frequency ultrasound backscatter with tumor microstructure in iris melanoma. *Ophthalmology* **105,** 906–912.
24. Lizzi, F. L., Astor, M., Feleppa, E. J., Shao, M. and Kalisz, A. (1997) Statistical framework for ultrasonic spectral parameter imaging. *Ultrasound Med. Biol.* **23,** 1371–1382.
25. D. J. Coleman, D. J., Silverman, R. H., Rondeau, M. J., Coleman, J. A., Rosberger, D., Ellsworth, R. M. and Lizzi, F. L. (1991) Ultrasonic tissue characterization of uveal melanoma and prediction of patient survival after enucleation and brachytherapy. *American J. Ophth.* **112,** 682–688.
26. Hunt, J. W., Worthington, A. E., and Kerr, A. T. (1995) The subtleties of ultrasound images of an ensemble of cells: simulation from regular and more random distribution of scatterers. *Ultrasound in Med & Biol.* **21,** 329–341.
27. Zamble, D. S., and Leopard, C. J. (1995) Cisplatin and DNA repair in cancer chemotherapy. *Trends Biochem. Sci.* **20,** 435–439.
28. Dustin, P. (1980) Microtubules. *Sci. Am.* **243,** 66–76.
29. Li, Y. Q., Guo, Y. P., Jay, V., Stewart, P. A., and Wong, C. S. (1996) Time course of radiation-induced apoptosis in the adult rat spinal cord. *Radiotherapy and Oncology* **39,** 35–42.
30. Matsumoto, Y., Muro, Y., Banno, S., Okasaki, M., and Tamada, Y. (1996) Differential apoptotic pattern induced by photodynamic therapy. *Arch. Derm. Res.* **289,** 52–54.
31. Webber, J., Luo, Y., Crihy, R., Fromm, D., and Kessel, D. (1996) An apoptotic response to photodynamic therapy with endogenous protoporphyrin *in vivo*. *Photochem. Photobiol*. **35,** 209–211.

21

p53 Induction as an Indicator of DNA Damage

Galina Selivanova

1. Introduction

p53 plays a central role in the cellular response to DNA damage. Induction of this protein is triggered by DNA breaks and correlates with their presence ***(1,2)***. In addition, p53 is upregulated by a number of different stress conditions including hypoxia, oncogene activation, viral infection, and ribonucleotide depletion (reviewed in ***(3)***). The ability of C-terminal domain of p53 to bind DNA ends ***(4,5)***, insertion/deletion mismatches ***(6)***, recombination intermediates ***(7)*** and gamma-irradiated DNA in vitro ***(8)*** implies that direct recognition of DNA lesions by p53 can play a role in its induction ***(9)***.

Under normal conditions p53 protein levels are kept low due to ubiquitin-dependent degradation mediated by E3 ubiquitin ligase Mdm-2 (mouse double minute) ***(10–12)***. Upon DNA damage the series of phosphorylation events results in release of p53 from Mdm-2 complexing followed by accumulation of high levels of the protein. The PI-3 family kinases ATM (ataxia-telangiectasia mutated) and ATR (AT-related) are probably the most upstream kinases that respond to DNA damage by phosphorylating p53, along with Mdm-2 and the checkpoint kinases chk2 and chk1 (checkpoint kinases 2 and 1), respectively. ATM-dependent phosphorylation of Ser15 enhances the transcriptional transactivation function of p53, whereas chk2-mediated Ser20 phosphorylation inhibits Mdm-2 binding and thus prevents p53 degradation ***(13–19)***. Mdm-2 protein expression is activated by p53 itself, creating a negative feedback loop, which secure to cease p53 response in the absence of stress conditions. Transcriptionally inactive mutant p53 found in tumors is unable to induce the expression of its destructor Mdm-2. As a result, mutant p53 is usually expressed at high levels in tumor cells and is not further induced by DNA damage ***(20)***.

From: *Methods in Molecular Biology, vol. 203:* In Situ *Detection of DNA Damage: Methods and Protocols*
Edited by: V. V. Didenko

Induction of p53 results either in growth arrest, to allow time for DNA repair, or in apoptosis *(21,22)*. By eliminating the cells carrying potential genetic alterations p53 prevents tumor development (reviewed in *(23)*). In addition p53 can preserve genomic integrity by promoting DNA repair (reviewed in *(24)*). It is conceivable that p53 bound to damaged DNA facilitates the recruitment of DNA repair factors to the sites of DNA damage via protein-protein interaction. Loss of p53 function leads to the deregulation of DNA repair and causes gross structural changes in the genome. Disruption of p53 function in some systems resulted in a deficiency in a rate and extent of nucleotide excision repair *(25–27)*.

p53 induction can serve as an indicator of DNA damage in situations where the other sources of its upregulation, such as mutation, hypoxia or virus infection, are excluded. Immunohistochemical detection of p53 can provide an indirect tool for detection of DNA damage. The extent of p53 induction upon DNA damage is inversely correlated with the efficiency/intactness of the DNA repair system in a cell *(28)*. Thus persistent p53 staining after exposure to DNA damaging agents might signal the defect in DNA repair. However, one should keep in mind that in spite of a correlation between the extent of DNA damage and the level of p53 induction, the amount of p53 could hardly serve as a quantitative indicator of DNA damage.

Accumulation of p53 could be used as tool for the detection of DNA damage in situ. For example, p53 induction was shown to serve as a marker for detection of DNA lesions produced by sunlight *(29)*. Increase in p53 level in human skin following UVAI, UVAI+II and solar stimulating radiation was used to estimate the efficacy of protective measures, such as sunscreens or protective clothing, against both UVB- and UVA-induced damage in human skin *(30)*.

A correlation between p53 induction pattern and DNA damaging mechanism of carcinogenes was demonstrated *(31,32)*. Thus, p53 appears to be a promising candidate for a low cost predictive assay of genotoxic damage and probably an effective tool for identifying environmental genotoxins.

This chapter describes the protocols for immunohistochemical detection of p53 in cultured primary cells after mitomycin C treatment as an example of DNA damage. Staining of tissue sections where p53 induction can serve as an indicator of DNA damages also described.

2. Materials

1. Primary culture of human diploid fibroblasts (*see* **Note 1**).
2. Fixed, paraffin-embedded tissue sections prepared according to standard paraffin embedding procedures.
3. IMDM culture medium supplemented with 10% heat-inactivated fetal bovine serum (Invitrogen Corporation, Carlsbad, CA) , 2 m*M* L-glutamine, penicillin (50 µg/mL) and streptomycin (50 µg/mL).

4. Fixative for cells (*see* **Note 2**): 4% formaldehyde in phosphate-buffered saline (PBS): Wear mask and gloves and use the hood when preparing formaldehyde fixative.
   a. Solution A, PBS: Fill 1 L beaker with 900 mL of distilled water and dissolve 0.23 g of NaH_2PO_4 (anhydrous), 1.15 g Na_2HPO_4 (anhydrous) and 9 g NaCl. Adjust pH to 7.4 using 1 *M* NaOH and/or 1 *M* HCl;
   b. Solution B, 4% formaldehyde: Dilute 37% formaldehyde (Sigma, St. Louis, MO) in PBS 1:9. Store at 4°C, protect from daylight. Avoid using this fixative after being stored longer than three weeks.
5. Cell culture tools and accessories: Multi-well (4 or 8 wells) chamber slides (Nalge Nunc International, St Louis, MO), 70% alcohol, pasteur pipets, sterile hood, incubator to culture cells in a humidified atmosphere containing 5% CO_2 at 37°C.
6. Permeabilization buffer: 0.2% Triton-X100 in PBS.
7. 0.01 *M* citrate buffer: 2.1 g of citric acid per 1 L, pH adjusted to 6.0 with 2 *M* NaOH. For microwave antigen unmasking for tissue sections.
8. DNA damage reagent: mitomycin C: prepare 10 mg/mL stock solution in sterile water, store at –20°C.
9. Blocking buffer: PBS containing 2% BSA, 5% glycerol, 0.2% Tween 20 and 0.01% sodium azide or 5–10% preimmune serum in PBS.
10. Primary anti-p53 antibodies: human specific DO1 or PAb1801 (Oncogene Research Products, San Diego, CA). Working dilution for DO1 is 1:250 in blocking buffer, for PAb1801 1:100 (*see* **Note 5**).
11. Fluorescent secondary antibodies: rabbit anti-mouse conjugated with fluorescein isothiocyanate (FITC; DAKO, Carpinteria, CA). Make 1: 50 working dilution in blocking buffer. For tissue sections use HRP-DAB Cell and Tissue Staining kit combined with DAB enhancer (R&D Systems, Minneapolis, MN).
12. Mounting medium for fluorescent labels from DAKO. This medium minimizes loss of fluorescence by FITC photobleaching during examination under the fluorescence microscope. Add Hoechst 33258 (Oncogene Research Products, San Diego, CA) for staining of DNA at a final concentration of 1 mg/mL. Hoechst 33258 is a potential carcinogen, therefore wear gloves while working with it. Mounting medium for chromogenic labels: aqueous mounting medium (R&D Systems, Minneapolis, MN).
13. Wax pen to label the tissue area.
14. Pen to label slides: SHUR/MARK pen (Fisher Scientific, Pittsburgh, PA).
15. Humidified incubation chamber for cell and tissue staining: Staining tray of 5-slide capacity with a cover (Signet Laboratories, Dedham, MA).
16. Bright field/fluorescence microscope (Olympus Optical Co. Ltd, Tokyo, Japan) equipped with fluorescence filter set to visualize FITC (460–490 nm excitation and 510–550 nm emission).

3. Methods

Unless otherwise stated, all incubations are performed at room temperature in a humid chamber.

3.1. Immunostaining of Cultured Cells

1. Seed the cells in multiwell chamber slide and incubate them for 18–24 h before treatment with DNA damaging agent.
2. In a sterile hood gently remove the culture medium from each well using a sterile pipette. Position the tip of the pipette into the corner of the well to avoid disturbing cells.
3. Dilute stock solution of mitomycin C 1:1000 in a warm (37°C) culture medium. Final concentration of mitomycin C should be 10 μg/mL. Add mitomycin C into designated wells. In control wells, add culture medium. Return the chamber slide into the 37°C/CO_2 humidified incubator and incubate for 24 h.
4. Remove the chamber slides from the incubator, discard the culture medium and add fixative into each well. Fix for 10 min and then wash 3 × 10 min with PBS.
5. Permeabilize cells for 2–5 min in 0.2% Triton in PBS.
6. Wash 3 × 10 min in PBS.
7. Remove the upper part of the slide as described by manufacturer. Place slides horizontally into humidified chamber, add anti-p53 antibodies (30 μL per sample) and incubate for 1 h. Alternatively, cells may be incubated with primary antibody overnight at 4°C. In the latter case you might need to use a higher dilution of the primary antibody.
8. Wash slides 3 × 10 min in PBS and incubate with secondary anti-mouse FITC-conjugated antibodies for 1 h (30 μL per sample).
9. Wash 3 × 10 min in PBS. Wipe of excess buffer around the sample but do not let the sample dry.
10. Apply mounting medium for fluorescent labels (DAKO, Carpinteria, CA), 10 μL per sample and put cover slip. Apply a drop of immersion oil on top and examine under the fluorescence microscope.

3.2. p53 Detection in Paraffin-Embedded Tissue Sections

For the staining of tissue sections chromogenic rather than fluorescent detection systems are recommended, due to the lower sensitivity of the latter in tissues. To prevent drying out of the sections, the whole staining procedure is performed in a humid chamber.

1. Label the slides using SHUR/MARK pen.
2. On the slide outline the tissue section with wax pen and let it dry for 5 min.
3. Dewax and rehydrate the sections by incubating slides at room temperature in a glass Coplin jar as follows:
   a. xylene—2× 10 min
   b. 100% ethanol—2× 10 min
   c. 95% ethanol—2× 10 min
   d. 70% ethanol—2× 10 min
4. Wash the slides (2 × 5 min) in PBS.
5. Antigen unmasking on paraffin sections is achieved by mild proteolytic diges-

tion or microwave treatment of the sections. Here we will describe microwave treatment.

a. place the slides in a jar with 0.01 *M* citrate buffer (pH 6.0), cover it with paraffin and puncture the film.
b. heat the sections for 2 min (the buffer should boil, the sections should not dry during the procedure; refill it with distilled water, if necessary).
c. incubate for 15 min at room temperature, then rinse with distilled water.

6. Remove the slides from the jar, shake excess water, place them horizontally and add 3–5 drops of 0.5% H_2O_2 in methanol to block endogenous peroxidase activity. Incubate 10 min.
7. Rinse the slides in distilled water for 5 min, then in PBS for 5 min.
8. Block nonspecific binding of primary antibodies by incubation with 5–20% solution of preimmune mouse serum for 20 min at room temperature in a humid chamber. Blot excess blocking serum from sections.
9. Apply primary antibody PAb1801 diluted 1:100 in PBS with carrier protein (3% BSA or 10% serum) and incubate 1 hour at 37°C (or overnight at +4°C).
10. Wash slides in PBS 3× 5 min.
11. Run avidin-biotin block using reagents from Cell and Tissue Staining kit (R&D Systems, Minneapolis, MN). Place slides horizontally into a humid chamber and add 3–5 drops of avidin blocking solution and incubate for 15 min. Rinse slides in PBS, place them horizontally and add 3–5 drops of biotin blocking solution from the kit and incubate 15 min. Wash slides in PBS for 20 min.
12. Incubate slides with biotinylated anti-mouse secondary antibody from Cell and Tissue Staining kit for 1 h at room temperature.
13. Wash slides 3 × 5 min in PBS.
14. Incubate sections with horseradish peroxidase conjugated with streptavidin from Cell and Tissue Staining kit for 1 h at room temperature.
15. Wash the slides 3 × 5 min in PBS.
16. Apply DAB mixture together with DAB enhancer to the sections, incubate 1–15 min (until desired stain intensity develops) at room temperature. DAB is a potential carcinogen, therefore wear gloves while working with it. Monitor the development of color under the microscope using 4× or 10× power lens.
17. Discard DAB mixture, rinse the slides in water and air-dry the sections.
18. Mount the slides in aqueous mounting media: add a small drop of the mounting media on the section, carefully place a coverslip on the drop, avoiding air bubbles. Leave the mounted slides on a bench to allow the mounting medium to set overnight, then store in light-tight boxes at room temperature until evaluation.

4. Notes

1. The use of primary cultures (such as human diploid fibroblasts) is recommended. Since p53 is mutated in most of the transformed or tumor-derived cell lines, these cells should note be used for such type of experiments. Positive p53 staining before any treatment usually indicates the presence of nonfunctional mutant p53.

2. An alternative to the formaldehyde fixation is methanol/acetone fixation protocol, which could be used when the slides are intended for storage before performing the immunostaining. Prepare 1:1 solution of methanol and acetone and keep it at –20°C at least two hours before use. Fix the cells in methanol/acetone at –20°C for at least 30 min. Slides could be kept in the solution at –20°C up to one month. Remove the slide from the fixative, drain off/wipe off organic solvent without disturbing the cell smear. Immediately rehydrate the cells in PBS for 10 min. Stain the cells as it is described in the protocol. Methanol/acetone fixation does not require permeabilization.
3. When using immunoenzymatic detection system make sure that the buffers used to dilute the reagents and to wash the slides do not contain any inhibitors of the enzyme (e.g., no sodium azide in case of peroxidase-based system).
4. Do not allow cell and tissue samples to dry during the incubation and washing steps. Cell or/and tissues samples that were found dry should be excluded from experiment. Also watch for partial drying of tissue section margins: this may result in strong and not necessarily specific staining. Since partial drying may be overlooked (i.e. when staining a large number of slides) during the staining procedure, it is recommended to interpret "marginal" results cautiously. The staining in the central part of the tissue will be more specific than that one on the tissue edges.
5. Crossreactivity of some antibodies to p53 with cytoplasmic intermediate filaments (PAb421, Oncogene Research Products, San Diego, CA) or granular cytoplasmic structures (PAb1801, Oncogene Research Products, San Diego, CA) and possibly artifactual cytoplasmic staining caused by inappropriate fixation of samples ***(33)*** underline the significance of controls (*see* below).
6. It is recommended to employ different types of controls to be sure that immunohistochemistry displays p53-expressing cells rather than non-specific cell and tissue binding sites. Therefore treatment-specific control should be employed, which will address the question of selectivity. This is done by comparing staining in untreated cells/tissues vs. samples treated with DNA damaging agents. Even though normal specimens may contain cells with p53-positive nuclei, their number and the level of p53 expression are expected to be extremely low in comparison with treated samples.
7. The specificity of staining is determined by two factors: (a) specificity of anti-p53 antibodies and (b) specificity of immunohistochemical reagents.
    a. The purpose of determining the specificity of anti-p53 antibodies is to confirm whether cell or tissue staining resulted from the interaction of antibodies with specific target (p53) or caused by their cross-reaction with irrelevant antigens. The efficient way to study the specificity is to block anti-p53 antibodies taken in working dilution with the peptide corresponding to the antibody epitope on p53 taken in concentration 10 μg/mL. Mix well and incubate either 5 h at room temperature or overnight at 4°C. It is expected that cell and tissue staining will be decreased when using peptide-blocked antibodies since

peptide will occupy binding sites on anti-p53 antibodies and thus reduce or abolish their capacity to interact with cellular protein.

b. The analysis of the specificity of immunohistochemical reagents needs to be done to demonstrate that such reagents as anti-mouse secondary antibodies, avidin-HRP or fluorescein-conjugated antibody do not bind to cells and tissues per se. The simplest way to answer this question is to omit anti-p53 antibody: lack of labeling will be indicative for the specificity of immunohistochemical reagents. In addition, the enzyme reaction should be performed on a section to check for potential endogenous enzyme activity. If non-specific labeling is observed, additional steps are required to minimize it.
   Nonspecific staining can be eliminated by:
   - Titration of the primary antibodies.
   - Diluting the reagents in buffers containing higher concentration of the blocking protein (for example, serum).
   - Reducing the incubation times with antibodies and/or more extensive washes between the individual steps.
   - Application of avidin-biotin block using reagents from Cell and Tissue Staining kit.
   - Frequently a high non-specific background is caused by free aldehyde groups present in tissues that are fixed with paraformaldehyde or glutaraldehyde: free aldehyde groups are capable of reacting with secondary antibodies and "crosslinking" them to the tissue. Free aldehyde groups can be blocked by incubating specimens before applying primary antibodies with 0.5 µg/mL of sodium borohydrate ($NaBH_4$) for 10–20 min at room temperature.

8. The specificity of staining is evaluated using (a) negative control and (b) positive control.
   a. Negative control constitutes a specimen, which does not contain p53. Human tumor cell lines carrying p53 gene deletion, which could be used for this purpose. These include for example osteosarcoma Saos 2, lung cancer H1299, or ovarian cancer SKOV cell lines.
   b. Tumor-derived cell lines with high level of mutant p53 expression can serve as a positive control. For example: colon carcinoma SW480 or A431 and many others ***(34)***.

The staining techniques described in this article could be used as a research tool to study DNA damage *in situ*. For instance, these techniques could be applied for qualitative measurement of genotoxicity of different carcinogens and hence can help to monitor pollution using cultured cells as a model.

Acknowledgments

This work was supported by grants from the Swedish Cancer Society, Swedish Royal Academy of Sciences and Swedish Medical Research Council.

References

1. Nelson, W. G., and Kastan, M. B. (1994) DNA strand breaks: the DNA template alterations that trigger p53- dependent DNA damage response pathways. *Mol. Cell. Biol.* **14,** 1815–1823.
2. Huang, L. C., Clarkin, K. C., and Wahl, G. M. (1996) Sensitivity and selectivity of the DNA damage sensor responsible for activating p53-dependent G1 arrest. *Proc. Natl. Acad. Sci. U S A* **93,** 4827–4832.
3. Giaccia, A. J., and Kastan, M. B. (1998) The complexity of p53 modulation: emerging patterns from divergent signals. *Genes Dev.* **12,** 2973–2983.
4. Bakalkin, G., Yakovleva, T., Selivanova, G., Magnusson, K. P., Szekely, L., Kiseleva, E., Klein, G., Terenius, L., and Wiman, K. G. (1994) p53 binds single-stranded DNA ends and catalyzes DNA renaturation and strand transfer. *Proc. Natl. Acad. Sci. U S A* **91,** 413–417.
5. Bakalkin, G., Selivanova, G., Yakovleva, T., Kiseleva, E., Kashuba, E., Magnusson, K. P., Szekely, L., Klein, G., Terenius, L., and Wiman, K. G. (1995) p53 binds single-stranded DNA ends through the C-terminal domain and internal DNA segments via the middle domain. *Nucleic Acids Res.* **23,** 362–369
6. Lee, S., Elenbaas, B., Levine, A., and Griffith, J. (1995) p53 and its 14 kDa C-terminal domain recognize primary DNA damage in the form of insertion/deletion mismatches. *Cell* **81,** 1013–1020.
7. Dudenhoffer, C., Rohaly, G., Will, K., Deppert, W., and Wiesmuller, L. (1998) Specific mismatch recognition in heteroduplex intermediates by p53 suggests a role in fidelity control of homologous recombination. *Mol. Cell. Biol.* **18,** 5332–5342.
8. Reed, M., Woelker, B., Wang, P., Wang, Y., Anderson, M. E., and Tegtmeyer, P. (1995) The C-terminal domain of p53 recognizes DNA damaged by ionizing radiation. *Proc. Natl. Acad. Sci. U S A* **92,** 9455–9459.
9. Selivanova, G., and Wiman, K. G. (1995).p53: a cell cycle regulator activated by DNA damage. *Adv. Cancer Res.* **66,** 143–180.
10. Haupt, Y., Maya, R., Kazaz, A., and Oren, M. (1997) Mdm2 promotes the rapid degradation of p53. *Nature* **387,** 296–299.
11. Kubbutat, M. H., Jones, S. N., and Vousden, K. H. (1997) Regulation of p53 stability by Mdm2. *Nature* **387,** 299–303.
12. Midgley, C. A., and Lane, D. P. (1997) p53 protein stability in tumour cells is not determined by mutation but is dependent on Mdm2 binding. *Oncogene* **15,** 1179–1189.
13. Shieh, S. Y., Ikeda, M., Taya, Y., and Prives, C. (1997) DNA damage-induced phosphorylation of p53 alleviates inhibition by MDM2. *Cell* **91,** 325–334.
14. Shieh, S. Y., Taya, Y., and Prives, C. (1999) DNA damage-inducible phosphorylation of p53 at N-terminal sites including a novel site, Ser20, requires tetramerization. *EMBO J.* **18,** 1815–1823.
15. Unger, T., Juven-Gershon, T., Moallem, E., Berger, M., Vogt Sionov, R., Lozano, G., Oren, M., and Haupt, Y. (1999) Critical role for Ser20 of human p53 in the negative regulation of p53 by Mdm2. *EMBO J.* **18,** 1805–1814.

16. Chehab, N. H., Malikzay, A., Stavridi, E. S., and Halazonetis, T. D. (1999) Phosphorylation of Ser-20 mediates stabilization of human p53 in response to DNA damage. *Proc Natl Acad Sci U S A* **96,** 13,777–13,782.
17. Chehab, N. H., Malikzay, A., Appel, M., and Halazonetis, T. D. (2000) Chk2/hCds1 functions as a DNA damage checkpoint in G(1) by stabilizing p53. *Genes Dev* **14,** 278–288.
18. Shieh, S. Y., Ahn, J., Tamai, K., Taya, Y., and Prives, C. (2000) The human homologs of checkpoint kinases Chk1 and Cds1 (Chk2) phosphorylate p53 at multiple DNA damage-inducible sites. *Genes Dev.* **14,** 289–300.
19. Khosravi, R., Maya, R., Gottlieb, T., Oren, M., Shiloh, Y., and Shkedy, D. (1999) Rapid ATM-dependent phosphorylation of MDM2 precedes p53 accumulation in response to DNA damage. *Proc. Natl. Acad. Sci. U S A* **96,** 14,973–14,977.
20. Sigal, A., and Rotter, V. (2000) Oncogenic mutations of the p53 tumor suppressor: the demons of the guardian of the genome. *Cancer Res* **60,** 6788–6793.
21. Kastan, M. B., Onyekwere, O., Sidransky, D., Vogelstein, B., and Craig, R. W. (1991) Participation of p53 protein in the cellular response to DNA damage. *Cancer Res.* **51,** 6304–6311.
22. Yonish-Rouach, E., Resnitzky, D., Lotem, J., Sachs, L., Kimchi, A., and Oren, M. (1991) Wild-type p53 induces apoptosis of myeloid leukaemic cells that is inhibited by interleukin-6. *Nature* **352,** 345–347.
23. Lowe, S. W., Bodis, S., McClatchey, A., Remington, L., Ruley, H. E., Fisher, D. E., Housman, D. E., and Jacks, T. (1994) p53 status and the efficacy of cancer therapy in vivo. *Science* **266,** 807–810.
24. Albrechtsen, N., Dornreiter, I., Grosse, F., Kim, E., Wiesmuller, L., and Deppert, W. (1999) Maintenance of genomic integrity by p53: complementary roles for activated and non-activated p53. *Oncogene* **18,** 7706–7717.
25. Ford, J. M., and Hanawalt, P. C. (1997) Expression of wild-type p53 is required for efficient global genomic nucleotide excision repair in UV-irradiated human fibroblasts. *J. Biol. Chem.* **272,** 28,073–28,880.
26. Courtemanche, C., and Anderson, A. (1999) The p53 tumor suppressor protein reduces mutation frequency of a shuttle vector modified by the chemical mutagens (+/–)7, 8-hydroxy-9, 10-epoxy-7,8,9,10,-tetrahydrobenzo(a)pyrene, aflatoxin B1 and meta-chloroproxybenzoic acid. *Oncogene* **18,** 4672–4680.
27. Zhu, Q., Wani, M. A., El-Mahdy, M., and Wani, A. A. (2000) Decreased DNA repair efficiency by loss or disruption of p53 function preferentially affects removal of cyclobutane pyrimidine dimers from non-transcribed strand and slow repair sites in transcribed strand. *J. Biol. Chem.* **275,** 11,492–11,497.
28. Mirzayans, R., Bashir, S., Murray, D., and Paterson, M. C. (1999) Inverse correlation between p53 protein levels and DNA repair efficiency in human fibroblast strains treated with 4-nitroquinoline 1- oxide: evidence that lesions other than DNA strand breaks trigger the p53 response. *Carcinogenesis* **20,** 941–946.
29. Hall, P. A., McKee, P. H., Menage, H. D., Dover, R., and Lane, D. P. (1993) High levels of p53 protein in UV-irradiated normal human skin. *Oncogene* **8,** 203–207.

30. Burren, R., Scaletta, C., Frenk, E., Panizzon, R. G., and Applegate, L. A. (1998) Sunlight and carcinogenesis: expression of p53 and pyrimidine dimers in human skin following UVA I, UVA I + II and solar simulating radiations. *Int. J. Cancer* **76,** 201–206.
31. Yang, J., and Duerksen-Hughes, P. (1998). A new approach to identifying genotoxic carcinogens: p53 induction as an indicator of genotoxic damage. *Carcinogenesis* **19,** 1117–1125.
32. Duerksen-Hughes, P. J., Yang, J., and Ozcan, O. (1999) p53 induction as a genotoxic test for twenty-five chemicals undergoing in vivo carcinogenicity testing. *Environ. Health Perspec.* **107,** 805–812.
33. Bartek, J., Bartkova, J., Lukas, J., Staskova, Z., Vojtesek, B., and Lane, D. P. (1993) Immunohistochemical analysis of the p53 oncoprotein on paraffin sections using a series of novel monoclonal antibodies. *J. Pathol.* **169,** 27–34.
34. Bartek, J., Bartkova, J., Vojtesek, B., Staskova, Z., Lukas, J., Rejthar, A., Kovarik, J., Midgley, C. A., Gannon, J. V., and Lane, D. P. (1991) Aberrant expression of the p53 oncoprotein is a common feature of a wide spectrum of human malignancies. *Oncogene* **6,** 1699–1703.

22

Detection of Caspases Activation *In Situ* by Fluorochrome-Labeled Inhibitors of Caspases (FLICA)

Zbigniew Darzynkiewicz, Elzbieta Bedner, Piotr Smolewski, Brian W. Lee and Gary L. Johnson

1. Introduction

Caspases are cysteine-aspartic acid specific proteases that are activated in response to different cell death inducing stimuli ***(1–3)***. Their activation initiates specific cleavage of the respective target proteins and therefore is considered to be a marker of the irreversible steps that lead to cell demise (reviews ***4,5***). Caspases specifically recognize a four-amino acid sequence on their substrate proteins; the carboxyl end of aspartic acid within this sequence is the target for cleavage. Several approaches have been developed to detect the process of caspases activation. Because the activation involves the transcatalytic cleavage of the zymogen pro-caspases (reviews ***6–8***) the cleavage products having lower molecular weight than the zymogen can be revealed electrophoretically and identified in Western blots using caspase-specific antibodies. Another approach utilizes the fluorogenic (or chromogenic) substrates of caspases. Peptide substrates were developed which are colorless or non-fluorescent, but upon cleavage, generate colored or fluorescing products ***(9–11)***. Utility of these two approaches, however, was limited to the measurement of caspases activation in cell extracts thereby providing no information on the *in situ* caspases activation. This would allow one to study individual cells, assess heterogeneity of cell populations, or reveal correlation with other cell attributes.

Among the approaches that can be applied to study activation of caspases *in situ* are the methods based on immunocytochemical detection of the epitope that is characteristic of the caspases' active form. Antibodies that react only with the activated caspases have recently become available ***(12)***, but little has been published utilizing such antibodies in cytometric assays. Activation of

From: *Methods in Molecular Biology, vol. 203:* In Situ *Detection of DNA Damage: Methods and Protocols*
Edited by: V. V. Didenko

caspases, however, can be detected indirectly, by immunocytochemical identification of the specific cleavage products e.g. the p89 fragment of poly(ADP-ribose) polymerase and this method has been adapted to cytometry ***(13,14)***.

The method described here relies on the use of the fluorochrome-labeled inhibitors of caspases (FLICA; refs. ***15,16***). The principle of this methodology was introduced long ago in the studies of the esterases and proteases utilizing radiolabeled specific inhibitors that bound to the active centers of these enzymes and were detected by autoradiography ***(17)***. In the case of caspases the ligands that specifically and covalently bind to their active centers are carboxyfluorescein (FAM) or FITC- labeled peptide-fluoromethyl ketone (FMK) inhibitors (**Fig. 1**). These ketone reagents penetrate through the plasma membrane of live cells and are relatively nontoxic to the cell, at least in short-term incubations. Actually, in some cell systems these inhibitors promote cell survival, protecting them from apoptosis ***(4,5,18)***. The recognition peptide moiety of these reagents provides some level of specificity between ligand and a particular caspase. Several FLICAs are commercially available [Serologicals Corp. (formerly Intergen), Gaithersburg, MD; Promega, Madison, WI], including FAM (or FITC)-VAD-FMK which contains the valylalanyl aspartic acid residue sequence. This target sequence allows this inhibitor to irreversibly bind to activated caspases -1, -3 -4, -5, -7, -8 and -9. Other inhibitors such as VDVAD, DEVD, VEID, YVAD, LETD, LEHD, and AEVD contain peptide residues which preferentially bind to the activated caspases -2, -3, -6, -1, -8, -9, and -10, respectively.

Exposure of live cells to FLICAs results in the uptake of these reagents followed by their covalent binding to activated caspases within the cells that undergo apoptosis. Unbound FLICAs are removed from the nonapoptotic cells that lack activated caspases by rinsing the cells with wash-buffer. The protocols given below describe labeling cells that contain activated caspases using FAM-VAD-FMK . This reagent which, as mentioned above, lacks specificity and labels all caspases. The same protocol can be applied to other FLICA with VDVAD, DEVD, VEID, YVAD, LETD, LEHD, or AEVD recognition peptides. Cells labeled with FLICAs can be examined by fluorescence microscopy, or subjected to quantitative analysis by flow cytometry or laser scanning cytometry (LSC). The latter instrumentation (LSC), which combines several features of flow cytometry and image analysis (reviews, ***19,20***), is particularly useful in studies of apoptosis (***21,22***; review ***23***)

2. Materials

1. Cells to be analyzed: Can be grown on slides (*see* **Subheading 3.1**) or in suspension.
2. Microscope slides, coverslips: *see* **Subheading 3.1.**
3. Fluorescence microscope, or laser scanning cytometer (LSC, manufactured by CompuCyte, Cambridge, MA) or flow cytometer, each with appropriate fluores-

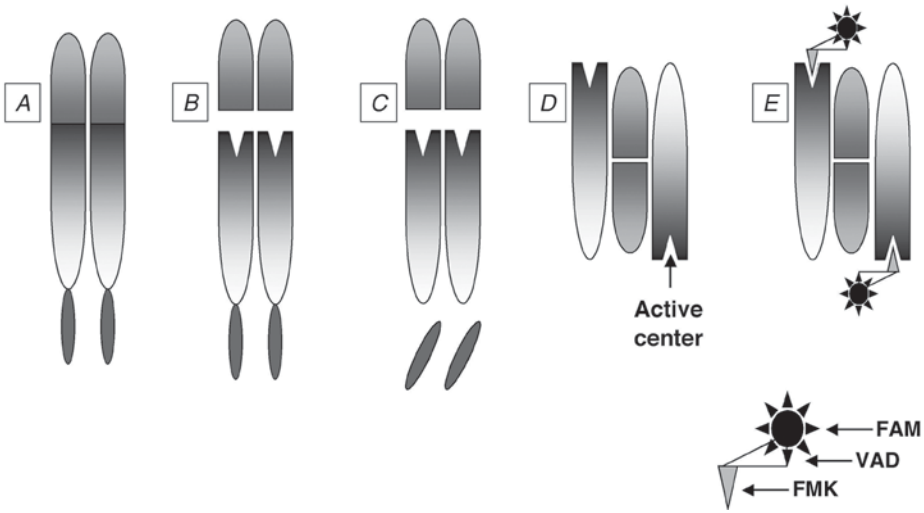

Fig. 1. Schematic illustration of FLICA binding to activated caspases. Caspases are present in the cell as zymogens containing N-terminal prodomain followed by a large (~20 kDa) and a small (~10 kDa) catalytic subunit **(A)**. The size of the prodomain segment varies between caspases. A large prodomain size is typical of initiator caspases while effector caspases have short prodomain regions. Two related motifs are present in prodomains: the death effector domain (DED) and caspase recruitment domain (CARD). When activated by the death signal the pro-caspases are initially cleaved at Asp-X bonds between the large and small subunits which results in separation of subunits **(B)**. The second cleavage takes place also at Asp site and leads to separation of the prodomain **(C)**. The subunits from two caspases then assemble into a hetero-tetramer to form the active protease that has two active centers at opposite ends of the molecule **(D)**. The active enzymatic centers are accessible to the substrates and also can bind FLICA **(E)**. The covalent binding of FLICAs is mediated by the fluoromethyl ketone (FMK) moiety which interacts with the cysteine of the active center forming a thiomethyl ketone II and irreversibly inactivates the enzyme ***(24)***. The specificity of binding is provided by the sequence of amino acids in the tetra-peptide moiety (e.g., DEVD for caspase-3). The tri-peptide (VAD) moiety FLICA binds to all caspases and thus is pan-caspase inhibitor/marker. The fluorescent tag (carboxyfluorescein, FAM) is located on the other end of the FLICA molecule.

cence excitation source and emission filters. Flow cytometers of different types, offered by several manufacturers, can be used to measure cell fluorescence following staining according to the procedures described below. The manufacturers of the most common flow cytometers are Coulter Corporation (Miami, FL), Becton Dickinson Immunocytometry Systems (San Jose, CA), Cytomation (Fort Collins, CO) and PARTEC (Zurich, Switzerland).

4. Phosphate-buffered saline (PBS).

5. Dimethyl sulfoxide (DMSO).
6. Stock solution of PI: Dissolve 1 mg of PI (Molecular Probes) in 1 mL of distilled water. This solution can be stored at 4°C in the dark for several months.
7. Stock FLICA solution: Dissolve lyophilized FLICA (e.g. FAM-VAD-FMK; available as a component of the CaspaTag™ Fluorescein Caspase Activity kit from Serologicals, Cat No. S7300) in dimethyl sulfoxide (DMSO) as specified in the kit to obtain 150× concentrated (stock) solution of this inhibitor. Also available from Serologicals are caspase-2 (VDVAD), caspase-3 (DEVD), caspase-6 (VEID), caspase-1 (YVAD), caspase-8 (LETD), caspase-9 (LEHD), and caspase-10 (AEVD) FLICAs. Aliquots of FLICAs solution may be stored at –20°C in the dark for several months.
8. Intermediate (30 × concentrated) FLICA solution: Prepare a 30 × concentrated solution of FAM-VAD-FMK by diluting the stock solution 1:5 in PBS. Mix the vial until the contents become transparent and homogenous. This solution should be made freshly. Protect all FLICA solutions from light.
9. FLICA staining solution: just prior to the use add 3 µL of 30 × concentrated FAM-VAD-FMK solution into 100 µL of culture medium.
10. Rinsing solution: 1% (w/v) BSA in PBS.
11. Staining solution of PI: Add 10 µL of stock solution of PI to 1 mL of the rinsing solution.

3. Methods

3.1. Attachment of Cells to Slides (Cells to be Analyzed by Microscopy and/or LSC)

The procedure requires incubation of live (unfixed, not permeabilized) cells with solutions of FLICAs. A variety of adherent cells are available for growth in cell culture flasks. Such cells can be attached to microscope slides by culturing them on slides or coverslips. Culture vessels that have a microscope slide at the bottom of the chamber are commercially available (e.g. "Chamberslide", Nunc, Inc., Naperville, Il). Adherent cells may be detached from culture flasks using trypsin-EDTA solution (BioWhittaker, Inc., Walkersville, MD). A suspension of these cells can be prepared using cell culture media plus 7–10% fetal bovine serum. The cells growing in these chambers spread and attach to the slide surface after incubation at 37°C for several hours. Glass rather than plastic slides are preferred as the latter often have high autofluorescence that interferes with measurements by LSC. Alternatively, the cells can be grown on coverslips e.g. placed on the bottom of Petri dishes. The coverslips are then inverted over shallow (< 1 mm) wells on the microscope slides. The wells can be prepared by constructing the well walls (~ 2 × 1 cm) with either a pen that deposits a hydrophobic barrier ("Isolator", Shandon Scientific), nail polish, or melted paraffin. The wells also may be made by preparing a strip of Parafilm "M" (American National Can, Greenwich, CT) of the size of the slide, cutting a hole ~2 × 1 cm in the middle of

this strip, placing the strip on the microscope slide and heating the slide on a warm plate until the Parafilm starts to melt. It should be stressed, however, that because the cells detach during late stages of apoptosis these cells may be selectively lost if the analysis is limited to attached cells.

Cells that normally grow in suspension can be attached to glass slides by electrostatic forces. This is due to the fact that sialic acid residues which cover the cell surface have a net negative charge in contrast to the glass surface which is positively charged. Incubation of cells on microscope slides in the absence of any serum or serum proteins (which otherwise neutralize the charge), thus, leads to their attachment. The cells taken from culture should be rinsed in PBS in order to remove serum proteins contained in the cell culture media and then resuspended in PBS at a concentration of 2×10^5 cells/mL . An aliquot (50–100 µL) of this suspension should be deposited within a shallow well (prepared as described above) on the horizontally placed microscope slide. To prevent drying, a small piece (~2 × 2 cm) of a thin polyethylene foil or Parafilm may be placed atop of the cell suspension drop. A short (15–20 min) incubation of such cell suspension at room temperature in a closed box containing wet tissue or filter paper that provides 100% humidity is adequate to ensure that most cells will firmly attach to the slide surface. Cells attached in this manner remain viable for several hours and can be subjected to surface immmunophenotyping, viability tests or intracellular enzyme kinetics assays ***(20)***. Such preparations can be fixed (e.g. in formaldehyde) without a significant loss of cells from the slide. However, as in the case of cell growth on glass, late apoptotic cells have a tendency to detach after the initial attachment.

It should be stressed that the microscope slide to which the cells are going to be attached electrostatically should be extra clean. Fingerprints leave oils on the slide that interferes with cell attachment. To remove possible contamination of the glass surface that may interfere with cell attachment it is advised to soak the microscope slides in a household detergent, and then rinse in water and 100% ethanol respectively. Slides should be allowed to air dry and used the same day they are cleaned.

3.2. Cell Staining and Analysis by Microscopy or LSC

1. Attach the cells to the microscope slide as described in **Subheading 3.1.** Keep the cells immersed in the culture medium by adding 100 µL of the medium (with 10% serum) into the well on the microscope slide to cover the area with the cells.
2. Remove the medium and replace it with 100 µL of the 1 × FLICA (e.g. FAM-VAD-FMK) staining solution (*see* **Note 1**).
3. Place a ~ 2 × 4 cm strip of Parafilm atop the staining solution to prevent drying. Incubate the slides horizontally for 1 h at 37°C in a closed box with wet tissue or filter paper to ensure 100% humidity, in the dark.

4. Remove the staining solution with Pasteur pipet. Rinse thrice with the rinsing solution each time, adding a new aliquot, gently mixing, and after 2 min replacing with the next rinse (*see* **Note 2**).
5. Apply one or two drops of the PI staining solution atop of the cells deposited on the slide. Cover with a coverslip and seal the edges to prevent drying (*see* **Note 3**).
6. Within the next 30–40 min following incubation with FLICA observe the cells under fluorescence microscope (blue light illumination) or measure cell fluorescence on LSC. Use the argon ion laser (488 nm) of LSC to excite fluorescence, contour on light scatter and measure green fluorescence of FLICA at 530 ± 20 nm and red fluorescence of PI at >600 nm.

3.3. Cell Staining and Analysis by Flow Cytometry (see Notes 4–8)

1. Suspend 5×10^5–10^6 cells in 0.3 mL of full culture medium (with 10% serum) in centrifuge tube.
2. Add 10 µL of the 30 × concentrated ("intermediate") FLICA solution to this cell suspension. Mix the cell suspension by flicking the tube (*see* **Note 1**).
3. Incubate for 60 min at 37°C in atmosphere of air with 5% CO_2, at 100% humidity, in the dark.
4. Add to the cell suspension with FLICA 5 mL of the rinsing solution (PBS with BSA) and gently mix the cell suspension. Alternatively, the rinsing solution may be replaced by using the 1 × Wash Buffer" provided as a 10 × concentrate with the FLICA kit (CaspaTag™; Serologicals)
5. Centrifuge at 300*g* for 5 min at room temperature and remove supernatant by aspiration.
6. Resuspend cell pellet in 2 mL of the rinsing solution or in "1 × Wash Buffer".
7. Centrifuge at 300*g* for 5 min and aspirate supernatant (*see* **Note 2**).
8. Resuspend cells in 1 mL of the PI staining solution. Place the tube on ice (*see* **Note 3**).
9. Measure cell fluorescence by flow cytometry
   a. excite cell fluorescence with blue light (488 nm laser line, or when using mercury arc lamp, apply BG12 excitation filter)
   b. measure green fluorescence of FLICA at 530 ± 20 nm.
   c. measure red fluorescence of PI at >600 nm.

Some problems that should be taken into account when using FLICA and **Figs. 2** and **3** are discussed in **Notes 4–8**.

4. Notes

1. Protect cells from light throughout the procedure.
2. After step 4 (**Subheading 3.2**) or step 7 (**Subheading 3.3**) the cells may be fixed in 1% formaldehyde followed by 70% ethanol and then subjected to staining with PI in the presence of RNase or stained with 7-aminoactinomycin D. Analysis of the FLICA *vs* PI fluorescence by LSC of flow cytometry allows then to correlate

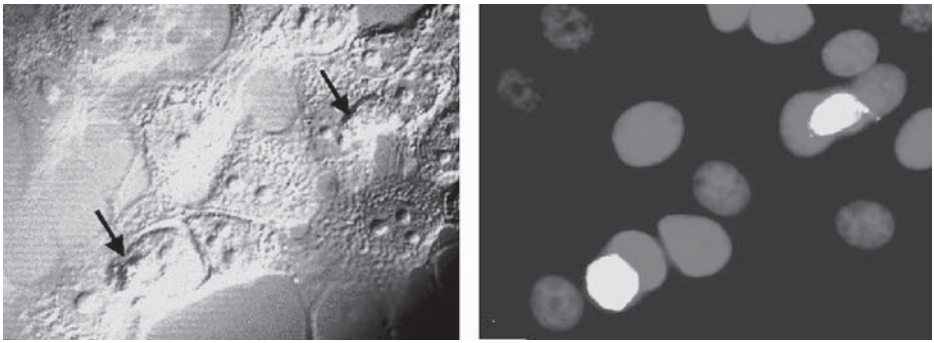

Fig. 2. Interference (Nomarski) contrast (left) and fluorescence microscopy (right) photomicrographs of MCF-7 cells labeled with FLICA and stained with PI. The cells growing in microscope slide-chambers were treated with 0. 15 μ*M* camptothecin (CTP) for 24 h and then incubated with FAM-VAD-FMK for 1 h, as described in the protocol. The cells were subsequently fixed in 1% formaldehyde followed by 70% ethanol, and their DNA counterstained with PI in the presence of RNase (*see* **Note 3**). Apparent are two apoptotic cells with changed morphology (diminished size, rounded shape; marked with arrows) detaching from the slide that are labeled with FAM-VAD-FMK.

activation of caspases with cellular DNA content i.e. the cell cycle position or DNA ploidy. Details of this procedure are provided in reference ***(16)***. Alternatively, when two-laser excitation is available and one of the lasers produces UV light, the cellular DNA may be counterstained with Hoechst 33342.

3. Staining with PI is optional. It allows us to identify the cells that have integrity of plasma membrane compromised to the extent that they cannot exclude PI (necrotic and late apoptotic cells, cells with mechanically damaged membranes, isolated cell nuclei; **Fig. 3**).
4. One has to keep in mind that FLICAs are not passive reagents that mark the activated caspases, but react directly with the caspase by covalent interaction with the active site of the enzyme. This inhibits caspase activity suppressing the process of apoptosis. Thus, the rate of apoptosis progression and all the events related to caspases activity are suppressed by FLICAs. The degree of suppression depends on their concentration, their target four peptide sequence, and the time of the cell exposure, *vis-à-vis* the induction of apoptosis.
5. Another problem that should be taken into an account when using FLICA to mark the activated caspases in live cells pertains to fragility of apoptotic cells. The assay requires incubation of live cells with these reagents followed by repeated rinsing to remove unbound FLICA from the non-apoptotic cells. Apoptotic cells, particularly at late stages of apoptosis, are fragile and are preferentially lost during the centrifugations. A certain degree of stability is derived from the presence of serum (up to 20% v/v) or BSA (up to 2% w/v) in the rinsing buffers. Also, the cells should be sedimented with minimal *g* force and short

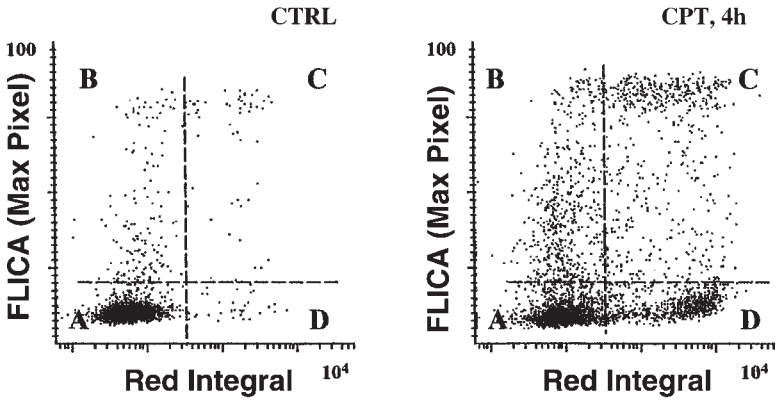

Fig. 3. The bivariate distributions (scatterplots) of FAM-VAD-FMK (FLICA; green maximal pixel) *vs* PI (red integral) fluorescence of the control (CTR) and CPT-treated HL-60 cells. The cells were stained according to the protocol (**Subheading 3.2**) and their fluorescence was measured by LSC. The live non-apoptotic cells, which are predominant in CTR are unlabeled (quadrant A). Early apoptotic cells have increased FLICA fluorescence but minimal fluorescence of PI (quadrant B). The cells more advanced in apoptosis show variable degrees of both, FLICA- and PI-, fluorescence (quadrant C). At terminal stages of apoptosis, caspases become unreactive with FLICA and very late apoptotic cells FLICA-negative and PI- positive (quadrant D).

centrifugation time. Some cell loss, however, does occur even when the cells are treated with the utmost caution. Because of cell loss one has to be careful drawing conclusions about the frequency of apoptosis based on the percentage of FLICA positive cells in the samples assayed by flow cytometry. In contrast to flow cytometry, analysis by LSC does not does not require the use of multiple centrifugation steps. Once cells are attached to microscope slides, they can be conveniently rinsed and analyzed for apoptotic activity. In the case of LSC, however, the propensity of apoptotic cells to detach from the glass should be taken into account, as it also may bias the analysis of apoptosis frequency.

6. It is difficult to assess the specificity of *in situ* bound individual FLICA sequences designed to be markers for their respective caspases. Certainly, the inhibitor with the VAD peptide sequence lacks specificity and binds to all caspases. An exception may be caspase-2 to which VAD has a low binding constant ***(24)***. The inhibitor with the DEVD sequence designed to be caspase-3 specific is expected also to interact with several other caspases. The inhibitory constant (K_i) of Ac-DEVD-CHO is 0.2–2.2 n*M* for caspase-3, 0.9 n*M* for caspase-8 and 1.6 n*M* for caspase-7 ***(24)***. In the present study we did observe that MCF-7 cells, (cells that do not express caspase-3) were quite strongly labeled with FAM-DEVD-FMK. This would suggest that in the absence of caspase-3, caspases-7 and -8, and perhaps other caspases were labeled with FAM-DEVD-FMK in MCF-7 cells. Other inhib-

itors also have strong affinity to more than a single caspase ***(24–27)***. Moreover, since little is known about the effective concentration of the different FLICA sequences within the confines of the cell and also about their binding constants to the respective caspases *in situ*, one has to be careful not to draw too many conclusions about their specificity based on binding in live cells. It was observed, however, that when the cells were pre-treated with a high concentration of the inhibitor (Z-VAD-FMK) the subsequent binding of the labeled inhibitor was reduced by over 90% ***(16)***. Likewise, when fixed and permeabilized cells were treated with an excess of the caspase-3 substrate (Ac-DEVD-pNA) the binding of the respective FLICA was inhibited ***(16)***.

7. **Fig. 2** shows the photomicrographs of MCF-7 cells treated for 24 h with camptothecin (CPT) to induce apoptosis and then stained with FAM-VAD-FMK according to the protocol described above. The cells were then fixed in formaldehyde followed by ethanol and their DNA stained with PI in the presence of RNase as described in **Note 3**. Notice two strongly fluorescing cells with changed morphology, typical of apoptosis.
8. The bivariate distributions (scatterplots) of FAM-VAD-FMK (FLICA; maximal pixel) *vs* PI (integral) fluorescence of the control and CPT-treated HL-60 cells are presented in **Fig. 3**. Cells were stained according to the protocol presented above and their fluorescence was measured by LSC. The live non-apoptotic cells have neither FLICA nor PI fluorescence (quadrant A). Early apoptotic cells have increased FLICA fluorescence but no red fluorescence of PI (quadrant B). Late apoptotic cells show variable degree of FLICA- and also PI- fluorescence (quadrant C). Very late apoptotic or necrotic cells are FLICA-negative and PI- positive (quadrant D).

Acknowledgment

Supported by NCI grant RO1 28704, "This Close" Foundation for Cancer Research and Chemotherapy Foundation

References

1. Alnemri, E. S., Livingston, D. I., Nicholson, D. W., Salvesen, G, Thornberry, N. A., Wong, W. W., and Yuan, J. (1996) Human ICE/CED-4 protease nomenclature. *Cell* **87,** 171–173.
2. Kaufmann, S. H., Desnoyers, S., Ottaviano, Y., Davidson, N. E., and Poirier, G. G. (1993) Specific proteolytic cleavage of poly(ADP-ribose) polymerase: an early marker of chemotherapy-induced apoptosis. *Cancer Res.* **53,** 3976–3985.
3. Lazebnik, Y. A., Kaufmann, S. H., Desnoyers, S., Poirier, G. G., and Earnshaw, W. C. (1994) Cleavage of poly(ADP-ribose) polymerase by proteinase with properties like ICE. *Nature* **371,** 346–347.
4. Budihardjo, I., Oliver, H., Lutter, M., and Luo, X. (1999) Biochemical pathways of caspase activation during apoptosis. *Annu. Rev. Cell Dev. Biol.* **15,** 269–290.
5. Earnshaw, W. C., Martins, L. M., and Kaufmann, S. H. (1999) Mammalian caspases: structure, activation, substrates, and functions during apoptosis. *Annu. Rev. Biochem.* **68,** 383–424.

6. Nicholson, D. W. (1999) Caspase structure, proteolytic substrates and function during apoptotic cell death. *Cell Death Differ.* **6,** 1028–1042.
7. Zhang, T. S., Hunort, S., Kuida, K., and Flavell, R. A. (1999) Caspase knockouts: matters of life and death. *Cell Death Differ.* **6,** 1043–1053.
8. Stennicke, H. R., and Salvesen, G. S. (1999) Catalytic properties of caspases. *Cell Death Differ.* **6,** 1060–1066.
9. Gorman, A. M., Hirt, U. A., Zhivotovsky, B., Orrenius, S., and Ceccatelliu, S. (1999) Application of a fluorometric assay to detect caspase activity in thymus tissue undergoing apoptosis *in vivo*. *J. Immunol. Methods* **226,** 43–48.
10. Liu, J., Bhalgat, M., Zhang, C., Diwu, Z., Hoyland, B., and Klaubert, D. H. (1999) Fluorescent molecular probes V: a sensitive caspase-3 substrate for fluorometric assays. *Bioorg. Med. Chem. Lett.* **9,** 3231–3236.
11. Komoriya, A., Packard, B. Z., Brown, M. J., Wu, M. L., and Henkart. P. A. (2000) Assessment of caspase activities in intact apoptotic thymocytes using cell-permeable fluorogenic caspase substrates. *J. Exp. Med.* **191,** 1819–1828.
12. Tanaka, M., Momoi, T., and Marunouchi, T. (2000) *In situ* detection of activated caspase-3 in apoptotic granule neurons in the developing cerebellum in slice cultures and *in vivo*. *Brain Res. Dev.* **121,** 223–228.
13. Li, X., and Darzynkiewicz, Z. (2000) Cleavage of poly(ADP-ribose) polymerase measured *in situ* in individual cells: relationship to DNA fragmentation and cell cycle position during apoptosis. *Exp. Cell Res.* **255,** 125–132.
14. Li, X., Du, L., and Darzynkiewicz, Z. (2000) During apoptosis of HL-60 and U-937 cells caspases are activated independently of dissipation of mitochondrial electrochemical potential. *Exp. Cell Res.* **257,** 290–297.
15. Bedner, E., Smolewski, P., Amstad, P., and Darzynkiewicz, Z. (2000) Activation of caspases measured in situ by binding of fluorochrome-labeled inhibitors of caspases (FLICA): correlation with DNA fragmentation. *Exp. Cell Res.* **259,** 308–313.
16. Smolewski, P., Bedner, E., Du, L., Hsieh, T.-C., Wu, J. M., Phelps, D. J., and Darzynkiewicz, Z. (2001) Detection of caspases activation by fluorochrome-labeled inhibitors: Multiparameter analysis by laser scanning cytometry. *Cytometry* **44,** 73–82.
17. Darzynkiewicz, Z., and Barnard, E. A. (1967) Specific proteases of mast cells. *Nature* **213,** 1198–1203.
18. Zhivotovsky, B., Samali, A., Gahm, A., and Orrenius, S. (1999) Caspases: their intracellular localization and translocation during apoptosis. *Cell Death Differ.* **8,** 644–651.
19. Kamentsky, L. A. (2001) Laser scanning cytometry. *Meth Cell Biol.* **63,** 51–87.
20. Darzynkiewicz, Z., Bedner, E., Li, X., Gorczyca, W., and Melamed, M. R. (1999) Laser scanning cytometry. A new instrumentation with many applications. *Exp. Cell Res.* **249,** 1–12.
21. Bedner, E., Li, X., Kunicki, J., and Darzynkiewicz, Z. (2000) Translocation of Bax to mitochondria during apoptosis measured by laser scanning cytometry. *Cytometry* **41,** 83–88.

22. Li, X., and Darzynkiewicz, Z. (2000) The Schrödinger's cat quandary in cell biology: integration of live cell functional assays with measurements of fixed cells in analysis of apoptosis. *Exp. Cell Res.* **249,** 404–412.
23. Bedner, E., Li, X., Gorczyca, W., Melamed, M. R. and Darzynkiewicz, Z. (1999) Analysis of apoptosis by laser scanning cytometry. *Cytometry,* **35,** 181–195
24. Ekert, P. G., Silke, J., and Vaux, D.,L. (1999) Caspase inhibitors. *Cell Death Differ.* **6,**1081–1086.
25. Thornberry, N. A., Peterson, E. P., Zhao, J. J., Howard, A. D., Griffin, P. R., and Chapman, K. T. (1994) Inactivation of interleukin-1 beta converting enzyme by peptide(acyloxy)methyl ketones. *Biochemistry* **33,** 3934–3940.
26. Garcia-Calvo, M., Peterson, E. P., Leiting, B., Ruel, R., Nicholson, D. W., and Thornberry, N. A. (1998) Inhibition of human caspases by peptide-based and macromolecular inhibitors. *J. Biol. Chem.* **273,** 32,608–32,613.
27. Thornberry, N. A., Rano, T. A., Peterson, E. P., Rasper, D. M., Timkey, T., Garcia-Calvo, M., Houtzager, V. M., Nordstrom, P. A., Roy, S., Valliancourt, J. P., Chapman, K. T., and Nicholson, D. W. (1997) A combinatorial approach defines specificities of members of the caspase family and granzyme B. *J. Biol. Chem.* **272,** 17,907–17,911.